



**TECHNISCHE  
UNIVERSITÄT  
DRESDEN**

Fakultät Mathematik und Naturwissenschaften

Fachrichtung Physik, Institut für Theoretische Physik

# QCD sum rules for D mesons: In-medium effects, chiral symmetry aspects and higher orders

**Thomas Buchheim**

geboren am 09. Januar 1987 in Wurzen

## Dissertation

zur Erlangung des akademischen Grades

**Doctor rerum naturalium (Dr. rer. nat.)**

angefertigt unter der wissenschaftlichen Betreuung von

**Prof. Dr. Burkhard Kämpfer**

am Helmholtz-Zentrum Dresden-Rossendorf e. V.

**HZDR**

 **HELMHOLTZ  
ZENTRUM DRESDEN  
ROSSENDORF**

eingereicht am 02. Dezember 2016

1. Gutachter: Prof. Dr. Burkhard Kämpfer
2. Gutachter: Prof. Dr. Dominik Stöckinger
3. Gutachter: Prof. Dr. Stefan Leupold

verteidigt am 11. April 2017

## Abstract

Heavy open flavor mesons can serve as probes of hot and dense, strongly interacting matter in heavy-ion collisions suitable to mimic the extreme conditions shortly after the big-bang or in compact stars. Thus, the thorough theoretical investigation of medium modifications of D mesons is of utmost importance for the interpretation of the experimental data. Even at finite thermodynamic parameters, such as temperature and density, the non-perturbative framework of QCD sum rules allows for the determination of hadronic properties which are not accessible in perturbative quantum chromodynamics (QCD). By virtue of the separation of scales, long-range effects of hadrons are related to quark and gluon degrees of freedom, where features of the hadron spectrum are linked to condensates parameterizing the complex QCD ground state.

This thesis furnishes the conception and calculus of QCD sum rules with emphasis on in-medium effects which are inevitable when addressing such effects in higher order contributions. In this regard, the notion and implications of medium-specific condensates are elucidated. Motivated by the significant numerical impact of four-quark condensates to the  $\rho$  meson sum rule we evaluate, for the first time, the corresponding in-medium mass-dimension 6 terms for D mesons tentatively employing the factorization hypothesis. Four-quark condensates containing heavy-quark operators may be included into the sum rule analysis utilizing the in-medium heavy-quark expansion made available here. Particular quark condensates are potential order parameters of chiral symmetry breaking, which is the mass generating mechanism of QCD giving the essential mass fraction to light hadrons. The interplay of altered spectral properties with changing in-medium QCD condensates, i. e. the chiral order parameters, can be studied with chiral partner sum rules. Although, introduced for light spin-1 mesons we foster their generalization to spin-0 open charm mesons demonstrating their sensitivity to chiral dynamics. In particular, signals of chiral restorations at higher temperatures are evident which are compatible with results from hadronic effective theories.

## Kurzdarstellung

Schwere Mesonen mit offenem Flavor können als Sonden heißer und dichter, stark wechselwirkender Materie in Schwerionenkollisionen dienen, die geeignet sind, die extremen Bedingungen kurz nach dem Urknall oder im Inneren kompakter Sterne zu imitieren. Daher ist die sorgfältige theoretische Untersuchung der Mediummodifikationen von D-Mesonen von größter Wichtigkeit für die Interpretation der experimentellen Daten. Sogar bei endlichen thermodynamischen Parametern, wie Temperatur und Dichte, lassen sich hadronische Eigenschaften im Rahmen von QCD-Summenregeln bestimmen, die der störungstheoretischen Quantenchromodynamik (QCD) nicht zugänglich sind. Vermöge einer Separation der Skalen sind langreichweitige Effekte der Hadronen analytisch mit Quark- und Gluon-Freiheitsgraden verbunden. Dabei werden Charakteristika des Hadronenspektrums mit Kondensaten verknüpft, welche den komplexen QCD-Grundzustand parametrisieren.

In dieser Arbeit wird das Kalkül der QCD-Summenregeln mit Augenmerk auf Mediumeffekte dargestellt, die unabdingbar sind, wenn solche Effekte in Beiträgen höherer Ordnung adressiert werden sollen. In diesem Zusammenhang werden die Begrifflichkeiten der medium-spezifischen Kondensate und deren Implikationen erläutert. Motiviert durch den

signifikanten numerischen Beitrag von Vier-Quark-Kondensaten zur  $\rho$ -Meson-Summenregel evaluieren wir zum ersten Mal die entsprechenden Mediumbeiträge der Massendimension 6 zum D-Meson, wobei die Faktorisierungshypothese tentativ zur Anwendung kommt. Vier-Quark-Kondensate, die Operatoren schwerer Quarks enthalten, mögen der hier bereitgestellten Schwer-Quark-Massen-Entwicklung im Medium unterzogen werden, um ebenso zur Summenregelanalyse herangezogen werden zu können. Bestimmte Quark-Kondensate sind potentielle Ordnungsparameter der chiralen Symmetriebrechung, welche der massegenerierende Mechanismus der QCD ist und den essentiellen Masseanteil der leichten Hadronen liefert. Das Zusammenspiel von geänderten spektralen Eigenschaften mit mediumabhängigen QCD-Kondensaten, d. h. den chiralen Ordnungsparametern, kann mit Hilfe von chiralen Partner-Summenregeln studiert werden. Obwohl diese für leichte Spin-1-Mesonen eingeführt wurden, plädieren wir für deren Erweiterung auf Spin-0-Mesonen mit offenem Charm und demonstrieren deren Sensitivität auf chirale Dynamik. Insbesondere werden Signale für eine chirale Restauration bei hohen Temperaturen evident, die mit den Resultaten aus hadronischen effektiven Theorien kompatibel sind.

# Contents

<b>1</b>	<b>Introduction</b>	<b>7</b>
1.1	Probes of strongly interacting matter . . . . .	7
1.2	QCD in the low-energy regime . . . . .	8
1.3	Structure of the thesis . . . . .	10
<b>2</b>	<b>QCD sum rules</b>	<b>13</b>
2.1	Current-current correlator . . . . .	13
2.1.1	Vacuum dispersion relation . . . . .	15
2.1.2	Medium dispersion relation . . . . .	17
2.2	Operator product expansion . . . . .	19
2.2.1	Background field expansion in Fock-Schwinger gauge . . . . .	21
2.2.2	Renormalization . . . . .	25
2.2.3	Structure of the OPE . . . . .	31
2.3	Nature of condensates . . . . .	35
2.3.1	Universality . . . . .	35
2.3.2	Order parameters . . . . .	36
2.3.3	Condensates in a strongly interacting medium . . . . .	39
2.4	Evaluation of QCD sum rules . . . . .	43
2.4.1	Model-independent resonance properties . . . . .	47
2.4.2	Resonance properties from a spectral density ansatz . . . . .	48
<b>3</b>	<b>Medium modifications of D mesons</b>	<b>53</b>
3.1	Motivation . . . . .	53
3.2	QCD sum rules for $qQ$ mesons . . . . .	55
3.3	Four-quark condensate contributions . . . . .	57
3.3.1	Wilson coefficients . . . . .	57
3.3.2	Chirally odd four-quark condensate in D meson QSR . . . . .	60
3.3.3	Estimates of four-quark condensates – factorization . . . . .	60
3.4	Numerical evaluation . . . . .	62
3.5	Comparison of four-quark condensates in $\rho$ meson and D meson sum rules . .	66
3.6	Heavy-quark expansion . . . . .	68
3.6.1	HQE in vacuum. A recollection . . . . .	68
3.6.2	Application of HQE to in-medium heavy-light four-quark condensates	69
3.7	Algebraic vacuum limits of QCD condensates . . . . .	70
3.8	Interim summary . . . . .	75
<b>4</b>	<b>Chiral partner sum rules</b>	<b>77</b>
4.1	Motivation . . . . .	77
4.2	Temperature dependences of pseudo-scalar and scalar D meson properties . .	78
4.2.1	Conventional Borel analysis . . . . .	81

4.2.2	Borel analysis with given meson mass input . . . . .	87
4.3	Weinberg sum rules . . . . .	91
4.3.1	Extending Weinberg-type sum rules for spin-0 heavy-light mesons . . .	92
4.3.2	Comments on chirally odd condensates . . . . .	93
4.4	D meson properties from chiral partner sum rules . . . . .	95
4.5	Interim summary . . . . .	97
<b>5</b>	<b>Summary and outlook</b>	<b>101</b>
<b>A</b>	<b>Quantum chromodynamics. An overview</b>	<b>105</b>
<b>B</b>	<b>Chiral symmetry</b>	<b>111</b>
B.1	Chiral symmetry group, related transformations and currents . . . . .	111
B.2	Derivation of the GOR relation . . . . .	115
B.3	Finite chiral transformations in the heavy-light sector . . . . .	116
<b>C</b>	<b>Operator product expansion. Addendum</b>	<b>119</b>
C.1	Technicalities on condensates . . . . .	119
C.1.1	Projection of Dirac indices . . . . .	119
C.1.2	Projection of color indices . . . . .	120
C.1.3	Fierz transformations . . . . .	121
C.2	In-medium projection of Lorentz tensors and algebraic vacuum limits . . . .	123
C.2.1	General framework . . . . .	123
C.2.2	Application to four-quark condensates . . . . .	131
C.2.3	Discussion of factorization and ground state saturation hypothesis . .	140
C.2.4	Equivalence of two approaches to the medium-specific decomposition .	142
C.3	Calculation of Wilson coefficients of light-quark condensates of mass dimen- sion 6 . . . . .	144
<b>D</b>	<b>Borel transformation</b>	<b>147</b>
<b>E</b>	<b>Monte-Carlo sum rule analysis</b>	<b>151</b>
	<b>Acronyms</b>	<b>155</b>
	<b>List of Figures</b>	<b>157</b>
	<b>List of Tables</b>	<b>159</b>
	<b>Bibliography</b>	<b>161</b>

# 1 Introduction

Richard Feynman’s statement ‘All mass is interaction.’ [Gle92] seems ultimately validated by the discovery of the Higgs boson [Aad12, Cha12] which is key to the understanding of the masses of the elementary particles constituting the standard model. By coupling to the scalar Higgs boson, these elementary particles acquire their respective masses. In particular, the heavy masses of  $W$  and  $Z$  bosons, mediating the weak force, can be generated by the Higgs mechanism [Hig64a, Hig64b, Eng64] which is based on a spontaneously broken symmetry principle. In the realm of theoretical physics, symmetries play an important role with applications in many fields but with outstanding relevance in particle physics. Local gauge symmetries are the defining properties of the quantum field theories describing the fundamental interactions between elementary particles. Studying unitary symmetry groups has lead Zweig [Zwe64] and Gell-Mann [GM62, GM64] to introduce the quark model underlying the structure of baryons and mesons. These are strongly interacting particles and collectively referred to as hadrons.

The essential mass contribution to the visible universe, however, does not originate from elementary particles but from massive hadrons, i. e. nucleons, being the building blocks of nuclei. Controversially, the nucleon mass is orders of magnitude larger than the sum of the masses of its constituents [Pat16], which is in conflict with the concept of binding energy in electrodynamics suggesting an underlying theory with vastly different characteristics. Due to the success of quantum chromodynamics (QCD) [Fri73] in describing high-energy processes involving hadrons, where quarks can be treated as quasi-free particles, its validity also in the low-energy regime is assumed. Thus, QCD is believed to provide an adequate description of the experimentally observable degrees of freedom (DoF), namely hadrons, which are bound states of elementary quarks and massless gluons being the force carrying gauge bosons of the strong interaction, i. e. it incloses the famous confinement problem. Interestingly, QCD bears a mass generating mechanism for strongly interacting particles dissolving the nucleon mass puzzle. It grounds on the spontaneous breaking of chiral symmetry, besides confinement, the central research subject in contemporary hadron physics.

## 1.1 Probes of strongly interacting matter

In order to shed light on the subatomic processes in the early stages of the universe characterized by enormously high temperatures and to elucidate the formation and stability of very dense cosmological object like neutron stars an understanding of strong interactions in such extreme conditions is inevitable, i. e. a comprehensive picture how the microcosm of particles physics determines the behavior of the macroscopic world even up to cosmological scales must be envisaged. The thermodynamics of strongly interacting matter is quantified by equations of state and the QCD phase diagram which features the phase transition or crossover from hadronic matter to the quark-gluon-plasma, where quarks and gluons are liberated. Associated with this transition are the confinement–deconfinement transition as well

as the chiral symmetry breaking and restoration mechanism. Hence, the exact characterization of the QCD phase diagram, e. g. the determination of the order of the phase transition, the possible occurrence of a critical end point and/or crossover as well as the location of the phase boundary, is the very focus of many theoretical and experimental efforts.

Heavy-ion collisions are an appropriate tool to explore the QCD phase diagram studying the behavior of strongly interacting matter at finite temperatures and net-baryon densities. The current experimental set ups at LHC [Aam08] and RHIC [Adc05, Ada05] produce a wealth of data at high temperatures and low densities, thus, providing a glimpse on the young universe, while the forthcoming experiments at FAIR [Fri06, Sch14, Bri07, Pre16], NICA [Sis09, Kek16] and J-PARC [Sak14] are designed to study finite baryon densities giving insights into dense stellar objects.<sup>1</sup> Heavy open flavor mesons, e. g. D and B mesons, can serve as probes of hot and dense matter. They are produced in initial interactions of the collision and can carry signals of the subsequent stages of the fireball; their identification is facilitated by the heavy-quark content. To interpret these signals correctly, the medium modifications of D mesons are of utmost importance and the main focus of this work.

Triggered by the Brown-Rho scaling law [Bro91], medium modifications of light hadrons, in particular vector mesons, have been studied extensively. Experiments, e. g. at GSI [Aga07, Aga12], CERN-SPS [Aga95, Arn06], JLab [Nas07] and KEK [Nar06], used direct photons and dileptons to detect altered spectral properties of  $\rho$  and  $\omega$  mesons in a strongly interacting environment. Such investigations enable studies of the in-medium behavior of light chiral partner mesons, which are of particular interest, because the difference of their spectral functions quantifies the degree of the dynamical breaking of chiral symmetry. Hence, they elucidate important features of the mass generating mechanism of QCD. In this thesis, we dwell on the advantageous evaluation of chiral effects in the heavy-light meson sector, and therefore, foster D mesons as adequate probes of chiral dynamics.

## 1.2 QCD in the low-energy regime

QCD, being an integral part of the standard model, is understood as the theory of the strong interaction on quark level. It is formulated as a non-Abelian SU(3) gauge theory defined by its Lagrangian density. Accordingly, each quark flavor exhibits a third degree degeneracy, where the additional quantum number is the color charge. Quark interactions are mediated by massless gauge bosons, i. e. the gluons. Corresponding to the adjoint representation of the SU(3) symmetry group, there exist eight gluons which carry color charge and anti-charge. Thus, gluons are self-interacting gauge bosons resulting in a strong coupling and gluon field strength at large distances, i. e. the QCD vacuum is highly non-trivial featuring anti-screening. In contrast to electrodynamics, an effective quark–anti-quark potential linearly rises with growing distance. Hence, quarks are always confined into colorless hadrons. The origin of this phenomenon, dubbed confinement, and its derivation from QCD is a pending problem. Hadrons are of two kinds: either bosonic mesons with an even number of valence quarks or fermionic baryons with an odd number of valence quarks.<sup>2</sup> The interaction of protons and neutrons has been described by the strong iso-spin symmetry, where the nucleon coupling is realized by an effective strong force via light-meson exchange, which is the actual

<sup>1</sup>See the list of acronyms below for the various accelerator facilities and experiments.

<sup>2</sup>The classification of the newly observed exotic states is a current matter of debate.



origin of the name 'strong' nuclear force, as it (over)compensates the Coulomb repulsion of protons in the nucleus.

From QCD renormalization calculations one obtains quantum corrections to tree-level vertices which yield a running coupling  $\alpha_s$  with negative derivative, therefore, the coupling decreases for a growing renormalization scale, known as asymptotic freedom [Gro73, Pol73]. However, in the low-energy regime the coupling becomes large, thus, spoiling a perturbative expansion, i.e. a power series in the coupling strength in order to compute observables becomes useless. Accordingly, non-perturbative methods are to be utilized to treat hadrons within the framework of QCD. In the following, a few particularly successful approaches are presented.

Effective theories, e.g. chiral perturbation theory [Wei67a, Wei68], obey the relevant symmetries of the QCD Lagrangian and describe the physically realized DoF, namely hadrons. Imposing a rigorous power counting scheme on all possible terms consistent with the symmetries gives excellent control over the relevance of the considered terms, in particular, it allows to distinguish leading order contributions from negligible higher order terms. Calculation of observables in these theories rely on the numerical values of particle masses and couplings, so-called low-energy constants, as input parameters which are to be fitted from experimental data or derived from the underlying theory.

Lattice QCD ( $\ell$ QCD) [Wil74] aims for numerically solving QCD by literal evaluation of path integrals on a finite, periodic, Euclidean space-time grid with finite lattice spacing  $a$ . To obtain comparable results, a fit of intermediate data to observables fixing intrinsic parameters and to perturbative results in the continuum limit  $a \rightarrow 0$  is in order. While  $\ell$ QCD is limitedly suitable to disclose the intrinsic mechanisms of QCD, it has already proved to be a very successful tool for particle spectroscopy, despite some issues with the treatment of Goldstone bosons and hadrons in a strongly interacting environment characterized by finite chemical potentials.

The Dyson-Schwinger–Bethe-Salpeter approach based on the pioneering works [Dys49, Sch51b, Sal51] can be also applied to quark–anti-quark bound states providing their masses and decay constants [Mun92]. Infinitely many coupled integral equations describe the bound state by virtue of dressed quark and gluon propagators and a relativistic Bethe-Salpeter interaction kernel. A truncation of the iteratively generated integral equations has to be performed in order to obtain a feasible numerical approach. The hierarchy of contributions beyond standard truncation schemes, e.g. rainbow-ladder approximation, w.r.t. their numerical impact is a recent matter of debate as well as different interaction models entering the Bethe-Salpeter kernel. There are many further attempts to extract the low-energy dynamics of strongly interacting matter availing, e.g., current algebra, resummation and renormalization group techniques, AdS/CFT correspondence, potential models, bag models as well as instanton models.

Among the analytic approaches with intimate contact to QCD are QCD sum rules (QSRs) which are pursued in this thesis. Introduced by Shifman, Vainshtein and Zakharov [Shi79] they proved particularly successful in deducing spectral properties of low-lying hadronic resonances. QSRs connect QCD with phenomenology, i.e. quark DoF are linked to hadronic DoF, by means of a dispersion relation of the current-current correlator. The dispersion relation can be derived from Cauchy's formula and the analytic properties of the correlator. It builds a bridge between the low-energy spectrum of the considered current and the cor-

relator at deep Euclidean momenta, where perturbative methods are applicable. Thereby, integrated spectral properties are linked to QCD ground state expectation values of quark and gluon operators, the celebrated condensates. An infinite tower of such condensates characterizes the highly non-trivial QCD ground state, as they quantify the interaction of quarks and gluons with the vacuum. Particular condensates, e. g. the famous chiral condensate  $\langle \bar{q}q \rangle$ , can serve as essential parts of order parameters of chiral symmetry and are therefore integral to the understanding of the mass generating mechanism of QCD.

The conceptional strength of QSRs is apparent, inter alia, in the generalization of the framework to in-medium situations [Boc86]. Due to the separation of scales, finite temperature and/or baryon density effects on hadronic spectra by virtue of a strongly interacting environment can be comprehensively traced back to numerically changing condensates in low-temperature and -density approximations. The temperature and density dependence of condensates can be deduced model independently by evaluation of the Gibbs averages of the respective quark and gluon operators. The determination of their medium behavior from QSRs, where always a combination of condensates enter, is more involved. However, the limitations in extracting individual condensates, e. g. a particular order parameter, from channel-specific QSRs can be circumvented by Weinberg sum rules (WSRs) [Wei67b] which are sensitive to individual chirally odd condensates being potential order parameters of chiral symmetry. Thus, WSRs are a valuable tool to study chiral dynamics by means of testable implications of changing chirally odd condensate on chiral partner meson spectra.

### 1.3 Structure of the thesis

In this thesis, QSRs are utilized to determine medium modifications of the spectral properties of heavy-light mesons, in particular D mesons. A careful foundation of the QSR framework with emphasis on its generalization to medium situations is provided in Chap. 2 ensuring the correct applications of the operator product expansion (OPE) machinery to higher order condensate contributions. Thereby, current discussions on the meaning of condensates and different QSR evaluation strategies are reviewed. Chapter 3 is devoted to the calculation of light four-quark condensate contributions to the pseudo-scalar D meson OPE in nuclear matter, motivated by their large numerical impact to the  $\rho$  meson sum rule and their crucial role as potential order parameters of chiral symmetry. For the interested reader, many of the intricate details of the in-medium computation are made available in App. C. Chiral symmetry aspects of open charm mesons in a heat bath are presented in Chap. 4. Channel-specific as well as chiral partner sum rules of pseudo-scalar and scalar D mesons are evaluated at finite temperatures to test heavy-light mesons as probes of chiral symmetry restoration assumed at high temperatures. The notion of chiral symmetry presented in App. B is a prerequisite to this analysis. The key results of this work are summarized and discussed in Chap. 5 supplemented by an outlook focusing on a promising QSR evaluation method as well as on critical aspects of low-energy QCD, e. g. the value of the QSR framework and its beneficial contribution to modern hadron physics. Appendix A recalls basics of (classical) chromodynamics in order to clarify the notation used throughout this thesis, while Apps. D and E describe techniques improving the reliability of QSR results.

In the course of elaborating this thesis, the following publications have been written (in chronological order):

- (i) T. BUCHHEIM, T. HILGER and B. KÄMPFER: *In-medium QCD sum rules for D mesons: A projection method for higher order contributions*, J. Phys. Conf. Ser. **503**, 012006 (2014).
- (ii) T. BUCHHEIM, T. HILGER and B. KÄMPFER: *Heavy-quark expansion for D and B mesons in nuclear matter*, EPJ Web Conf. **81**, 05007 (2014).
- (iii) T. BUCHHEIM, T. HILGER and B. KÄMPFER: *Defining medium-specific condensates in QCD sum rules for D and B mesons*, Nucl. Part. Phys. Proc. **258-259**, 213 (2015).
- (iv) T. BUCHHEIM, T. HILGER and B. KÄMPFER: *Wilson coefficients and four-quark condensates in QCD sum rules for medium modifications of D mesons*, Phys. Rev. C **91**, 015205 (2015).
- (v) T. BUCHHEIM, T. HILGER and B. KÄMPFER: *Chiral symmetry aspects in the open charm sector*, J. Phys. Conf. Ser. **668**, 012047 (2016).
- (vi) T. BUCHHEIM, B. KÄMPFER and T. HILGER: *Algebraic vacuum limits of QCD condensates from in-medium projections of Lorentz tensors*, J. Phys. G **43**, 055105 (2016).



## 2 QCD sum rules

The conceptional ideas and the theoretical foundation of QSRs were introduced by Shifman, Vainshtein and Zakharov (SVZ) providing a systematic study of non-perturbative effects in QCD [Shi79] which circumvent complications arising for this non-Abelian gauge theory in the low-energy regime. Originally applied to resonances of vector mesons in vacuum the ideas and notions of the QSR framework have been extended to allow for a description of baryons [Iof81], and more recently, also tetra- and penta-quark systems [Lat85, Zhu03]. Also further hadronic properties are accessible, e.g. form factors [Nes82] and hadronic coupling constants [Rei83], inter alia, utilizing light-cone sum rules [Bal89, Bra89, Che90]. The valuable generalization of the scope of the QSR framework to cover single hadrons in a strongly interacting medium at finite temperatures [Boc86, Hat93] and net-baryon densities [Fur92] enables an understanding of recent and envisaged experimental results.<sup>1</sup>

The introduction to QSRs in this chapter builds on the original articles [Shi79, Boc86, Fur92, Hat93] and is also based on reviews [Rei85, Col01], textbooks [Pas84, Nar07] and more detailed papers [Nov84, Jin93, Gro95] dedicated to different technical aspects of the framework.

### 2.1 Current-current correlator

In the framework of QSRs phenomenological hadronic properties are connected to QCD parameters. By virtue of a dispersion relation (see below) the causal current-current correlator

$$\Pi(q) = i \int d^4x e^{iqx} \langle \Omega | T [J(x) J^\dagger(0)] | \Omega \rangle \quad (2.1)$$

can be evaluated in a twofold way, where the short-range effects of quarks and gluons are linked to the long-range effects of hadrons. The two-point function (2.1) is defined as the Fourier transform of the time-ordered expectation value (EV) of the interpolating currents  $J$  and  $J^\dagger$ . They are formed by quark and/or gluon operators in the Heisenberg representation reflecting the partonic content and quantum numbers, e.g. parity and spin, of the hadron under consideration. The QCD ground state  $|\Omega\rangle$  differs from the vacuum of the free theory  $|0\rangle$ , in particular  $a|\Omega\rangle \neq 0$  with  $a$  being an annihilation operator of the free theory.<sup>2</sup>

Although the vacuum ground state  $|\Omega\rangle$  must be understood as a non-perturbative ground state it is defined to satisfy  $E_\Omega = 0$ , and hadrons as excitations of that ground state thus have an energy equal to their mass in the rest frame. The QCD ground state is Lorentz invariant and invariant under parity and time reversal transformations. While the QCD ground state is not translational invariant, but acquires a phase factor when the translation

---

<sup>1</sup>Attempts are recently pursued in order to include effects of high magnetic fields into the framework [Mac14, Cho15] which may occur in ultra-peripheral heavy-ion collisions.

<sup>2</sup>In the Lagrangian of the 'free theory', interaction terms are absent.

operator is applied, EVs in this state are invariant under space-time translations as the phase factors cancel each other.

The Gell-Mann–Low formula [Pas84, Ste93] connects EVs of Heisenberg operators, evaluated with the interacting states of the full theory, with EVs of operators in the interaction representation, evaluated with states of the free theory [GM51]. For the relevant two-point function one obtains

$$\langle \Omega | T \left[ J(x) J^\dagger(0) \right] | \Omega \rangle = \frac{\langle 0 | T \left[ j(x) j^\dagger(0) e^{i \int d^4 y \mathcal{L}_{\text{int}}(y)} \right] | 0 \rangle}{\langle 0 | T \left[ e^{i \int d^4 y \mathcal{L}_{\text{int}}(y)} \right] | 0 \rangle}, \quad (2.2)$$

where  $\mathcal{L}_{\text{int}}$  (A.15) is the interaction term of the Lagrangian comprising free fields. Whenever the coupling  $g$  in  $\mathcal{L}_{\text{int}}$  obeys  $g \ll 1$ , a series expansion of the operator-valued exponentials is a suitable starting point for a perturbative evaluation.

The current-current correlator (2.1) uncovers two particularly important regimes: (i) for large space-like momenta, it represents the short-range quark–anti-quark fluctuations, perturbatively assessable, whereas (ii) long-range hadronic properties are encoded for positive momenta  $q^2 > 0$ . For instance, the correlator of the vector meson current  $j_V = \bar{q} \gamma_\mu q$  can be linked to the hadron production cross section  $\sigma$  in  $e^+ e^-$  annihilation via [Rei85]

$$\text{Im} \Pi(q^2) = \frac{9}{64\pi^2 \alpha^2} q^2 \sigma(e^+ e^- \rightarrow \text{hadrons}), \quad (2.3)$$

where  $\alpha = e^2/(4\pi)$  is the quantum electrodynamics (QED) fine structure constant. This formula already discloses a severe restriction to the interpretation of QSR results. The phenomenological information provided by Eq. (2.3) is not unique to one specific vector meson, but the cross section includes the complete spectrum of hadrons, and even multi-particle excitation, with the quantum numbers of the considered vector meson. This becomes obvious from explicitly writing out the time-ordering in Eq. (2.1) employing the integral representation of the Heaviside function (and intermediate insertion of a complete set of hadronic states) which leads to the Källén-Lehmann representation [Käl52, Leh54] of the correlator

$$\Pi(q) = - \int d\omega \left( \frac{\rho(\omega, \vec{q})}{q_0 - \omega + i\epsilon} - \frac{\tilde{\rho}(\omega, \vec{q})}{q_0 - \omega - i\epsilon} \right) \quad (2.4)$$

with independent spectral densities

$$\rho(p) = \frac{1}{2\pi} \int d^4 x e^{ipx} \langle \Omega | j(x) j^\dagger(0) | \Omega \rangle, \quad (2.5)$$

$$\tilde{\rho}(p) = \frac{1}{2\pi} \int d^4 x e^{ipx} \langle \Omega | j^\dagger(0) j(x) | \Omega \rangle \quad (2.6)$$

for particles ( $\rho$ ) and anti-particles ( $\tilde{\rho}$ ). However, in vacuum (due to the assumed symmetries of the QCD ground state) or for self-adjoint particles (e.g. the  $\rho^0$  meson) with  $\tilde{\rho}(\omega) = -\rho(-\omega)$  the correlator reads

$$\Pi(q) = \int_0^\infty ds \frac{\rho(s)}{s - q^2}. \quad (2.7)$$

Insertion of a complete set of hadronic states  $\{|h\rangle\}$  into the definition (2.5) of the spectral density

$$\rho(p) = (2\pi)^3 \sum_h \delta^{(4)}(p - (p_h - p_\Omega)) \langle \Omega | j(0) | h \rangle \langle h | j^\dagger(0) | \Omega \rangle \quad (2.8)$$

reveals that all hadronic states  $|h\rangle$  with the quantum numbers of the considered current, i. e.  $\langle \Omega | j(0) | h \rangle \neq 0$ , contribute to the spectral density (and thus to the correlator). In Eq. (2.8),  $p_\Omega$  ( $p_h$ ) denotes the eigen value of the momentum operator applied to the QCD ground state  $|\Omega\rangle$  (hadronic state  $|h\rangle$ ). In vacuum one can choose  $p_\Omega = 0$  due to Lorentz invariance of the QCD ground state.

In a strongly interacting environment characterized by a medium velocity  $v_\mu$  and some intensive thermodynamic properties, the current product of the correlator (2.1) is not evaluated with the QCD ground state  $|\Omega\rangle$ , but it is Gibbs averaged, i. e. the substitution [Boc86]

$$\langle \Omega | \cdots | \Omega \rangle \longrightarrow \langle\langle \cdots \rangle\rangle = \frac{1}{Z} \text{Tr} \left[ \cdots e^{-(H-\mu N)/T} \right] \quad (2.9)$$

is required to generalize the correlator to cover in-medium situations.<sup>3</sup> The quantity  $Z = \text{Tr}[e^{-(H-\mu N)/T}]$  is the grand-canonical partition function, where  $H$  denotes the QCD Hamiltonian operator (emerging from Lagrangian (A.1)),  $T$  is the temperature of the system,  $N$  symbolizes some additive quantum number, e. g. baryon number, strangeness, etc., and  $\mu$  is the corresponding chemical potential. The trace represents the summation over complete sets of states to any particle number (baryon number, strangeness, etc.)  $N$ . As the presence of the strongly interacting medium breaks Lorentz invariance, the correlator depends on  $q_0$  and  $\vec{q}$  separately. Generalized formulae for the Källén-Lehmann representation (2.4) of the Gibbs averaged causal correlator (2.1) as well as retarded and advanced correlators are presented in [Neg88].

The in-medium ground state is understood as a many-particle state. In contrast to the vacuum QCD ground state, it is only assumed to be invariant under parity and time reversal transformations in its local rest frame and it is not invariant under all Lorentz transformations [Fur92]. However, EVs calculated in this state, e. g. the current-current correlator (2.1), do have well defined Lorentz transformation properties. The new feature in the medium is the additional four-vector  $v_\mu$  that must be transformed when making the comparison of observables in different reference frames and must be included when building tensors or identifying invariant functions [Fur92]. Analogous to the QCD ground state EV, translational invariance is assumed for the Gibbs average, i. e.  $\langle\langle O(x) \rangle\rangle = \langle\langle O(x+a) \rangle\rangle$  for arbitrary operators  $O$  [Jin93].

### 2.1.1 Vacuum dispersion relation

On grounds of analyticity a dispersion relation can be derived connecting the current-current correlator (2.1), expressed in QCD DoF for deep-Euclidean momenta, to the hadronic sum in Eq. (2.8) at physical momenta. Assuming analyticity of the correlator  $\Pi(q^2)$  within the

<sup>3</sup>In subsequent parts of this work, where vacuum and in-medium ground state EVs are not distinguished explicitly, the common symbol  $\langle \cdots \rangle$  is used.

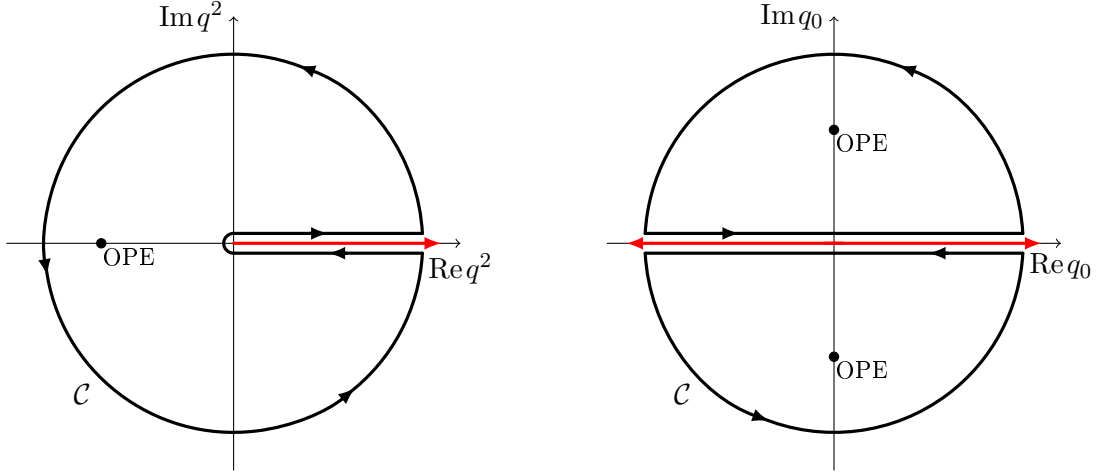


**Figure 2.1:** The integration contours  $\mathcal{C}$  for a derivation of the dispersion relations in vacuum (left panel) and in medium (right panel) using Cauchy's integral theorem. The operator product expansion (OPE) is employed at bold dots either in the complex momentum  $q^2$  plane (left) or complex energy  $q_0$  plane at fixed  $\vec{q}$  (right), respectively. Red lines indicate positions of hadronic poles and cuts of the correlator along the real axis.

contour  $\mathcal{C}$ , where the poles of the correlator along the positive real axis are excluded, cf. left panel of Fig. 2.1, Cauchy's integral theorem is applicable, i. e.

$$\Pi(q^2) = \frac{1}{2\pi i} \oint_{\mathcal{C}} ds \frac{\Pi(s)}{s - q^2} \quad (2.10)$$

$$= \frac{1}{2\pi i} \oint_{|s|=R} ds \frac{\Pi(s)}{s - q^2} + \frac{1}{2\pi i} \int_{0^+}^R ds \frac{\Pi(s + i\epsilon) - \Pi(s - i\epsilon)}{s - q^2}. \quad (2.11)$$

The integration contour of the second integral in Eq. (2.11) runs on both sides along the positive real axis with  $\epsilon > 0$ . Thus, the Schwarz reflection principle  $\Pi(z^*) = \Pi^*(z)$  can be applied to the discontinuity

$$\Delta\Pi(s) = \frac{1}{2i} \lim_{\epsilon \rightarrow 0} [\Pi(s + i\epsilon) - \Pi(s - i\epsilon)] \quad (2.12)$$

and one can identify the spectral density by comparing with the Källén-Lehmann representation (2.7) of the correlator, i. e.

$$\Delta\Pi(s) = \text{Im}\Pi(s) = \pi\rho(s). \quad (2.13)$$

The first integral in Eq. (2.11) over the circle with radius  $R$  vanishes, if the current-current correlator on this circle for  $R \rightarrow \infty$  decreases sufficiently rapidly, i. e.  $\lim_{|s| \rightarrow \infty} \Pi(s) \propto 1/|s|^\eta$  is satisfied for arbitrary  $\eta > 0$ . The resulting dispersion relation

$$\Pi(q^2) = \frac{1}{\pi} \int_0^\infty ds \frac{\text{Im}\Pi(s)}{s - q^2} \quad (2.14)$$



as one possible representation of the correlator (2.1) is the starting point of a QSR analysis in vacuum [Shi79]. Another representation of the correlator (2.1) in terms of quark and gluon DoF utilizes the OPE, which is presented in Sec. 2.2.

If the integrand in the first integral in Eq. (2.11) does not decrease rapidly enough for  $|q^2| \rightarrow \infty$ , as required in the derivation of Eq. (2.14), the integral along the circle  $R$  does not vanish, but converges to a finite-degree polynomial instead [Sug61]. Assuming  $|\Pi(s)| \leq |s|^N$  for  $s \rightarrow \infty$  with  $N \in \mathbb{N}$  a finite fixed integer and  $R \rightarrow \infty$  one can prove this statement. As  $|q^2| < |s|$ , if  $s$  is on the circle, the integrand can be expanded in a geometric series. If  $\Pi(s)$  obeys the above assumption the power series in  $q^2/s$  breaks down at the power  $N$ . Thus, in such a case the vacuum dispersion relation reads

$$\Pi(q^2) = \frac{1}{\pi} \int_0^\infty ds \frac{\text{Im}\Pi(s)}{s - q^2} + \sum_{n=0}^N a_n q^{2n}, \quad (2.15)$$

instead of (2.14), with  $a_n = \frac{1}{2\pi} \lim_{|s| \rightarrow \infty} \int_0^{2\pi} d\varphi \Pi(s)/s^n$ . For clarity, one may point out that the coefficients  $a_n$  are not proportional to derivatives of  $\Pi(s)$  at  $s = 0$  which enter the forthcoming subtracted dispersion relation. The  $(N + 1)$ -th derivative with respect to  $q^2$  of Eq. (2.15) eliminates the polynomial.

If  $\Pi(q^2)$  is analytic in the vicinity of the origin a further approach to the dispersion relation is feasible leading to so-called subtraction terms but circumvents polynomials from the integral over the circle with radius  $R$ . If the lower limit of the integral along the positive real axis is a finite value  $s_0$ , which may be regarded as the energy squared of the first resonance of the spectral density, this approach can be pursued. Subtracting on both sides of Eq. (2.10) the Taylor polynomial of the correlator around the origin up to the power of  $N - 1$ ,

$$\Pi(q^2) - \sum_{n=0}^{N-1} \frac{\Pi^{(n)}(s)|_{s=0}}{n!} q^{2n} = \frac{1}{2\pi i} \oint_C ds \frac{\Pi(s)}{s - q^2} - \sum_{n=0}^{N-1} \frac{q^{2n}}{2\pi i} \oint_C ds \frac{\Pi(s)}{s^{n+1}}, \quad (2.16)$$

the assumption leading to the polynomial in Eq. (2.15) yields the  $N$ -fold subtracted dispersion relation in vacuum

$$\Pi(q^2) - \sum_{n=0}^{N-1} \frac{\Pi^{(n)}(s)|_{s=0}}{n!} q^{2n} = \frac{1}{\pi} \int_{s_0}^\infty ds \left( \frac{q^2}{s} \right)^N \frac{\text{Im}\Pi(s)}{s - q^2}, \quad (2.17)$$

where  $\Pi^{(n)}(s)|_{s=0}$  denotes the  $n$ -th derivative of the current-current correlator evaluated at the origin. The  $N$  terms of the polynomial in powers of  $q^2$  on the l. h. s. of Eq. (2.17), i. e. the terms of the sum, are dubbed subtraction terms.

### 2.1.2 Medium dispersion relation

The medium dispersion relation differs from that in vacuum. Due to the presence of the medium, represented by the medium velocity  $v_\mu$ , Lorentz invariance is broken and the current-current correlator does not solely depend on the outer hadron momentum  $q^2$ , but becomes a function of all possible scalar products of  $q_\mu$  and  $v_\mu$ , i. e.  $\Pi(q, v) = \Pi(q^2, v^2, vq)$ .

In the rest frame of the medium the correlator is a function of  $q_0$  and  $\vec{q}$ , i.e.  $\Pi(q_0, \vec{q})$  and one can make no further restrictions to the pole structure. In contrast to the vacuum, the correlator exhibits now poles along the complete energy axis [Fur92] and the desired dispersion relation must be derived on the complex energy plane rather than on the  $q^2$  plane. As the OPE building on perturbative methods is valid for large space-like momenta only, the correlator must be continued analytically for imaginary values of  $q_0$  performing a Wick rotation. For  $q_0 = iq'_0$  with  $q'_0 \in \mathbb{R}$ , the requirement  $q^2 < 0$  is satisfied.

Analogously to the derivation in vacuum, Cauchy's integral theorem

$$\Pi(q_0, \vec{q}) = \frac{1}{2\pi i} \oint_{\mathcal{C}} d\omega \frac{\Pi(\omega, \vec{q})}{\omega - q_0} \quad (2.18)$$

is applied to the integration contour  $\mathcal{C}$  in the right panel of Fig. 2.1 for fixed  $\vec{q}$ . The in-medium correlator can be decomposed into an even and odd part with respect to the hadron energy  $q_0$ :

$$\Pi(q_0, \vec{q}) = \Pi^{\text{even}}(q_0, \vec{q}) + q_0 \Pi^{\text{odd}}(q_0, \vec{q}) \quad (2.19)$$

with

$$\Pi^{\text{even}}(q_0, \vec{q}) = \frac{1}{2} [\Pi(q_0, \vec{q}) + \Pi(-q_0, \vec{q})] = \Pi^{\text{even}}(-q_0, \vec{q}), \quad (2.20a)$$

$$\Pi^{\text{odd}}(q_0, \vec{q}) = \frac{1}{2q_0} [\Pi(q_0, \vec{q}) - \Pi(-q_0, \vec{q})] = \Pi^{\text{odd}}(-q_0, \vec{q}). \quad (2.20b)$$

Provided that the discontinuity is restricted to the real axis, i.e.

$$\Delta \Pi(\omega, \vec{q}) = \frac{1}{2i} \lim_{\epsilon \rightarrow 0} [\Pi(\omega + i\epsilon, \vec{q}) - \Pi(\omega - i\epsilon, \vec{q})] = \text{Im} \Pi(\omega, \vec{q}), \quad (2.21)$$

the  $N$ -fold subtracted dispersion relation in medium of the even part takes the form

$$\begin{aligned} \Pi^{\text{even}}(q_0, \vec{q}) &= \frac{1}{2} \sum_{n=0}^{N-1} \frac{\Pi^{(n)}(\omega, \vec{q})|_{\omega=0}}{n!} (q_0)^n [1 + (-1)^n] \\ &= \frac{1}{2\pi} \int_{-\infty}^{\infty} d\omega \text{Im} \Pi(\omega, \vec{q}) \frac{q_0^N}{\omega^{N-1}} \frac{[1 + (-1)^N] + \frac{q_0}{\omega} [1 - (-1)^N]}{\omega^2 - q_0^2} \end{aligned} \quad (2.22)$$

and for the odd part it reads

$$\begin{aligned} \Pi^{\text{odd}}(q_0, \vec{q}) &= \frac{1}{2} \sum_{n=0}^{N-1} \frac{\Pi^{(n)}(\omega, \vec{q})|_{\omega=0}}{n!} (q_0)^{n-1} [1 - (-1)^n] \\ &= \frac{1}{2\pi} \int_{-\infty}^{\infty} d\omega \text{Im} \Pi(\omega, \vec{q}) \frac{q_0^{N-1}}{\omega^{N-1}} \frac{[1 - (-1)^N] + \frac{q_0}{\omega} [1 + (-1)^N]}{\omega^2 - q_0^2}. \end{aligned} \quad (2.23)$$

## 2.2 Operator product expansion

Utilizing Wilson's operator product expansion (OPE) the correlator is linked to the quark and gluon DoF [Wil69]. As hadrons are the relevant DoF of the strong interaction theory for low energies, whereas quarks can be resolved for large momentum transfer only, an expansion based on quark DoF is valid, intuitively, only for large outer momenta. The proof of the validity of the OPE is based on Feynman diagram techniques and is rigorously proven only for perturbation theory [Shi79]. Following Wilson, an operator product can be expanded into an asymptotic series of complex functions  $\tilde{C}_n$  and local operators  $O_n$  for short distances  $x - y$ :

$$A(x)B(y) = \sum_n \tilde{C}_n(x - y)O_n. \quad (2.24)$$

The Wilson coefficients  $\tilde{C}_n(x - y)$  are singular for  $x \rightarrow y$ . The full expansion features an infinite number of local operators  $O_n$  sorted by the degree of singularity rising with index  $n$ . Due to the constant mass dimension of the operator product  $A(x)B(y)$  the operators on the r. h. s. of Eq. (2.24) may be sorted by their mass dimension accordingly, where the sum runs over all products of operators in the theory under consideration. Apart from the perturbative contribution with  $O_n = \mathbb{1}$  ( $\dim_m = 0$ ) all possible products of the available operators in QCD, i. e. gauge covariant derivative  $D_\mu$  ( $\dim_m = 1$ ), quark operator  $q$  ( $\dim_m = 3/2$ ) and gauge field strength tensor  $G_{\mu\nu}$  ( $\dim_m = 2$ ) (Dirac, flavor and color indices are not displayed here), form local operators  $O_n$  with increasing mass dimension entering the expansion.

In momentum space the OPE reads

$$\int d^4x e^{iq(x-y)} A(x)B(y) = \sum_n C_n(q)O_n \quad (2.25)$$

with  $C_n \propto q^{-n+m}$ , where  $m$  is a constant value depending on the mass dimension of the operator product  $A(x)B(y)$ . Due to the polynomial structure of the Wilson coefficients the terms of the series (2.25) beyond the perturbative contribution are dubbed power corrections. As the series (2.25) is an expansion on operator level the complex valued Wilson coefficient do not depend on the state used to evaluate the operator product. In particular, the coefficients are not altered whether the OPE is evaluated in vacuum or medium. Despite further medium-specific condensates and associated Wilson coefficients entering the OPE for finite temperatures and/or baryon densities, the Wilson coefficients of the vacuum-specific condensates at low temperatures are (approximately) equal to the Wilson coefficients of these condensates in vacuum.<sup>4</sup> Wilson coefficients can be calculated utilizing the background field expansion in Fock-Schwinger gauge outlined in Subsec. 2.2.1 or further approaches, e. g. the plane wave method [Rei85, Bag94].

The evaluation of the current-current correlator (2.1) comprises the EV of the time-ordered operator product of the expansion (2.25) with  $A(x) = j(x)$  and  $B(y = 0) = j^\dagger(0)$ , i. e.

$$\Pi(q) = \sum_n C_n(q) \langle \Omega | O_n | \Omega \rangle. \quad (2.26)$$

---

<sup>4</sup>The notions of vacuum- and medium-specific condensates and its relevance for in-medium QSRs are explained in detail in App. C.2.

The quantity  $\langle \Omega | O_n | \Omega \rangle$  is referred to as a QCD condensate. If the OPE is calculated in perturbation theory solely the EV of the unit operator contributes, because all further EVs vanish. To account for non-perturbative effects also the EVs of higher mass dimension operators must not vanish. Due to the QCD ground state  $|\Omega\rangle$  the EVs of the operators  $O_n$  give finite results. Thus, non-perturbative effects are absorbed into condensates, whereas the Wilson coefficients contain the perturbative part. To ensure separation of long-range from short-range effects the introduction of a scale  $\mu$  is mandatory. The separation of scales is necessary for loop corrections, where small momentum contributions to the momentum integrals lead to Wilson coefficients which contain long-range effects. This requires the redefinition of condensates [Col01]. Therefore, the 'practical OPE' is introduced in [Shi98]. At finite loop order and with condensates up to a fixed mass dimension the separation of scales is achieved by a redefinition of the condensates.

If the OPE of a Gibbs averaged current-current correlator is performed, Gibbs averaged operators  $\langle\langle O_n \rangle\rangle$  will enter. As the QCD ground state is the lowest energy contribution to the trace in Eq. (2.9), the deviation of the numerical values of a Gibbs averaged operator  $\langle\langle O_n \rangle\rangle$  from its ground state EV  $\langle \Omega | O_n | \Omega \rangle$  grows for increasing intensive thermodynamic quantities of the system, e. g. temperature or baryon density, while their values coincide for vanishing thermodynamic parameters. The meaning of condensates beyond their role in an OPE, where they absorb the non-perturbative phenomena, and further details on in-medium condensates are presented in Sec. 2.3.

If the separation of scales is verified, perturbative methods can be utilized for actual calculations. Evaluation of the current-current correlator (2.1) in the deep-Euclidean region  $q^2 \ll 0$  allows for the application of Wick's theorem, which is based on the decomposition of field operators into positive and negative frequency parts with associated annihilation and creation operators. While such a Fourier decomposition is common for free field operators, it is impossible for interacting operators in the Heisenberg representation. However, the operators in the interaction representation of perturbation theory satisfy the equations of motion (EoMs) of the free theory enabling a decomposition similar to free fields. In this regard, Wick's theorem is a perturbative method [Rom69]. For a time-ordered product of  $n$  operators one has [Pes95]

$$\begin{aligned} T [\phi_1(x_1)\phi_2(x_2)\cdots\phi_n(x_n)] &= : \phi_1(x_1)\phi_2(x_2)\cdots\phi_n(x_n) : \\ &+ : \text{all possible contractions} :, \end{aligned} \quad (2.27)$$

where a contraction ' $\frown$ ' is defined by

$$\underbrace{\phi_1(x_1)\phi_2(x_2)} = \langle 0 | T [\phi_1(x_1)\phi_2(x_2)] | 0 \rangle \quad (2.28)$$

and ' $: \cdots :$ ' denotes normal-ordering, i. e. within the colons all annihilation operators are grouped to the right of creation operators. If Wick's theorem is applied to the vacuum EV of operators, the normal-ordered terms will vanish due to the definition of normal-ordering, in particular:  $\langle 0 | :(\text{odd number of operators}) : | 0 \rangle = 0$ . Thus, solely fully contracted terms remain. These considerations apply to the ground state  $|0\rangle$  of the free theory, due to  $a|0\rangle = 0$ , but do not apply the QCD ground state  $|\Omega\rangle$ . Hence, Wick-uncontracted operators sandwiched between QCD ground states can have non-zero values forming the celebrated condensates.

### 2.2.1 Background field expansion in Fock-Schwinger gauge

The correlators of color neutral currents considered in this thesis are gauge invariant [Nov84]. That is, every particular gauge condition on the gluonic background field yields the same results and, thus, can be chosen appropriately. The Fock-Schwinger gauge

$$(x^\mu - x_0^\mu)A_\mu(x) = 0, \quad (2.29)$$

independently introduced by Fock [Foc37] and Schwinger [Sch51a] in the framework of QED, is suitable for the OPE of current-current correlators. The SVZ sum rules widened the application of the gauge (2.29) introducing it to QCD calculations, because it allows for a compact formulation of quark and gluon propagators. The calculus presented in this section is derived from [Nov84, Pas84]. Usually, one chooses  $x_0^\mu = 0$ . Although the gauge condition (2.29) is scale independent as well as has an independence under parity and time reversal transformations it breaks translation symmetry. However, the cancellation of the  $x_0$  dependence in the calculation is supported by arguments in [Nov84].

The Fock-Schwinger gauge implies the relation

$$A_\mu(x) = \int_0^1 d\alpha \alpha x^\nu G_{\nu\mu}(\alpha x) \quad (2.30)$$

which connects the gluonic background field potential  $A_\mu$  to its field strength tensor  $G_{\nu\mu}$ . Furthermore, in the Taylor expansion of arbitrary fields

$$\phi(x) = \sum_{n=0}^{\infty} \frac{1}{n!} x^{\alpha_1} \dots x^{\alpha_n} (\partial_{\alpha_1} \dots \partial_{\alpha_n} \phi)_{x=0} \quad (2.31)$$

it allows for a substitution of the partial derivatives  $\partial_{\alpha_i} = \partial/\partial x_{\alpha_i}$  by covariant derivatives  $D_{\alpha_i}(x) = \partial_{\alpha_i} - igA_{\alpha_i}(x)$ :

$$x^{\alpha_1} \dots x^{\alpha_n} (\partial_{\alpha_1} \dots \partial_{\alpha_n} \phi)_{x=0} = x^{\alpha_1} \dots x^{\alpha_n} (D_{\alpha_1} \dots D_{\alpha_n} \phi)_{x=0}. \quad (2.32)$$

Expanding the field strength tensor  $G_{\nu\mu}$  in Eq. (2.30) at the origin using Eq. (2.32) with  $\phi = G_{\nu\mu}$  yields

$$A_\mu(x) = \int_0^1 d\alpha \alpha x^\nu \sum_{n=0}^{\infty} \frac{\alpha^n}{n!} x^{\alpha_1} \dots x^{\alpha_n} (D_{\alpha_1} \dots D_{\alpha_n} G_{\nu\mu})_{x=0} \quad (2.33)$$

$$= \sum_{n=0}^{\infty} \frac{1}{n!(n+2)} x^\nu x^{\alpha_1} \dots x^{\alpha_n} (D_{\alpha_1} \dots D_{\alpha_n} G_{\nu\mu})_{x=0}, \quad (2.34)$$

i.e. the covariant expansion of the gluon field in terms of the gluon field strength tensor. Analogously, within the Fock-Schwinger gauge one obtains the covariant expansion of fermion field operators by substituting  $\phi$  with  $\psi$  or its adjoint  $\bar{\psi}$  in Eq. (2.31):

$$\psi(x) = \sum_{n=0}^{\infty} \frac{1}{n!} x^{\alpha_1} \dots x^{\alpha_n} (D_{\alpha_1} \dots D_{\alpha_n} \psi)_{x=0}, \quad (2.35a)$$

$$\bar{\psi}(x) = \sum_{n=0}^{\infty} \frac{1}{n!} x^{\alpha_1} \dots x^{\alpha_n} (\bar{\psi} \overleftarrow{D}_{\alpha_1} \dots \overleftarrow{D}_{\alpha_n})_{x=0}. \quad (2.35b)$$

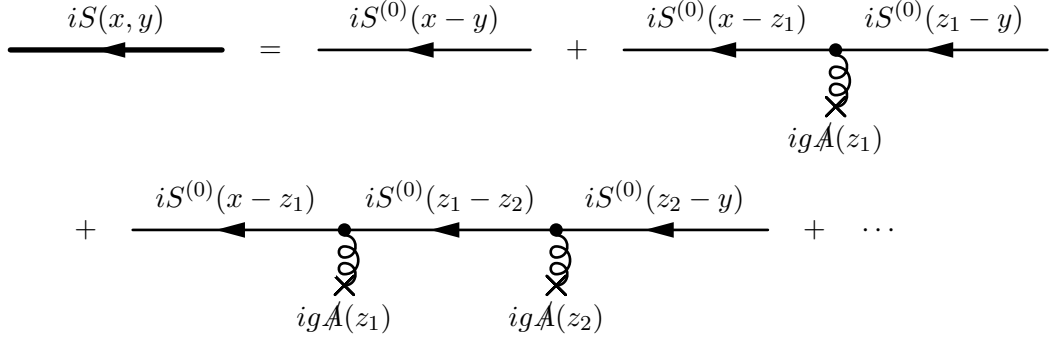


**Figure 2.2:** Diagrammatic representation of the perturbative quark propagator  $S$  (thick solid line) in a classical, weak, gluonic background field yielding a series of the free quark propagator  $S^{(0)}$  (thin solid lines) coupled via soft-gluon exchange (curly lines) to the background (crosses). The vertices originate from the interaction Lagrangian.

The background field method is utilized to model non-perturbative effects of the vacuum and the medium. The quark propagator  $S(x, y) = -i\langle T[q(x)\bar{q}(y)] \rangle$ , emerging from Wick's theorem, does not describe free propagation but the propagation of the quark in a classical, weak, gluonic background field  $A_\mu$ . This propagator is dubbed perturbative propagator throughout this thesis; it satisfies the relations

$$\left[ i\not{D}(z) - m_q \right] S(z, y) = \left[ i\not{\partial}_z + gA(z) - m_q \right] S(z, y) = \delta^{(4)}(z - y). \quad (2.36)$$

Provided the impact of the background field via  $gA_\mu$  is a small perturbation,  $S(z, y)$  can be expanded in an asymptotic series [Itz80, Nov84]. The derivation employs the free quark propagator  $iS^{(0)}(x, z) = iS^{(0)}(x - z)$ , which fulfills

$$S^{(0)}(x - z) \left[ -i\overleftarrow{\not{\partial}}_z - m_q \right] = \delta^{(4)}(x - z), \quad (2.37)$$

to obtain the implicit integral equation of the perturbative propagator

$$iS(x, y) = iS^{(0)}(x - y) + \int d^4z \, iS^{(0)}(x - z) igA(z) iS(z, y). \quad (2.38)$$

An iterative expansion of Eq. (2.38) yields

$$\begin{aligned} iS(x, y) &= iS^{(0)}(x - y) \\ &+ \sum_{n=1}^{\infty} \int d^4z_1 \cdots d^4z_n \, iS^{(0)}(x - z_1) igA(z_1) iS^{(0)}(z_1 - z_2) \cdots igA(z_n) iS^{(0)}(z_n - y). \end{aligned} \quad (2.39)$$

The diagrammatic interpretation of the first three terms of this expansion is illustrated in Fig. 2.2. Due to the gauge condition (2.29) the perturbative quark propagator (2.39) does not exhibit translation invariance, i.e. space-time shifts  $x \rightarrow x' = x - y$  do not give the same expression, in contrast to the free quark propagator. Thus,  $S(x, y)$  and  $S(x - y, 0)$  are different quantities. In order to preserve the gauge condition, two separate Fourier

transforms of the perturbative quark propagator are introduced:

$$S(p) = \int d^4x e^{ipx} S(x, 0), \quad (2.40)$$

$$\tilde{S}(p) = \int d^4x e^{-ipx} S(0, x). \quad (2.41)$$

The Fourier transforms of the free quark propagators and the gluonic background field read

$$S^{(0)}(q) = \int d^4x e^{iqx} S^{(0)}(x, 0) = \int d^4x e^{-iqx} S^{(0)}(0, x), \quad (2.42)$$

$$A_\mu(k) = \int d^4x e^{ikx} A_\mu(x). \quad (2.43)$$

Further utilizing momentum derivatives  $\partial_p$  of the Fourier exponentials to absorb the spatial dependence of the covariant expansion (2.34) the perturbative quark propagator in a classical, weak, gluonic background field can be expanded as

$$S(p) = \sum_{n=0}^{\infty} S^{(n)}(p) \quad (2.44)$$

with

$$\begin{aligned} S^{(n)}(p) &= -S^{(0)}(p) (\gamma \tilde{A}) S^{(n-1)}(p) \\ &= -S^{(n-1)}(p) (\gamma \tilde{A}) S^{(0)}(p) \\ &= (-1)^n S^{(0)}(p) \underbrace{(\gamma \tilde{A}) S^{(0)}(p) \cdots (\gamma \tilde{A}) S^{(0)}(p)}_{n \text{ times } (\gamma \tilde{A}) S^{(0)}(p)}, \end{aligned} \quad (2.45)$$

where the background field contribution  $(\gamma \tilde{A}) = \gamma^\mu \tilde{A}_\mu$  is inserted using the expansion

$$\tilde{A}_\mu = \sum_{k=0}^{\infty} \tilde{A}_\mu^{(k)}, \quad (2.46)$$

$$\tilde{A}_\mu^{(k)} = -g \frac{(-i)^{k+1}}{k!(k+2)} (D_{\alpha_1} \cdots D_{\alpha_k} G_{\nu\mu})_{x=0} \partial_p^\nu \partial_p^{\alpha_1} \cdots \partial_p^{\alpha_k}. \quad (2.47)$$

The partial derivatives  $\partial_p^{\alpha_i}$  contained in a particular  $(\gamma \tilde{A})$  act on all functions (quark propagators) to the right in Eq. (2.45), whereas the contained covariant derivatives  $D_{\alpha_i}$  solely affect the next gluonic field strength tensor  $G_{\nu\mu}$ . Analogously, one can derive the perturbative quark propagator

$$\tilde{S}(p) = S^{(0)}(p) + \sum_{n=1}^{\infty} (-1)^n S^{(0)}(p) \underbrace{(\overset{\leftarrow}{\gamma} \tilde{A}) S^{(0)}(p) \cdots (\overset{\leftarrow}{\gamma} \tilde{A}) S^{(0)}(p)}_{n \text{ times } (\overset{\leftarrow}{\gamma} \tilde{A}) S^{(0)}(p)}, \quad (2.48)$$

where the arrows indicate the direction of application of the partial derivatives in  $(\gamma \tilde{A})$ . Although, the perturbative quark propagator in position space (2.39) is not translation invariant, i. e.  $S(x, 0)$  differs from  $S(0, x)$ , Eqs. (2.48) and (2.44) are identical.

To denote the order of the background field expansion  $\tilde{A}^{(k_i)}$  contained in the perturbative quark propagator (2.44) one may introduce the notation

$$S_{(\tilde{A}^{(k_1)}, \dots, \tilde{A}^{(k_n)})}^{(n)}(p) = (-1)^n S^{(0)}(p) \gamma^{\mu_1} \tilde{A}_{\mu_1}^{(k_1)} S^{(0)}(p) \dots \gamma^{\mu_n} \tilde{A}_{\mu_n}^{(k_n)} S^{(0)}(p). \quad (2.49)$$

If  $k_1 = \dots = k_n = k$  is satisfied, the notation reduces to  $S_{(\tilde{A}^{(k)})}^{(n)}(p)$ .

As OPEs of current-current correlators to higher orders in the perturbative expansion are to be considered, also the perturbative gluon propagator in a classical, weak, gluonic background field needs to be introduced to achieve a complete evaluation. In this thesis, no contributions are evaluated which demand inclusion of the perturbative gluon propagator. Accordingly, only a brief, schematic derivation is presented in the following.

Propagation of the gluon is modeled by further terms entering the QCD Lagrangian if the gauge field is substituted by [Shu82b, Gro95]

$$A_\mu^A + a_\mu^A. \quad (2.50)$$

In this derivation, the gluon field strength tensors  $G_{\mu\nu}^A$  and the covariant derivatives  $D_\mu$  solely contain the background field  $A_\mu^A$ . Similarly as above, the Fock-Schwinger gauge is chosen for  $A_\mu^A$  retaining the purely gluonic QCD Lagrangian

$$\mathcal{L}_{\text{glu}} = -\frac{1}{4} G_{\mu\nu}^A G^{A\mu\nu} - \frac{1}{2} (D_\mu a_\nu^A)^2 + \frac{1}{2} (D_\mu a_\nu^A) (D^\nu a^{A\mu}) + \frac{1}{2} g a^{A\mu} G_{\mu\nu}^{AB} a^{B\nu} + \dots \quad (2.51)$$

with

$$D_\mu a_\nu^A = \partial_\mu a_\nu^A + g A_\mu^{AC} a_\nu^C, \quad (2.52a)$$

$$A_\mu^{AC} = f^{ABC} A_\mu^B, \quad (2.52b)$$

$$G_{\mu\nu}^{AB} = f^{ABC} G_{\mu\nu}^C \quad (2.52c)$$

being gauge invariant with respect to the free gluon field  $a_\mu^A$  [Nov84]. The fourth term of the Lagrangian (2.51) yields only vertex functions  $\Gamma_{\mu\nu}^{(1)}$  containing one background field, whereas the second and third term in Eq. (2.51) provide, apart from  $\Gamma_{\mu\nu}^{(1)}$ , further vertex functions  $\Gamma_{\mu\nu}^{(2)}$  containing two background fields. The perturbative gluon propagator in a classical, weak, gluonic background field is defined by

$$D_{\mu\nu}^{AB}(x, y) = -i \langle T [a_\mu^A(x) a_\nu^B(y)] \rangle. \quad (2.53)$$

Its diagrammatic representation is displayed in Fig. 2.3. If the Lagrangian (2.51) is supplemented by the gauge fixing term  $-\frac{1}{2} (D^\mu a_\mu^A)^2$ , ensuring canonical quantization, the resulting free gluon propagator is  $D_{\mu\nu}^{(0)}(p) = -g_{\mu\nu}/p^2$  and the corresponding vertex functions are  $\Gamma_{\mu\nu}^{(1)} = ig A_\lambda^{AB} (p_1^\lambda + p_2^\lambda) g_{\mu\nu} - ig A_\mu^{AB} (p_{1\nu} - p_{2\nu}) - ig A_\nu^{AB} (p_{2\mu} - p_{1\mu}) - ig G_{\mu\nu}^{AB}$  as well as  $\Gamma_{\mu\nu}^{(2)} = -g^2 A_\lambda^{AC} A^{CB\lambda} g_{\mu\nu} - g^2 A_\mu^{AC} A_\nu^{CB} + g^2 A_\nu^{AC} A_\mu^{CB}$ , where  $p_1$  is the incoming and  $p_2$  the outgoing momentum of the propagating gluon. Construction of the perturbative gluon



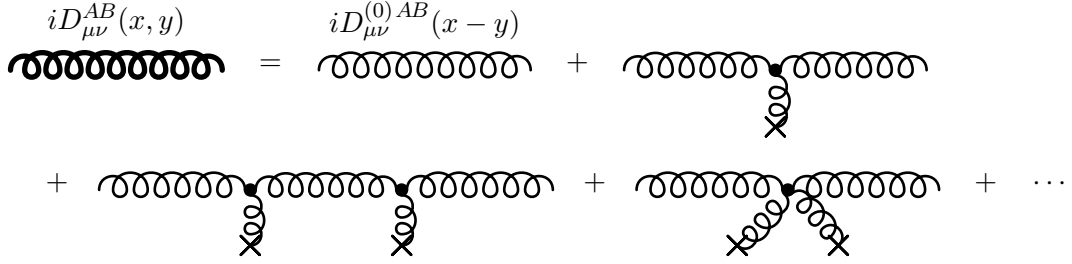


**Figure 2.3:** Diagrammatic representation of the perturbative gluon propagator  $D$  (thick curly line) in a classical, weak, gluonic background field yielding a series of the free gluon propagator  $D^{(0)}$  (thin curly lines) coupled via soft-gluon exchange to the background (crosses). The vertices originate from the interaction part of the Lagrangian (2.51).

propagator up to order  $1/p^6$  as in Fig. 2.3 using Eq. (2.34) yields

$$\begin{aligned}
 D_{\mu\nu}(p) &= \int d^4x e^{ip(x-y)} D_{\mu\nu}(x, y) \\
 &= -\frac{g_{\mu\nu}}{p^2} + g\frac{2}{p^4}G_{\mu\nu} + g\frac{4i}{p^6}(pD)G_{\mu\nu} - g\frac{2i}{3p^6}g_{\mu\nu}D^\lambda G_{\lambda\sigma}p^\sigma \\
 &\quad + g\frac{2}{p^8}(pD)g_{\mu\nu}D^\lambda G_{\lambda\sigma}p^\sigma + g\frac{2}{p^8}\left(p^2D^2G_{\mu\nu} - 4(pD)^2G_{\mu\nu}\right) \\
 &\quad - g^2\frac{1}{2p^8}g_{\mu\nu}\left(p^2(G_{\lambda\sigma})^2 - 4(p^\lambda G_{\lambda\sigma})^2\right) + g^2\frac{4}{p^6}g^{\lambda\sigma}G_{\mu\lambda}G_{\sigma\nu}. \tag{2.54}
 \end{aligned}$$

The Fock-Schwinger gauge allows to compute the OPE (2.26) of the current-current correlator (2.1) in a systematic and profound way not relying on 'appropriate' states to single out particular Wilson coefficients of the OPE as necessary for the plane wave method [Rei85]. Applying Wick's theorem to the components of the interpolating currents  $j(x)$  and  $j^\dagger(0)$  in Eq. (2.1) leads to perturbative quark and/or gluon propagators, i. e. the expansions (2.44) and/or (2.54) emerge, respectively. Remaining Wick-uncontracted partonic operators and the background fields entering through the perturbative quark and gluon propagators form the normal-ordered condensates. Accordingly, the free propagators and the vertex functions entering the expansions (2.44) and/or (2.54) form the Wilson coefficients. Starting from the very first terms of the expansions (2.44) one recognizes the perturbative contribution and the well known low mass dimension condensates, e. g. the chiral condensate  $\langle\bar{q}q\rangle$  and the gluon condensate  $\langle G^2\rangle$ . For higher order  $\alpha_s$  contributions and for more exotic hadrons comprising gluonic valence partons or pure glueballs the expansion (2.54) becomes relevant.

### 2.2.2 Renormalization

Following Ref. [Pas84] the renormalization procedure is reviewed to arrive at the running coupling, quark masses and renormalized condensates. These are employed in vacuum QSR analyses by authors which aim for the extraction of hadronic and/or QCD parameters with the highest accuracy allowed by the framework, e. g. [Nar13, Luc15]. If the impact of a strongly interacting medium on hadronic observables is envisaged one may refrain from using the running quantities. In order to gain further insights into the convergence behavior of the OPE such efforts are worthwhile.

Experimentally observable quantities can be calculated by means of Green's functions in perturbative quantum field theories. If quantum corrections to the classical description are addressed one encounters (superficially) divergent momentum integrals in intermediate steps of the calculation which must vanish in the final result. These divergences are associated to loops in the corresponding Feynman diagrams, e.g. self-energies or vertex-corrections. To treat the divergences one has to fix a regularization and a renormalization scheme, e.g. dimensional renormalization and the  $\overline{\text{MS}}$  scheme, respectively. While the former casts the divergences into a rigorous form, e.g. a pole  $1/\epsilon$  in the limit  $\epsilon \rightarrow 0$  after introducing a scale  $\mu$  to preserve mass dimension, the latter eliminates them by inserting appropriate counter terms proportional to  $C_i$  into the Lagrangian, which exactly cancel the divergences in a given loop order, i.e. the counter terms are a power series in  $g^2$  up to the given loop order. One then defines the renormalization constants

$$Z_i = 1 - C_i \quad (2.55)$$

for each term in the Lagrangian, which allow to write the constituting fields and parameters (couplings, masses, gauge) as bare quantities absorbing the renormalization constants. Gauge invariance of the Lagrangian requires the bare couplings of each single interaction term to coincide, i.e. the Slavnov-Taylor identities give restrictions on renormalization constant ratios. As the counter terms are not unique various renormalization schemes can be applied in order to calculate Green's functions.

Renormalization invariance means independence of physical observables of the renormalization scheme chosen for their theoretical calculation. The group structure within classes of renormalization can be easily exhibited for multiplicatively renormalizable, general Green's functions

$$\Gamma_R(\cdots) = Z_R \Gamma(\cdots), \quad (2.56)$$

where  $Z_R$  denotes the appropriate product of renormalization constants in the renormalization scheme  $R$ . For a different scheme  $R'$  one has  $\Gamma_{R'}(\cdots) = Z_{R'} \Gamma(\cdots)$  analogously. Thus, the differently normalized Green's functions satisfy

$$\Gamma_{R'}(\cdots) = Z_{R'R} \Gamma_R(\cdots) \quad \text{with} \quad Z_{R'R} = Z_{R'}/Z_R. \quad (2.57)$$

Therefore, for the set of all possible  $Z_{R'R}$  with arbitrary  $R$  and  $R'$  there exist the composition law

$$Z_{R''R} = Z_{R''R'} Z_{R'R}. \quad (2.58)$$

For each element  $Z_{R'R}$  one can associate an inverse  $Z_{R'R}^{-1} = Z_{RR'}$  and a unit element  $Z_{RR} = \mathbb{1}$ . These relations define a group structure. Notice that the composition law is not defined for two arbitrary elements of the group, because the resulting product  $Z_{R_i R_j} Z_{R_k R_l}$  is an element of the group for  $j = k$  only.

The relation between the renormalized and bare Green's function which depend on the gauge coupling  $\alpha_s$ , the quark masses  $m_q$  and the gauge fixing parameter  $\xi$  reads

$$\Gamma_R(p_1, \dots, p_N; \alpha_s, m_q, \xi; \mu) = \lim_{\epsilon \rightarrow 0} \left\{ Z_\Gamma(\mu, \epsilon) \Gamma_0(p_1, \dots, p_N; \alpha_{s0}, m_{q0}, \xi_0; \epsilon) \right\} \quad (2.59)$$

with the combined field renormalization constant  $Z_\Gamma(\mu, \epsilon)$  depending on the number and type of fundamental QCD field operators contained in the Green's function  $\Gamma_R$  with mass dimension  $d_\Gamma$ . The  $\mu$ -independence of the bare Green's function, i. e.  $\frac{d}{d\mu}\Gamma_0 = 0$ , implies

$$\left[ \mu \frac{\partial}{\partial \mu} + \mu \frac{d\alpha_s}{d\mu} \frac{\partial}{\partial \alpha_s} + \sum_q \mu \frac{dm_q}{d\mu} \frac{\partial}{\partial m_q} + \mu \frac{d\xi}{d\mu} \frac{\partial}{\partial \xi} \right] \Gamma_R = \frac{\mu}{Z_\Gamma} \frac{dZ_\Gamma}{d\mu} \Gamma_R, \quad (2.60)$$

where one can introduce a set of universal functions  $\beta$ ,  $\gamma_i$  and  $\delta$  depending on  $\alpha_s$ ,  $m_q$  and  $\xi$ :

$$\begin{aligned} \mu \frac{d\alpha_s}{d\mu} &= \alpha_s \beta(\alpha_s, m_q, \xi), & \frac{\mu}{m_q} \frac{dm_q}{d\mu} &= -\gamma_q(\alpha_s, m_q, \xi), \\ \mu \frac{d\xi}{d\mu} &= \xi \delta(\alpha_s, m_q, \xi), & \frac{\mu}{Z_\Gamma} \frac{dZ_\Gamma}{d\mu} &= \gamma_\Gamma(\alpha_s, m_q, \xi) \end{aligned} \quad (2.61)$$

with the famous  $\beta$  function determining the behavior of the running coupling and the anomalous dimension  $\gamma_\Gamma$  of the Green's function from the (combined) field renormalization. These functions convert Eq. (2.60) into the renormalization group equation (RGE)

$$\left[ \mu \frac{\partial}{\partial \mu} + \beta(\alpha_s) \alpha_s \frac{\partial}{\partial \alpha_s} - \sum_q \gamma_q(\alpha_s) m_q \frac{\partial}{\partial m_q} + \delta(\alpha_s) \xi \frac{\partial}{\partial \xi} - \gamma_\Gamma(\alpha_s) \right] \Gamma_R = 0, \quad (2.62)$$

where only the  $\alpha_s$ -dependence of the universal functions in Eqs. (2.61) has been written explicitly. The expressions for these functions can be obtained from the corresponding renormalization constants (2.55) calculated in a given renormalization scheme. In the  $\overline{\text{MS}}$  scheme applied throughout this thesis, these fundamental functions are  $m_q$ -independent, while the  $\beta$  function is also independent of the gauge parameter  $\xi$ .

Dimensional analysis puts another constraint on the Green's function. Scaling the momenta  $p_i$  by a dimensionless parameter  $\lambda$  one has

$$\Gamma_R(\lambda p_1, \dots, \lambda p_N; \alpha_s, m_q, \xi; \mu) = \lambda^{d_\Gamma} \Gamma_R(p_1, \dots, p_N; \alpha_s, m_q/\lambda, \xi; \mu/\lambda) \quad (2.63)$$

resulting in

$$\left[ \lambda \frac{\partial}{\partial \lambda} + \sum_q m_q \frac{\partial}{\partial m_q} + \mu \frac{\partial}{\partial \mu} - d_\Gamma \right] \Gamma_R(\lambda p_1, \dots, \lambda p_N; \alpha_s, m_q, \xi; \mu) = 0 \quad (2.64)$$

which is known from Euler's homogenous function theorem. Introducing the dimensionless quantities

$$t = \ln \lambda \quad \text{and} \quad x_q = m_q/\mu \quad (2.65)$$

for convenience and upon application of Eq. (2.64) one obtains the RGE (2.62) in the desired form

$$\begin{aligned} \left[ -\frac{\partial}{\partial t} + \beta(\alpha_s) \alpha_s \frac{\partial}{\partial \alpha_s} + \delta(\alpha_s) \xi \frac{\partial}{\partial \xi} - \sum_q \{1 + \gamma_q(\alpha_s)\} x_q \frac{\partial}{\partial x_q} \right. \\ \left. + d_\Gamma - \gamma_\Gamma(\alpha_s) \right] \Gamma_R(e^t p_1, \dots, e^t p_N; \alpha_s, x_q, \xi; \mu) = 0 \end{aligned} \quad (2.66)$$

which is the fundamental equation of the renormalization group. As above, the fundamental functions appearing in Eq. (2.66) do not only depend on  $\alpha_s$  but also on  $x_q$  and  $\xi$ . The general solution of Eq. (2.66) reads<sup>5</sup>

$$\begin{aligned} \Gamma_R(e^t p_1, \dots, e^t p_N; \alpha_s, x_q, \xi; \mu) \\ = \lambda^{d_\Gamma} \Gamma_R(p_1, \dots, p_N; \bar{\alpha}_s(t), \bar{x}_q(t), \bar{\xi}(t); \mu) e^{-\int_0^t dt' \gamma_\Gamma(\bar{\alpha}_s(t'), \bar{x}_q(t'), \bar{\xi}(t'))}, \end{aligned} \quad (2.67)$$

where the running coupling  $\bar{\alpha}_s(t)$ , mass  $\bar{x}_q(t)$  and gauge  $\bar{\xi}(t)$  expressions are obtained via the method of characteristics. Thus, first one must solve the system of coupled ordinary differential equations

$$\frac{d\bar{\alpha}_s(t)}{dt} = \bar{\alpha}_s(t) \beta(\bar{\alpha}_s(t), \bar{x}_q(t), \bar{\xi}(t)), \quad \bar{\alpha}_s(0) = \alpha_s, \quad (2.68)$$

$$\frac{d\bar{x}_q(t)}{dt} = -\bar{x}_q(t) [1 + \gamma_q(\bar{\alpha}_s(t), \bar{x}_q(t), \bar{\xi}(t))], \quad \bar{x}_q(0) = x_q, \quad (2.69)$$

$$\frac{d\bar{\xi}(t)}{dt} = \bar{\xi}(t) \delta(\bar{\alpha}_s(t), \bar{x}_q(t), \bar{\xi}(t)), \quad \bar{\xi}(0) = \xi. \quad (2.70)$$

As we work in the  $\overline{\text{MS}}$  scheme and are interested in the running coupling and mass, only the  $\beta$  function and the mass anomalous dimension  $\gamma_q$  need to be specified. They are polynomials in the coupling  $a_s = \alpha_s/\pi$ , i. e.

$$\beta(\alpha_s) = \beta_1 a_s + \beta_2 a_s^2 + \dots \quad \text{and} \quad \gamma_q(\alpha_s) = \gamma_1 a_s + \gamma_2 a_s^2 + \dots \quad (2.71)$$

with the coefficients [Pas84, Ynd06]

$$\beta_1 = -\frac{1}{2} \left( 11 - \frac{2}{3} N_f \right), \quad \gamma_1 = 2, \quad (2.72)$$

$$\beta_2 = -\frac{1}{4} \left( 51 - \frac{19}{3} N_f \right), \quad \gamma_2 = \frac{1}{12} \left( 101 - \frac{10}{3} N_f \right) \quad (2.73)$$

which are determined from the one- and two-loop contributions to the renormalization constants  $Z_{\alpha_s}$  and  $Z_{m_q}$  evaluated in the  $\overline{\text{MS}}$  scheme for  $N_c = 3$  and  $N_f$  flavors. One introduces the renormalization group invariant (RGI) scale  $\Lambda$  and the RGI quark mass  $\hat{m}_q$  and obtains for the corresponding two-loop result of the running coupling

$$\bar{\alpha}_s^{(2)}(q^2) = \bar{\alpha}_s^{(1)}(q^2) \left[ 1 - \frac{\beta_2}{\beta_1} \frac{\bar{\alpha}_s^{(1)}(q^2)}{\pi} \ln \left( \frac{1}{2} \ln \frac{-q^2}{\Lambda^2} \right) \right] \quad (2.74)$$

with the one-loop expression

$$\bar{\alpha}_s^{(1)}(q^2) = \frac{\pi}{-\beta_1 \frac{1}{2} \ln \frac{-q^2}{\Lambda^2}} \quad (2.75)$$

and for the running mass

$$\bar{m}_q^{(2)}(q^2) = \bar{m}_q^{(1)}(q^2) \left\{ 1 + \left[ \gamma_1 \frac{\beta_2}{\beta_1^2} \ln \left( \frac{1}{2} \ln \frac{-q^2}{\Lambda^2} \right) - \frac{1}{\beta_1} \left( \gamma_2 - \gamma_1 \frac{\beta_2}{\beta_1} \right) \right] \frac{\bar{\alpha}_s^{(1)}(q^2)}{\pi} \right\} \quad (2.76)$$

<sup>5</sup>Comparing this result with Eq. (2.63) exhibits that the global scale factor of the Green's function is not the naively expected  $\lambda^{d_\Gamma}$  but  $\exp(t d_\Gamma - \int_0^t dt' \gamma_\Gamma(\bar{\alpha}_s(t'), \bar{x}_q(t'), \bar{\xi}(t')))$  which is the reason that  $\gamma_\Gamma$  is dubbed the anomalous dimension.

with the one-loop expression

$$\bar{m}_q^{(1)}(q^2) = \hat{m}_q \left( \frac{1}{2} \ln \frac{-q^2}{\Lambda^2} \right)^{\gamma_1/\beta_1} = \hat{m}_q \left[ -\beta_1 \frac{\bar{\alpha}_s^{(1)}(q^2)}{\pi} \right]^{-\gamma_1/\beta_1}. \quad (2.77)$$

The QCD condensates entering the OPE are EVs of composite operators which in general also require renormalization [Pas84, Nar89, Ynd06, Nar07]. Due to the short distance singularities of composite local operators their very definition and renormalization is a subject by itself [Zim73]. However, the situation for the QSR relevant quantities is much simpler, because EVs of such operators are considered which is similar to perturbation theory, where Green's functions are expanded in the coupling times the interaction Lagrangian being a local composite operator of free fields. In perturbation theory, the renormalization of the fields composing the interaction Lagrangian does not absorb the ultra-violet divergences associated with the vertex described by the considered interaction term, but requires the renormalization of the coupling as well. Similarly, the renormalization of other composite operators demands an additional overall renormalization constant beyond the renormalization of their component fields.

In QCD, the fundamental fields can be renormalized multiplicatively, i. e. there exists a one-to-one correspondence between bare and renormalized fields, because all fundamental fields entering the action have different quantum numbers, thus they do not mix under renormalization. In contrast, composite operators can and do mix, as there are usually several of them which share the same quantum numbers. Renormalization of a composite operator involves three types of bare composite operators: *(I)* gauge invariant operators which do not vanish by virtue of the classical EoMs (A.17), (A.18) and (A.19), *(II)* gauge invariant operators which do vanish due to the EoMs and *(III)* gauge dependent operators of the same mass dimension, quantum numbers and Lorentz structure. Generically, one may write for a composite operator  $O$

$$O_R(\mu) = Z_I(\mu)O_0^{(I)} + Z_{II}(\mu)O_0^{(II)} + Z_{III}(\mu)O_0^{(III)} \quad (2.78)$$

with  $O_0^{(J)}$  being vectors of the three types of bare composite operators and corresponding renormalization constant matrices  $Z_J$ . It is particularly advantageous to work in the Landau background field gauge [Shi79, Pas84], where type-*(III)* operators  $O_0^{(III)}$  do not enter the renormalized expression of type-*(I)* operators  $O_0^{(I)}$ , i. e.  $Z_{III} = 0$ , while type-*(II)* and -*(III)* operators are renormalized among themselves. Physical relevance resides in the gauge invariant operators of type-*(I)* alone, cf. QCD condensates.

The components of the renormalization matrix  $Z_I$  and the corresponding anomalous dimensions, cf. lower right Eq. (2.61), are determined from suitable  $N$ -point Green's functions

$$\Gamma_R^O(p_1, \dots, p_{N-1}; \mu) \propto \langle \phi_1(x_1) \cdots \phi_N(x_N) O_R(\mu) \rangle \quad (2.79)$$

with fundamental QCD fields  $\phi_i$  and inserted zero-momentum composite operator  $O_R$ , e. g. the quark propagators  $\Gamma_R^O(p; \mu) = -i \int d^4x e^{ipx} \langle T[q(x) \bar{q}(0) O_R(\mu)] \rangle$ , the gluon propagators  $\Gamma_R^O(k; \mu) = -i \int d^4x e^{ikx} \langle T[A_\mu^A(x) A_\nu^B(0) O_R(\mu)] \rangle$  and the vertices  $\Gamma_R^O(q, q'; \mu) = i \int d^4x d^4y e^{-iqx} e^{-iq'y} \langle T[q(x) \bar{q}(y) A_\mu^A(0) O_R(\mu)] \rangle$  are evaluated up to the envisaged loop order. Thus, these Green's functions being combination of Green's functions with inserted

bare operators, cf. Eq. (2.78), and expressed by free fundamental fields in the interaction representation allow for a perturbative treatment [Ynd06]. Diagrammatic techniques can be employed, i. e. the well known Feynman rules of QCD supplemented by the Feynman rules for the zero-momentum insertion of the composite operators, which are readily obtained from derivatives w. r. t. their component fields, can be used to calculate the divergent parts of the Green's functions  $\Gamma_R^O$  up to a given loop order. The renormalization constants  $Z_I$  are chosen to absorb these arising divergences. The desired renormalization constants of dimension-4 QCD condensates can be deduced by comparison with the vertex corrections and self-energies from the renormalization (2.55) of the QCD Lagrangian to a given loop-order.

Once the renormalization constants are deduced, one may write the renormalization of fixed-mass dimension condensates in component notation (with implicit summation over repeated indices and omission of the label  $I$ )

$$\langle O_R \rangle_i(\mu) = Z_{ij}(\mu) \langle O_0 \rangle_j, \quad (2.80)$$

where the renormalization matrix in the  $\overline{\text{MS}}$  scheme has the form

$$Z_{ij}(\mu) = \delta_{ij} + \sum_{n=1}^{\infty} \frac{Z_{ij}^{(n)}[\alpha_s(\mu)]}{\epsilon^n}. \quad (2.81)$$

The corresponding anomalous dimension matrix  $\gamma_{\langle O \rangle}^{ij}$ , defined by

$$\gamma_{\langle O \rangle}^{ij} \langle O_R \rangle_j = \mu \frac{d \langle O_R \rangle_i}{d\mu}, \quad (2.82)$$

can be expressed by the renormalization matrix yielding  $\gamma_{\langle O \rangle}^{ij} = \mu(dZ_{ik}/d\mu)(Z^{-1})_{kj}$ , where Eq. (2.80) and  $\delta_{jl} = (Z^{-1})_{jk}Z_{kl}$  have been employed. Since the  $\mu$ -dependence of the renormalization matrix is exclusively contained within the coupling, which is not dimensionless for arbitrary space-time dimensions, i. e.  $\alpha_s(\mu, \epsilon) = \mu^{2\epsilon}\alpha_s(\mu)$ , one can rewrite the anomalous dimension matrix

$$\gamma_{\langle O \rangle}^{ij}(\alpha_s, \epsilon) = \mu \frac{d\alpha_s(\mu, \epsilon)}{d\mu} \frac{\partial Z_{ik}(\alpha_s)}{\partial \alpha_s} (Z^{-1})_{kj} = [2\alpha_s\epsilon + \alpha_s\beta(\alpha_s)] \frac{\partial Z_{ik}(\alpha_s)}{\partial \alpha_s} (Z^{-1})_{kj}. \quad (2.83)$$

Substituting Eq. (2.81) in Eq. (2.83) and comparison of equal powers of  $\epsilon$  yields in order  $\epsilon^0$

$$\gamma_{\langle O \rangle}^{ij}(\alpha_s) = 2\alpha_s\epsilon \frac{\partial Z_{ik}^{(1)}/\epsilon}{\partial \alpha_s} \delta_{kj} = 2\alpha_s \frac{\partial Z_{ij}^{(1)}(\alpha_s)}{\partial \alpha_s} \quad (2.84)$$

$$\equiv \gamma_{\langle O \rangle,1}^{ij} a_s + \gamma_{\langle O \rangle,2}^{ij} a_s^2 + \dots, \quad (2.85)$$

where analogous relations to (2.84) from further powers of  $\epsilon$  must be satisfied which ensure that  $\gamma_{\langle O \rangle}^{ij}$  has no poles in  $\epsilon$  [Pas84]. Often, a multiplicatively renormalizable operator combination can be found [Tar82, Nar83, Gri89] considerably reducing evaluational efforts. In particular, in the light chiral limit, the renormalization matrices of dimension-4 and -5 vacuum condensates reduce to scalars. Hence, the indices in the above relations can be omitted and the RGI condensate  $\langle O \rangle^{\text{RGI}}$  can be introduced analogous to the RGI quark mass

$\hat{m}_q$ . The running condensate  $\langle O_R \rangle(\mu)$  to one-loop order is obtained from an integration of Eq. (2.82) with  $\gamma_{\langle O \rangle} = \gamma_{\langle O \rangle,1} a_s$

$$\int \frac{d\langle O_R \rangle}{\langle O_R \rangle} = \frac{\gamma_{\langle O \rangle,1}}{\pi} \int d\mu \frac{\alpha_s(\mu)}{\mu}. \quad (2.86)$$

Using the one-loop result for the running coupling (2.75) allows for the evaluation of the  $\mu$ -integral, i. e.

$$\begin{aligned} \ln \langle O_R \rangle(\mu) &= -\frac{\gamma_{\langle O \rangle,1}}{\pi} \frac{\pi}{\beta_1} \int d(\mu/\Lambda) \left( \frac{\mu}{\Lambda} \ln \frac{\mu}{\Lambda} \right)^{-1} + \text{const.} \\ &= -\frac{\gamma_{\langle O \rangle,1}}{\beta_1} \ln \left( \ln \frac{\mu}{\Lambda} \right) + \ln \langle O \rangle^{\text{RGI}}, \end{aligned} \quad (2.87)$$

and one readily obtains the one-loop result for the running condensate in the desired form

$$\langle O_R \rangle(\mu) = \left[ -\beta_1 \frac{\bar{\alpha}_s^{(1)}(-\mu^2)}{\pi} \right]^{\gamma_{\langle O \rangle,1}/\beta_1} \langle O \rangle^{\text{RGI}}. \quad (2.88)$$

Pseudo-conserved currents, such as the gauge invariant vector and axial-vector currents which have a vanishing divergence in the massless quark limit, do not get renormalized in contrast to the EVs entering the OPE. The chiral condensate is conveniently renormalized from the quark mass renormalization result using the RGI of the Gell-Mann–Oakes–Renner (GOR) relation (B.23), cf. Eqs. (2.89) and (2.77). The gluon condensate and higher mass dimension vacuum condensates are renormalized according to the above prescription. Results for mass dimension-5 and -6 condensates are obtained in [Nar83, Jam86]. As renormalization of four-quark condensates is incompatible with factorization of these condensates [Nar83] and the corrections from their anomalous dimensions are approximately canceled by the running coupling anyway [Shi79], RGI four-quark condensates are commonly not used in the renormalization group improved QSR, e. g. [Nar13]. The renormalization results to order  $\alpha_s$  in the light chiral limit,  $m_q \rightarrow 0$ , are [Nar13]

$$\langle \bar{q}q \rangle(q^2) = \hat{\mu}_q^3 [-\beta_1 a_s(q^2)]^{2/\beta_1}, \quad (2.89)$$

$$\langle \bar{q}g\sigma Gq \rangle(q^2) = M_0^2 \hat{\mu}_q^3 [-\beta_1 a_s(q^2)]^{1/(3\beta_1)}, \quad (2.90)$$

where  $\hat{\mu}_q^3$  denotes the RGI chiral condensate and  $M_0^2$ , numerically fixed from B and  $B^*$  masses in Ref. [Nar88], is a mass dimension-2 parameter to scale the mixed quark-gluon condensate  $\langle \bar{q}g\sigma Gq \rangle$  with the chiral condensate  $\langle \bar{q}q \rangle$ . To one loop level, the gluon condensate  $\langle (\alpha_s/\pi) G^2 \rangle$  does not require renormalization in the light chiral limit,  $m_q \rightarrow 0$ .

### 2.2.3 Structure of the OPE

The operator product expansion (OPE) is an expansion in two distinct variables. On one hand, the current-current correlator  $\Pi(q)$ , defined in Eq. (2.1), is expanded into a perturbative series of the strong coupling  $\alpha_s$

$$\Pi(q) = i \int d^4x e^{iqx} \langle T \left[ j(x) j^\dagger(0) \sum_{n=0}^{\infty} \frac{(i)^n}{n!} \int d^4y_1 \cdots d^4y_n \mathcal{L}_{\text{int}}(y_1) \cdots \mathcal{L}_{\text{int}}(y_n) \right] \rangle, \quad (2.91)$$

where  $\mathcal{L}_{\text{int}}$  is a function of  $\alpha_s$  according to Eqs. (A.15) and (A.16). On the other hand, an expansion of  $\Pi(q)$  in powers of  $1/q^2$  is performed, which are contained in the Wilson coefficients  $C_n(q)$  of the OPE

$$\Pi(q) = \sum_n C_n(q) \langle O_n \rangle. \quad (2.92)$$

This expansion entails the introduction of condensates  $\langle O_n \rangle$  of the respective mass dimensions compensating the mass dimensions of the Wilson coefficients in order to ensure the fixed mass dimension of their product.

In general, there are two options of how to perform the expansions – commencing with the OPE (2.92) followed by the perturbative series (2.91), or vice versa. The equation<sup>6</sup>

$$\begin{aligned} \Pi^{\text{OPE}}(q) &= \sum_n \langle O_n \rangle \left( \sum_{k=0}^{\infty} C_n^{(k)}(q) \alpha_s^k \right) \\ &= \mathbb{1} \left( C_0^{(0)}(q) + C_0^{(1)}(q) \alpha_s^1 + C_0^{(2)}(q) \alpha_s^2 + \dots \right) \\ &\quad + \langle g^2 G^2 \rangle \left( C_{4_G}^{(0)}(q) + C_{4_G}^{(1)}(q) \alpha_s^1 + C_{4_G}^{(2)}(q) \alpha_s^2 + \dots \right) \\ &\quad + m \langle \bar{q} q \rangle \left( C_{4_q}^{(0)}(q) + C_{4_q}^{(1)}(q) \alpha_s^1 + C_{4_q}^{(2)}(q) \alpha_s^2 + \dots \right) \\ &\quad + \langle \bar{q} g \sigma G q \rangle \left( C_5^{(0)}(q) + C_5^{(1)}(q) \alpha_s^1 + C_5^{(2)}(q) \alpha_s^2 + \dots \right) \\ &\quad + \langle g^3 G^3 \rangle \left( C_{6_G}^{(0)}(q) + C_{6_G}^{(1)}(q) \alpha_s^1 + C_{6_G}^{(2)}(q) \alpha_s^2 + \dots \right) \\ &\quad + \langle g^2 \bar{q} q \sum_f \bar{f} f \rangle \left( C_{6_q}^{(0)}(q) + C_{6_q}^{(1)}(q) \alpha_s^1 + C_{6_q}^{(2)}(q) \alpha_s^2 + \dots \right) \\ &\quad + \dots \end{aligned} \quad (2.93)$$

prepends the expansion in the series of power corrections (2.92) following the introductory work [Shi79]. The lower index of the coefficient  $C_n^{(k)}$  denotes the mass dimension of the associated condensate, and the upper index gives the order of the  $\alpha_s$  expansion. Perturbative corrections to the Wilson coefficient of a particular condensate are subsequently evaluated employing diagrammatic techniques. Hence, four-quark condensates originating from tree-level diagrams of the next-to-leading order (NLO) correlator, cf. Fig. 3.3, remain disregarded.

In contrast, the equation<sup>6</sup>

$$\Pi^{\text{OPE}}(q) = \sum_{k=0}^{\infty} \alpha_s^k \left( \sum_n C_k^{(n)}(q) \langle O_{n(k)} \rangle \right) \quad (2.95)$$

---

<sup>6</sup>While the notation  $G^2$ ,  $\bar{q} \sigma G q$  and  $G^3$  is often employed for the gauge invariant operator combinations (A.27), the expressions  $\bar{q} q \sum_f \bar{f} f$  and  $\bar{q} q \bar{q} q$  merely symbolize generic four-quark terms entering the leading order and next-to-leading order correlator, respectively.



$$\begin{aligned}
 &= \alpha_s^0 \left( C_0^{(0)}(q) \mathbb{1} + C_0^{(4G)}(q) \langle g^2 G^2 \rangle + C_0^{(4q)}(q) m \langle \bar{q} q \rangle + C_0^{(6G)(q)} \langle g^3 G^3 \rangle \right. \\
 &\quad \left. + C_0^{(6q)}(q) \langle g^2 \bar{q} q \sum_f \bar{f} f \rangle + \dots \right) \\
 &+ \alpha_s^1 \left( C_1^{(0)}(q) \mathbb{1} + C_1^{(4G)}(q) \langle g^2 G^2 \rangle + C_1^{(4q)}(q) m \langle \bar{q} q \rangle + C_1^{(6G)(q)} \langle g^3 G^3 \rangle \right. \\
 &\quad \left. + C_1^{(6q)}(q) \langle g^2 \bar{q} q \sum_f \bar{f} f \rangle + C_1'^{(6q)}(q) \langle \bar{q} q \bar{q} q \rangle + \dots \right) \\
 &+ \dots
 \end{aligned} \tag{2.96}$$

prepends the expansion in the perturbative series (2.91). Such a view is advantageous when dealing with four-quark condensates [Pas84] and it is also suggested by the diagrammatic interpretation of the OPE in Figs. 2.4 and 2.5. The lower index of the coefficient  $C_k^{(n)}$  denotes the order of the  $\alpha_s$  expansion, while the upper index provides the mass dimension of the associated condensate. The condensate  $\langle O_{n(k)} \rangle$  carries an additional lower index denoting the order of the  $\alpha_s$  expansion, because certain condensates (disregarded in Eq. (2.93)) enter the OPE starting from the NLO of the  $\alpha_s$  expansion, e.g.  $\langle \bar{q} q \bar{q} q \rangle$ . The Eq. (2.92) is applied systematically in each considered order of the perturbative expansion. Application of Wick's theorem produces perturbative quark and gluon propagators, Eqs. (2.44) and (2.54), and condensates emerge from the ground state EVs of remaining Wick-uncontracted QCD operators. Thus, the OPE results in order  $\alpha_s^1$  of the perturbative expansion contain tree-level diagrams associated with four-quark condensates  $\alpha_s \langle \bar{q} q \bar{q} q \rangle$  as well as loop corrections to the coefficients associated with  $\alpha_s g^2 \langle \bar{q} q \sum_f \bar{f} f \rangle$  originating from the perturbative quark propagator.

The diagrammatic representation of the perturbative expansion of the current-current correlator is depicted in Fig. 2.4. The QCD quark propagator displayed therein corresponds to the perturbative quark propagator supplemented by the quark condensate [Jin93] as depicted in Fig. 2.5. To graphically generate diagrams contributing to the OPE of the correlator, the QCD quark propagator construction is inserted at the respective positions in Fig. 2.4, where resulting disconnected diagrams are to be avoided.

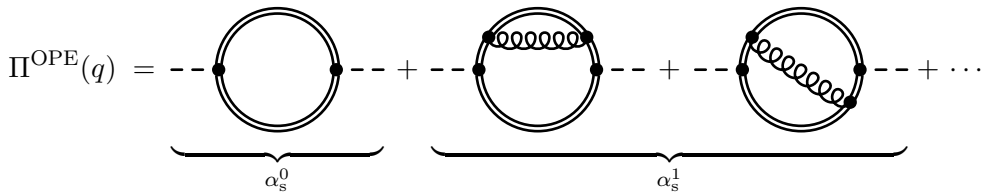


**Figure 2.4:** Diagrammatic representation of the perturbative expansion of the current-current correlator into a power series of  $\alpha_s$ , where the dashed lines depict meson currents and the quark propagators are specified in Fig. 2.5. Vacuum and tadpole diagrams are not displayed here.

$$\begin{array}{c}
\text{QCD quark} \\
\text{propagator}
\end{array}
=
\begin{array}{c}
\text{perturbative} \\
\text{contribution}
\end{array}
+
\underbrace{
\begin{array}{c}
+ \text{---} \times \text{---} \times \text{---} \propto \langle \bar{q}q \rangle \\
+ \text{---} \times \text{---} \times \text{---} \times \text{---} \times \text{---} \propto \langle \bar{q}q \sum_f \bar{f}f \rangle \\
+ \text{---} \times \text{---} \times \text{---} \times \text{---} \times \text{---} \times \text{---} \propto \langle G^2 \rangle \\
+ \text{---} \times \text{---} \times \text{---} \times \text{---} \times \text{---} \times \text{---} \times \text{---} \propto \langle G^3 \rangle \\
+ \text{---} \times \text{---} \times \text{---} \times \text{---} \times \text{---} \times \text{---} \times \text{---} \times \text{---} \propto \langle \bar{q}\sigma Gq \rangle \\
+ \dots
\end{array}
}_{\text{non-perturbative contributions}}$$

**Figure 2.5:** Diagrammatic representation of the QCD quark propagator associated with the expansion (2.92) containing the perturbative contribution and vacuum condensate terms, explicitly depicted up to mass dimension 6.

Superficially, the OPE may appear as an expansion in two variables, the coupling  $\alpha_s$  and the power correction  $1/q^2$ . However, the series of the power corrections involves three expansions, in fact: (i) the covariant Taylor expansion of the quark field (2.35), (ii) the perturbative quark propagator (2.44), and (iii) the therein enclosed expansion of the gluonic background field (2.46). Although, these expansions are utilized to compute the power corrections they implicitly entail an expansion in the coupling  $g$ . The perturbative quark propagator contains powers of the coupling constant depending on the order of the expansion in the gluonic background field. While the coupling  $g$  in the expansion (2.44) is absorbed by the definition of  $\tilde{A}_\mu$  it is apparent in Eq. (2.39). Furthermore, the coupling strength comes into play by virtue of commutations of covariant derivatives  $D_\mu$  and gluonic EoMs.

In this subsection, we attribute a different meaning to the strong coupling  $\alpha_s$  distinct from the one of the coupling strength  $g$ , despite their obvious relation (A.16). In order to comprehensively distinguish the origin of couplings,  $\alpha_s$  is used in the loop expansion (2.91) whereas  $g$  is employed in the three expansions described in the previous paragraph resulting in Eq. (2.92). Although, the power corrections are related to the coupling strength  $g$  the mass dimension of a particular condensate does not uniquely determine its power of  $g$ , e.g. it differs for different mass dimension-6 vacuum condensates: the triple gluon condensate  $\langle G^3 \rangle$  is of order  $g^3$  while the four-quark condensate  $\langle \bar{q}q \sum_f \bar{f}f \rangle$  (order  $\alpha_s^0$ ) scales with  $g^2$ . Albeit, distinguishing the couplings,  $\alpha_s$  and  $g$ , originating from the different expansions, a complete evaluation of the current-current correlator up to a given order in each expansion is impossible.

The complexity of the OPE computation grows further if the gluons of the loop expansion are expressed by perturbative gluon propagators (2.54) which also couple to the classical, weak, gluonic background field, thus, entailing a further expansion in the coupling  $g$ . Apart from this, one may also consider to expand condensates which contain heavy-quark operators in the inverse heavy-quark mass, cf. Sec. 3.6. Therefore, an order scheme which sorts OPE terms by numerical relevance due to their orders in the individual expansions has limited significance. As the individual expansions can not be disentangled it is impossible to

complete each expansion up to a particular order. The multiple expansions entering an OPE evaluation compromise an order scheme based on only two or three parameters.

## 2.3 Nature of condensates

The OPE techniques outlined in Sec. 2.2 demonstrate how QCD condensates emerge ‘naturally’ in the asymptotic expansion of the current-current correlator (2.1) as correction to the perturbative results accounting for the long-range effects of the theory. Formally, QCD condensates are ground state EVs of Hermitian products of local QCD operators, i. e. they are real-valued. Only EVs which obey the assumed symmetries of the QCD ground state, i. e. invariance under parity and time reversal transformations (cf. Tab. A.1), do not vanish a priori. Condensates are to be color singlets as well as Dirac and Lorentz scalars. To satisfy the latter requirements the projection of color, Dirac and Lorentz indices has to be performed (cf. App. C for details). The origin and the physical meaning of condensates is a very recent matter of debate [Bro10, Bro11, Bro12, Cha13, Clo14].

### 2.3.1 Universality

Following the common perception on condensates advocated since the advent of the QSR framework, QCD condensates are understood as numerical values parameterizing the interaction of quarks and gluons with the non-trivial QCD ground state. Light quarks and gluons couple to the QCD ground state, where annihilation with the corresponding virtual particles occurs. In vacuum, condensates attain fixed, finite numerical values, which can be employed for any QSR evaluation once they are known.<sup>7</sup> That is, condensates are of universal character reflecting the vacuum structure of QCD [Shi79]. Thus, an infinite tower of condensates being spread in space-time characterizes the complex QCD ground state which can be visualized in  $\ell$ QCD [Lei99]. The numerical values may be deduced from QSRs employing known hadronic properties and they are accessible in  $\ell$ QCD. The vacuum condensates have been the central object of many studies since their introduction.

In QSR analyses at finite temperatures and/or net-baryon densities, the numerical values of vacuum condensates change whereas the Wilson coefficients of vacuum condensates are unaltered (at least in low-temperature and -density approximations) [Hat93]. However, further condensates contribute to in-medium QSRs which do vanish identically in vacuum. The common idea of hadrons being excitations of the QCD vacuum characterized by quark and gluon condensates immediately suggests the following interpretation of the in-medium changes of the condensate values: As the properties of low mass hadrons are closely connected with vacuum structure, in-medium changes of hadron properties carry signals of the way the vacuum changes in a nuclear environment [Wei94].<sup>8</sup>

Despite the overwhelming success of the QSR framework, relying on the above perception, doubts have been raised about the meaning of condensates [Bro10, Bro12]. Supported

<sup>7</sup>There are concerns by Shifman that this may not apply to glueballs, cf. §8 in Ref. [Shi98].

<sup>8</sup>A different point of view is presented in [Koi97], where in-medium effects described by QSRs are interpreted as the scattering of the considered hadron with medium particles (quantified to leading order by the scattering length) rather than a change of the QCD vacuum caused by ambient strongly interacting particles.

by cosmological arguments the perception of condensates is changed from a space-time-independent quantity extending throughout all of space to a quantity having spatial support within hadrons only. The presence of confinement, where condensates can not be considered as space-time-independent vacuum properties of QCD's elementary DoF, and the measurable impact of the condensates is expressed entirely in the properties of QCD's asymptotically realizable states, namely hadrons [Bro12]. Thus, the notion of 'in-hadron condensates' is introduced [Bro10] emphasizing their spatial restrictions and the close connection of condensates to hadronic wave functions [Cas74].

Observations of supernovae as well as the systematics of the cosmic microwave background anisotropies showed the accelerated expansion of the universe, consistent with the hypothesis that this accelerated expansion can be ascribed to a cosmological constant [Bro11]. However, if the contribution of condensates to the energy-momentum tensor in Einstein's equations are accounted for, e.g. the gluon condensate having the dimension of an energy density, QCD would lead to a cosmological constant of some 45 orders of magnitude larger than observed. This conflict is avoided if strong interaction condensates are properties of rigorously well-defined wave function of the hadrons, rather than the hadronless ground state of QCD [Bro10]. Following this view, QCD condensates would contribute to the energy-momentum tensor through the hadrons masses, leaving the cosmological constant compatible with an accelerated expansion of the universe.

In this perception, not the interactions of the light quarks and gluons with the QCD ground state cause non-vanishing condensates but the quark and gluon propagator dressings as described by Dyson-Schwinger equations. However, with regard to QSRs the essential question is whether also in-hadron condensates are universal, i.e. whether they exhibit no dependence on the host hadron and the same numerical values may be used for QSR evaluations of different hadrons. At least for the quark condensate, a particularly weak sensitivity to its host hadron could be verified [Bro12]. The new perception suggests to consider condensates entering the OPE as merely mass-dependent parameters in a theoretical truncation scheme, such that the OPE techniques presented in the previous section and in App. C remain valid despite the shift of paradigm. The insensitivity to the host hadronic state of all QCD condensates is yet to be proven. Supported by the already achieved positive proof for the quark condensate universality of all QCD condensates is assumed throughout this thesis being aware that cosmological observations strongly favor in-hadron condensates.

### 2.3.2 Order parameters

Condensates parametrize the QCD ground state and concentrate much of the complexity of the theory of QCD. Partially such EVs can also be related to (broken) symmetries of the theory. The gluon condensate  $\langle(\alpha_s/\pi)G_{\mu\nu}^A G^{A\mu\nu}\rangle$  is related to the energy density via the trace of the symmetric energy-momentum tensor  $T^{\mu\nu}$ . For zero quark masses, classical chromodynamics exhibits an invariance under the scale transformation  $x \rightarrow x' = e^{-\sigma}x$ , i.e. it obeys dilatation symmetry, because the classical action contains no parameters with mass dimension. On the quantum level, i.e. in QCD, this symmetry is broken by the regularization scale parameter  $\mu$ . The divergence of the dilatation current  $J_{\text{dil}}^\mu = x_\nu T^{\mu\nu}$  (which vanishes in the classical theory due to Noether's theorem) is then determined by the trace of the

energy-momentum tensor, the so-called QCD trace anomaly

$$\partial_\mu J_{\text{dil}}^\mu = T_\mu^\mu = \frac{\beta(g)}{2g} G_{\mu\nu}^A G^{A\mu\nu} + \sum_q m_q \bar{q}q, \quad (2.97)$$

where the Callan-Symanzik  $\beta$  function describes the scale dependence of the renormalized coupling  $g$  which is shifted to  $g' = g + \sigma\beta(g)$  by the above transformation [Pes95]. Besides the finite quark masses  $m_q$ , breaking the scale invariance explicitly, it is the non-zero gluon condensate which drives the dilatation symmetry breaking<sup>9</sup> of QCD (apart from multi-loop corrections  $\mathcal{O}(\alpha_s^2)$ ). The numerical value  $\langle(\alpha_s/\pi)G^2\rangle = (0.33 \text{ GeV})^4$  has been deduced from the charmonium QSRs, where this quantity gives the dominant condensate contribution.

A further global symmetry of QCD related to quark condensates is chiral symmetry, which is particularly interesting as the experimentally accessible chiral partner meson spectra can be used to study chiral symmetry breaking or restoration patterns. Chiral symmetry is the invariance of the QCD Lagrangian under flavor rotations acting separately on the left-handed and right-handed quark spinors. Details on chiral symmetry transformations and chiral partner currents are relegated to App. B. As finite quark masses break the symmetry explicitly only the light-quark sector of QCD exhibits an approximately invariant Lagrangian. However, even if massless quarks are assumed, chiral symmetry is dynamically broken because the QCD ground state is not invariant under chiral transformations. The violation of chiral symmetry by the ground state can be quantified by particular QCD ground state EVs of quark operators which were already introduced as QCD condensates. Suitable quantities which measure the degree of dynamical chiral symmetry breaking (D $\chi$ SB) are dubbed order parameters. To attribute the new meaning to these quark condensates, the relevant notions of Noether's and Goldstone's theorem are formally introduced following [Pas84, Kug97, Bur00, Gre02, Tho08a, Fuk13].

Noether's theorem provides a conserved current  $j_\mu^a$ , i. e.  $\partial^\mu j_\mu^a = 0$ , for each global continuous symmetry of the action  $S = \int d^4x \mathcal{L}(x)$  and guarantees the time independence of the charge

$$Q^a(x_0) = \int d^3x j_0^a(x). \quad (2.98)$$

These charges are the generators of the symmetry group, because their commutators with the field give the infinitesimal symmetry transformations  $\delta\phi = \phi' - \phi$  in  $a$ -direction by

$$[iQ^a, \phi] = \delta^a \phi. \quad (2.99)$$

The existence of such a conserved current carries special information whether the symmetry involved should be spontaneously broken.

The symmetry exhibited by the action may or may not hold for the ground state. If the ground state  $|\Omega\rangle$  is symmetric with respect to the transformation generated by  $Q^a$  one has  $e^{i\omega^a Q^a}|\Omega\rangle = |\Omega\rangle$  (implicit summation over  $a$ ) which is equivalent to

$$Q^a|\Omega\rangle = 0, \quad (2.100)$$

---

<sup>9</sup>However, the situation is more intricate, due to the absence of a quasi-conserved quantum number or an identifiable physical quantity related to this ground state EV, cf. Ref. [Rei85].

and the symmetry realized in the system is in the Wigner-Weyl phase. In this phase, the invariance of the system is manifest in the spectrum exhibiting degenerate patterns for states which are related by the transformation generated by  $Q^a$ . However, if the ground state is not invariant under such a transformation one can formally write

$$Q^a|\Omega\rangle \neq 0 \quad (2.101)$$

which is actually ill-defined, because the integral over the conserved current in Eq. (2.98) is convergent, thus exists, only in the symmetric case. This issue can be circumvented by introducing the commutator of the charge with a local Heisenberg field  $\Phi(y)$ , i.e. a field with limited support in space-time, which renders the commutator finite. Thus, a rigorous definition of the degree of symmetry breaking by the ground state  $|\Omega\rangle$  can be provided by the ground state EV of the commutator  $[iQ^a(x_0), \Phi(x)]$ . A symmetric ground state which fulfills Eq. (2.100) yields

$$\langle\Omega|[iQ^a(x_0), \Phi(x)]|\Omega\rangle = 0, \quad (2.102)$$

while violation of the symmetry by the ground state requires

$$\langle\Omega|[iQ^a(x_0), \Phi(x)]|\Omega\rangle \neq 0. \quad (2.103)$$

The field  $\Phi$  does not need to be an elementary field  $\phi$ , instead a polynomial in  $\phi$  with finite support is allowed as well. The proof of Goldstone's theorem utilizes the conservation of the charge (2.98) and insertion of a complete set of energy eigenstates on either side of  $j_0^a(x)$  in the commutator. The condition (2.103) is satisfied only when excited states couple to  $j_0^a(x)$  as well as to  $\Phi$ . These states are to be identified with the Goldstone bosons, which are massless excitations with the quantum numbers of  $j_0^a(x)$ . Otherwise, the EV of the commutator vanishes, and the system resides in the Wigner-Weyl realization of the symmetry. Thus, the quantity in Eq. (2.103) distinguishes the symmetric from asymmetric mode and qualifies as an order parameter. Employing the generating property of the charge, Eq. (2.99), this order parameter reads

$$\langle\Omega|[iQ^a(x_0), \Phi(x)]|\Omega\rangle = \langle\Omega|\delta^a\Phi(x)|\Omega\rangle. \quad (2.104)$$

Composing the field  $\Phi$  from elementary fields  $\phi$  allows for the evaluation of the abstract commutator (2.104) by common equal-time (anti-)commutation relations leading to QCD condensates which can be interpreted as order parameters of spontaneous symmetry breaking.

The essential property of an order parameter, as defined in Eq. (2.104), is its sensitivity on the symmetry of the ground state. It vanishes if the system is in the symmetric Wigner-Weyl phase and acquires a non-zero value if the system resides in the asymmetric Nambu-Goldstone phase, i.e. it allows to distinguish the realizations of the considered symmetry. This distinction is caused by the ground state alone, while the Lagrangian and therefore the action obey the considered symmetry in any case.

The above digression on order parameters is not restricted to specific symmetries. Working in this approach the chiral condensate serves as an example for an order parameter of spontaneous  $SU(N_f)_A$  symmetry breaking. This symmetry is a sub-group of the chiral symmetry group  $U(N_f)_L \times U(N_f)_R$  specified in App. B.

Utilizing the equal-time anti-commutation relations of the quark operators (with Dirac indices  $i, j$ , color indices  $\alpha, \beta$  and flavor indices  $q, q'$  (fundamental representation))

$$\left\{ \psi_{i,\alpha,q}(x), \psi_{j,\beta,q'}^\dagger(y) \right\} = \delta_{ij} \delta_{\alpha\beta} \delta_{qq'} \delta^{(3)}(\vec{x} - \vec{y}), \quad (2.105a)$$

$$\left\{ \psi_{i,\alpha,q}(x), \psi_{j,\beta,q'}(y) \right\} = \left\{ \psi_{i,\alpha,q}^\dagger(x), \psi_{j,\beta,q'}^\dagger(y) \right\} = 0 \quad (2.105b)$$

and the relation  $[AB, C] = A\{B, C\} - \{A, C\}B$  the variations (2.99) of the quark field generated by the  $SU(N_f)_A$  charge (with flavor index  $a$  in the adjoint representation)

$$Q_A^a(x_0) = \int d^3x \bar{\psi}(x) \gamma_0 \gamma_5 \tau^a \psi(x) \quad (2.106)$$

are readily obtained:

$$\left[ Q_A^a(x_0), \psi(x) \right] = -\gamma_5 \tau^a \psi(x), \quad (2.107a)$$

$$\left[ Q_A^a(x_0), \psi^\dagger(x) \right] = \psi^\dagger(x) \gamma_5 \tau^a. \quad (2.107b)$$

In order to identify the chiral condensate in Eq. (2.104) we chose the local field  $\Phi$  to be the pseudo-scalar current  $\Phi^b(x) = \bar{\psi}(x) \gamma_5 \tau^b \psi(x)$ . The commutator in (2.104) can be evaluated by means of Eqs. (2.107). For  $N_f = 2$ , i. e.  $2\tau^a = \sigma^a$  are Pauli matrices with  $\{\sigma^a, \sigma^b\} = 2\delta^{ab} \mathbb{1}_2$ , one recovers in

$$\langle \Omega | \left[ iQ_A^a(x_0), \Phi^b(x) \right] | \Omega \rangle = -\frac{i}{2} \delta^{ab} \langle \Omega | \bar{\psi}(x) \psi(x) | \Omega \rangle \quad (2.108)$$

the (local) chiral condensate  $\langle \Omega | \bar{\psi} \psi | \Omega \rangle$  as an order parameter in the spirit of Eq. (2.104). Setting  $b = a$ , the field  $\Phi^b$  directly induces the chiral condensate as an order parameter of  $D\chi$ SB associated with the charge  $Q_A^a$ . Its non-zero numerical value can be deduced from the GOR relation (B.23) with the pion mass  $m_\pi \simeq 140$  MeV, the pion leptonic decay constant  $f_\pi \simeq 93$  MeV and the combined light-quark masses  $m_u + m_d \simeq 11$  MeV resulting in  $\langle \Omega | \bar{q}q | \Omega \rangle \simeq (-0.249 \text{ GeV})^3$ , where  $q$  denotes either up- or down-quark operators.

However, chiral order parameters may acquire a zero numerical value due to residual symmetries although  $SU(N_f)_A$  is broken. Hence, it is important to choose EVs  $\langle \Omega | \delta^a \Phi(x) | \Omega \rangle$  that are insensitive to further symmetries, i. e. they are to be invariant under other symmetry transformations to possess discriminating potential. In particular, they must be invariant under parity and time reversal transformations as well as Lorentz scalars and color singlets previously introduced as the assumed symmetries of the QCD ground state. A specific example of a chiral symmetry breaking pattern with vanishing chiral condensate due to center symmetry, but with broken axial-vector symmetry, is outlined in Subsec. 4.3.2. In this scenario, chirally odd four-quark condensates can serve as meaningful order parameters. The procedure described above for the chiral condensate has been thoroughly applied to four-quark operators in Ref. [Tho08a] to identify such potential order parameters in the spirit of Eq. (2.104) among the light four-quark condensates.

### 2.3.3 Condensates in a strongly interacting medium

In the common perception on QCD condensates, cf. Subsec. 2.3.1, these quantities enter the QSRs as universal parameters which determine hadronic properties. Thus, changing

condensates are presumed to govern changes of the spectral density of hadrons which are embedded in a strongly interacting medium. To account for in-medium effects in the QSR framework, the current-current correlator (2.1) is evaluated in Gibbs averaged form (2.9) leading to Gibbs averaged operators  $\langle\langle O \rangle\rangle$  in the OPE eventually [Boc86]. Thus, formally, in-medium changes are caused by deviations of the Gibbs average  $\langle\langle O \rangle\rangle$  from the ground state EV  $\langle\Omega|O|\Omega\rangle$  as well as by the advent of further operators with vanishing ground state EV in vacuum.

The dependence of the in-medium condensates  $\langle\langle O \rangle\rangle$  on temperature  $T$  and chemical potentials  $\mu_h$  (for particular hadron species  $h$ ) could be estimated in several ways: the direct  $\ell$ QCD computation, or calculations based on low-energy effective theories, or within QSRs from modifications of hadron spectra, or the low-temperature expansion etc. However,  $\ell$ QCD results are available for few of the needed quantities only and they suffer from problems at finite chemical potentials. Estimates from effective theories inhere model dependences. While the extraction of the medium dependences from QSRs might be feasible for a few condensates, ambiguities arise for the multitude of condensates.

In this thesis, the approach based on low-temperature ( $T$ ) and low-baryon density ( $n$ ) approximations is pursued in accordance with the conceptional limitation of QSRs to small deviations from the vacuum case. Since the QSR relies on the power counting of hadron momenta, high temperatures and baryo-chemical potentials compatible with these momenta would require a complete rearrangement of the OPE.<sup>10</sup> With the restriction to low temperatures and low densities the assumption of medium-independent Wilson coefficients is justified as well as the expansion of the condensate changes to leading order (LO) in these parameters. Extrapolations of condensate modifications and QSR results, e. g. to the phase transition boundary in the QCD phase diagram, must be taken with care.

In the low-temperature approximation the strongly interacting medium is assumed to be a thermal gas of free hadrons [Gas87]. Due to its partial Goldstone boson character the pion is the lowest hadronic excitation above the QCD ground state. As long as  $T$  is moderate and the thermal pion gas is dilute the temperature dependent condensates  $\langle O \rangle_T$  are approximated by [Hat93]

$$\langle O \rangle_T \simeq \langle O \rangle_0 + \sum_{a=1}^3 \int \frac{d^3p}{2E_p(2\pi)^3} \langle \pi^a(\vec{p}) | O | \pi^a(\vec{p}) \rangle n_B(E_p/T) \quad (2.109)$$

with adapted notation for the ground state EV  $\langle O \rangle_0 = \langle \Omega | O | \Omega \rangle$  which are used interchangeably throughout this thesis. The pion energy is given by  $E_p = (\vec{p}^2 + m_\pi^2)^{1/2}$ ,  $a$  denotes the iso-spin state and  $n_B(x) = (e^x - 1)^{-1}$  is the Bose-Einstein distribution. The pion states are covariantly normalized, i. e.  $\langle \pi^a(\vec{p}) | \pi^b(\vec{p}') \rangle = 2E_p(2\pi)^3 \delta^{ab} \delta^{(3)}(\vec{p} - \vec{p}')$ . If the pion matrix element is diagonal in iso-spin and independent of the pion momentum,  $\langle \pi^a(\vec{p}) | O | \pi^b(\vec{p}) \rangle = \delta^{ab} \langle \pi | O | \pi \rangle$ , the integral further reduces to

$$\langle O \rangle_T \simeq \langle O \rangle_0 + \frac{T^2}{8} B_1(m_\pi/T) \langle \pi | O | \pi \rangle \quad (2.110)$$

with the function  $B_1(z) = \frac{6}{\pi^2} \int_z^\infty dy \sqrt{y^2 - z^2} / (e^y - 1)$  converging to 1 for  $z \rightarrow 0$ . Especially in the chiral limit,  $m_\pi = 0$ , the condensate scales as  $T^2$ .

---

<sup>10</sup>Feynman diagram techniques in the Matsubara representation should be considered to determine the QCD expression of the correlator (2.1) at high temperatures [Boc86].



For some purposes, (cold) nuclear matter can be approximated by a non-interacting Fermi gas of nucleons [Dru91]. The density dependence of condensates is governed by spin-averaged and iso-spin-averaged nucleon matrix elements taken for nucleons at rest [Coh92] and has yet to be found for particular operators, especially condensates with  $\dim_m \geq 6$ . Analogous to Eq. (2.109) the nucleon density dependent condensates  $\langle O \rangle_n$  are approximated by

$$\langle O \rangle_n \simeq \langle O \rangle_0 + \int \frac{d^3k}{2E_k(2\pi)^3} \langle N(\vec{k}) | O | N(\vec{k}) \rangle n_F([E_k - \mu_N]/T), \quad (2.111)$$

where the Fermi-Dirac distribution  $n_F(x) = (e^x + 1)^{-1}$  reduces to the step function  $\Theta(\mu_N - E_k)$  in the zero temperature limit. The nucleon energy is given by  $E_k = (\vec{k}^2 + m_N^2)^{1/2}$  and the nucleon states are normalized as  $\langle N(\vec{k}) | N(\vec{k}') \rangle = 2E_k(2\pi)^3 \delta^{(3)}(\vec{k} - \vec{k}')$ . Thus, if the nucleon matrix element is independent of the nucleon momentum the remaining integral equals the number density of nucleons, i.e. the baryon density  $n = \int dE n_F([E - \mu_N]/T) D(E)$  with the density of states  $D(E) = \int \frac{d^3k}{(2\pi)^3} \delta(E - E_k)$ . Accordingly, the condensates

$$\langle O \rangle_n \simeq \langle O \rangle_0 + \frac{n}{2m_N} \langle N | O | N \rangle \quad (2.112)$$

change linearly with density  $n$ .

The combination of the two approximations gives the leading terms to the Gibbs average

$$\langle\langle O \rangle\rangle = \langle O \rangle_0 + \frac{T^2}{8} B_1(m_\pi/T) \langle \pi | O | \pi \rangle + \frac{n}{2m_N} \langle N | O | N \rangle + \dots \quad (2.113)$$

For larger temperatures and baryon densities, the effects of higher powers of pion and baryon densities supplementing the leading terms in Eqs. (2.109) and (2.111) as well as further massive excitations, i.e.  $K$ ,  $\eta$ , etc., start to become important [Hat93]. While for a general operator  $O$  it is hard to make model independent predictions for higher order density corrections [Leu06], contributions beyond linear density approximation to the chiral condensate can be systematically studied by an application of the Hellmann-Feynman theorem [Coh92]. The resonance gas approximation partly accounts for many-body correlations of the stable hadronic states forming the medium, in this way going beyond linear density approximation [Leu06]. We rely on the LO temperature and baryon density terms, which give an adequate description of the medium modifications of condensates up to  $T \sim 150$  MeV and nuclear matter saturation density  $n_0 = 0.17 \text{ fm}^{-3} \simeq (110 \text{ MeV})^3$ . To deduce the in-medium behavior of the condensate  $\langle\langle O \rangle\rangle$  the pion and nucleon matrix elements are to be evaluated. They dictate the in-medium changes of condensates, which will be explicated in the following for the famous chiral and gluon condensates.

The pionic matrix element  $\langle \pi | \bar{q}q | \pi \rangle$  is estimated by applying the soft-pion theorem twice [Hat93]:

$$\lim_{\vec{p}, \vec{p}' \rightarrow 0} \langle \pi^a(\vec{p}) | \bar{q}q | \pi^b(\vec{p}') \rangle = -\frac{1}{f_\pi^2} \langle [Q_A^a, [Q_A^b, \bar{q}q]] \rangle_0, \quad (2.114)$$

where  $Q_A^a$  is the iso-vector axial charge (2.106),  $f_\pi$  is the pion decay constant and  $a = 1, 2, 3$ . Using the anti-commutation relations of the quark operators (2.105) one obtains

$$\langle \pi | \bar{q}q | \pi \rangle = \lim_{\vec{p}, \vec{p}' \rightarrow 0} \langle \pi^a(\vec{p}) | \bar{q}q | \pi^b(\vec{p}') \rangle = -\frac{\delta^{ab}}{f_\pi^2} \langle \bar{q}q \rangle_0 \quad (2.115)$$

resulting in the temperature dependence

$$\langle \bar{q}q \rangle_T \simeq \langle \bar{q}q \rangle_0 \left( 1 - \frac{T^2}{8f_\pi^2} \right). \quad (2.116)$$

Comparison of this result with the three-loop calculation in chiral perturbation theory [Ger89] exhibits deviations up to 5 % only, even at  $T = 160$  MeV. For temperatures below 140 MeV, the thermal  $\ell$ QCD results [Bor10] agree with the hadronic resonance gas model, whose leading non-trivial term is given in Eq. (2.116), but show a stronger fall off beyond this temperature [Hoh14].

The nucleon matrix element  $\langle N | \bar{q}q | N \rangle$  merely defines the nucleon sigma term  $\sigma_N = (m_u + m_d) \langle N | \bar{q}q | N \rangle / (2m_N)$ . Using the Hellmann-Feynman theorem  $\frac{\partial}{\partial m_q} m_N = \langle N | \bar{q}q | N \rangle / (2m_N)$  it can be expressed by  $\sigma_N = (m_u + m_d) \frac{\partial}{\partial m_q} m_N$ . Application of the GOR relation (B.23) to eliminate the light-quark masses yields

$$\langle \bar{q}q \rangle_n \simeq \langle \bar{q}q \rangle_0 \left( 1 - \frac{\sigma_N n}{m_\pi^2 f_\pi^2} \right), \quad (2.117)$$

i. e. a decreasing magnitude of the chiral condensate for growing density analogous to the low-temperature approximation (2.116).

The behavior of the chiral condensate at finite temperature (2.116) or baryon density (2.117), where the modulus of the chiral condensate is diminished for an increase in the intensive thermodynamic quantity, has far-reaching implications. Due to its role as an order parameter of chiral symmetry, a reduced magnitude of the chiral condensate may be interpreted as a signal of (partial) chiral restoration at higher temperatures and/or densities. In a chiral restoration scenario, where the system falls back into the Wigner-Weyl realization of chiral symmetry, the chiral condensate would vanish.

The hadronic matrix elements  $\langle h | (\alpha_s/\pi) G^2 | h \rangle$  of the gluon operators can be evaluated using the trace anomaly (2.97). Hence, for the hadron  $h$  one arrives at

$$\langle h | T_\mu^\mu | h \rangle = 2m_h^2 \quad (2.118)$$

$$= -\frac{1}{8} \left( 11 - \frac{2}{3} N_f \right) \langle h | \frac{\alpha_s}{\pi} G^2 | h \rangle + \sum_f m_f \langle h | \bar{f}f | h \rangle, \quad (2.119)$$

where we chose the number of quark flavors  $N_f = 6$ , thus the sum runs over the three light ( $q = u, d, s$ ) and the three heavy ( $Q = c, b, t$ ) quark flavors. By means of the heavy-quark expansion (HQE) the heavy-quark matrix elements are related to the gluon matrix element. Thus, they are eliminated by employing Eq. (3.17). The hadronic gluon matrix element then reads

$$\langle h | \frac{\alpha_s}{\pi} G^2 | h \rangle = -\frac{8}{9} \left( 2m_h^2 - \sum_q m_q \langle h | \bar{q}q | h \rangle \right). \quad (2.120)$$

Utilizing the Hellmann-Feynman theorem  $\frac{\partial}{\partial m_q} m_\pi = \langle \pi | \bar{q}q | \pi \rangle / (2m_\pi)$  for the pion with the GOR relation (B.23) inserted (expressed as a function  $m_\pi(m_q)$ ) one obtains [Hat92a]

$$\langle \pi | \bar{u}u | \pi \rangle = \langle \pi | \bar{d}d | \pi \rangle = \frac{m_\pi^2}{m_u + m_d} \quad \text{and} \quad \langle \pi | \bar{s}s | \pi \rangle = m_\pi^2 \frac{\partial}{\partial m_s} \ln \left( \frac{|\langle \bar{u}u \rangle_0|}{f_\pi^2} \right), \quad (2.121)$$

where  $\langle \pi | \bar{s}s | \pi \rangle$  in Eq. (2.121) can be explicitly calculated in the Nambu–Jona-Lasinio model. Substituting the pionic quark matrix elements in Eq. (2.120) yields the desired quantity

$$\langle \pi | \frac{\alpha_s}{\pi} G^2 | \pi \rangle = -\frac{8}{9} (m_\pi^2 - m_s \langle \pi | \bar{s}s | \pi \rangle) \quad (2.122)$$

which vanishes in the chiral limit,  $m_\pi \rightarrow 0$ . Thus, to LO the gluon condensate

$$\langle \frac{\alpha_s}{\pi} G^2 \rangle_T \simeq \langle \frac{\alpha_s}{\pi} G^2 \rangle_0 - \frac{T^2}{9} (m_\pi^2 - m_s \langle \pi | \bar{s}s | \pi \rangle) \quad (2.123)$$

is temperature independent in that limit.

Applying nucleon states in Eq. (2.120) and introducing the nucleon sigma term  $\sigma_N$  as well as an analogous quantity  $S_N = m_s \langle N | \bar{s}s | N \rangle / (2m_N)$ , measuring the strangeness contribution to the nucleon mass, the matrix element reads [Jin93]

$$\langle N | \frac{\alpha_s}{\pi} G^2 | N \rangle = -\frac{16}{9} m_N (m_N - \sigma_N - S_N). \quad (2.124)$$

The quantity  $S_N$  is commonly parametrized as  $S_N = (\sigma_N - \sigma_N^0) m_s / (m_u + m_d)$ , where one takes  $\sigma_N = 45$  MeV,  $\sigma_N^0 = 35$  MeV (from second order perturbation theory in  $m_s - m_q$ ), and  $m_s / (m_u + m_d) \simeq 13$ . These numerical estimates suggest  $m_N > \sigma_N + S_N$  resulting in a mildly decreasing gluon condensate

$$\langle \frac{\alpha_s}{\pi} G^2 \rangle_n \simeq \langle \frac{\alpha_s}{\pi} G^2 \rangle_0 - \frac{8}{9} (m_N - \sigma_N - S_N) n \quad (2.125)$$

for growing baryon density  $n$ , i. e. at nuclear matter saturation density  $\langle (\alpha_s/\pi) G^2 \rangle_n$  drops to 90 – 95 % of its vacuum value.

In order to study the temperature and baryon density dependences of four-quark condensates  $\langle \bar{q} A q \bar{q}' B q' \rangle$ , where  $A$  and  $B$  denote certain Dirac and color matrices to ensure parity and time reversal invariance, the corresponding pion and nucleon matrix elements are needed, i. e.  $\langle \pi | \bar{q} A q \bar{q}' B q' | \pi \rangle$  and  $\langle N | \bar{q} A q \bar{q}' B q' | N \rangle$ . While the pion matrix elements can be calculated by means of the soft-pion theorem (2.114) [Hat93, Dru02], the nucleon matrix element has to be computed from the overlap of the four-quark operator with an assumed quark structure of the nucleon [Dru03]. Intermediate steps of the computation rely on the factorization hypothesis which is questionable in QCD, cf. Subsec. 3.3.3. Also the medium dependence of many further condensates can only be estimated utilizing model assumptions or from comparison to deep inelastic scattering (DIS) data [Jin93].

## 2.4 Evaluation of QCD sum rules

QCD sum rules offer two evaluation strategies due to the two representations of the current-current correlator (2.1). On the one hand, known phenomenological spectral information or, preferably, the actual spectral density can be utilized to determine QCD parameters such as the condensates, quark masses or the strong coupling constant and, on the other hand, the QCD parameters entering the OPE can be employed to deduce hadronic spectral properties.<sup>11</sup>

<sup>11</sup>Furthermore, QSRs can serve as a consistency check for theoretical hadronic models requiring reasonably small deviations of the QSR's l. h. s. and r. h. s. in a sufficiently wide Borel window [Leu98], see the details below.

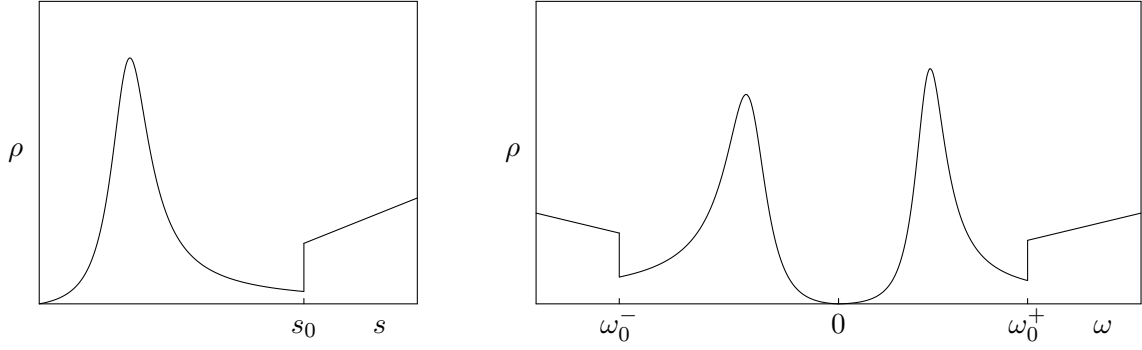


**Figure 2.6:** Sketches of generic spectral densities  $\rho$  comprising the lowest resonances and the continua for vacuum (left panel) and in-medium (right panel) situations.

In order to estimate the spectral properties of the lowest hadronic resonance  $\rho^{\text{res}}$  coupling to the current  $j$ , it is separated from higher excitations forming a continuum  $\rho^{\text{cont}}$  which emerges from the continuum threshold parameter<sup>12</sup>  $s_0$  onwards, i.e. the vacuum spectral density, cf. left panel of Fig. 2.6, is of the form

$$\rho(s) = \Theta(s_0 - s)\rho^{\text{res}}(s) + \Theta(s - s_0)\rho^{\text{cont}}(s). \quad (2.126)$$

The continuum threshold parameter is chosen to be located above the resonance. Representing the higher excitations by a continuum is adequate as higher hadronic states are increasingly short-lived, thus, acquiring large widths which smear out the individual resonances.<sup>13</sup> While for large momenta  $\rho^{\text{cont}}(s) = \text{Im}\Pi^{\text{OPE}}(s)/\pi$  may be considered a valid representation of the continuum, it is mainly justified by its successful application in numerous QSRs. According to Eq. (2.126), the dispersion integral splits into a low-momentum and a high-momentum part and the vacuum QSR reads

$$\begin{aligned} \Pi^{\text{OPE}}(q^2) &= \sum_{n=0}^{N-1} \frac{\Pi^{(n)}(s)|_{s=0}}{n!} q^{2n} \\ &= \int_0^{s_0} ds \left(\frac{q^2}{s}\right)^N \frac{\rho^{\text{res}}(s)}{s - q^2} + \frac{1}{\pi} \int_{s_0}^{\infty} ds \left(\frac{q^2}{s}\right)^N \frac{\text{Im}\Pi^{\text{OPE}}(s)}{s - q^2}. \end{aligned} \quad (2.127)$$

A further assumption is often employed in QSRs to simplify the structure of the continuum part of the spectral density [Rei85, Col01]. In the limit  $q^2 \rightarrow -\infty$ , the dispersion integral satisfies the relation

$$\int_{s_0}^{\infty} ds \left(\frac{q^2}{s}\right)^N \frac{\text{Im}\Pi(s)}{s - q^2} \approx \int_{s_0}^{\infty} ds \left(\frac{q^2}{s}\right)^N \frac{\text{Im}\Pi^{\text{pert}}(s)}{s - q^2}, \quad (2.128)$$

which is dubbed global (or semi-local) quark-hadron duality. The quantity  $\text{Im}\Pi^{\text{pert}}$  denotes the perturbative part of the OPE of the current-current correlator. This assumption is the

<sup>12</sup>The continuum threshold parameter must not be confused with  $s_0$  in Sec. 2.1, which was introduced there to define the radius of a circle around the origin wherein the current-current correlator is analytic.

<sup>13</sup>See Ref. [Shi98] for a detailed discussion of the transition from comb-like toy spectral densities to more realistic ones considering finite width resonances.

attenuated form of the local quark-hadron duality, i.e.  $\text{Im}\Pi(s) \rightarrow \text{Im}\Pi^{\text{pert}}(s)$  for  $s \rightarrow \infty$ . Presuming quark-hadron duality the continuum term  $\text{Im}\Pi^{\text{OPE}}$  in Eq. (2.127) is replaced by  $\text{Im}\Pi^{\text{pert}}$ .

Depending on the evaluation strategy pursued, a phenomenological hadronic model is employed for the resonant part of the spectral density,  $\rho^{\text{res}}$ , in order to determine hadron properties from the QSR, or the experimentally accessible low-energy spectrum may be used directly to gain information about the QCD parameters. While often ansätze are utilized to shape the lowest excitation of the spectral density, cf. Subsec. 2.4.2, moments of the spectral density below the continuum threshold  $s_0$  can provide some model-independent information on the spectral distribution function, cf. Subsec. 2.4.1.

Also in a medium, the spectral density is split into low-energy and high-energy parts. However, the spectral density contains two resonances and continua situated to the left and the right of the origin on the real  $q_0 = \omega$  axis, cf. right panel of Fig. 2.6, representing excitations of the currents  $j$  and  $j^\dagger$ , i.e. hadrons and anti-hadrons. Accordingly, the in-medium QSR for the even and odd parts of the correlator are obtained:

$$\begin{aligned} \Pi_{\text{OPE}}^{\text{even}}(q_0, \vec{q}) &= \frac{1}{2} \sum_{n=0}^{N-1} \frac{\Pi^{(n)}(\omega, \vec{q})|_{\omega=0}}{n!} (q_0)^n (1 + (-1)^n) \\ &= \frac{1}{2} \int_{\omega_0^-}^{\omega_0^+} d\omega \rho^{\text{res}}(\omega, \vec{q}) \frac{q_0^N}{\omega^{N-1}} \frac{(1 + (-1)^N) + \frac{q_0}{\omega} (1 - (-1)^N)}{\omega^2 - q_0^2} \\ &\quad + \frac{1}{2\pi} \left( \int_{-\infty}^{\omega_0^-} + \int_{\omega_0^+}^{\infty} \right) d\omega \text{Im}\Pi^{\text{OPE}}(\omega, \vec{q}) \frac{q_0^N}{\omega^{N-1}} \frac{(1 + (-1)^N) + \frac{q_0}{\omega} (1 - (-1)^N)}{\omega^2 - q_0^2}, \end{aligned} \quad (2.129a)$$

$$\begin{aligned} \Pi_{\text{OPE}}^{\text{odd}}(q_0, \vec{q}) &= \frac{1}{2} \sum_{n=0}^{N-1} \frac{\Pi^{(n)}(\omega, \vec{q})|_{\omega=0}}{n!} (q_0)^{n-1} (1 - (-1)^n) \\ &= \frac{1}{2} \int_{\omega_0^-}^{\omega_0^+} d\omega \rho^{\text{res}}(\omega, \vec{q}) \frac{q_0^{N-1}}{\omega^{N-1}} \frac{(1 - (-1)^N) + \frac{q_0}{\omega} (1 + (-1)^N)}{\omega^2 - q_0^2} \\ &\quad + \frac{1}{2\pi} \left( \int_{-\infty}^{\omega_0^-} + \int_{\omega_0^+}^{\infty} \right) d\omega \text{Im}\Pi^{\text{OPE}}(\omega, \vec{q}) \frac{q_0^{N-1}}{\omega^{N-1}} \frac{(1 - (-1)^N) + \frac{q_0}{\omega} (1 + (-1)^N)}{\omega^2 - q_0^2}. \end{aligned} \quad (2.129b)$$

Often, the continuum threshold parameters are chosen symmetrically w.r.t. the origin, i.e. one takes  $\omega_0^+ = -\omega_0^-$  as an ad hoc assumption.

The major inherent malaise of the QSR framework is that only integrated hadronic spectral properties are probed and only combinations of QCD condensates enter. The accuracy of extracted spectral parameters is therefore limited and isolation of a single condensate,

e. g. a particularly interesting order parameter, is hampered.<sup>14</sup> To improve the sensitivity of QSRs to the lowest excitation of the spectrum a Borel transformation can be applied converting the momentum dependence to a dependence on the Borel mass  $M$ . Thus, the spectral integrals as given in Eqs. (2.127) and (2.129) comprise Laplace transformed integrands, i. e. the spectral densities are integrated with an exponential weight. While subtraction terms are eliminated by virtue of the Borel transformation, higher order power corrections are factorially suppressed improving the convergence of the OPE. The result is a Borel sum of the OPE, where Borel summation is a technique to sum divergent series. The definition and properties of the Borel transformation as well as the relevant expressions are presented in App. D. Applying the Borel transformation to the vacuum QSR (2.127) employing Eq. (D.16) with  $Q^2 = -q^2$ ,  $a = s$ ,  $k = 1$  and  $m = N$  yields

$$\begin{aligned} \mathcal{B} [\Pi^{\text{OPE}}(Q^2)] (M^2) &\equiv \hat{\Pi}^{\text{OPE}}(M^2) \\ &= \int_0^{s_0} ds e^{-s/M^2} \rho^{\text{res}}(s) + \frac{1}{\pi} \int_{s_0}^{\infty} ds e^{-s/M^2} \text{Im} \Pi^{\text{OPE}}(s) \end{aligned} \quad (2.130)$$

and similar expressions for the in-medium sum rules (2.129) with  $Q^2 = -q_0^2$ , where the subtraction terms are eliminated and the polynomial weight in the spectral integral replaced by the exponential. However, one may apply the Borel transform to a  $N$ -fold subtracted dispersion relation  $\Pi/Q^{2m}$  with  $m < N$  in order to further suppress the continuum part by  $1/s^m$  in the spectral integral as commonly employed in twice subtracted  $\rho$  meson QSRs with  $m = 1$ . Of course, in the Borel transform of  $\Pi/Q^{2m}$ ,  $m$  subtraction terms remain which can be easily understood from the point of view of subtracted dispersion relations: the suppression of high-energy contributions has to be compensated for by a more detailed knowledge of the function at the subtraction point [Leu98].<sup>15</sup>

Although the Borel transformation attenuates shortcomings of the QSR method by suppressing the continuum states and higher order power corrections, sufficiently reliable spectral information about the lowest resonance can be extracted only within a certain Borel mass range. This range is a compromise as particularly small or large numerical values of the Borel mass  $M$  influence the sum rule in a two-fold way. While for large  $M$  higher order power corrections are strongly suppressed, contributions to the spectral integral of higher hadronic excitations, only grossly modeled by the continuum, are enhanced ultimately exceeding the contribution of the lowest resonance of the spectrum. The beneficial enhancement of the lowest resonance and the exponential suppression of the continuum for small  $M$  are counteracted by increasing numerical impact of higher order power corrections worsening the convergence behavior of the OPE.

In order to ensure the validity of the QSR, criteria for a maximal and minimal Borel mass are selected. The Borel mass interval estimated on grounds of those criteria is referred to as the Borel window. The commonly chosen criteria on the upper and lower limit of the Borel window are the following [Lei97]: The upper limit  $M_{\text{max}}$  is selected such that the integral over the lowest excitation contributes at least 50 % to the integral over the

---

<sup>14</sup>Weinberg sum rules, introduced below in this thesis, can overcome this limitation to some extent, because they are only sensitive to order parameters of DxSB.

<sup>15</sup>Care needs to be taken here, because a naive approach may lead to opposite medium modifications of the very same hadron from the sum rules of  $\Pi$  and  $\Pi/Q^2$  [Koi95, Hat95], i. e. suppressed in-medium OPE information must be compensated by a relation constraining the in-medium spectral parameters [Koi97].

full spectral function. The lower limit  $M_{\min}$  is evaluated requiring that the highest mass-dimension condensate term considered contributes less than 10 % to the complete OPE. The actually used percentages for individual QSR analyses may vary, but the result should be robust with respect to slight changes of that figures. The existence of a Borel window is a priori not guaranteed. One may face a QSR with very narrow Borel window worsening accuracy of the method, or even a closed Borel window, i. e.  $M_{\max} < M_{\min}$ , causing a failure of the QSR framework.

This method of deducing the Borel window for a certain confidence level associated with the chosen percentage criteria might be contrasted by an approach based on Hölder inequalities [Ben95]. Using these inequalities one can construct fundamental constraints on the QSR that must be satisfied if the sum rule is consistent with its phenomenological relation to the integral over the spectral density. The constraints can be viewed as a test of both the validity of the continuum hypothesis, i. e. the quark-hadron duality above  $s_0$ , and of the lower bound on the Borel mass, i. e.  $M_{\min}$ , beyond which the neglected or unknown effects in the QSR become substantial. Thus, these constraints shift the notion of QSR validity from the Borel window, being an Borel mass range with an associated confidence level, to an admissible region in the  $M$ - $s_0$  plane, providing a minimal Borel mass  $M_{\min}$  for every continuum threshold  $s_0$ .

Having outlined the concept of QSRs, let us summarize the essential content: The correlator (2.1) (the l. h. s.) is cast in a dispersion relation form, where an integral of the discontinuity (or the spectral density) appears as the relevant quantity, while the r. h. s. of (2.1) employs the OPE. Within this thesis, we take the attitude to assume that the r. h. s. quantities (Wilson coefficients and condensates) are known and study the implications for the l. h. s. which encodes hadron properties.

### 2.4.1 Model-independent resonance properties

Extraction of the integrated spectral information concealed in hadronic Green's functions, e. g. the current-current correlator (2.1), calculated by means of an OPE or in the  $\ell$ QCD framework is limited. Model-independent estimates about the shape of the particularly interesting low-energy part of the spectral density  $\rho^{\text{res}}$  may be obtained from moments of the spectral distribution,<sup>16</sup> if multi-resonance structures can be excluded. The center of gravity of the distribution is provided by the first weighted moment

$$\bar{m}^2 = \frac{\int_0^{s_0} ds s e^{-s/M^2} \rho^{\text{res}}(s)}{\int_0^{s_0} ds e^{-s/M^2} \rho^{\text{res}}(s)}, \quad (2.131)$$

where the spectral integrals of the denominator and the numerator can be expressed by the OPE employing the QSR (2.130) and the derivative of Eq. (2.130) w. r. t.  $-1/M^2$ , dubbed derivative sum rule, respectively. Higher central moments

$$\bar{m}_{(n)}^2 = \frac{\int_0^{s_0} ds (s - \bar{m}^2)^n e^{-s/M^2} \rho^{\text{res}}(s)}{\int_0^{s_0} ds e^{-s/M^2} \rho^{\text{res}}(s)} \quad (2.132)$$

<sup>16</sup>Note that not the bare spectral function but  $\rho^{\text{res}}(s)$  weighted by the Borel exponential  $e^{-s/M^2}$  enters the spectral integral of the QSR (2.130).

may be used to estimate the shape of the spectral distribution, i. e. variance  $\bar{m}_{(2)}^2$ , skewness  $\bar{m}_{(3)}^2/\bar{m}_{(2)}^3$  and kurtosis  $\bar{m}_{(4)}^2/\bar{m}_{(2)}^4$  measuring width, asymmetry and flatness of the distribution, respectively. Further odd (even) central moments would give additional information on the asymmetry (flatness) of the spectral distribution. Such higher central moments would be evaluated by means of higher derivative sum rules which have inherent shortcomings as we will dwell on in the following Subsec. 2.4.2.

Euclidean time correlators of hadrons are successfully computed within the scope of  $\ell$ QCD. As also these correlators incorporate the integrated spectral density, the same difficulties in deducing the hadronic spectral properties are encountered. In the lattice community, the maximum entropy method, based on Bayesian inference theory, has been introduced to extract the spectral density from the correlators [Nak99]. These ideas have been adopted to QSR analyses [Gub10], recently. The maximum entropy method which does not fix the functional form of the spectral density seems to be less restrictive than a model ansatz for the resonance, but it relies on a 'default model', used to fix the value of the spectral function at low and high energies, which might influence the results as well. The pending problem of deducing the spectral density from the correlator deserves intense investigations, cf. [Bur13] for a slightly improved Bayesian approach based on reassessed axioms.

### 2.4.2 Resonance properties from a spectral density ansatz

The parametrization of the lowest excitation of the spectrum by a pole,

$$\rho^{\text{res}}(s) = R_h \delta(s - m_h^2), \quad (2.133)$$

is suggested by the spectral density (2.8), where one can identify  $R_h = (2\pi)^3 |\langle \Omega | j(0) | h \rangle|^2$  for a hadron  $h$  at rest, i. e.  $p_h = (m_h, \vec{0})$ , and for  $p_\Omega = 0$ . This simple parametrization of the lowest resonance has been employed to QSR evaluations to estimate hadron masses since the advent of the method. Although application of the admittedly rough model seems not suitable for short-lived states or brought resonances, e. g. the  $\rho$  meson, it yields acceptable results building confidence in the framework.

The center of gravity  $\bar{m}$  (2.131) of a general spectral function  $\rho(s)$  in the low-energy region, i. e.  $s < s_0$ , coincides with the mass parameter  $m_h$  of the pole ansatz (2.133). Thus, the standard QSR evaluation procedure utilizes the normalized first moment of the spectral integral over the low energies, dubbed ratio sum rule by some authors. A further advantage of the pole + continuum ansatz is its small number of parameters. The hadron mass  $m_h$ , the residuum  $R_h$  and the continuum threshold parameter  $s_0$  can be determined from the QSR (2.130) and its derivative w. r. t.  $-1/M^2$  alone, because the continuum threshold parameter is fixed by the requirement of maximal flatness of the mass Borel curve

$$m_h(M) = \sqrt{\frac{1}{\tilde{\Pi}(M)} \frac{d\tilde{\Pi}(M)}{d(-1/M^2)}} \quad (2.134)$$

and the residuum Borel curve

$$R_h(M) = e^{m_h^2/M^2} \tilde{\Pi}(M) \quad (2.135)$$



in the Borel window with  $\tilde{\Pi} = \hat{\Pi}^{\text{OPE}} - \hat{\Pi}^{\text{cont}}$  and  $\hat{\Pi}^{\text{cont}}(M) = \int_{s_0}^{\infty} ds e^{-s/M^2} \rho^{\text{cont}}(s)$ . The spectral parameters are extracted consecutively from these equations, where the flatness can be quantified as<sup>17</sup>

$$d(s_0) = \frac{1}{M_{\text{max}}(s_0) - M_{\text{min}}} \int_{M_{\text{min}}}^{M_{\text{max}}(s_0)} dM [m_h(M; s_0) - m_h(s_0)]^2, \quad (2.136)$$

where  $m_h(s_0)$  is obtained from Eq. (2.134) averaged within the Borel window. Once the continuum threshold parameter  $s_0$  is fixed by requiring maximal flatness, i. e.

$$d(s_0) = \min_{s'_0 > m_h} d(s'_0), \quad (2.137)$$

the corresponding  $m_h$  provides the hadron mass parameter. Subsequently, the Borel window averaged residuum parameter  $R_h$  is estimated from Eq. (2.135) employing the average Borel mass parameter  $m_h$  or the mass Borel curve  $m_h(M)$ .

The requirement of flatness in the Borel window emerges from the derivation of the mass Borel curve (ratio QSR) using

$$\frac{d}{d(1/M^2)} \tilde{\Pi}(M^2) = \frac{d}{d(1/M^2)} R_h e^{-m_h^2/M^2} \quad (2.138)$$

$$= -m_h^2 \tilde{\Pi}(M^2) + \frac{\partial \tilde{\Pi}}{\partial m_h} \frac{dm_h}{d(1/M^2)} + \frac{\partial \tilde{\Pi}}{\partial R_h} \frac{dR_h}{d(1/M^2)}. \quad (2.139)$$

If this requirement cannot be met for a physical continuum threshold parameter  $s_0$ , the ratio QSR might give wrong results. In this case, one should not rely on the ratio QSRs [Lei97], especially not on higher derivative QSRs, where exemplarily the  $n$ -th derivative QSR of the  $\rho$  meson in generic form is given by [Hil12c]<sup>18</sup>

$$\begin{aligned} R_h m_h^{2n} e^{-m_h^2/M^2} &= \int_0^{s_0} ds s^{n-1} \text{Im} \tilde{\Pi}(s) e^{-s/M^2} \\ &= n! c_0 M^2 \left[ 1 - e^{-s_0/M^2} \sum_{k=0}^n \frac{(s_0/M^2)^k}{k!} \right] + (-1)^n \sum_{k=0}^{\infty} \frac{c_{k+n+1}}{k! M^{2(k+n)}}, \end{aligned} \quad (2.140)$$

because of three main reasons [Jin95, Lei97]: (i) The importance of the perturbative term increases for increasing  $n$ , due to the  $n!$  factor, implying that higher derivative QSRs probe the continuum instead of the resonance. (ii) Power corrections proportional to  $c_1, \dots, c_n$  do not contribute to the  $n$ -th derivative sum rule, i. e. if one truncates the OPE, part or

<sup>17</sup>While the presented criterion utilizes the deviation  $d(s_0)$  from mean in the  $L^2$  norm an extension to the  $L^p$  norm is conceivable producing the supremum norm for  $p \rightarrow \infty$ .

<sup>18</sup>The here introduced OPE coefficients  $c_i$  of the power corrections are related to the Wilson coefficients  $C_j$  and the condensates  $\langle \Omega | O_j | \Omega \rangle$  in Eq. (2.26). In order to keep track of the derivatives w. r. t.  $-1/M^2$ , the expansion in condensates is rewritten in a power series in  $1/M^2$  such that the coefficients  $c_i$  contain all condensates of mass dimension  $2i$  and the momentum independent factors of the corresponding coefficients  $C_j$ .

all of the non-perturbative information will be lost in this derivative sum rule. (iii) In the original QSR, the power correction  $c_i$  is suppressed by a factor of  $1/(i-1)!$ , while it is only suppressed by  $1/k! = 1/(i-n-1)!$  in the  $n$ -th derivative sum rule ( $i > n$ ) implying a much slower convergence of the OPE and thus, making it even more restrictive to define the lower Borel window boundary. Following the same reasoning, the accuracy of the information on the spectral shape from higher moments of the spectral distribution (2.132) must be doubted, because they build on higher derivative sum rules as well.

One may also evaluate QSRs by expanding the exponential in the spectral integral and a term-by-term comparison in Eq. (2.130) giving a set of QSRs for moments of the spectral density. The first moments obtained this way are advocated by some authors [Wei00] due to their independence of the auxiliary parameter  $M$  and the absence of higher mass dimension condensates with notoriously poorly known numerical values. However, these moments are essentially derivative sum rules evaluated at  $1/M^2 = 0$  which is far above the actual Borel window, i.e. the continuum is probed instead of the resonance. The sensitivity of these moments on the spectral shape of the lowest resonance seems to be insufficient, such that extracted spectral properties must be questioned as well as the discriminating potential of the moments whether the QSRs are compatible with a particular hadronic model.

The Monte-Carlo QSR analysis suggested in Ref. [Lei97] does genuinely rely on the original QSR (2.130) avoiding the shortcomings of derivative sum rules (2.140) altogether. This analysis procedure, where hadronic parameters of the spectral density ansatz are extracted by means of a maximum likelihood method for Gaussianly distributed input parameters, allows for a rigorous uncertainty analysis. The details of the Monte-Carlo QSR method are outlined in App. E. So far, the Monte-Carlo analysis has been done for the  $\rho$  meson and the nucleon only, which feature well-performing QSRs and have been extensively studied. The  $\rho$  channel is most favorable from the point of view of applications of the SVZ sum rules. In a sense, this is a dream case: the role of the continuum with respect to  $\rho$  is as tempered as it can possibly be, and higher (unknown) condensates in the truncated condensate expansion show up at remarkably low values of  $M^2$  so that the working window is comfortably wide [Shi98]. The successful application of the Monte-Carlo QSR analysis to a wider range of hadrons is still pending. We follow the conservative approach using the first derivative sum rule for the mass Borel curve being aware of its limited reliability if the mass Borel curve is not sufficiently flat in the Borel window, but we refrain from using higher order derivative sum rules. Nonetheless, the Monte-Carlo QSR analysis is a promising tool for extracting spectral properties of hadrons which are not biased from derivative sum rules given that a reliable minimization procedure is employed.

In a strongly interacting medium, affecting hadrons and anti-hadrons differently, e.g. non-self-adjoint mesons embedded in nuclear matter, the odd OPE does not vanish a priori and the spectral parameters double:

$$\rho^{\text{res}}(\omega, \vec{0}) = R_+ \delta(\omega - m_+) + R_- \delta(\omega + m_-) \quad (2.141)$$

(cf. the schematic in-medium spectral density in Fig. 2.6 right panel). Hence, the Borel transformed even sum rule ( $e \equiv \hat{\Pi}^{\text{even}}(M^2) = m_+ R_+ e^{-m_+^2/M^2} + m_- R_- e^{-m_-^2/M^2}$ ) and odd sum rule ( $o \equiv \hat{\Pi}^{\text{odd}}(M^2) = R_+ e^{-m_+^2/M^2} - R_- e^{-m_-^2/M^2}$ ) are coupled, cf. Eqs. (2.129). Introducing a mass centroid  $\bar{m}_h = (m_+ + m_-)/2$  and mass splitting  $\Delta m_h = (m_+ - m_-)/2$  they

can be disentangled by a generalization of Eq. (2.134) [Hil09]

$$\Delta m_h(M) = \frac{1}{2} \frac{oe' - eo'}{e^2 + oo'}, \quad (2.142)$$

$$\bar{m}_h(M) = \sqrt{\Delta m_h^2 - \frac{ee' + (o')^2}{e^2 + oo'}}, \quad (2.143)$$

where here, for brevity, a prime denotes the derivative w.r.t.  $1/M^2$ . If one furthermore decomposes  $R_{\pm} = \bar{R}_h \pm \Delta R_h$ , the even sum rule  $\propto \bar{m}_h \bar{R}_h e^{-\bar{m}_h^2/M^2}$  exhibits its dependence on averaged  $h + \bar{h}$  properties while the odd sum rule  $\propto (\Delta R_h - 2\Delta m_h \bar{R}_h \frac{\bar{m}_h}{M^2}) e^{-\bar{m}^2/M^2}$  reveals its relation to the  $h - \bar{h}$  splitting which vanishes for self-adjoint hadrons  $h$  and at zero nucleon density. Obviously, the residuum Borel curves  $R_{\pm}(M)$  can be conveniently deduced from the original even and odd sum rules.

A broad resonance in the low-energy region of the spectral density may be adequately parametrized by a Breit-Wigner distribution [Hat93]

$$\rho^{\text{res}}(s) = \frac{F_h}{\pi} \frac{m_h \Gamma_h}{(s - m_h^2)^2 + m_h^2 \Gamma_h^2}. \quad (2.144)$$

In contrast to the pole ansatz characterized by a residuum  $R_h$  (here:  $F_h$ ) and the hadron mass  $m_h$ , this distribution contains a further parameter  $\Gamma_h$  describing the width of the spectral distribution. However, QSRs are hardly sensitive on the width  $\Gamma_h$  of the distribution (2.144), because it probes the integrated spectral density. One may circumvent this problem by calculating the decay constant  $f_h^2 = R_h/m_h^2$  from the pole ansatz first and subsequently computing the rate for the related decay of the hadron using  $f_h$  [Hat93, Nar99]. This rate coincides with the desired (partial) width  $\Gamma_h$  for  $\Gamma_h \ll m_h$  [Pes95].

Anyway, the three parameters of the above ansatz (2.144) can not be extracted from the standard procedure employing the original QSR and its first derivative sum rule alone (analogous to Eqs. (2.135) and (2.134), respectively). In order to actually fix three resonance parameters one is forced to use a further derivative sum rule. Otherwise, only relations among the spectral parameters can be obtained, e.g. mass-width correlations [Hil12c]. Utilizing a more complex spectral ansatz one faces the same problems in an enhanced manner, where even more spectral parameters are to be determined from the same set of equations. Thus, relying on the original QSRs and their first derivatives alone, does not allow for the evaluation of even and odd in-medium sum rules with complicated spectral ansätze which produce unique results for the doubled parameters, analogous to Eq. (2.141). However, if the QSR study focuses on in-medium changes of hadronic spectral properties one might choose a sophisticated ansatz, e.g. Breit-Wigner distributions with energy dependent widths and taking production thresholds into account. If good reasons can be provided one may allow for only two of the parameters, optimized to reproduce experimental vacuum data, to deviate from their vacuum values.



### 3 Medium modifications of D mesons

The D meson has been considered the 'hydrogen problem' of QCD. Its characteristics resemble those of a hydrogen atom, because it is a bound state with vastly different mass scales – a particularly light quark ( $q$ ) of up or down flavor and a heavy charm quark ( $Q$ ) – albeit with strongly interacting particles. Exposing a hydrogen atom to electromagnetic fields alters the properties of the level scheme known as Stark and Zeeman effects. Similarly, the D meson is expected to exhibit changing properties in a strongly interacting environment. Medium modifications of D mesons have become an interesting topic in recent years, since open charm mesons and charmonium serve as probes of hot nuclear matter and deconfinement effects [Fri11]. Mesons with charm (or bottom) can serve equally well as probes of dense or even saturated nuclear matter (cf. [Tol09, Tol13, Kum10, Kum11, Bla12, He13, Yas13a, Yas13b, Yas14] for recent works and further references). For such theoretical investigations the finite-density QSRs look promising [Hay00, Hil09, Zsc11, Wan11, Wan13]. However, these studies are restricted hitherto to condensate contributions up to mass dimension 5. Motivated by the significant contributions of four-quark condensate terms to the  $\rho$  meson QSR we aim for higher order contributions of mass dimension 6 to study their impact on the in-medium D meson QSR. This chapter is based on the results presented in Ref. [Buc15b] as well as in Ref. [Buc16b] dealing with a vital technical aspect and its implications.

#### 3.1 Motivation

Among the central issues of hadron physics in the light-quark sector are chiral symmetry and its breaking pattern. If one relates spontaneous chiral symmetry breaking with the non-zero value of the chiral condensate in vacuum,  $\langle \bar{q}q \rangle_0 \simeq (-245 \text{ MeV})^3$ , one is tempted to ask for observable consequences of chiral restoration, i. e. to which extent do hadron observables change under a change of the chiral condensate [Wei94]. In LO, at non-zero temperature  $T$  and/or density  $n$ , the chiral condensate is modified according to  $\langle \bar{q}q \rangle_{T,n} \simeq \langle \bar{q}q \rangle_0 \left( 1 - \frac{T^2}{8f_\pi^2} - \frac{\sigma_N n}{m_\pi^2 f_\pi^2} \right)$  (cf. Eqs. (2.116) and (2.117)), i. e. it is diminished relative to its vacuum value. Chiral restoration may be understood accordingly as being necessarily accompanied by  $\langle \bar{q}q \rangle_{T,n} \rightarrow 0$ . Also further condensates, especially four-quark condensates, exhibit non-invariant behavior under chiral transformations [Leu06, Tho07, Hil11]. Such condensates are candidates for order parameters of spontaneous chiral symmetry breaking and restoration, similarly to the chiral condensate, cf. Subsec. 2.3.2. While deconfinement accompanied by dissolving hadron states is the obviously strongest medium modification of hadrons, more modest modifications are envisaged during the last two decennia (cf. [Hat93, Jin93, Coh95] for surveys on medium modifications of hadrons). The seminal paper by Hatsuda and Lee [Hat92b] devices a scenario where spectral properties of mesons (most notably condensed into moments characterizing masses and widths) do change in a strongly interacting medium. Clearly, there are further condensates which change at non-zero temperature and density [Hat93, Jin93].

In order to judge the impact of particular condensates on the hadronic spectral function, we estimate their contributions to the OPE side of the QSR (2.130). For the  $\rho$  meson at rest the Borel transformed OPE series reads<sup>1</sup>

$$\widehat{\Pi}^{(\rho)}(M^2) = C_0^{(\rho)} M^2 + \frac{C_1^{(\rho)}}{M^2} \langle \bar{q}q \rangle + \frac{C_2^{(\rho)}}{M^2} \langle \frac{\alpha_s}{\pi} G^2 \rangle + \frac{C_3^{(\rho)}}{M^4} \langle \mathcal{O}_3 \rangle + \dots, \quad (3.1)$$

where the superscript ' $(\rho)$ ' is a reminder that, for the moment, we are talking about the  $\rho$  meson which has been analyzed extensively [Fri11]. Writing schematically  $\langle \mathcal{O}_3 \rangle = \kappa \langle \bar{q}q \rangle^2$  with a fudge factor  $\kappa$  one observes in fact that, for Borel masses  $M \sim 1$  GeV, the chiral condensate term  $\propto C_1^{(\rho)}/M^2$  is numerically suppressed, and the gluon condensate term  $\propto C_2^{(\rho)}/M^2$  as well as the four-quark condensate combinations  $\propto C_3^{(\rho)}/M^4$  are of the same order of magnitude for a typical choice  $\kappa \sim 2$  [Rap10]:

$$\begin{aligned} \widehat{\Pi}^{(\rho)}(M^2) &= \frac{1 + \frac{\alpha_s}{\pi}}{8\pi^2} M^2 + \frac{m_q}{M^2} \langle \bar{q}q \rangle + \frac{1}{24M^2} \langle \frac{\alpha_s}{\pi} G^2 \rangle - \frac{112\pi\alpha_s\kappa}{81M^4} \frac{1}{2} \langle \bar{q}q \rangle^2 + \dots \\ &= \frac{M^2}{8\pi^2} \left( 1.11 - 0.006 \frac{\text{GeV}^4}{M^4} + 0.039 \frac{\text{GeV}^4}{M^4} - 0.026 \frac{\text{GeV}^6}{M^6} + \dots \right), \end{aligned} \quad (3.2)$$

where  $\alpha_s = 0.35$ ,  $m_q = 0.005$  GeV,  $\langle \bar{q}q \rangle = (-0.245 \text{ GeV})^3$  and  $\langle (\alpha_s/\pi) G^2 \rangle = 0.012 \text{ GeV}^4$  have been used.

While the separation of scales in the OPE seems unproblematic in the light-quark sector extra effort is required to include heavy quarks, because their masses enter the scheme as additional scales. Nevertheless, since other methods (such as  $\ell$ QCD evaluations, Schrödinger equation approaches with potentials, Dyson-Schwinger–Bethe-Salpeter equations, etc.) are at our disposal, a mutual judging is of interest. In the  $qQ$  sector<sup>2</sup> the chiral condensate appears in the scale-dependent combination<sup>3</sup>  $m_Q \langle \bar{q}q \rangle$ , i.e. the heavy-quark mass  $m_Q$  acts as an amplification factor of the chiral condensate term with sizable impact on spectral properties of  $qQ$  mesons [Hil11]. Furthermore, the in-medium sum rule has an even and an odd part w.r.t. the meson energy  $p_0$ , cf. Eqs. (2.20), since particles and anti-particles are to be distinguished and the corresponding dispersion integrals run over positive and negative frequencies. In the light chiral limit,  $m_q \rightarrow 0$ , the first known terms have the structure [Hil09, Zsc11]

$$\widehat{\Pi}^{\text{even}}(M^2) = C_0 + e^{-m_Q^2/M^2} \sum_{k=1}^6 c_k^{\text{even}}(M^2) \langle \mathcal{O}_k \rangle^{\text{even}}, \quad (3.3a)$$

$$\widehat{\Pi}^{\text{odd}}(M^2) = e^{-m_Q^2/M^2} \sum_{k=1}^3 c_k^{\text{odd}}(M^2) \langle \mathcal{O}_k \rangle^{\text{odd}} \quad (3.3b)$$

with the perturbative term  $C_0$  and the condensates  $\langle \mathcal{O}_1 \rangle^{\text{even}} = \langle \bar{q}q \rangle$ ,  $\langle \mathcal{O}_2 \rangle^{\text{even}} = \langle \bar{q}g\sigma Gq \rangle$ ,  $\langle \mathcal{O}_3 \rangle^{\text{even}} = \langle (\alpha_s/\pi) G^2 \rangle$ ,  $\langle \mathcal{O}_4 \rangle^{\text{even}} = \langle (\alpha_s/\pi) [(vG)^2/v^2 - G^2/4] \rangle$ ,  $\langle \mathcal{O}_5 \rangle^{\text{even}} = \langle q^\dagger i D_0 q \rangle$  and

<sup>1</sup>The ellipses in the displayed series denote higher power corrections which may break down the expansion, thus, requiring a careful evaluation of the OPE's convergence behavior.

<sup>2</sup>We use henceforth the shorthand notation  $qQ$  for  $\bar{q}Q$  and  $\bar{Q}q$  mesons. The correlators of mesons  $\bar{q}Q$  and anti-mesons  $\bar{Q}q$  satisfy the relation  $\Pi_{\bar{q}Q}(p) = \Pi_{\bar{Q}q}(-p)$  [Zsc11]. The  $D$  meson four-momentum is denoted by  $p$  instead of  $q$  in this chapter in order to obtain a clear distinction from the light-quark operator  $q$ .

<sup>3</sup>Although, the running heavy-quark mass (2.77) compensates the scale-dependence of the running chiral condensate (2.89) to one-loop order, we tentatively refer to  $m_Q \langle \bar{q}q \rangle$  as a scale-dependent combination in contrast to  $m_q \langle \bar{q}q \rangle$  since  $m_q$  and  $m_Q$  might have different anomalous dimensions in higher loop orders.

$\langle \mathcal{O}_6 \rangle^{\text{even}} = \langle \bar{q} [D_0^2 - g\sigma G/8] q \rangle$  as well as  $\langle \mathcal{O}_1 \rangle^{\text{odd}} = \langle \bar{q}^\dagger q \rangle$ ,  $\langle \mathcal{O}_2 \rangle^{\text{odd}} = \langle \bar{q}^\dagger D_0^2 q \rangle$  and  $\langle \mathcal{O}_3 \rangle^{\text{odd}} = \langle \bar{q}^\dagger g\sigma G q \rangle$ . The coefficients  $c_k^{\text{even,odd}}(M^2)$  are the Wilson coefficients modulo a common factor  $e^{-m_Q^2/M^2}$ . Without knowledge of the Wilson coefficients of the four-quark condensates it is hardly possible to estimate their impact on  $\hat{\Pi}$  in the sum rule and a simple order-of-magnitude comparison can be misleading. (For example, in the above  $\rho$  meson sum rule (3.2),  $\langle (\alpha_s/\pi) G^2 \rangle = 0.012 \text{ GeV}^4$  and  $\langle \bar{q}q \rangle^2 = 0.00022 \text{ GeV}^6$  would one lead to guess that the latter condensate contribution is negligible at  $M \sim 1 \text{ GeV}$ . However, it is the Wilson coefficient  $C_2^{(\rho)} = 1/24$  which makes the gluon contribution comparable to the four-quark condensate term with  $C_3^{(\rho)} = (112/81)\pi\alpha_s$ .) Therefore, a calculation of Wilson coefficients of the in-medium four-quark condensates entering QSRs for  $qQ$  mesons is mandatory. This is the goal of the present chapter. Equipped with these four-quark condensate contributions one can extend previous OPE/QSR studies of spectral properties of pseudo-scalar  $qQ$  mesons. Furthermore, and more importantly, one is able to identify four-quark condensate contributions which are not invariant under chiral transformations and, thus, may serve as elements of order parameters of spontaneous chiral symmetry breaking. As pointed out in Sec. 4.1 and Ref. [Hil11], also in  $qQ$  meson systems, the splitting of the spectral densities between parity partners is driven by such order parameters.

Although four-quark condensates can influence the in-medium properties significantly, as recalled above for the  $\rho$  meson, no light four-quark condensate contributions of the OPE have been used so far to improve the evaluation of in-medium modifications of  $qQ$  mesons. Accordingly, we are going to include here light four-quark condensate contributions, thus, extending the previous studies.

The common problem of presently poorly known numerical values of four-quark condensates requires a further treatment of these contributions. Thus, we resort here to the argument that heavy quarks are static and do not condense, i.e. one neglects all contributions of condensates containing heavy-quark operators [Rei85]. To arrive at an order of magnitude estimate of their impact, light four-quark condensates are eventually factorized and equipped with fudge factors to correct potential failure of the ground state saturation hypothesis.

Including four-quark condensates is a difficult task and has only been done in vacuum  $qQ$  systems employing factorization up to now. In vacuum, the number of terms involves only a small amount of the possible in-medium contributions. Furthermore, assuming vacuum saturation from the very beginning in order to factorize four-quark condensates simplifies evaluations drastically. This is the reason why even in vacuum only few papers deal with non-factorized four-quark condensates [Hil12c, Hoh14], whereby even factorized four-quark condensates have never been considered in  $qQ$  systems in the medium.

## 3.2 QCD sum rules for $qQ$ mesons

We consider the causal current-current correlator (2.1) in LO perturbation theory  $\propto \alpha_s^0$

$$\Pi(p) = i \int d^4x e^{ipx} \langle \text{T} [j(x) j^\dagger(0)] \rangle \quad (3.4)$$

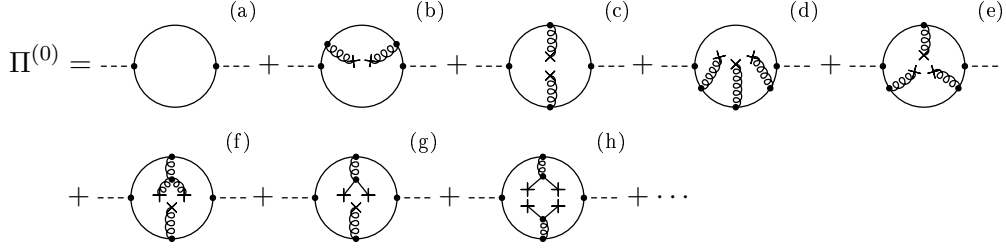


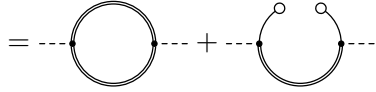
**Figure 3.1:** Diagrammatic representation of the contribution (3.7a) to the current-current correlator, where a selection of topologically relevant diagrams is displayed. Solid lines stand for free quark propagators, wiggly lines are for gluons and crosses symbolize local quark or gluon condensation. In our expansion scheme, we retain only the diagrams (a)–(c) contributing to the perturbative term  $C_0$ , (a), and yielding the Wilson coefficients  $c_3^{\text{even}}$  and  $c_4^{\text{even}}$ , (b) and (c), in Eq. (3.3a) since the other ones, (d)–(h), are of higher order in  $g$ .

with the interpolating pseudo-scalar current

$$j(x) = i\bar{q}(x)\gamma_5 Q(x). \quad (3.5)$$

The Wilson coefficients are calculated using the background field method in Fock-Schwinger gauge  $x^\mu A_\mu(x) = 0$ . The general ideas of the calculus are provided in Sec. 2.2, while a compact description in LO perturbation theory is given in [Zsc11, Hil11]. Utilizing Wick's theorem the correlator (3.4) decomposes as

$$\Pi(p) = \Pi^{(0)}(p) + \Pi^{(2)}(p) \quad (3.6)$$



with

$$\Pi^{(0)}(p) = -i \int d^4x e^{ipx} \langle\langle : \text{Tr}_{c,D} [S_q(0, x) \gamma_5 S_Q(x, 0) \gamma_5] : \rangle\rangle, \quad (3.7a)$$

$$\Pi^{(2)}(p) = + \int d^4x e^{ipx} \langle\langle : \bar{Q}(0) \gamma_5 S_q(0, x) \gamma_5 Q(x) + \bar{q}(x) \gamma_5 S_Q(x, 0) \gamma_5 q(0) : \rangle\rangle, \quad (3.7b)$$

where terms associated with disconnected diagrams are omitted. The notation  $\text{Tr}_{c,D}$  means traces over color and Dirac indices respectively.  $\Pi^{(0)}(p)$  denotes the fully Wick-contracted term and  $\Pi^{(2)}(p)$  is the two-quark term, i.e. the superscript number in parentheses refers to the number of Wick-uncontracted quark field operators of the interpolating currents. The full light-quark propagator in the gluonic background field is defined as  $S_q(x, y) = -i \langle T [q(x) \bar{q}(y)] \rangle$  (and with  $q \rightarrow Q$  for the full heavy-quark propagator, cf. App. C.3 for further details). In the diagrammatic representation of the decomposition (3.6), dashed lines denote the pseudo-scalar current, double lines symbolize full quark propagators whereas single lines are for free quark propagators, and circles denote non-local quark condensation.

Employing the expansion (2.44) in (3.7a) generates a series of terms where a (few) soft gluon(s) couple to quark, gluon and quark-gluon condensates (cf. Fig. 3.1), while an analog



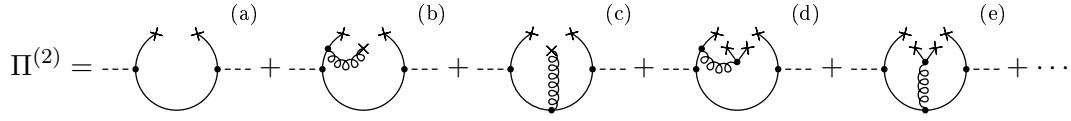


**Figure 3.2:** Diagrammatic representation of the contribution (3.7b), where a selection of topologically relevant diagrams is displayed as in Fig. 3.1, too.

series emerges from (3.7b) utilizing the covariant expansion (2.35) of the quark operator additionally, see Fig. 3.2.

Up to mass dimension 5 the corresponding infra-red stable Wilson coefficients can be found in [Hil09, Zsc11], providing coefficients for the vacuum- and medium-specific quark, gluon and mixed quark-gluon condensates listed below Eq. (3.3). These refer to diagrams (a)–(c) in Fig. 3.1 and (a)–(c) in Fig. 3.2 as well as diagrams associated to non-local condensation. Using the formulae in [Zsc11, Hil11] one also obtains Wilson coefficients of light four-quark condensates, where the corresponding tree-level diagrams (cf. Fig. 3.2, diagrams (d) and (e)) contain one soft-momentum gluon line.

Since we truncate here the series expansion of (3.7a) and (3.7b) at order  $g^2$ , light four-quark condensate contributions arise only from (3.7b), i. e. diagrams (d) and (e) in Fig. 3.2. The other diagrams in Fig. 3.2 refer to the two-quark (a) and the quark-gluon condensate contributions (b) and (c), respectively.

### 3.3 Four-quark condensate contributions

#### 3.3.1 Wilson coefficients

We focus now on the evaluation of the light-quark condensate contributions in mass dimension 6 containing the particularly interesting four-quark condensates.<sup>4</sup> For a handy notation, we denote by  $\Pi_{\text{dim}6}$  those contributions to  $\Pi^{(2)}$ , cf. (3.6), where dimension-6 light-quark condensates are involved (e. g. the four-quark condensate contributions in diagrams (d) and (e) in Fig. 3.2). We note that the gluon in the contributions to  $\Pi^{(2)}$  may have an arbitrarily small momentum, and thus they are dubbed soft-gluon contributions. However, also tree-level four-quark contributions exist, where the gluon must carry the full momentum  $p$  of the meson (cf. Fig. 3.3). These contributions are dubbed hard-gluon ones, and they arise with the NLO interaction term inserted into the correlator [Shi79, Pas84, Nar07]. However, their corresponding condensates contain heavy-quark operators and are neglected according to arguments in [Rei85, Nar05]: heavy quarks do hardly condense. In principle, heavy-quark condensates could be considered rigorously using the HQE, where the condensate is expanded in inverse powers of the heavy-quark mass. Unfortunately, for in-medium condensates of mass dimension 6 this procedure leads to numerous unknown condensates which are merely used to approximate the magnitude of the heavy-quark condensate, i. e. an

<sup>4</sup>In medium, four-quark condensates can not be considered solely, but inclusion of corresponding light-quark condensates in mass dimension 6, which can not be reduced to four-quark condensates, is required in order to ensure a continuous transition to the vacuum (cf. App. C.3 for technical details).

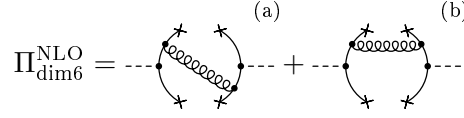


**Figure 3.3:** Diagrammatic representation of hard-gluon contributions giving tree-level four-quark condensate terms for the correlator in NLO perturbation theory  $\propto \alpha_s^1$ .

inherently small quantity compared to light-quark condensates. Therefore, we neglect such heavy-quark terms in the present analysis, but provide the description how to generalize the original vacuum HQE to in-medium situations in Sec. 3.6. Note that we also disregard higher order light four-quark condensate contributions  $\propto g^{2n}$  with  $n \geq 2$ , such as diagram (h) in Fig. 3.1.

In the light chiral limit,  $m_q \rightarrow 0$ , the exact result reads

$$\begin{aligned}
 \Pi_{\text{dim6}}(p) = & \frac{1}{3} \frac{1}{(p^2 - m_Q^2)^2} \left( 1 + \frac{1}{2} \frac{m_Q^2}{p^2 - m_Q^2} - \frac{1}{2} \frac{m_Q^4}{(p^2 - m_Q^2)^2} \right) g^2 \langle\langle :O_1: \rangle\rangle \\
 & + \frac{1}{9} \frac{1}{(p^2 - m_Q^2)^3} \left( p^2 - 4 \frac{(vp)^2}{v^2} \right) \left[ \langle\langle :g^2 O_1 - \frac{2}{v^2} (g^2 O_2 - 2g O_3 + 6g O_4): \rangle\rangle \right. \\
 & \quad - \langle\langle :g^2 O_1 - \frac{2}{v^2} (g^2 O_2 + g O_5): \rangle\rangle + \frac{2}{v^2} \langle\langle :g^2 O_2 + 3g O_5 - g O_6: \rangle\rangle \\
 & \quad \left. + \frac{2}{v^2} g \langle\langle :O_3: \rangle\rangle - \frac{3}{2} \langle\langle :3g^2 O_1 - \frac{4}{v^2} (g^2 O_2 + 2g O_4 - g O_7): \rangle\rangle \right] \\
 & - \frac{2}{15} \frac{1}{(p^2 - m_Q^2)^4} \left( p^4 - 7p^2 \frac{(vp)^2}{v^2} + 6 \frac{(vp)^4}{v^4} \right) \left[ \frac{2}{v^2} g \langle\langle :O_3: \rangle\rangle \right. \\
 & \quad \left. + \langle\langle :g^2 O_1 - \frac{2}{v^2} (g^2 O_2 - 2g O_3 + 6g O_4): \rangle\rangle \right] \\
 & + \frac{1}{30} \frac{1}{(p^2 - m_Q^2)^4} \left( p^4 - 12p^2 \frac{(vp)^2}{v^2} + 16 \frac{(vp)^4}{v^4} \right) \langle\langle :g^2 O_1 - \frac{48}{v^4} O_8: \rangle\rangle \\
 & - 2 \frac{m_Q}{(p^2 - m_Q^2)^3} \frac{(vp)}{v^2} \left[ g^2 \langle\langle :O_9: \rangle\rangle + 2g (\langle\langle :O_{10}: \rangle\rangle + \langle\langle :O_{11}: \rangle\rangle) \right. \\
 & \quad \left. - \frac{1}{3} g \langle\langle :O_{12}: \rangle\rangle + \frac{1}{3} g \langle\langle :O_{13}: \rangle\rangle \right] \\
 & + \frac{8}{3} \frac{m_Q}{(p^2 - m_Q^2)^4} \frac{(vp)}{v^2} \left( p^2 - \frac{(vp)^2}{v^2} \right) \left[ g^2 \langle\langle :O_9: \rangle\rangle + \frac{3}{2} g \langle\langle :O_{10}: \rangle\rangle \right] \\
 & - 8 \frac{m_Q}{(p^2 - m_Q^2)^4} \frac{(vp)}{v^4} \left( p^2 - 2 \frac{(vp)^2}{v^2} \right) \langle\langle :O_{14}: \rangle\rangle, \tag{3.8}
 \end{aligned}$$

where the operators  $O_k$  are listed in Tab. 3.1. The incorporated four-quark operators are obtained from the perturbative quark propagator exploiting the gluonic EoM (A.19). Even in medium, the number of such operators is limited, because the EoM predetermines Dirac and color structures. Current-current correlators with a single quark flavor  $q$  form three

**Table 3.1:** List of light-quark operators of mass dimension 6 forming condensates which enter the results for soft-gluon diagram contributions to  $\Pi^{(2)}$  (cf. Fig. 3.2) emerging from (3.7b).  $\sum_f$  means summing over light-quark flavors  $u, d, s$ . The quantity  $\not{v}$  denotes the medium four-velocity contracted with a Dirac matrix and  $(vD)$  its contraction with the covariant derivative.

$k$	$O_k$	$k$	$O_k$	$k$	$O_k$
1	$\bar{q}\gamma^\nu t^A q \sum_f \bar{f}\gamma_\nu t^A f$	6	$\bar{q}\not{v}\sigma^{\nu\mu}[(viD), G_{\nu\mu}]q$	11	$\bar{q}(vi\overleftrightarrow{D})\sigma Gq$
2	$\bar{q}\not{v}t^A q \sum_f \bar{f}\not{v}t^A f$	7	$\bar{q}i\overleftrightarrow{D}_\mu\gamma_5\not{v}G_{\nu\lambda}q\varepsilon^{\mu\nu\lambda\tau}v_\tau$	12	$\bar{q}\sigma^{\mu\nu}[iD_\mu, G_{\nu\lambda}]v^\lambda q$
3	$\bar{q}(vi\overleftrightarrow{D})\sigma G\not{v}q$	8	$\bar{q}(vi\overleftrightarrow{D})^3\not{v}q$	13	$\bar{q}\sigma^{\nu\mu}[(viD), G_{\nu\mu}]q$
4	$\bar{q}(v\overleftrightarrow{D})\gamma^\mu G_{\nu\mu}v^\nu q$	9	$\bar{q}t^A q \sum_f \bar{f}\not{v}t^A f$	14	$\bar{q}(vi\overleftrightarrow{D})^3q$
5	$\bar{q}\gamma^\nu[(vD), G_{\nu\mu}]v^\mu q$	10	$\bar{q}\sigma G(viD)q$		

**Table 3.2:** List of medium-specific light-quark operator combinations in mass dimension 6 incorporating operators related to  $O_1$  which already occurs in vacuum.

$$\begin{aligned}
 &g^2 O_1 - \frac{2}{v^2} (g^2 O_2 - 2gO_3 + 6gO_4) \\
 &g^2 O_1 - \frac{2}{v^2} (g^2 O_2 + gO_5) \\
 &\frac{2}{v^2} (g^2 O_2 + 3gO_5 - gO_6) \\
 &\frac{2}{v^2} gO_3 \\
 &3g^2 O_1 - \frac{4}{v^2} (g^2 O_2 + 2gO_4 - gO_7) \\
 &g^2 O_1 - \frac{48}{v^4} O_8
 \end{aligned}$$

different four-quark operators (of this origin) according to Eq. (C.118) which are invariant under parity and time reversal transformations. The corresponding condensates, i. e.  $\langle\langle O_k \rangle\rangle$  with  $k = 1, 2$  and 9, are classified as full condensates with indices 2v, 2v' and 2vs in Tab. 1 (for  $q = f$ ) and with indices 4v, 4v', 4vs and 6vs in Tab. 2 (for  $q \neq f$ ) of Ref. [Tho07] which provides an exhaustive list of independent light four-quark condensates.

Only the first line in (3.8) contains the vacuum contribution whereas the remaining terms are medium-specific and consequently must vanish in vacuum [Buc15a]. Furthermore, it can be shown by consistency arguments alone that the particular linear combinations of operators collected in Tab. 3.2 must vanish identically in vacuum. This imposes vacuum constraints as interrelations among the operators of Tab. 3.1, in particular also between terms which already occur in vacuum, i. e.  $O_1$ , and those which additionally and exclusively enter in the medium [Buc16b]. Note that vacuum-specific terms additionally exhibit an own medium dependence. These ideas are presented in Sec. 3.7, while the details on this rather technical aspect are relegated to App. C.2.

In order to test our computational procedure we consider the light four-quark condensate contributions of pseudo-scalar  $D$  mesons in vacuum. Employing the Borel transformation and a factorization of the four-quark condensates (cf. Section 3.3.3), we recover the result first calculated by Aliev and Eletsky [Ali83] and confirmed by Narison [Nar01]:

$$\widehat{\Pi}_{4q}^{\text{vac}}(M) = -\frac{16\pi}{27} \frac{e^{-m_Q^2/M^2}}{M^2} \left\{ 1 - \frac{1}{4} \frac{m_Q^2}{M^2} - \frac{1}{12} \frac{m_Q^4}{M^4} \right\} \alpha_s \kappa_0 \langle \bar{q}q \rangle_0^2. \quad (3.9)$$

The result of Hayashigaki and Terasaki [Hay04] differs by a factor of  $-2$  in the second of the three terms in  $\{\dots\}$  forming the Wilson coefficient. It is conceivable that they missed one of the three terms of mass dimension 6 leading to light four-quark condensate contributions eventually (cf. [Pas84] and the details in App. C.3). In fact, omitting the four-quark term in (C.116) would recover the result in [Hay04].

Having accomplished the evaluation of the OPE for light-quark condensates in mass dimension 6, one has to note that, in our expansion scheme, further diagrams contribute in LO. These are, for example, the gluon condensates depicted in Fig. 3.1 by diagrams (d), (e) and (f) which deserve separate elaborations beyond the scope of this work.

### 3.3.2 Chirally odd four-quark condensate in $D$ meson QSR

As stressed in Sec. 3.1, the chiral condensate  $\langle\langle \bar{q}q \rangle\rangle$  may serve as an order parameter of spontaneous chiral symmetry breaking (or can constitute an element thereof), since it is not invariant under chiral transformations. Other quark condensates reveal invariant as well as non-invariant behavior under chiral transformations, thus, they are dubbed chirally even or chirally odd condensates, respectively. Four-quark condensates entering the OPE (3.8) are of both kinds. Since these condensates (cf. Tab. 3.1) are flavor singlet structures, such four-quark condensates containing exclusively  $\gamma_\mu$  and/or  $\gamma_5 \gamma_\mu$  as Dirac structures are invariant under chiral transformations (B.5). Therefore, the first two entries in Tab. 3.1, i. e.  $\langle\langle :O_1: \rangle\rangle$  and  $\langle\langle :O_2: \rangle\rangle$ , are invariant under chiral transformations (B.5), whereas the condensate

$$\langle\langle :O_9: \rangle\rangle \propto \langle\langle : \bar{\psi}_R t^A \psi_L \bar{\psi}_L \not{t}^A \psi_L : \rangle\rangle + \langle\langle : \bar{\psi}_L t^A \psi_R \bar{\psi}_R \not{t}^A \psi_L : \rangle\rangle + (\text{L} \longleftrightarrow \text{R}) \quad (3.10)$$

is chirally odd, i. e. it can be turned into its negative, e. g. for  $|\Theta_R^a - \Theta_L^a|/\sqrt{2N_f} = (2k+1)\pi$  with integer  $k$  and vanishing of the remaining rotation parameters  $\Theta_{R,L}^b$  with  $b \neq a$ , cf. Eq. (B.10). We note that this chirally odd four-quark condensate is medium-specific contrary to the chiral condensate. The chirally odd nature of  $\langle\langle :O_9: \rangle\rangle$  can be also deduced from the difference of chiral partner spectra (Weinberg-type sum rules), where the dependence on chirally symmetric condensates cancels out [Hil11]. Furthermore, the operator  $O_9$  emerges from the commutator (2.104) with the generator of the axial-vector transformation [Tho08a], similarly to operators providing potential order parameters, e. g. the chiral condensate. Thus, the chirally odd four-quark condensate contributions may give insight to the breaking patterns of chiral symmetry as well as symmetry restoration scenarios [Hoh12, Hoh13, Hoh14].

### 3.3.3 Estimates of four-quark condensates – factorization

Once the evaluation of the OPE is completed, even in a truncated form and according to a particular organization of the nested multiple expansion schemes, one needs numerical

**Table 3.3:** List of light four-quark condensates  $\langle\langle :O_k: \rangle\rangle$ , with  $k = 1, 2$  and 9, entering the result (3.8) in genuine and factorized form. Resulting from the two-quark condensates in linear density approximation, the third column depicts the density dependent and factorized four-quark condensates  $\langle :O_k: \rangle_n$ , utilized in Sec. 3.4.

$\langle\langle :O_k: \rangle\rangle$	factorization	density dependence
$\langle\langle :\bar{q}\gamma^\nu t^A q \sum_f \bar{f}\gamma_\nu t^A f: \rangle\rangle$	$-\frac{2}{9}\kappa_0 \left[ 2\langle\langle :\bar{q}q: \rangle\rangle^2 - \frac{1}{v^2} \langle\langle :\bar{q}\not{v}q: \rangle\rangle^2 \right]$	$-\frac{4}{9}\kappa_0 \left[ \langle : \bar{q}q : \rangle_0^2 \left( 1 - \frac{\sigma_N n}{m_\pi^2 f_\pi^2} \right)^2 - \frac{9}{8} n^2 \right]$
$\langle\langle :\bar{q}\not{v} t^A q \sum_f \bar{f}\not{v} t^A f: \rangle\rangle$	$-\frac{1}{9}\kappa_1 \left[ v^2 \langle\langle :\bar{q}q: \rangle\rangle^2 + \langle\langle :\bar{q}\not{v}q: \rangle\rangle^2 \right]$	$-\frac{1}{9}\kappa_1 \left[ \langle : \bar{q}q : \rangle_0^2 \left( 1 - \frac{\sigma_N n}{m_\pi^2 f_\pi^2} \right)^2 + \frac{9}{4} n^2 \right]$
$\langle\langle :\bar{q} t^A q \sum_f \bar{f}\not{v} t^A f: \rangle\rangle$	$-\frac{2}{9}\kappa_2 \langle\langle :\bar{q}q: \rangle\rangle \langle\langle :\bar{q}\not{v}q: \rangle\rangle$	$-\frac{1}{3}\kappa_2 \langle : \bar{q}q : \rangle_0 \left( 1 - \frac{\sigma_N n}{m_\pi^2 f_\pi^2} \right) n$

values of the various condensates. The low mass dimension condensates are constrained fairly well, even with some debate on the gluon condensates [Shu04]. The mass dimension-6 four-quark condensates are less well investigated. They enter QSRs in different combinations, as exemplified, for instance, in [Tho07] for the nucleon and in [Hil12c] for the  $\rho$  meson.

To arrive at some numerical estimates of the impact of the light four-quark condensates we employ tentatively the factorization hypothesis, being aware of its limited reliability and lacking foundation [Lau84, Koi93, Leu05, Dru12, Bra15]. Despite the validity of the factorization ansatz for an infinite number of colors, its accuracy for QCD is still questionable. Factorization of four-quark condensates is based on the ground state saturation hypothesis. Accordingly, only the ground state is assumed to yield a relevant contribution after insertion of a complete set of hadronic states into the four-quark condensate. In Ref. [Shi79] the contribution of the lightest hadronic state, the pion state, is estimated as 1/20 of the ground state contribution. Thus, the four-quark condensate is assumed to factorize into two ground state EVs of two-quark operators. In a medium, two different two-quark condensates exist,  $\langle\langle :\bar{q}q: \rangle\rangle$  and  $\langle\langle :\bar{q}\gamma^\mu q: \rangle\rangle$ , where the latter one is employed as  $\langle\langle :\bar{q}\not{v}q: \rangle\rangle v^\mu/v^2$  after projection of the Lorentz index. Factorization formulae for in-medium contributions can be found in [Jin93]. Our investigation uses

$$\begin{aligned}
 \langle\langle :\bar{q}\Gamma_1 t^A q \bar{q}\Gamma_2 t^A q: \rangle\rangle &= -\frac{\kappa(\Gamma_1, \Gamma_2)}{36} \left\{ \langle\langle :\bar{q}q: \rangle\rangle^2 \text{Tr}_D [\Gamma_1 \Gamma_2] \right. \\
 &\quad + \langle\langle :\bar{q}q: \rangle\rangle \langle\langle :\bar{q}\gamma_\mu q: \rangle\rangle (\text{Tr}_D [\Gamma_1 \gamma^\mu \Gamma_2] + \text{Tr}_D [\gamma^\mu \Gamma_1 \Gamma_2]) \\
 &\quad \left. + \langle\langle :\bar{q}\gamma_\mu q: \rangle\rangle \langle\langle :\bar{q}\gamma_\nu q: \rangle\rangle \text{Tr}_D [\gamma^\mu \Gamma_1 \gamma^\nu \Gamma_2] \right\}, \quad (3.11)
 \end{aligned}$$

$$\langle\langle :\bar{q}\Gamma_1 t^A q \bar{q}'\Gamma_2 t^A q': \rangle\rangle = 0, \quad (3.12)$$

where  $\Gamma_1$  and  $\Gamma_2$  denote the Dirac structures of the condensates and  $q \neq q' = f$  in Eq. (3.12). The factors  $\kappa(\Gamma_1, \Gamma_2)$  may be introduced to account for deviations from strict factorization, which is recovered for  $\kappa(\Gamma_1, \Gamma_2) = 1$ . The relevant expressions are listed in Tab. 3.3.

However, Tab. 3.3 exhibits further issues which arise due to factorization of four-quark condensates. Condensates originally considered chirally even, such as  $\langle\langle :O_1: \rangle\rangle$  and  $\langle\langle :O_2: \rangle\rangle$ ,

factorize into powers of the chiral condensate  $\langle\langle:\bar{q}q:\rangle\rangle$  which is genuinely chirally odd. Since factorization changes the behavior of four-quark condensates under chiral transformations, the transformation properties of the OPE and, therefore, of the (operator product) expanded correlator are altered. Apart from lacking accuracy, factorization is also disputable with respect to chiral symmetry. A procedure analog to the one in [Hil12c] can overcome such artifacts.

### 3.4 Numerical evaluation

The Borel transform [Fur92, Coh95], cf. App. D, of the light-quark condensate contributions in the meson's rest frame,  $p_\mu = (p_0, \vec{0})$ ,  $v_\mu = (1, \vec{0})$ , and after a Wick rotation  $p_0 = i\omega$ , reads

$$\begin{aligned}\hat{\Pi}_{\text{dim6}}^{\text{even}}(M^2) = & \frac{1}{3} \frac{e^{-m_Q^2/M^2}}{M^2} \left( 1 - \frac{1}{4} \frac{m_Q^2}{M^2} - \frac{1}{12} \frac{m_Q^4}{M^4} \right) g^2 \langle\langle:O_1:\rangle\rangle \\ & - \frac{1}{3} \frac{e^{-m_Q^2/M^2}}{M^2} \left( 1 - \frac{1}{2} \frac{m_Q^2}{M^2} \right) \left[ \langle\langle:g^2 O_1 - 2(g^2 O_2 - 2g O_3 + 6g O_4):\rangle\rangle \right. \\ & \quad - \langle\langle:g^2 O_1 - 2(g^2 O_2 + g O_5):\rangle\rangle + 2\langle\langle:g^2 O_2 + 3g O_5 - g O_6:\rangle\rangle \\ & \quad \left. + 2g \langle\langle:O_3:\rangle\rangle - \frac{3}{2} \langle\langle:3g^2 O_1 - 4(g^2 O_2 + 2g O_4 - g O_7):\rangle\rangle \right] \\ & + \frac{1}{6} \frac{e^{-m_Q^2/M^2}}{M^2} \left( 1 - \frac{m_Q^2}{M^2} + \frac{1}{6} \frac{m_Q^4}{M^4} \right) \langle\langle:g^2 O_1 - 48 O_8:\rangle\rangle, \quad (3.13a)\end{aligned}$$

$$\begin{aligned}\hat{\Pi}_{\text{dim6}}^{\text{odd}}(M^2) = & \frac{e^{-m_Q^2/M^2} m_Q}{M^4} \left[ g^2 \langle\langle:O_9:\rangle\rangle + 2g (\langle\langle:O_{10}:\rangle\rangle + \langle\langle:O_{11}:\rangle\rangle) \right. \\ & \quad \left. - \frac{1}{3} g \langle\langle:O_{12}:\rangle\rangle + \frac{1}{3} g \langle\langle:O_{13}:\rangle\rangle \right] \\ & - 4 \frac{e^{-m_Q^2/M^2} m_Q}{M^4} \left( 1 - \frac{1}{3} \frac{m_Q^2}{M^2} \right) \langle\langle:O_{14}:\rangle\rangle \quad (3.13b)\end{aligned}$$

which is the basis of the following numerical evaluation in nuclear matter, i. e. in a particle–anti-particle asymmetric environment. Accordingly, even and odd parts w. r. t.  $p_0$  have been separated. As described in Subsec. 3.3.1 the medium-specific condensates entering the results (3.13) must vanish for zero nucleon density per construction. This can be satisfied for the odd OPE (3.13b) by vanishing of the square bracketed terms and  $\langle\langle:O_{14}:\rangle\rangle$ , and it implies non-trivial constraints on the vacuum EVs of operators in the even OPE (3.13a) containing the medium velocity  $v_\mu$ . These vacuum constraints can be formulated in terms of a system of linear equations which can be solved and which ensures vanishing of all medium-specific condensates in vacuum, cf. Eqs. (3.24).

As, however, the density dependence of the medium-specific light-quark condensates in mass dimension 6 is still unrestricted, we assume that it is dominated by the four-quark condensate contribution whose medium dependence can be estimated by factorization (cf. Tab. 3.3), i. e. only  $O_i$  with  $i = 1, 2$  and  $9$  exhibit a medium dependence  $\langle\langle:O_i:\rangle\rangle = \langle:O_i:\rangle_n$ .

The other condensates are constant w.r.t. density (and temperature) and remain at their vacuum values dictated by the vacuum constraints (3.24). This reduces the numerical values of the medium-specific condensates to the density dependent terms of the four-quark condensate contributions of the third column in Tab. 3.3. Furthermore, the factorization parameters  $\kappa_i$  are also related via such constraints (C.88). One has  $\kappa_0(n=0) = \kappa_1(n=0)$ .<sup>5</sup> In order to indicate the numerical evaluation of  $\hat{\Pi}_{\text{dim6}}$  under these assumptions we introduce the notation  $\hat{\Pi}_{4\text{q-dom}}$ .

Note that we utilize four-quark condensates beyond linear density approximation with the following reasoning. Taking into account only the linear density terms in the third column of Tab. 3.3 yields a chirally odd condensate, namely  $\langle :O_9: \rangle_n$ , which does not vanish at higher densities, i.e. exhibits no signals of chiral restoration, in contradiction with the chiral condensate (2.117). However, employing the linear density approximation to the two-quark condensates entering the factorized four-quark condensates provides a quadratic density dependence which overcomes such issues. (It turns out that imposing the above described constraints and using the linear density dependence of factorized four-quark condensates, only the odd term carries a medium dependence, whereas the medium dependence of the even term – including the vacuum specific term – completely cancels out.)

Assuming constant  $\kappa$ 's w.r.t. density and using the notation  $\langle O_i^n \rangle = \langle O_i \rangle_n - \langle O_i^0 \rangle$  with the vacuum part  $\langle O_i^0 \rangle = -\frac{5-i^2}{9}\kappa_{i-1}\langle \bar{q}q \rangle_0^2$  for  $i = 1$  and  $2$  the Borel transformed density dependent result reads

$$\begin{aligned} \hat{\Pi}_{4\text{q-dom}}^{\text{even}}(M^2) = & \frac{1}{3} \frac{e^{-m_Q^2/M^2}}{M^2} \left( 1 - \frac{1}{4} \frac{m_Q^2}{M^2} - \frac{1}{12} \frac{m_Q^4}{M^4} \right) g^2 \langle O_1 \rangle_n \\ & - \frac{1}{3} \frac{e^{-m_Q^2/M^2}}{M^2} \left( 1 - \frac{1}{2} \frac{m_Q^2}{M^2} \right) \left[ 2g^2 \langle O_2^n \rangle - \frac{3}{2} g^2 \langle 3O_1^n - 4O_2^n \rangle \right] \\ & + \frac{1}{6} \frac{e^{-m_Q^2/M^2}}{M^2} \left( 1 - \frac{m_Q^2}{M^2} + \frac{1}{6} \frac{m_Q^4}{M^4} \right) g^2 \langle O_1^n \rangle, \end{aligned} \quad (3.14a)$$

$$\hat{\Pi}_{4\text{q-dom}}^{\text{odd}}(M^2) = \frac{e^{-m_Q^2/M^2} m_Q}{M^4} g^2 \langle O_9 \rangle_n, \quad (3.14b)$$

where condensates are displayed without normal ordering, since we introduce physical condensates by renormalization of the normal-ordered condensates to one-loop level as described in [Jam93]. According to arguments in [Jam93, Zsc11] for gluon condensates we obtain no further terms upon renormalization since four-quark condensate contributions are already of order  $\alpha_s$ . Note that the vacuum constraints are the minimal requirements for a consistent vacuum limit. Any more sophisticated medium dependence must go beyond factorization with constant parameters and/or it also imposes medium dependence to the terms  $O_i$  with  $i = 3, \dots, 8$  and  $10, \dots, 14$  in Tab. 3.1.

<sup>5</sup>This relation differs from the one provided in Ref. [Buc15b], because here we additionally include the vacuum constraints (C.72) of four-quark condensates which enter the light meson OPE of the correlator with the NLO interaction term inserted and assumed universality of these condensates. If only the  $qQ$  OPE is considered the relation of  $\kappa_0$  and  $\kappa_1$  is unrestricted, cf. App. C.2.2. The different  $\kappa$  value does not alter the meaning of our findings or conclusive statements on the numerical impact of four-quark condensates.

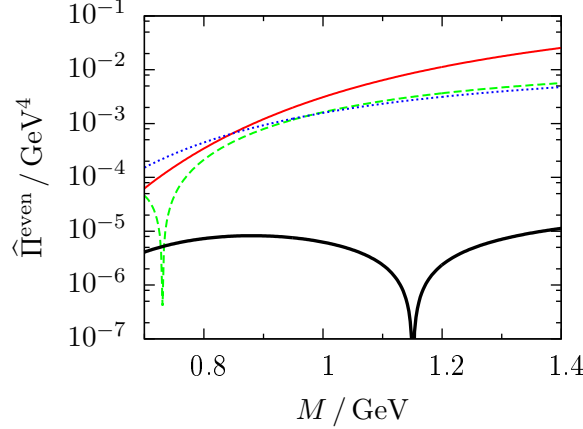


**Figure 3.4:** Various contributions to the even OPE part of the  $qQ$  sum rule at saturation density. The red solid curve depicts the perturbative term subtracted by the continuum contribution of the phenomenological side of the sum rule according to quark-hadron duality, i. e.  $\tilde{C}_0 = C_0 - \frac{1}{\pi} \left( \int_{-\infty}^{\omega_0^-} + \int_{\omega_0^+}^{\infty} \right) d\omega \omega e^{-\omega^2/M^2} \text{Im} C_0(\omega^2) = \frac{1}{\pi} \int_{m_Q^2}^{\omega_0^2} ds e^{-s/M^2} \text{Im} C_0(s)$ , where we assume  $\omega_0^+ = -\omega_0^- = \omega_0$  for the second equality with the symmetric continuum threshold parameter  $\omega_0^2 = 6 \text{ GeV}^2$  (cf. [Hil09]). The green dashed curve is the modulus of the power correction  $e^{-m_Q^2/M^2} \sum_{k=1}^6 c_k^{\text{even}} \langle \mathcal{O}_k \rangle^{\text{even}}$  of the in-medium OPE (3.3a) up to mass dimension 5 according to [Hil09]. The contribution of the chiral condensate, i. e.  $-e^{-m_Q^2/M^2} m_Q \langle \bar{q}q \rangle_{n_0}$ , is shown by the blue dotted curve. The modulus of the four-quark condensate contribution  $\hat{\Pi}_{4q\text{-dom}}^{\text{even}}$  (3.14a) is displayed by the thick solid black curve. For the curves with sign flips in the depicted region the left branches originates from negative values.

Our numerical evaluation employs the values of the condensates including their nucleon density dependences presented in [Hil09]. We resort here to the four-quark condensate factorization parameters  $\kappa_0 = \kappa_1 = \kappa_2 = 1$ , bearing in mind that the actual values may considerably deviate from these assumed values. We use for the heavy-quark mass  $m_Q = 1.5 \text{ GeV}$  and determine the strong coupling from the one-loop result (2.75) with the renormalization scale  $\mu = 1 \text{ GeV}$ , the dimensional QCD parameter  $\Lambda = 0.25 \text{ GeV}$  and the number of light-quark flavors  $N_f = 3$ . The nucleon saturation density is  $n_0 = 0.15 \text{ fm}^{-3}$ .

Subject to the following investigation is the OPE side of the Borel transformed QSR of  $qQ$  mesons (cf. Eq. (3.3))

$$\hat{\Pi}^{\text{even}}(M^2) = C_0 + e^{-m_Q^2/M^2} \sum_{k=1}^6 c_k^{\text{even}}(M^2) \langle \mathcal{O}_k \rangle^{\text{even}} + \hat{\Pi}_{4q\text{-dom}}^{\text{even}}(M^2), \quad (3.15a)$$

$$\hat{\Pi}^{\text{odd}}(M^2) = e^{-m_Q^2/M^2} \sum_{k=1}^3 c_k^{\text{odd}}(M^2) \langle \mathcal{O}_k \rangle^{\text{odd}} + \hat{\Pi}_{4q\text{-dom}}^{\text{odd}}(M^2). \quad (3.15b)$$

Utilizing the spectral density ansatz (2.141), the sum rule analysis up to condensates of mass dimension 5 shows that the density dependence of the mass centroid for  $D$  and  $\bar{D}$  mesons is mainly determined by the even part, while the mass splitting of the meson–anti-meson



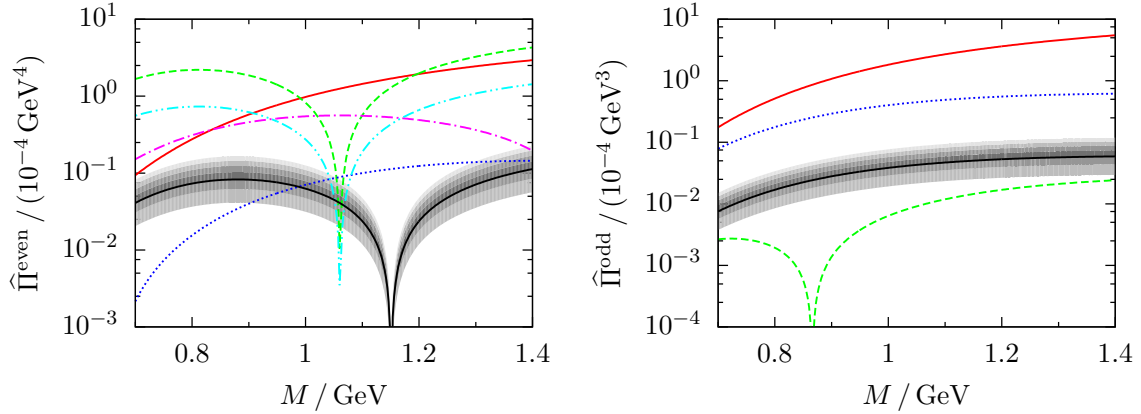


**Figure 3.5:** Modulus of the individual contributions to the even (left panel) and the odd (right panel) OPE (3.3) at saturation density up to mass dimension 5 according to [Hil09] supplemented by the four-quark condensate contributions exhibited by the solid black curves and the contours with  $\kappa_0 = \kappa_1 = \kappa_2 \in [0.5, 2]$ . Using the notation of the contributions according to the condensates  $\langle \mathcal{O}_k \rangle^{\text{even, odd}}$  listed below (3.3) for the even OPE on the left panel the following line code applies:  $\langle \mathcal{O}_2 \rangle^{\text{even}}$  – red solid curve,  $\langle \mathcal{O}_3 \rangle^{\text{even}}$  – green dashed curve,  $\langle \mathcal{O}_4 \rangle^{\text{even}}$  – blue dotted curve,  $\langle \mathcal{O}_5 \rangle^{\text{even}}$  – magenta dot-dashed curve and  $\langle \mathcal{O}_6 \rangle^{\text{even}}$  – cyan dot-dot-dashed curve. For the curves with sign flips in the depicted region, the left branches originate from negative values. On the right panel the red solid curve depicts the  $\langle \mathcal{O}_1 \rangle^{\text{odd}}$  contribution, the green dashed curve displays the  $\langle \mathcal{O}_2 \rangle^{\text{odd}}$  contribution, where the right branch originates from negative values, and the blue dotted curve shows the sign flipped  $\langle \mathcal{O}_3 \rangle^{\text{odd}}$  contribution.

pair is influenced by the odd part of the OPE [Hil09].<sup>6</sup> To get an estimate on the impact of light-quark condensate contributions in mass dimension 6, especially four-quark condensate contributions, on the meson properties we compare them to contributions of condensates up to mass dimension 5.

The QSRs of  $qQ$  mesons are governed by the perturbative and the chiral condensate contributions (cf. Fig. 3.4). The purely perturbative contribution is even more prominent than displayed in Fig. 3.4, where we already subtracted the continuum contribution of the spectral density of the sum rule employing the quark-hadron duality (2.128). The continuum threshold  $\omega_0^2$ , which needs to be chosen to meet stability criteria of the sum rule, is set to the typical value of 6 GeV<sup>2</sup> in our investigation (cf. [Nar05]). The chiral condensate contribution (blue dotted curve) has the strongest impact on the sum rule among the power corrections (green dashed curve). However, at typical Borel masses  $M = 0.9 - 1.3$  GeV [Hil09] further condensates contribute weakly.

The absolute numerical values of light four-quark condensate contributions  $\hat{\Pi}_{4q\text{-dom}}^{\text{even}}$  (thick black solid curve) are two orders of magnitude below the chiral condensate contribution in the presumed Borel window, due to the heavy-quark mass accompanying the chiral condensate acting as an amplification factor. Evaluation of individual contributions to the even and odd OPE exhibited in Fig. 3.5 shows the tendency of decreasing values of the contributions of

<sup>6</sup>If four-quark condensates are included in linear density approximation into the sum rule their medium modification effects only the odd OPE, and thus only the mass splitting of D and  $\bar{D}$ . The mass centroid remains unaffected by such four-quark condensate contributions.

the condensates with increasing mass dimension. The four-quark condensate contributions are of mass dimension 6 and therefore the highest order contribution of the evaluated OPE. Despite varying  $\kappa_0 = \kappa_1 = \kappa_2$  between 0.5 and 2 they are more than one order of magnitude smaller than most other contributions of the OPE up to mass dimension 5 yielding small absolute values which supports the convergence of the OPE. Moreover, trusting the order of magnitude of light four-quark condensate contributions exhibited in Fig. 3.4 lends credibility to the previous analyses, e. g. [Hil09], which were truncated at mass dimension 5.

Besides four-quark condensates also gluonic condensates contribute additionally to the in-medium OPE (3.15) in mass dimension 6. Their contributions may numerically influence the OPE as strongly as the presented light-quark condensate terms, thus, they deserve separate further investigation. We choose the light four-quark condensates to serve as the starting point for the analysis of the OPE in mass dimension 6, because they are especially important in other meson sum rules, as stressed above.

### 3.5 Comparison of four-quark condensates in $\rho$ meson and $D$ meson sum rules

To compare with the  $\rho$  meson OPE neglecting higher-twist terms, where the gluon and four-quark condensate contributions are of similar magnitude (cf. upper left panel in Fig. 3.6), we consider the vacuum four-quark condensate term of the  $D$  meson (cf. upper right panel in Fig. 3.6). Its contribution is up to one order of magnitude smaller than the vacuum gluon condensate term. This order of magnitude difference arises from the  $\rho$  meson OPE where the soft-gluon diagrams (d) and (e) in Fig. 3.2 are supplemented by hard-gluon diagrams (a) and (b) in Fig. 3.3 whose numerical contributions exceed the soft-gluon contributions by a factor of five (cf. left panels in Fig. 3.6) and the gluon condensate term contributes half as much as the gluon condensate contribution in the  $D$  meson sum rule. We argue that this can be disentangled as follows. While terms proportional to positive integer powers of the light-quark mass squared are neglected in the  $\rho$  meson OPE, analogous heavy-quark terms significantly contribute to the  $D$  meson OPE, where additionally the chiral condensate as well as the quark-gluon condensate are redefined to render the gluon condensate term free of infra-red mass singularities which is necessary in heavy-light systems [Jam93].

Wilson coefficients of the OPEs for  $qQ$  meson systems exhibit a non-monotonic behavior for varying Borel mass parameters in contrast to light meson systems, due to the non-zero heavy-quark mass entering QSRs of heavy-light systems as an additional scale. Non-negligible terms proportional to positive integer powers of the heavy-quark mass squared (cf. Eq. (3.9)) lead to roots of the Wilson coefficient in the Borel mass region near  $M = 1$  GeV (cf. Fig. 3.5), which is in the Borel window of  $D$  meson sum rules resulting in small OPE contributions for terms with altering Wilson coefficients, such as light four-quark condensate contributions.

Studying the  $\rho$  meson sum rule in the VOC (Vanishing of chirally Odd Condensates) scenario (cf. Ref. [Hil12c]), where the mass and/or width of the  $\rho$  meson are evaluated in a hypothetical chirally symmetric world, the omission of medium-specific contributions<sup>7</sup> is jus-

---

<sup>7</sup>Medium-specific contributions of the  $\rho$  meson OPE are usually denoted non-scalar or higher-twist terms [Leu98].

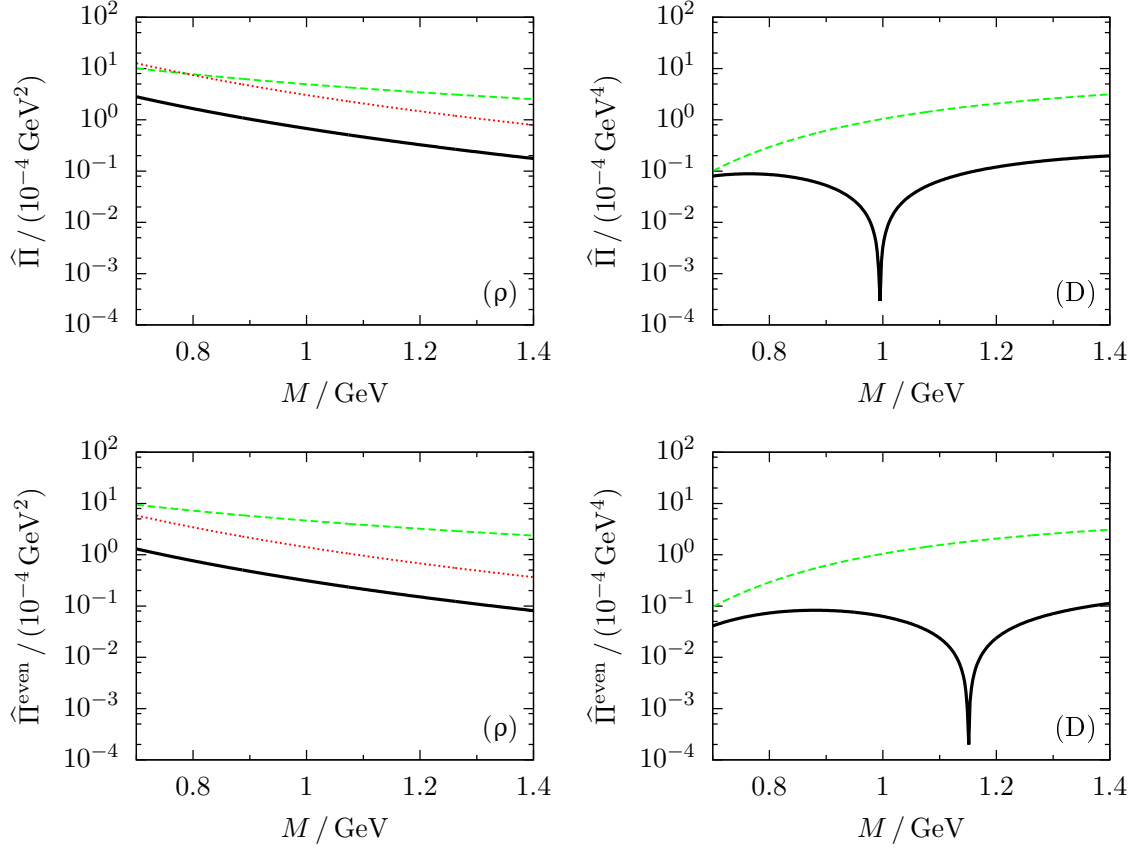


**Figure 3.6:** Comparison of  $\rho$  meson (left panels) and  $D$  meson (right panels) contributions in vacuum (upper panels) and at nucleon saturation density (lower panels). Dashed green curves denote the gluon condensate contributions and thick solid black curves display the modulus of light four-quark condensate contributions containing the soft-gluon diagrams (d) and (e) in Fig. 3.2. The modulus of the four-quark condensate contribution of the  $\rho$  meson from hard-gluon diagrams in Fig. 3.3 is depicted by the dotted red curve.

tified. In such a clear-cut scenario, the chirally odd objects, e. g. the chiral condensate, do not vanish due to their medium modifications, but are set to zero, while the chirally symmetric condensates retain their vacuum values. In contrast, investigating signals of chiral restoration in the chirally broken world, chirally odd condensates are diminished due to an ambient medium. Thus, the inclusion of medium-specific contributions to the  $\rho$  meson OPE is mandatory for a consistent in-medium description. Four-quark condensate contributions without their medium-specific parts exhibit an artificially strong medium dependence in comparison with the complete  $D$  meson four-quark terms which show a minor medium dependence only (cf. Fig. 3.6 lower panels compared to upper ones). Furthermore, these medium-specific contributions also contain chirally odd objects, e. g.  $\langle (\bar{\psi}\not{\epsilon}\gamma_5\lambda^a\tau_3\psi)^2 - (\bar{\psi}\not{\epsilon}\lambda^a\tau_3\psi)^2 \rangle$  traceable to the Gibbs averaged twist-4 operator  $\langle \mathcal{T}(\bar{\psi}\gamma_\mu\gamma_5\lambda^a\tau_3\psi)(\bar{\psi}\gamma_\nu\gamma_5\lambda^a\tau_3\psi) \rangle$  (with adopted notation from [Hil12c]). However, identification of such chirally odd objects requires the decomposition of the non-scalar terms analogous to the procedure presented here for the  $D$  meson and deserves further investigations.

### 3.6 Heavy-quark expansion

The heavy-quark expansion (HQE), originally introduced in [Shi79] for the heavy two-quark condensate  $\langle \bar{Q}Q \rangle$  in vacuum, is extended here to four-quark condensates and to the in-medium case, thus going beyond previous approaches to  $D$  and  $B$  meson QSR analyses, e.g. [Nar13]. Specific formulas are derived and presented in Ref. [Buc14a] which provide important pieces to a complete QSR analysis of  $qQ$  mesons in a strongly interacting medium, which includes the contributions of the first term in Eq. (3.7b) and the four-quark condensate contributions depicted in Fig. 3.3. While the calculation of the former contribution proceeds along the lines of App. C.3 the latter contributions originating from the NLO correlator are derived in Ref. [Buc12].

#### 3.6.1 HQE in vacuum. A recollection

In [Gen84], a general method is developed for vacuum condensates involving heavy quarks  $Q$  with mass  $m_Q$ . The heavy-quark condensate is considered as the one-point function

$$\langle \Omega | \bar{Q}Q | \Omega \rangle = -i \int \frac{d^4 p}{(2\pi)^4} \langle \Omega | \text{Tr}_{c,D} S_Q(p) | \Omega \rangle \quad (3.16)$$

expressed by the heavy-quark propagator  $S_Q$  in a weak, classical, gluonic background field in Fock-Schwinger gauge, cf. Eq. (2.44), which interacts with the complex QCD ground state via soft gluons generating a series expansion in the inverse heavy-quark mass. The compact notation (3.16) differs from [Gen84], but provides a comprehensive scheme easily extendable to in-medium condensates. The first HQE terms of the heavy two-quark condensate (3.16) reproduce [Gen84]:

$$\begin{aligned} \langle \Omega | \bar{Q}Q | \Omega \rangle &= -\frac{g^2}{48\pi^2 m_Q} \langle G^2 \rangle - \frac{g^3}{1440\pi^2 m_Q^3} \langle G^3 \rangle - \frac{g^4}{120\pi^2 m_Q^3} \langle (DG)^2 \rangle + \dots \\ &= \text{diagram 1} + \left( \text{diagram 2} + \text{diagram 3} \right) + \text{diagram 4} + \dots \end{aligned} \quad (3.17)$$

with the notation

$$\langle G^2 \rangle = \langle \Omega | G_{\mu\nu}^A G^{A\mu\nu} | \Omega \rangle, \quad (3.18a)$$

$$\langle G^3 \rangle = \langle \Omega | f^{ABC} G_{\mu\nu}^A G^{B\nu}{}_\lambda G^{C\lambda\mu} | \Omega \rangle, \quad (3.18b)$$

$$\langle (DG)^2 \rangle = \langle \Omega | \left( \sum_f \bar{f} \gamma_\mu t^A f \right)^2 | \Omega \rangle. \quad (3.18c)$$

The diagrammatic interpretation of the terms in (3.17) is depicted too: the solid lines denote the free heavy-quark propagators and the curly lines are for soft gluons whose condensation is symbolized by the crosses, whereas the heavy-quark condensate is symbolized by the crossed circles [Bag86]. An analogous expression for the mixed heavy-quark gluon condensate can be obtained along those lines which contains, however, a term proportional to  $m_Q$ . The LO term in (3.17) was employed already in [Shi79] in evaluating the sum rule for charmonia.

The vacuum HQE method was rendered free of ultra-violet divergent results for higher mass-dimension heavy-quark condensates by requiring at least one condensing gluon per condensed heavy-quark [Shi79, Bag85], which prevents unphysical results, where the condensation probability of heavy-quark condensates rises for an increasing heavy-quark mass.

### 3.6.2 Application of HQE to in-medium heavy-light four-quark condensates

The above method can be extended to in-medium situations. Our approach contains two new aspects: (i) formulas analogous to equation (3.16) are to be derived for heavy-quark condensates, e.g.  $\langle\langle \bar{Q}\psi Q \rangle\rangle$ ,  $\langle\langle \bar{Q}\psi\sigma GQ \rangle\rangle$ ,  $\langle\langle \bar{q}\psi t^A q \bar{Q}\psi t^A Q \rangle\rangle$ , which additionally contribute to the in-medium OPE and (ii) medium-specific gluonic condensates, e.g.  $\langle\langle G^2/4 - (vG)^2/v^2 \rangle\rangle$ ,  $\langle\langle G^3/4 - f^{ABC} G_{\mu\nu}^A G^{B\nu}{}_\lambda G^{C\lambda\kappa} v^\mu v_\kappa/v^2 \rangle\rangle$ , enter the HQE of heavy-quark condensates for both, vacuum and additional medium condensates.

We are especially interested in heavy-light four-quark condensates entering the OPE of  $qQ$  mesons, inter alia, in terms corresponding to the NLO perturbative diagrams in Fig. 3.3 with one light-quark ( $q$ ) and one heavy-quark ( $Q$ ) line cut. There are 24 two-flavor four-quark condensates in the nuclear medium [Tho07] represented here in a compact notation by  $\langle\langle \bar{q}\Gamma T^A q \bar{Q}\Gamma' T^A Q \rangle\rangle$ , where  $\Gamma$  and  $\Gamma'$  denote Dirac structures and  $T^A$  with  $A = 0, \dots, 8$  are the generators of  $SU(N_c = 3)$  supplemented by the unit element ( $A = 0$ ). We obtain the analogous formula to (3.16) for heavy-light four-quark condensates:

$$\langle\langle \bar{q}\Gamma T^A q \bar{Q}\Gamma' T^A Q \rangle\rangle = -i \int \frac{d^4 p}{(2\pi)^4} \langle\langle \bar{q}\Gamma T^A q \text{Tr}_{c,D} [\Gamma' T^A S_Q(p)] \rangle\rangle. \quad (3.19)$$

The LO terms of this HQE are obtained for the heavy-quark propagators  $S_Q^{(1)}(\tilde{A}^{(1)})$  and  $S_Q^{(2)}(\tilde{A}^{(0)})$  with NLO and LO background fields, respectively:

$$\begin{aligned} & \langle\langle \bar{q}\Gamma T^A q \bar{Q}\Gamma' T^A Q \rangle\rangle \\ &= -i \int \frac{d^4 p}{(2\pi)^4} \langle\langle \bar{q}\Gamma T^A q \text{Tr}_{c,D} [\Gamma' T^A (S_Q^{(1)}(\tilde{A}^{(1)})(p) + S_Q^{(2)}(\tilde{A}^{(0)})(p) + \dots)] \rangle\rangle \\ &\equiv \langle\langle \bar{q}\Gamma T^A q \bar{Q}\Gamma' T^A Q \rangle\rangle^{(0)} + \langle\langle \bar{q}\Gamma T^A q \bar{Q}\Gamma' T^A Q \rangle\rangle^{(1)} + \dots \\ &= \text{[Diagram 1]} + \text{[Diagram 2]} + \dots \end{aligned} \quad (3.20)$$

Evaluation of the first term of the expansion (3.20) for the complete list of two-flavor four-quark condensates in [Tho07] gives three non-zero results:

$$\langle\langle \bar{q}\gamma^\nu t^A q \bar{Q}\gamma_\nu t^A Q \rangle\rangle^{(0)} = -\frac{2}{3} \frac{g^2}{(4\pi)^2} \left( \ln \frac{\mu^2}{m_Q^2} + \frac{1}{2} \right) \langle\langle \bar{q}\gamma^\nu t^A q \sum_f \bar{q}_f \gamma_\nu t^A q_f \rangle\rangle, \quad (3.21a)$$

$$\langle\langle \bar{q}\psi t^A q \bar{Q}\psi t^A Q \rangle\rangle^{(0)} = -\frac{2}{3} \frac{g^2}{(4\pi)^2} \left( \ln \frac{\mu^2}{m_Q^2} + \frac{1}{3} \right) \langle\langle \bar{q}\psi t^A q \sum_f \bar{q}_f \psi t^A q_f \rangle\rangle, \quad (3.21b)$$

$$\langle\langle \bar{q}t^A q \bar{Q}\psi t^A Q \rangle\rangle^{(0)} = -\frac{4}{3} \frac{g^2}{(4\pi)^2} \left( \ln \frac{\mu^2}{m_Q^2} - \frac{1}{8} \right) \langle\langle \bar{q}t^A q \sum_f \bar{q}_f \psi t^A q_f \rangle\rangle, \quad (3.21c)$$

where logarithmic singularities are calculated in the  $\overline{\text{MS}}$  scheme,  $\mu$  is the renormalization scale, and  $t^A = T^A$  for  $A = 1, \dots, 8$ . The non-zero contributions for the second term of (3.20) read

$$\langle\langle \bar{q}q\bar{Q}Q \rangle\rangle^{(1)} = -\frac{1}{3} \frac{g^2}{(4\pi)^2} \frac{1}{m_Q} \langle\langle \bar{q}q G_{\mu\nu}^A G^{A\mu\nu} \rangle\rangle, \quad (3.22a)$$

$$\langle\langle \bar{q}t^A q \bar{Q}t^A Q \rangle\rangle^{(1)} = -\frac{1}{6} \frac{g^2}{(4\pi)^2} \frac{1}{m_Q} \langle\langle d^{ABC} \bar{q}t^A q G_{\mu\nu}^B G^{C\mu\nu} \rangle\rangle, \quad (3.22b)$$

$$\langle\langle \bar{q}\gamma_5 q \bar{Q}\gamma_5 Q \rangle\rangle^{(1)} = -\frac{1}{4} \frac{g^2}{(4\pi)^2} \frac{1}{m_Q} \langle\langle i\bar{q}\gamma_5 q G_{\mu\nu}^A G_{\alpha\beta}^A \varepsilon^{\mu\nu\alpha\beta} \rangle\rangle, \quad (3.22c)$$

$$\langle\langle \bar{q}\gamma_5 t^A q \bar{Q}\gamma_5 t^A Q \rangle\rangle^{(1)} = -\frac{1}{8} \frac{g^2}{(4\pi)^2} \frac{1}{m_Q} \langle\langle i d^{ABC} \bar{q}\gamma_5 t^A q G_{\mu\nu}^B G_{\alpha\beta}^C \varepsilon^{\mu\nu\alpha\beta} \rangle\rangle, \quad (3.22d)$$

$$\langle\langle \bar{q}\psi q \bar{Q}Q \rangle\rangle^{(1)} = -\frac{1}{3} \frac{g^2}{(4\pi)^2} \frac{1}{m_Q} \langle\langle \bar{q}\psi q G_{\mu\nu}^A G^{A\mu\nu} \rangle\rangle, \quad (3.22e)$$

$$\langle\langle \bar{q}\psi t^A q \bar{Q}t^A Q \rangle\rangle^{(1)} = -\frac{1}{6} \frac{g^2}{(4\pi)^2} \frac{1}{m_Q} \langle\langle d^{ABC} \bar{q}\psi t^A q G_{\mu\nu}^B G^{C\mu\nu} \rangle\rangle, \quad (3.22f)$$

$$\langle\langle \bar{q}\sigma_{\mu\nu} t^A q \bar{Q}\sigma^{\mu\nu} t^A Q \rangle\rangle^{(1)} = -\frac{5}{6} \frac{g^2}{(4\pi)^2} \frac{1}{m_Q} \langle\langle f^{ABC} \bar{q}\sigma_{\mu\nu} t^A q G^{B\nu}{}_{\lambda} G^{C\lambda\mu} \rangle\rangle, \quad (3.22g)$$

$$\langle\langle \bar{q}\sigma_{\mu\nu} t^A q \bar{Q}\sigma_{\alpha\beta} t^A Q g^{\mu\alpha} v^\nu v^\beta \rangle\rangle^{(1)} = -\frac{5}{3} \frac{g^2}{(4\pi)^2} \frac{1}{m_Q} \langle\langle f^{ABC} \bar{q}\sigma_{\mu\nu} t^A q G^{B\nu}{}_{\alpha} G^{C\alpha\beta} v^\mu v_\beta \rangle\rangle, \quad (3.22h)$$

$$\langle\langle \bar{q}\gamma_5 \gamma_\lambda t^A q \bar{Q}\sigma_{\mu\nu} t^A Q \varepsilon^{\mu\nu\lambda\tau} v_\tau \rangle\rangle^{(1)} = -\frac{5}{6} \frac{g^2}{(4\pi)^2} \frac{1}{m_Q} \langle\langle f^{ABC} \bar{q}\gamma_5 \gamma_\lambda t^A q G_{\alpha\beta}^B G^{C\beta}{}_{\gamma} \varepsilon^{\gamma\alpha\lambda\tau} v_\tau \rangle\rangle, \quad (3.22i)$$

where  $f^{ABC}$  is the anti-symmetric structure constant of the color group and the corresponding symmetric object  $d^{ABC}$  is defined by the anti-commutator (A.5).

### 3.7 Algebraic vacuum limits of QCD condensates from in-medium projections of Lorentz tensors

The decomposition of operators with non-trivial Lorentz structure is a crucial step in setting up any in-medium QSR, as only there the difference between vacuum and medium in the scope of an OPE comes into play. The framework presented in App. C.2 builds on ideas first considered in finite-density nucleon QSRs [Coh91, Coh92, Fur92, Jin93], where the authors realized that a tensor decomposition of local operators as needed in OPE evaluations depends on the available tensors, e.g. the metric tensor  $g_{\mu\nu}$  and the Levi-Civita symbol  $\varepsilon_{\mu\nu\kappa\lambda}$ . In a strongly interacting medium the ground state is not Poincaré invariant, but there is an additional four-vector, the medium velocity  $v_\mu$ , which must be transformed when comparing observations in different reference frames, and must be included to build tensors or invariants [Jin93]. Thus, additional condensates give non-zero in-medium contributions which vanish in vacuum.

The number of Lorentz indices to be projected and the number of decomposition terms tends to increase with the mass dimension of the operator. As a consequence, one faces the

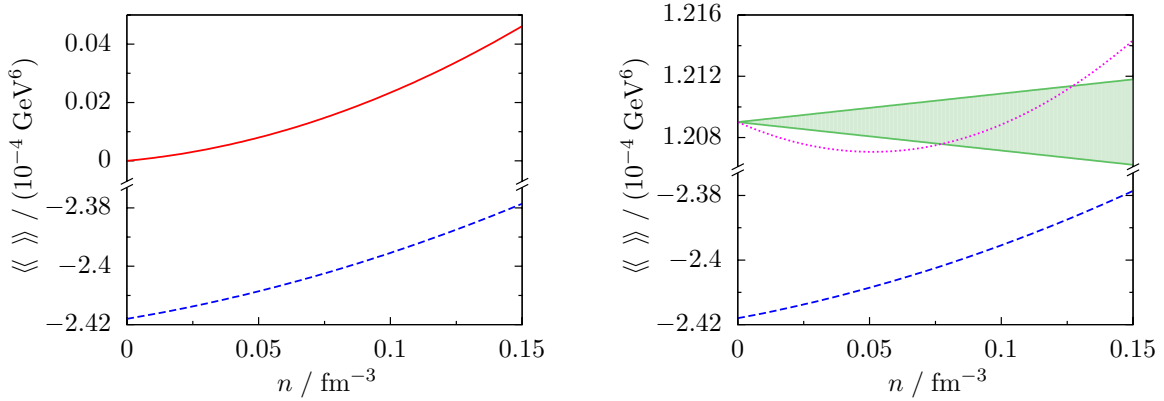


**Figure 3.7:** Left panel: The net-nucleon density dependences of the vacuum-specific condensate  $\langle\langle g\bar{q}\gamma_\mu t^A q \sum_f \bar{f}\gamma^\mu t^A f \rangle\rangle$  (blue dashed curve) and the medium-specific condensate  $\langle\langle g\bar{q}\gamma_\mu t^A q \sum_f \bar{f}\gamma^\mu t^A f - \frac{2}{v^2} (\bar{q}\gamma^\alpha[(vD), G_{\alpha\beta}]v^\beta q + g\bar{q}\psi t^A q \sum_f \bar{f}\psi t^A f) \rangle\rangle$  (red solid curve). Right panel: The individual contributions to the medium-specific condensate,  $-2\langle\langle g\bar{q}\psi t^A q \sum_f \bar{f}\psi t^A f \rangle\rangle/v^2$  (magenta dotted curve),  $-2\langle\langle \bar{q}\gamma^\alpha[(vD), G_{\alpha\beta}]v^\beta q \rangle\rangle/v^2$  (green band, generated by an assumed linear density dependence  $c_n n$  with  $c_n \in [-2, 2]$ ) and vacuum-specific condensate  $\langle\langle g\bar{q}\gamma_\mu t^A q \sum_f \bar{f}\gamma^\mu t^A f \rangle\rangle$  (blue dashed curve, as in left panel), which add up to the red solid curve displayed in the left panel for  $c_n = 1$ .

problem of an increasing number of numerically yet unknown condensates. To overcome this, condensates may be neglected, if good reasons could be provided, or the corrected vacuum saturation hypothesis may be employed from the very beginning. However, for the D meson this naive approach leads to an OPE which does not correctly reproduce the vacuum limit and consequently would not lead to a continuous dependence of the spectral properties on density and/or temperature [Hil12b, Buc15a, Buc15b]. The reason is that the additional medium contribution contains scalar operators that are also contained in the vacuum OPE. Retaining not the full additional medium contribution prevents a proper cancellation of terms and destroys the clean vanishing of the medium-specific contribution in vacuum. In this context, it is important to clearly distinguish between the notions of 'medium-specific scalar operator or condensate' on one side and, on the other side, the 'medium dependence of a condensate': A medium-specific scalar operator has a vanishing ground state EV; it only occurs in the medium. In contrast, a vacuum-specific condensate has a non-zero ground state EV; it already occurs in vacuum. Both have a medium dependence.

To illustrate this important point let us consider an example which is detailed below. In Fig. 3.7, left panel, the vacuum-specific condensate  $\langle\langle g\bar{q}\gamma_\mu t^A q \sum_f \bar{f}\gamma^\mu t^A f \rangle\rangle$  is exhibited as a function of the net-nucleon density  $n$  by the blue dashed curve. At  $n = 0$  it takes the value  $-2.42 \times 10^{-4} \text{ GeV}^6$ . According to our definition, this condensate obeys a density dependence, which is deduced here from the squared chiral condensate in nuclear matter. The according additional in-medium contributions only enter via the medium-specific condensate,  $\langle\langle g\bar{q}\gamma_\mu t^A q \sum_f \bar{f}\gamma^\mu t^A f - \frac{2}{v^2} (\bar{q}\gamma^\alpha[(vD), G_{\alpha\beta}]v^\beta q + g\bar{q}\psi t^A q \sum_f \bar{f}\psi t^A f) \rangle\rangle$ , which vanishes at  $n = 0$ . The individual contributions to the medium-specific condensate are the medium four-quark condensate  $\langle\langle g\bar{q}\psi t^A q \sum_f \bar{f}\psi t^A f \rangle\rangle/v^2 = g\langle\langle O_2 \rangle\rangle/v^2$ , the quark-gluon condensate  $\langle\langle \bar{q}\gamma^\alpha[(vD), G_{\alpha\beta}]v^\beta q \rangle\rangle/v^2 = \langle\langle O_5 \rangle\rangle/v^2$  and the already mentioned vacuum four-quark condensate  $\langle\langle g\bar{q}\gamma_\mu t^A q \sum_f \bar{f}\gamma^\mu t^A f \rangle\rangle = g\langle\langle O_1 \rangle\rangle$ , cf. the operator combination in the second line

of Tab. 3.2. These contributions, depicted as magenta dotted, green solid and blue dashed curves, respectively, in the right panel of Fig. 3.7 add up to the medium-specific condensate shown in the left panel (red solid curve).

This example should illustrate how the vacuum-specific and medium-specific condensates are interwoven in the formalism presented in App. C.2 which has the benefit of displaying a transparent limit  $T, n \rightarrow 0$ .

Requiring zero ground state EVs of medium-specific condensates entering the even  $qQ$  meson OPE, i.e. the operator combinations in Tab. 3.2, imposes constraints on the ground state EVs of these constituting operators. The obtained interrelations of the components of medium-specific condensates build on an unambiguous identification of these operator combinations by means of the algebraic decomposition of their Lorentz tensor structure. Setting the ground state EVs of the medium-specific operator combination in Tab. 3.2 to zero one yields a set of equations which corresponds to the general system (C.65) in the light chiral limit  $m_q \rightarrow 0$ . The solution of the underdetermined  $qQ$  meson system of equations, where we choose the ground state EV

$$g^2 \langle \Omega | O_2 | \Omega \rangle / v^2 = x \quad (3.23)$$

to be the free parameter of the solution, can be read off Eq. (C.67) for  $m_q \rightarrow 0$ :

$$g \langle \Omega | O_3 | \Omega \rangle / v^2 = 0, \quad (3.24a)$$

$$g \langle \Omega | O_4 | \Omega \rangle / v^2 = \frac{1}{12} (g^2 \langle \Omega | O_1 | \Omega \rangle - 2x), \quad (3.24b)$$

$$g \langle \Omega | O_5 | \Omega \rangle / v^2 = \frac{1}{2} (g^2 \langle \Omega | O_1 | \Omega \rangle - 2x), \quad (3.24c)$$

$$g \langle \Omega | O_6 | \Omega \rangle / v^2 = \frac{1}{2} (g^2 \langle \Omega | O_1 | \Omega \rangle - 4x), \quad (3.24d)$$

$$g \langle \Omega | O_7 | \Omega \rangle / v^2 = -\frac{1}{12} (-7g^2 \langle \Omega | O_1 | \Omega \rangle - 8x), \quad (3.24e)$$

$$\langle \Omega | O_8 | \Omega \rangle / v^4 = \frac{1}{48} g^2 \langle \Omega | O_1 | \Omega \rangle. \quad (3.24f)$$

The heretofore unknown condensates  $\langle \Omega | O_k | \Omega \rangle$  with  $k = 3, \dots, 8$  are related to the vacuum four-quark condensate  $\langle \Omega | O_1 | \Omega \rangle$  known from the vacuum QSR. As argued in App. C.2.2 one may choose on grounds of universality of condensates the arbitrary parameter to be  $x = g^2 \langle \Omega | O_1 | \Omega \rangle / 4$  as dictated by the algebraic vacuum limits (C.72) from in-medium light meson OPEs.

### Numerical estimates employing factorization

In order to benefit from the algebraic vacuum relations (3.24) one might employ the factorization formulae in Tab. 3.3 to arrive at a tentative numerical estimate of the previously unknown ground state EVs (only non-zero EVs are displayed)

$$g \langle \Omega | O_4 | \Omega \rangle / v^2 = -\frac{1}{54} (2\kappa_0 - \kappa_1) g^2 \langle \Omega | \bar{q}q | \Omega \rangle^2, \quad (3.25a)$$

$$g \langle \Omega | O_5 | \Omega \rangle / v^2 = -\frac{1}{9} (2\kappa_0 - \kappa_1) g^2 \langle \Omega | \bar{q}q | \Omega \rangle^2, \quad (3.25b)$$



$$g\langle\Omega|O_6|\Omega\rangle/v^2 = -\frac{2}{9}(\kappa_0 - \kappa_1)g^2\langle\Omega|\bar{q}q|\Omega\rangle^2, \quad (3.25c)$$

$$g\langle\Omega|O_7|\Omega\rangle/v^2 = \frac{1}{27}(7\kappa_0 - 2\kappa_1)g^2\langle\Omega|\bar{q}q|\Omega\rangle^2, \quad (3.25d)$$

$$\langle\Omega|O_8|\Omega\rangle/v^4 = -\frac{1}{108}\kappa_0g^2\langle\Omega|\bar{q}q|\Omega\rangle^2, \quad (3.25e)$$

while the medium dependence of these condensates remains unrestricted.

In Fig. 3.7 we employ the factorization formulae in Tab. 3.3 and Eq. (3.25b) to illustrate the numerical estimates of the vacuum-specific and medium-specific condensates occurring in the in-medium decomposition of the Gibbs average  $\langle\langle\bar{q}\gamma_\mu[D_\nu, G_{\kappa\lambda}]q\rangle\rangle$  which enters the OPE of  $qQ$  mesons, cf. App. C.3. After transformation to canonical condensates utilizing Eq. (C.58) the vacuum-specific condensate contained in Eq. (C.56) reads

$$\langle\langle g\bar{q}\gamma_\mu t^A q \sum_f \bar{f}\gamma^\mu t^A f \rangle\rangle$$

while the medium-specific condensate contained in Eq. (C.57) is

$$\begin{aligned} & \langle\langle g\bar{q}\gamma_\mu t^A q \sum_f \bar{f}\gamma^\mu t^A f - \frac{2}{v^2} \left( \bar{q}\gamma^\alpha[(vD), G_{\alpha\beta}]v^\beta q + g\bar{q}\not{v}t^A q \sum_f \bar{f}\not{v}t^A f \right) \rangle\rangle \\ &= \langle\langle g\bar{q}\gamma_\mu t^A q \sum_f \bar{f}\gamma^\mu t^A f \rangle\rangle - \frac{2}{v^2} \left( \langle\langle \bar{q}\gamma^\alpha[(vD), G_{\alpha\beta}]v^\beta q \rangle\rangle + \langle\langle g\bar{q}\not{v}t^A q \sum_f \bar{f}\not{v}t^A f \rangle\rangle \right). \end{aligned} \quad (3.26)$$

The factorized expressions in Tab. 3.3 denote in-medium relations suitable to deduce the medium dependences of the four-quark condensates from the medium behavior of the two-quark condensates. In the rest frame, where  $v_\mu = (1, \vec{0})$ , one obtains the LO net-nucleon density dependences of the chiral condensate (2.117) and the in-medium two-quark condensate  $\langle\langle\bar{q}\not{v}q\rangle\rangle = \langle\langle q^\dagger q \rangle\rangle = \frac{3}{2}n$  [Jin93]. Accordingly, the involved four-quark terms acquire the density dependences listed in the last column of Tab. 3.3. However, the EV of the third constituent of the medium-specific condensate (3.26), i.e. the quark-gluon condensate  $\langle\langle \bar{q}\gamma^\alpha[(vD), G_{\alpha\beta}]v^\beta q \rangle\rangle/v^2$ , is only known in vacuum from the algebraic vacuum limit (3.25b). We introduce 'by hand' a linear density dependence of this medium condensate modifying its vacuum value  $\langle\langle \bar{q}\gamma^\alpha[(vD), G_{\alpha\beta}]v^\beta q \rangle\rangle/v^2 = \langle\Omega|\bar{q}\gamma^\alpha[(vD), G_{\alpha\beta}]v^\beta q|\Omega\rangle/v^2 (1 + c_n n)$  with  $c_n \in [-2, 2]$  to exemplify a potential medium dependence of this particular condensate. The range of  $c_n$  is approximately in numerical agreement with the linear density dependences of the two-quark condensates. Accordingly, the quark-gluon condensate in (dense) nuclear matter reads

$$\langle\langle \bar{q}\gamma^\alpha[(vD), G_{\alpha\beta}]v^\beta q \rangle\rangle/v^2 = -\frac{1}{9} \left( 2\kappa_0(0) - \kappa_1(0) \right) g \langle\Omega|\bar{q}q|\Omega\rangle^2 (1 + c_n n). \quad (3.27)$$

For the parameters we choose  $\kappa_i(n) = \kappa_i(0) = 1$  for  $i = 0$  and 1 in accordance with relation (C.88a). The vacuum EV of the chiral condensate  $\langle\Omega|\bar{q}q|\Omega\rangle = (-0.245 \text{ GeV})^3$  is employed as well as  $g = \sqrt{4\pi\alpha_s}$  with  $\alpha_s = 0.5$ . The above derived formulae (3.26) and (3.27) are utilized to illustrate the important features of vacuum-specific and medium-specific condensates in Fig. 3.7.

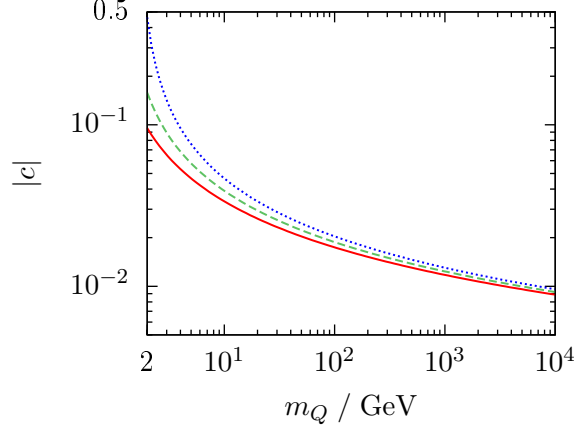


**Figure 3.8:** The modulus of  $c$  defined in (3.30) as a function of  $m_Q$ . The red solid, green dashed and blue dotted curves correspond to  $\mu^2 = 0.5, 1$  and  $2 \text{ GeV}^2$ , respectively.

### Discussion of heavy-quark expansion

Besides light-quark condensates also heavy-quark condensates enter  $D$  meson QSRs containing a light and a heavy quark [Zsc11, Buc12]. Although, these contributions are expected to have little numerical impact they can be included by means of a HQE, cf. Sec. 3.6. In order to check the compatibility of the HQE with the full set of algebraic vacuum limits, inter alia containing heavy-quark condensates with covariant derivatives, the approach presented in Ref. [Gro95] has to be extended to medium condensates.

We choose the algebraic vacuum constraint (C.72), with  $\Gamma' = \mathbb{1}_4$ ,  $T^A = t^A$  and one  $\bar{q} \cdots q$  pair substituted by a  $\bar{Q} \cdots Q$  pair, entering the  $qQ$  meson OPE from the correlator with inserted NLO interaction term [Buc12]

$$\langle \Omega | \bar{q} \not{t}^A q \bar{Q} \not{t}^A Q | \Omega \rangle / v^2 = \frac{1}{4} \langle \Omega | \bar{q} \gamma_\mu t^A q \bar{Q} \gamma^\mu t^A Q | \Omega \rangle \quad (3.28)$$

as the first algebraic vacuum limit deduced by the above formalism to be checked for the compatibility with HQE. Utilizing the LO HQE formulae for both sides of Eq. (3.28) separately, i.e. Eqs. (3.21a) and (3.21b), one obtains from (3.28) upon  $\lim_{T, n \rightarrow 0} \langle \cdots \rangle = \langle \Omega | \cdots | \Omega \rangle$

$$\langle \Omega | \bar{q} \not{t}^A q \sum_f \bar{f} \not{t}^A f | \Omega \rangle / v^2 = \frac{1+c}{4} \langle \Omega | \bar{q} \gamma_\mu t^A q \sum_f \bar{f} \gamma^\mu t^A f | \Omega \rangle \quad (3.29)$$

with HQE compatibility

$$c = \frac{1}{2} \left( 3 \ln \frac{\mu^2}{m_Q^2} + 1 \right)^{-1}. \quad (3.30)$$

However, the algebraic vacuum constraint (C.72), with  $\Gamma' = \mathbb{1}_4$  and  $T^A = t^A$ , entering the light-quark current OPE is satisfied solely for  $c = 0$ . Instead,  $c = c(m_Q)$  runs only logarithmically to zero for increasing heavy-quark masses  $m_Q$ , as exhibited in Fig. 3.8. Only in the limit of an infinite heavy-quark mass the algebraic vacuum limits deduced from

medium-specific condensates are compatible with LO HQE for this specific example, albeit showing strong deviations from  $c = 0$  for experimentally constrained values caused by the logarithmic HQE terms.

### 3.8 Interim summary

A systematic evaluation of the current-current correlator within the framework of QSRs leads to a series of EVs of combined QCD operators multiplied by Wilson coefficients. The seminal analysis of the  $\rho$  meson [Hat92b] points to the crucial impact of light four-quark operator structures (cf. [Hil12c, Hoh12, Hol13, Hoh14]). Driven by this insight we have evaluated the in-medium QSR for pseudo-scalar  $\bar{q}Q$  and  $\bar{Q}q$  mesons up to mass dimension 6 with emphasis on light four-quark condensate contributions, thus extending previous studies for vacuum [Shu82a, Ali83, Nar88, Nar94, Nar99, Nar01, Nar05, Nar13, Hay04] and medium [Hil09, Zsc11].

Due to lacking information on precise numerical values of four-quark condensates, we employed tentatively the factorization hypothesis to estimate the numerical importance of light four-quark condensate contributions. In contrast to the  $\rho$  meson sum rule, the power corrections of higher mass dimension are obviously consecutively smaller, as mentioned already in [Rei85] for vacuum and highlighted in [Hil09] for in-medium situations. The heavy-quark mass in the combination  $m_Q \langle \bar{q}q \rangle$  provides a numerically large contribution to the OPE making it dominating. Having now the exact Wilson coefficients for light four-quark condensates at our disposal their impact for in-medium situations can be quantified: Within the previously employed Borel window relevant for pseudo-scalar  $\bar{q}Q$  and  $\bar{Q}q$  excitations the individual contributions to the even part are one to two orders of magnitude smaller than most of the other known terms at saturation density. A similar statement holds for the contributions of the odd part. By comparing to the  $\rho$  meson OPE terms we are able to locate the origin of these order of magnitude differences in the D meson contributions: (i) the absence of light four-quark terms from hard-gluon diagrams and (ii) Wilson coefficients altering more strongly with changing Borel mass due to the non-negligible heavy-quark mass. Despite the small numerical impact of these higher mass dimension contributions, they are required for a profound estimate of the reliable Borel window: Extending the OPE up to light-quark condensates of mass dimension 6 delivers the bonus to allow for a better determination of the Borel window, because the lower limit is constrained by the highest order OPE terms which must not contribute more than  $\sim 10\%$  to the OPE [Lei97].

Our presentation makes obvious the avenue for improvements: Insertion of the NLO interaction term into the correlator provides loop corrections to the Wilson coefficients for condensates of lower mass dimension as well as further four-quark condensate contributions with associated diagrams on tree-level. We emphasize the rapidly growing complexity of higher order contributions, especially for in-medium situations. Our evaluation of the Wilson coefficients of LO  $\alpha_s$  terms related to light four-quark condensates demonstrates this already. Including, furthermore, condensation of heavy quarks can be accommodated in the present formalism, albeit resulting in cumbersome expressions. Probably new methods are needed for executing the OPE and subsequent evaluation of the sum rules as a complement to  $\ell$ QCD methods.

Although the numerical impact of light four-quark condensate terms on the OPE proved to be small, they are structurally important in hadron physics due to their close connection

to chiral symmetry. Apart from the chiral condensate which serves as an order parameter of spontaneous chiral symmetry breaking we identify a further chirally odd condensate,  $\langle\langle \bar{q}t^A q \sum_f \bar{f} \not{t}^A f \rangle\rangle$ , among the four-quark condensate contributions of the pseudo-scalar  $D$  meson sum rule. Chirally odd condensates quantify the difference of chiral partner spectra and can also be studied by Weinberg-type sum rules, proven, e. g. in [Hoh12,Hol13,Hoh14], as extremely useful when addressing issues of chiral restoration in a strongly interacting medium.

The physics motivation of the present investigation is clearly driven by the contemporary interest in open charm (also bottom) mesons as probes of the hot, strongly interacting medium created in ultra-relativistic heavy-ion collisions. Moreover, the planned experiments of the CBM and PANDA collaborations at FAIR will study charm degrees of freedom in proton and anti-proton induced reactions of nuclei and in heavy-ion collisions as well. For these experimental investigations a solid theoretical basis is mandatory. Among possible approaches with emphasis on medium modifications are QCD sum rules as a method with intimate contact to QCD.

## 4 Chiral partner sum rules

Chiral partner mesons are hadrons coupling to quark currents which mix under chiral transformations and transform into each other under a suitable finite chiral transformation with a specific set of rotation angles. Embedded in a system that obeys chiral symmetry the spectral densities of chiral partner mesons are degenerate. As chiral symmetry is (dynamically) broken in nature the spectra may differ. Studying the differences of chiral partner spectra, thus, allows to probe the breaking pattern of chiral symmetry. Canonically, currents sharing the same internal angular momentum but possess opposite parity are considered chiral partners. Often the light spin-1 mesons of vector (V) and axial-vector (A) type, e.g. the  $\rho$  and  $a_1$  mesons respectively, are investigated while we focus on heavy-light spin-0 mesons, in particular on pseudo-scalar (P) and scalar (S) D mesons. This chapter is partially based on Ref. [Buc16a] and builds on notions related to chiral symmetry which are introduced in App. B and Subsec. 2.3.2.

### 4.1 Motivation

In the scope of QCD sum rules, where the integrated spectral density of a hadron is related to QCD condensates, the difference of chiral partner spectra is quantified by chirally odd condensates entering with opposite sign. In a scenario of chiral restoration, which may be realized in a strongly interacting environment, these chirally odd condensates, e.g. the chiral condensate  $\langle \bar{q}q \rangle$ , must vanish. As non-vanishing chirally odd condensates necessitate the dynamical breakdown of chiral symmetry, their medium dependence [Hat93, Jin93, Fio12, God13] is of paramount importance [Wei94, Tho06], not only in the scope of QSRs [Rap99, Rap00, Har06]. However, as the vanishing of a single condensate does not necessarily imply chiral symmetry restoration (cf. [Kan15] for a recent discussion of a counter example), a more comprehensive view must be envisaged. The impact of higher order condensates, in particular of four-quark condensates, on  $\rho$  meson and nucleon properties is well-known [Leu98, Zsc02, Tho07]. In particular chirally odd four-quark condensates turn out to materially contribute to the spectral shape of the  $\rho$  meson [Hil12c].

While probing the degree of D $\chi$ SB with chiral partners composed of up- and down-quarks having negligible masses is a promising approach successfully applied to  $\rho$  and  $a_1$  mesons, studying patterns of D $\chi$ SB with mesons containing a heavy and a light quark seems to be superimposed by the explicit symmetry breaking due to the non-negligible heavy-quark mass. However, the original light-quark problem can be translated into the heavy-light sector, if the chiral symmetry transformations are restricted to the light-quark content. As exemplified in App. B.3 for the  $D^0$  meson, the pseudo-scalar current  $j_P = i\bar{u}\gamma_5 c$  can be transformed into the scalar current  $j_S = \bar{u}c$  by a finite chiral transformation (B.30) with a specific set of rotation parameters (B.32). Thus, the pseudo-scalar and scalar  $D^0$  mesons are chiral partners, which would have degenerate spectral properties in a chirally symmetric world. In contrast, the experimentally verified masses,  $m_P = 1.865$  GeV and

$m_S = 2.318$  GeV, deviate about 450 MeV (in accordance with the  $a_1$ - $\rho$  mass splitting) signaling the dynamical breakdown of chiral symmetry which is driven by order parameters [Hil11,Hil12b,Buc16a], e. g. most prominently by the chiral condensate as well as by chirally odd four-quark condensates. In order to obtain a comprehensive picture of the landscape of order parameters of D $\chi$ SB and their respective relations to the spectra of hadrons and medium modifications thereof, four-quark condensates must also be investigated in the scope of heavy-light quark mesons.

For instance, in the  $\rho$  and  $\omega$  meson sum rules the chiral condensate contribution is suppressed numerically due to the light-quark mass, i. e. the RGI combination  $m_q\langle\bar{q}q\rangle$ , whereas gluon and four-quark condensates are important instead [Tho08b,Rap10]. As a consequence, numerically relevant chiral symmetry effects enter the QSR via chirally odd four-quark condensates. Due to the approximation of four-quark condensates by the squared chiral condensate these chiral effects were mistakenly viewed to be caused by the chiral condensate. Such artifacts can be overcome if contributions from chirally odd condensate, being potential order parameters, are separated from chirally even terms [Hil12c]. However, the chiral condensate has a sizable impact on spectral properties in the heavy-light meson sector, since the heavy-quark mass acts as an amplification factor, i. e. the scale-dependent combination  $m_Q\langle\bar{q}q\rangle$  enters the QSR (3.3a) [Hil10,Rap11,Zsc11]. The chiral condensate dominates in fact the contributions to the pseudo-scalar D meson OPE in the region of interest (Borel window) in vacuum as well as at nucleon saturation density [Hil09,Buc15b]. Thus, the D meson QSR is highly sensitive to chiral symmetry effects mediated by  $\langle\bar{q}q\rangle$ . Chirally odd four-quark terms enter the Lorentz-odd in-medium OPE of the D meson (3.3b). Although, these condensates do not substantially contribute to the complete (Lorentz-odd) OPE as depicted in Fig. 3.5, they have significant impact on Weinberg-type sum rules which are sensitive to chirally odd condensates only, cf. Sec. 4.3.

While spectral properties of the pseudo-scalar D mesons are experimentally well constrained, only limited information on scalar D mesons is currently available. QSR investigations of these particular mesons exhibit a congruent pattern. Pseudo-scalar D mesons attracted much attention, where recent studies focus either on precise predictions of spectral or QCD parameters in vacuum [Nar16] or on medium modifications [Gub16,Suz16a], cf. also the references in Sec. 3.8; whereas scalar D meson QSRs have been rarely analyzed so far, primarily in the vacuum [Hay04,Nar05,Sun10,Wan15b] or in cold nuclear matter [Hil10]. As the idea of heavy-light mesons as probes of D $\chi$ SB gains acceptance also further investigations of chiral partners based on different approaches are performed emphasizing the role of the scalar D meson, e. g. hadronic model calculations [Sas14] exhibiting approaching chiral partner D meson masses at high temperatures. Accordingly, we are going to set up the in-medium QSR for the scalar D meson in order to seek for signals of chiral restoration at finite temperatures in a particle-anti-particle symmetric medium.

## 4.2 Temperature dependences of pseudo-scalar and scalar D meson properties

The temperature dependences of the masses, residua and decay constants of pseudo-scalar and scalar D mesons are addressed in this section, where the obtained vacuum results can be directly compared to decay constants from recent QSR analyses if the interpolating currents

entering the correlator (2.1) are slightly altered in comparison to Eq. (3.5), for example. Hence, we use here

$$j_P(x) = \partial_\mu j_A^\mu(x) = (m_Q + m_q) i \bar{q}(x) \gamma_5 Q(x), \quad (4.1a)$$

$$j_S(x) = i \partial_\mu j_V^\mu(x) = (m_Q - m_q) \bar{q}(x) Q(x) \quad (4.1b)$$

with the canonical definition of vector and axial-vector currents, i. e.  $j_V^\mu(x) = \bar{q}(x) \gamma^\mu Q(x)$  and  $j_A^\mu(x) = \bar{q}(x) \gamma^\mu \gamma_5 Q(x)$ , both being part of weak V – A currents. As demonstrated in Eqs. (4.1) by employing the quark EoMs, the pseudo-scalar and scalar currents overlap with  $j_A^\mu$  and  $j_V^\mu$ , respectively, admitting a weak decay of the D mesons, e. g.  $D^+ \rightarrow W^{+*} \rightarrow \ell^+ \nu_\ell$ . The pseudo-scalar D meson decay constant  $f_P$  defined as

$$\langle \Omega | j_A^\mu(x) | P(\vec{p}) \rangle = i p^\mu f_P e^{-i p x}, \quad (4.2)$$

analogously to  $f_\pi$  in Eq. (B.19), reappears in

$$\langle \Omega | j_P(0) | P \rangle = f_P m_P^2 \quad (4.3)$$

by virtue of Eq. (4.1a), where  $|P\rangle$  denotes the pseudo-scalar D meson state with mass  $m_P$ . Accordingly, the decay constant  $f_P$  contributes to the leptonic decay width of lepton flavor  $\ell$

$$\Gamma(P^+ \rightarrow \ell^+ \nu_\ell) = \frac{G_F^2}{8\pi} |V_{Qq}|^2 f_P^2 m_\ell^2 m_P \left(1 - \frac{m_\ell^2}{m_P^2}\right)^2, \quad (4.4)$$

the numerical value of which can be obtained from the branching ratio  $\Gamma(P^+ \rightarrow \ell^+ \nu_\ell)/\Gamma_{\text{tot}}$  in [Pat16]. Analogous definitions and relations hold for the scalar particle, however, experimental results for the wanted branching fraction of a decay into a specific leptonic channel,  $\Gamma(S^+ \rightarrow \ell^+ \nu_\ell)/\Gamma_{\text{tot}}$ , are not yet available.<sup>1</sup>

The Borel transformed in-medium dispersion relations as well as even and odd OPE formulas for pseudo-scalar currents [Hil09] can be easily rewritten for scalar mesons using Eqs. (4.20) and (4.21). At finite temperature but zero baryon density they reduce to

$$\int_0^\infty ds e^{-s/M^2} \rho_{P,S}(s; T) \tanh\left(\frac{\sqrt{s}}{2T}\right) = \hat{\Pi}_{P,S}(M^2; T) \quad (4.5)$$

with the finite-temperature OPE derived in the  $\overline{\text{MS}}$  scheme and in the light chiral limit,  $m_q \rightarrow 0$ ,

$$\begin{aligned} & \hat{\Pi}_{P,S}(M^2; T) \\ &= \frac{1}{\pi} \int_{m_Q^2}^\infty ds e^{-s/M^2} \text{Im} \Pi^{\text{pert}}(s) + e^{-m_Q^2/M^2} m_Q^2 \left\{ \mp m_Q \langle \bar{q}q \rangle_T + \frac{1}{12} \langle \frac{\alpha_s}{\pi} G^2 \rangle_T \right. \\ &+ \left[ \left( \frac{7}{18} + \frac{1}{3} \ln \frac{\mu^2 m_Q^2}{M^4} - \frac{2\gamma_E}{3} \right) \left( \frac{m_Q^2}{M^2} - 1 \right) - \frac{2}{3} \frac{m_Q^2}{M^2} \right] \langle \frac{\alpha_s}{\pi} \left( \frac{(vG)^2}{v^2} - \frac{G^2}{4} \right) \rangle_T \\ &+ \left. 2 \left( \frac{m_Q^2}{M^2} - 1 \right) \langle q^\dagger i D_0 q \rangle_T \pm \frac{1}{2} \left( \frac{m_Q^3}{2M^4} - \frac{m_Q}{M^2} \right) \left( \langle \bar{q}g\sigma Gq \rangle_T - \langle \Delta \rangle_T \right) \right\}, \quad (4.6) \end{aligned}$$

<sup>1</sup>Although, no charged scalar D meson  $S^+$  is listed in [Pat16] its mass is assumed to coincide with the uncharged D meson  $m_{S^+} \simeq m_{S^0}$  in this work due to iso-spin symmetry. This is also in agreement with the small SU(3) light-quark flavor breaking [Nar05], i. e.  $m_{S^+} \simeq m_{S^0}$ , and supported by analogy to the pseudo-scalar channel  $m_{P^+} \simeq m_{P^0}$ .

where the perturbative contribution  $\text{Im}\Pi^{\text{pert}}(s)$  obtained from Cutkosky's cutting rules can be found, e. g. in Ref. [Ali83, Zsc11] (mind the interpolating currents there which differ from Eq. (4.1a) by the quark mass factors). The quantity  $\mu$  denotes the renormalization scale and  $\gamma_E$  is the Euler-Mascheroni constant. The EVs  $\langle(\alpha_s/\pi)[(vG)^2/v^2 - G^2/4]\rangle_T$ ,  $\langle q^\dagger i D_0 q \rangle_T$  and  $\langle \Delta \rangle_T = 8\langle \bar{q} D_0^2 q \rangle_T - \langle \bar{q} g \sigma G q \rangle_T$  are medium-specific condensates [Buc16b], thus they vanish at zero temperature by definition. Dimension-6 four-quark condensate terms do not significantly contribute to  $\hat{\Pi}_P$ , cf. Fig. 3.4; the same holds true for the scalar OPE. Thus, we restrict the numerical evaluation to condensates up to mass dimension 5.

Henceforth, the pole + continuum ansatz for the spectral densities, cf. Sec. 2.4, is employed, because it adequately describes a narrow resonance, e. g. the pseudo-scalar D meson. The spectral density reads

$$\rho_X(s) = R_X \delta(s - m_X^2) + \frac{1}{\pi} \text{Im}\Pi^{\text{pert}}(s) \Theta(s - s_0^X), \quad (4.7)$$

where  $X$  denotes either P or S. The residue in vacuum is assumed to satisfy [Nar05, Bor05, Luc11a]

$$R_X = f_X^2 m_X^4, \quad (4.8)$$

justified by comparison of Eq. (4.7) with the spectral density (2.8) entering the Källén-Lehmann representation of the current-current correlator (2.1), where a complete set of hadronic states has been inserted – the lowest resonance with residuum  $|\langle \Omega | j_X(0) | X \rangle|^2$  and further (multi-particle) excitations combined to the continuum here. In order to render our results comparable with the findings in the above references, we resort to this assumption at finite temperatures as well. Employing the ansatz (4.7) the spectral integral in Eq. (4.5) yields

$$\begin{aligned} & \int_0^\infty ds e^{-s/M^2} \rho_X(s) \tanh\left(\frac{\sqrt{s}}{2T}\right) \\ &= R_X e^{-m_X^2/M^2} \tanh\left(\frac{m_X}{2T}\right) + \frac{1}{\pi} \int_{s_0^X}^\infty ds e^{-s/M^2} \tanh\left(\frac{\sqrt{s}}{2T}\right) \text{Im}\Pi^{\text{pert}}(s) \\ &\equiv \hat{\Pi}_X^{\text{res}}(M^2; T) + \hat{\Pi}_X^{\text{cont}}(M^2; T) \end{aligned} \quad (4.9)$$

conveniently split into the resonance and continuum parts,  $\hat{\Pi}_X^{\text{res}}$  and  $\hat{\Pi}_X^{\text{cont}}$ , respectively. The ratio QSRs (2.134) are utilized to deduce the meson masses from  $\tilde{\Pi}_X = \hat{\Pi}_X - \hat{\Pi}_X^{\text{cont}}$  while the residua are obtained from  $R_X = e^{m_X^2/M^2} \tanh^{-1}(m_X/(2T)) \tilde{\Pi}_X$ , cf. Eq. (2.135).

The temperature dependence of the phenomenological side due to  $\tanh(\sqrt{s}/(2T))$ , cf. Eq. (4.5), has only a minor numerical impact. Even for the lowest relevant energies  $\sqrt{s}$  and at temperatures as high as the chiral restoration temperature  $T_{\chi\text{rest}} \simeq 0.263$  GeV, estimated by  $\langle \bar{q} q \rangle_{T=T_{\chi\text{rest}}} \simeq 0$  from Eq. (2.116),<sup>2</sup> the D meson masses and residua are effected on a sub-percentage level. For  $\hat{\Pi}_X^{\text{cont}}$  entering the meson mass formula (2.134) one obtains deviations of

<sup>2</sup>To conservatively estimate the impact of the tanh-term on the QSR, we choose this rather high value of  $T_{\chi\text{rest}}$  compared to commonly reported values of  $\sim 0.15$  GeV. However, it is close to the critical temperature  $\sim 0.27$  GeV in pure Yang-Mills theory.



**Table 4.1:** List of relevant condensates entering the finite-temperature OPEs in Eq. (4.6). The second column contains the vacuum values while the last column provides the temperature dependent part of the condensates at  $\mu = 1.5$  GeV using a RGI chiral condensate  $\hat{\mu}_q^3 = (0.251 \text{ GeV})^3$  and the integral definitions  $B_i(z) = \frac{3(3i-1)}{\pi^{2i}} \int_z^\infty dy y^{2(i-1)} \sqrt{y^2 - z^2} / (e^y - 1)$  for  $i = 1$  and  $2$  [Hat93, Nar13].

condensate	vacuum value	temperature dependent part
$\langle \bar{q}q \rangle_T$	$(-0.268)^3 \text{ GeV}^3$	$(0.268)^3 \text{ GeV}^3 \frac{T^2}{8f_\pi^2} B_1\left(\frac{m_\pi}{T}\right) \simeq 0.278 \text{ GeV} T^2$
$\langle \bar{q}g\sigma Gq \rangle_T$	$0.8 \cdot (-0.246)^3 \text{ GeV}^5$	$0.8 \cdot (0.246)^3 \text{ GeV}^5 \frac{T^2}{8f_\pi^2} B_1\left(\frac{m_\pi}{T}\right) \simeq 0.172 \text{ GeV}^3 T^2$
$\langle \frac{\alpha_s}{\pi} G^2 \rangle_T$	$0.012 \text{ GeV}^4$	$-\frac{m_\pi^2}{9} T^2 B_1\left(\frac{m_\pi}{T}\right) \simeq 0$
$\langle q^\dagger i D_0 q \rangle_T$	$0$	$\frac{1}{8} \left[ \frac{\pi^2}{5} T^4 B_2\left(\frac{m_\pi}{T}\right) - \frac{m_\pi^2}{8} T^2 B_1\left(\frac{m_\pi}{T}\right) \right] \cdot 0.92 \simeq 0.247 T^4$

$1 - \hat{\Pi}_X^{\text{cont}} / [\frac{1}{\pi} \int_{s_0^X}^\infty ds e^{-s/M^2} \text{Im} \Pi^{\text{pert}}(s)] \leq 1 - \tanh(\sqrt{s_0^X}/(2T)) \leq 1 - \tanh(m_Q/(2T_{\chi\text{rest}})) \simeq 0.7\%$  for  $m_Q \sim 1.5$  GeV. The numerical values of the pole residuum  $R_X$  are altered by  $R_X/(e^{m_X^2/M^2} \tilde{\Pi}_X) - 1 = \tanh^{-1}(m_X/(2T)) - 1 \leq \tanh^{-1}(m_Q/(2T_{\chi\text{rest}})) - 1 \simeq 0.7\%$  for  $m_Q \sim 1.5$  GeV. Considering the inherent uncertainties of the QSR framework the factor  $\tanh(\sqrt{s}/(2T))$  may be safely neglected in the spectral integral kernel.

The numerical evaluations of the QSRs below utilize running QCD parameters in the  $\overline{\text{MS}}$  scheme on two-loop level with  $\mu = 1.5$  GeV, i.e. the strong coupling, quark mass and condensates according to Ref. [Nar13] and the derivations in Subsec. 2.2.2. The needed RGI quantities are deduced from experimental results listed in Ref. [Pat16]. In particular, the QCD scale  $\Lambda$  is directly determined from  $\alpha_s(\mu = m_Z = 91.2 \text{ GeV}) = 0.1184$  and the RGI quark mass  $\hat{m}_Q$  from  $m_Q(\mu = 2 \text{ GeV}) = 1.275 \text{ GeV}$  while the RGI chiral condensate  $\hat{\mu}_q^3$  employs the GOR relation (B.23) with  $f_\pi = 0.093 \text{ GeV}$ ,  $m_\pi = 0.14 \text{ GeV}$  and  $(m_u + m_d)(\mu = 2 \text{ GeV}) = 0.008 \text{ GeV}$ . The temperature behavior of the contributing condensates, estimated for an ambient non-interacting pion gas, have a sizable impact on the QSRs. The temperature dependences of numerically relevant condensates are listed in Tab. 4.1 whereas the medium-specific condensates  $\langle (\alpha_s/\pi) [(vG)^2/v^2 - G^2/4] \rangle_T$  and  $\langle \Delta \rangle_T$  are negligible [Hat93]. The above decay constant  $f_\pi$  and the pion mass in the chiral limit,  $m_\pi = 0$ , have been used to produce the numerical coefficients in the last column in Tab. 4.1.

### 4.2.1 Conventional Borel analysis

In the QSR framework meson masses are evaluated as the average of the particular meson mass Borel curve (2.134) which shows maximum flatness in the corresponding Borel window. This window is the Borel mass range where the phenomenological and OPE sides of the QSR can be reliably matched (to some extent), since it is constructed such that higher OPE terms do not contribute significantly and the phenomenological spectral density is dominated by the first excitation, cf. Sec. 2.4. The Borel window depends on the actual

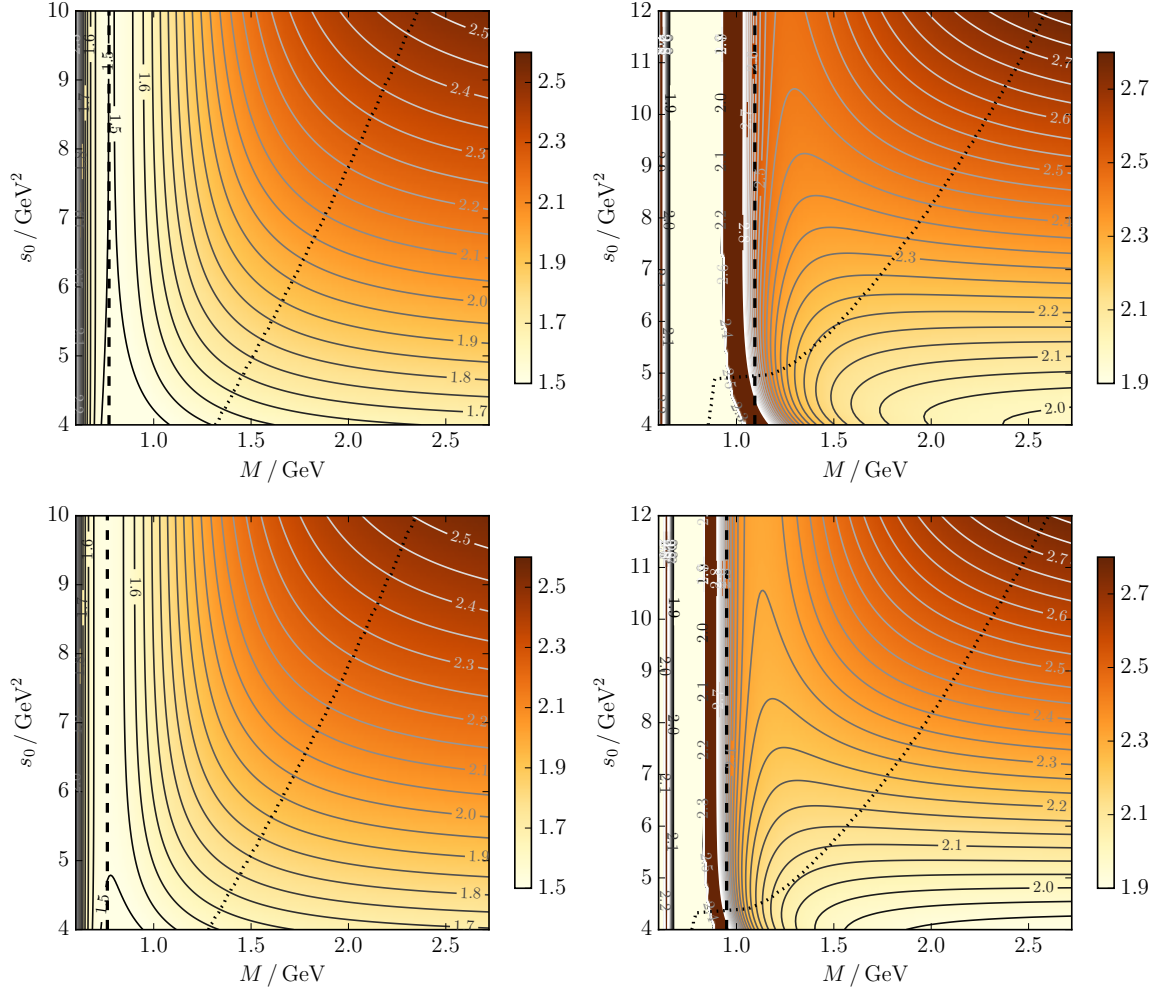


**Figure 4.1:** Comparison of pseudo-scalar (left panels) and scalar (right panels) D meson mass contours  $m_{P,S}(M, s_0) / \text{GeV}$ , in vacuum at  $T = 0$  (upper panels) and at  $T = 0.15 \text{ GeV}$  (lower panels). The dashed and dotted curves denote the lower and upper Borel window boundaries, respectively.

numerical restrictions of the particular QSR and, thus, differs for scalar and pseudo-scalar D mesons as well as for distinct temperatures as exhibited in Fig. 4.1.

The pseudo-scalar D meson mass  $m_P(M, s_0)$ , depicted in the left panels of Fig. 4.1, does not produce a flat area within the Borel window. Thus, a standard Borel analysis as outlined in Sec. 2.4 is not feasible which was already realized in Refs. [Hil09] and [Nar13]. While the authors of the former reference estimate the meson mass from the Borel curve minimum, accordingly, and focus on medium effects, the latter reference resorts to the Borel mass dependent renormalization scale,  $\mu = M$ , in order to obtain stable mass Borel curves. Here, no final conclusion about the numerical value of the pseudo-scalar D meson mass is drawn. However, the contour pattern of the meson mass hardly changes with increasing temperature (cf. left panels of Fig. 4.1) which might suggest only minor medium effects on the pseudo-scalar D meson mass in a heat bath consisting of non-interacting pions, thus, pointing to a pseudo-scalar D meson mass which approximately resides in the vicinity of its

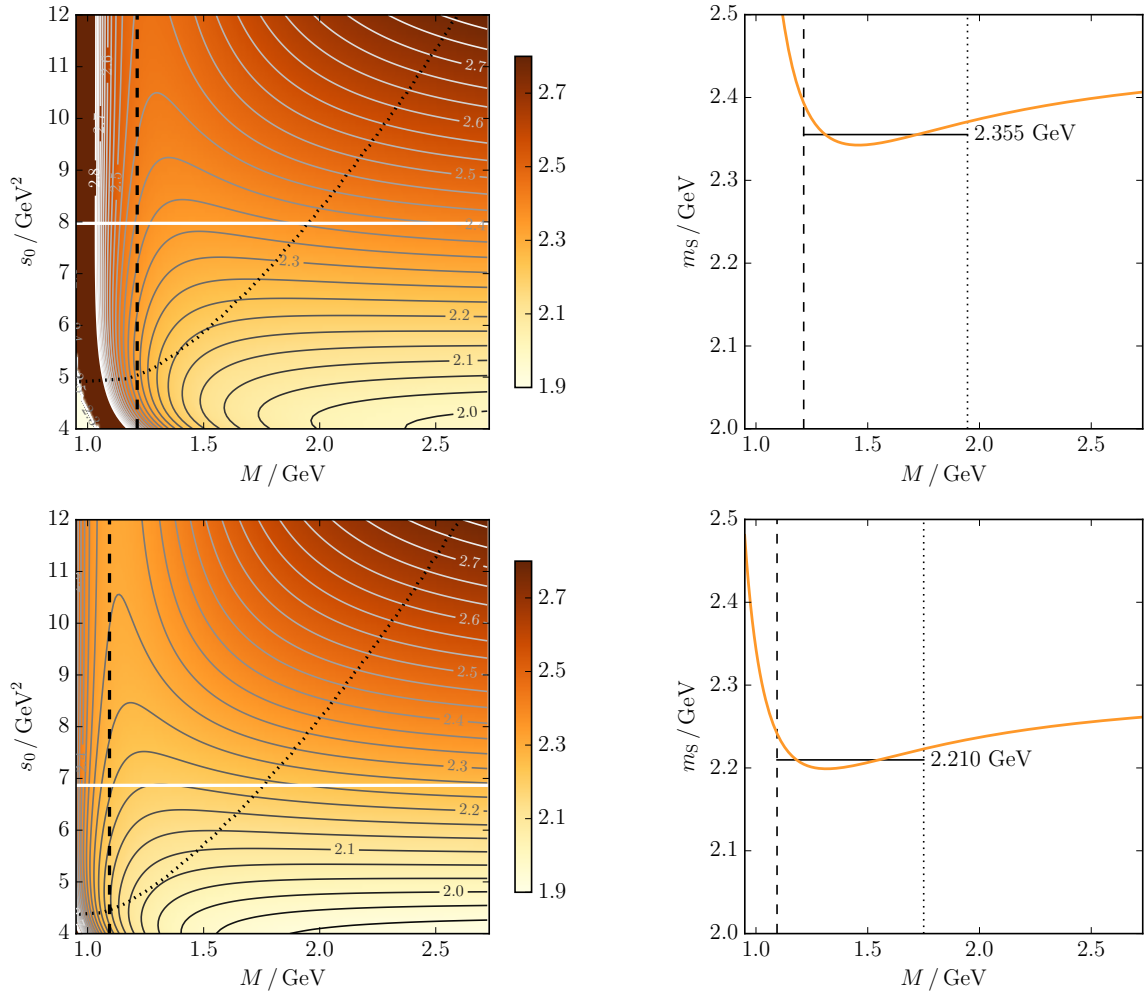


**Figure 4.2:** Scalar D meson mass contours  $m_S(M, s_0)/\text{GeV}$  (left panels), in vacuum at  $T = 0$  (upper panels) and at  $T = 0.15 \text{ GeV}$  (lower panels). The dashed and dotted curves denote the lower and upper Borel window boundaries, respectively. For both temperatures, the maximally flat mass Borel curves (together with the associated Borel averaged masses) are depicted in the right panels corresponding to the white cuts in the contour plots, where the optimal continuum threshold parameter can be read off.

experimentally confirmed vacuum value of  $m_P = 1.865 \text{ GeV}$ , also at finite temperatures. In contrast, the scalar D meson mass  $m_S(M, s_0)$ , depicted in the right panels of Fig. 4.1, is exploitable, i. e. there are contour lines displaying approximately horizontal sections within the Borel window. The relevant contour lines are well above the closing Borel window, preventing a Borel analysis for  $s_0 < 5 \text{ GeV}^2$  in vacuum and  $s_0 < 4.4 \text{ GeV}^2$  at  $T = 0.15 \text{ GeV}$ . The contour plot exhibits changing patterns for finite temperatures, where the contour lines with pronounced horizontal section within the Borel window signal a clear downshift of the scalar D meson mass.

A quantitative more robust analysis can be provided by the conventional approach requiring maximal flatness of the mass Borel curve within the Borel window, cf. Eq. (2.137). However, the lower limits of the standard Borel window, where the highest order condensate

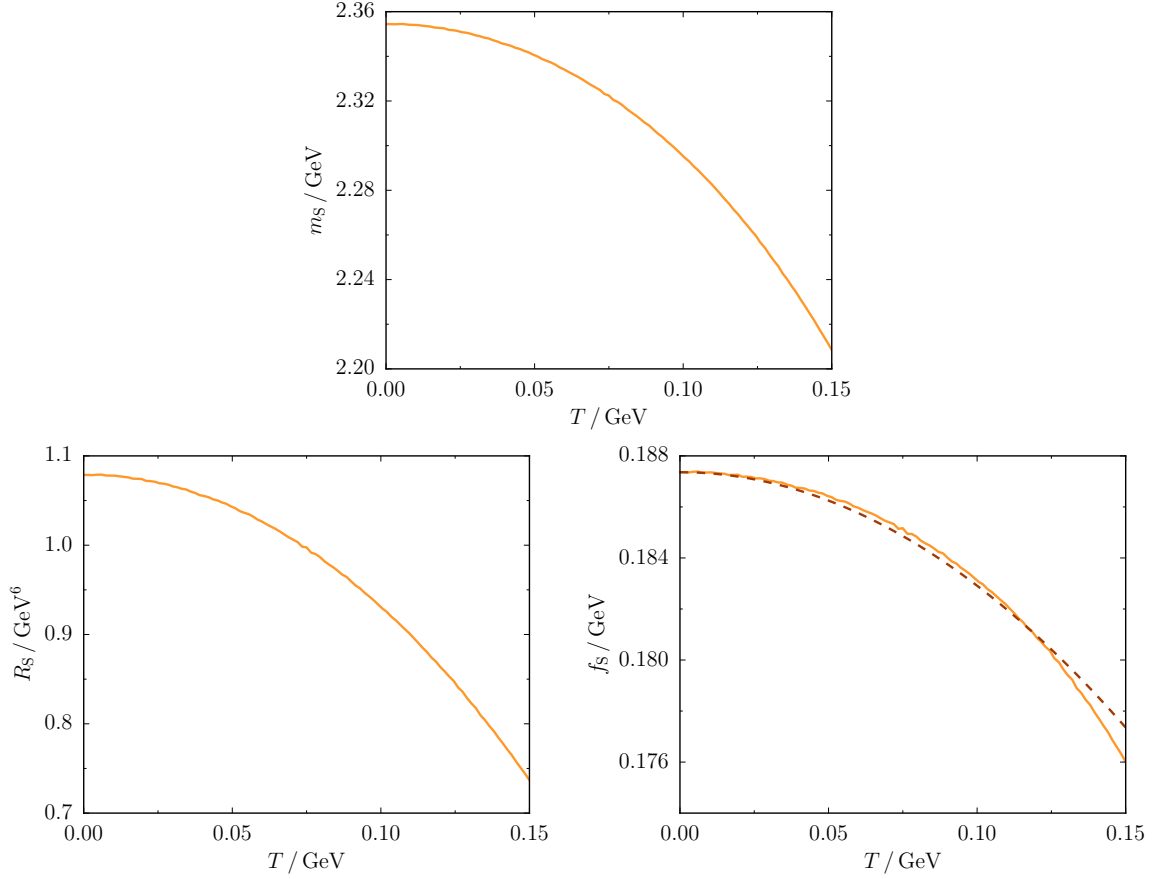


**Figure 4.3:** Temperature dependences of the spectral properties of the scalar D meson, where the upper panel depicts the mass parameter  $m_S$ , the lower left panel displays the residuum  $R_S$  and the lower right panel shows the decay constant  $f_S$  from our analysis (orange solid curve) as well as the temperature dependence of the decay constant deduced from Eq. (4.10) (brown dashed curve).

term is required to contribute less than 10 % to the OPE, are close to the steep slopes in the contour plots in Fig. 4.1, i.e. close to the poles of the Borel curves. Hence, they can significantly influence the meson masses  $m_{P,S}$  averaged within the Borel window, because it has a sizable impact on the value of the continuum threshold  $s_0^{P,S}$  resulting from an optimization of the Borel curve for maximal flatness. In order to reduce the impact of the steep Borel curve section spoiling the extraction method of the spectral meson parameters, we choose  $M_{\min}$  requiring the highest order OPE term to contribute less than 5 % to the complete OPE, while  $M_{\max}$  is extracted as usually by requiring the continuum to contribute less than 50 % to the QSR. The results exhibit a mass drop of the scalar D meson. As depicted in the right panels in Fig. 4.2, calculating the average of the mass Borel curve with optimal continuum threshold parameter, corresponding to the white cuts in the left panels in Fig. 4.2, yields the scalar D meson mass  $m_S = 2.355$  GeV (experimentally,  $m_S^{\text{exp}} = (2.318 \pm 0.029)$  GeV, cf. Ref. [Pat16]) in vacuum which drops to  $m_S = 2.210$  GeV at  $T = 0.15$  GeV.

A numerical Borel analysis for continuous temperatures up to 0.15 GeV, where the low-temperature expansion is assumed to hold [Hat93], yields temperature dependent scalar D

meson masses  $m_S$  and residua  $R_S$  averaged within the Borel window as depicted in Fig. 4.3. These results exhibiting a scalar  $D$  meson mass drop, while the pseudo-scalar  $D$  meson mass remains unaltered, point to approaching chiral partner meson masses for increasing temperatures, signaling chiral restoration.

The temperature behavior of the scalar  $D$  meson mass  $m_D$  depicted in Fig. 4.3 deviates from the result calculated from a hadronic effective theory incorporating chiral symmetry breaking terms [Sas14], cf. Fig. 4.7 below. Although, both approaches predict a significant mass drop at high temperatures, the  $D$  meson mass deduced from the effective theory remains almost constant before falling rapidly at  $T = 0.12$  GeV while our QSR evaluations points to a parabolic temperature dependence. Such behavior is transferred to the respective residuum  $R_S$  and decay constant  $f_S$  which approximately obeys

$$f_S(T) = f_S(0) \left( 1 - \frac{T^2}{12[f_S(0)]^2} \right), \quad (4.10)$$

cf. Fig. 4.3. In the framework of chiral perturbation theory, this functional form has been distilled from the LO temperature dependence of the axial-vector correlator at large space-like momenta determining the pion decay constant  $f_\pi$ , where massless pions have been assumed, i. e. a two-flavor system which imposes the factor  $1/12$  [Gas87].

Naively, the different temperature behaviors of the chiral partners may be regarded to canceling temperature dependences of the condensates in the pseudo-scalar OPE contrasted by accumulating temperature dependent contributions in the scalar OPE, i. e.

$$\tilde{\Pi}_{P,S}(M^2; T) = \Pi_0^{P,S}(M^2) + \Pi_T^{P,S}(M^2) \quad (4.11)$$

with

$$\begin{aligned} \Pi_0^{P,S}(M^2) = & \frac{1}{\pi} \int_{m_Q^2}^{s_0^{P,S}} d\omega e^{-\omega/M^2} \text{Im} \Pi^{\text{pert}}(\omega) + e^{-m_Q^2/M^2} m_Q^2 \left[ \mp m_Q \langle \bar{q}q \rangle_0 \right. \\ & \left. + \frac{1}{12} \langle \frac{\alpha_s}{\pi} G^2 \rangle_0 \pm \frac{1}{2} \left( \frac{m_Q^3}{2M^4} - \frac{m_Q}{M^2} \right) \langle \bar{q}g\sigma Gq \rangle_0 \right], \end{aligned} \quad (4.12a)$$

$$\begin{aligned} \Pi_T^{P,S}(M^2) = & T^2 B_1 \left( \frac{m_\pi}{T} \right) e^{-m_Q^2/M^2} m_Q^2 \left[ \pm \frac{m_Q}{8f_\pi^2} \langle \bar{q}q \rangle_0 + \frac{m_\pi^2}{18} + \frac{1}{4} \left( \frac{m_Q^2}{M^2} - 1 \right) \cdot 0.92 \right. \\ & \left. \times \left( \frac{\pi^2}{5} T^2 \frac{B_2 \left( \frac{m_\pi}{T} \right)}{B_1 \left( \frac{m_\pi}{T} \right)} - \frac{m_\pi^2}{8} \right) \mp \frac{1}{2} \left( \frac{m_Q^3}{2M^4} - \frac{m_Q}{M^2} \right) \frac{1}{8f_\pi^2} \langle \bar{q}g\sigma Gq \rangle_0 \right], \end{aligned} \quad (4.12b)$$

cf. Tab. 4.1. In the light chiral limit,  $m_\pi \rightarrow 0$ , the only relevant terms at low temperatures in Eq. (4.12b) arise from the chirally odd contributions, i. e. the chiral condensate and the mixed quark-gluon condensate. Hence, no significant cancellation of terms occurs, but the relevant temperature dependent terms enter the pseudo-scalar and scalar OPEs  $\tilde{\Pi}_{P,S}$  with opposite sign. Since the different temperature behaviors of pseudo-scalar and scalar mesons cannot be understood by comparing the temperature dependent OPE contributions  $\Pi_T^{P,S}$ , one needs to disclose intermediate steps of the Borel analysis to explain the phenomenon in the scope of QSRs.

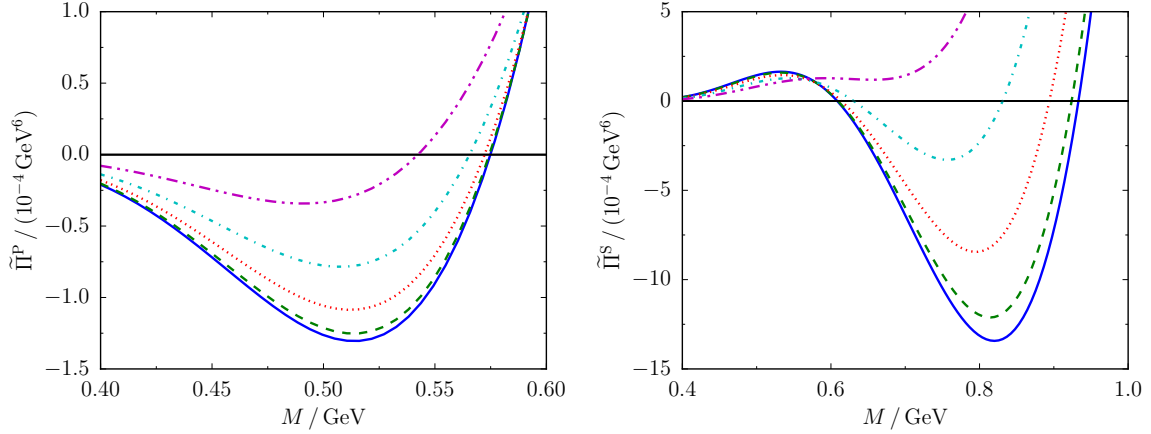


**Figure 4.4:** OPE Borel curves of pseudo-scalar (left panel) and scalar (right panel) D mesons containing condensate contributions up to mass dimension 5 and with fixed continuum threshold parameters  $s_0^{P,S} = 7 \text{ GeV}^2$  at different temperatures: blue solid curve – vacuum; green dashed, red dotted, cyan dot-dashed and magenta dot-dot-dashed curves are at  $T = 0.05, 0.1, 0.15$  and  $0.2 \text{ GeV}$ , respectively.

In this framework, meson masses are evaluated as the average of the particular meson mass Borel curve (2.134), which shows maximum flatness in the corresponding Borel window. The meson mass Borel curves of pseudo-scalar and scalar D mesons feature poles slightly below the Borel window, which lift the mass Borel curve in the Borel window and subsequently increase the averaged meson mass. These poles originate from zeros of the OPE, entering the denominator of the mass Borel curve formula (2.134), and are subject to changes at higher temperatures, which turn out very differently for pseudo-scalar and scalar mesons, cf. Fig. 4.4. While the pole in the pseudo-scalar curve persists, shifted slightly towards lower Borel masses, the poles of the scalar meson mass Borel curve vanish at high temperatures. Due to the vicinity of the Borel window the scalar D meson mass is effected by such a drastic temperature behavior of the pole structure of the scalar meson mass Borel curve. Vanishing of the poles at higher temperatures can be understood from the scalar OPE which drifts upwards for increasing temperatures featuring no zeros above a particular temperature, cf. Fig. 4.4.

The vanishing and persistence of zeros of the pseudo-scalar and scalar OPEs can also be understood if the major OPE contributions at the relevant Borel mass ranges are considered. In Fig. 4.5 the main contributions to the OPE are depicted: the perturbative term, the chiral condensate term and the mixed quark-gluon condensate term. The perturbative contribution remains the same while the condensate contributions decrease with increasing temperature. In vacuum, the dominant contribution to the OPE at high Borel mass  $M$  is the perturbative term consecutively superseded by the chiral and mixed condensate term for lower values of  $M$ . Due to the downshift of the condensate curves at high temperatures, e. g.  $T = 0.25 \text{ GeV}^2$ , the perturbative term as the dominating term of the OPE is directly superseded by the mixed condensate term for decreasing  $M$ . Depending on the particular signs of the single condensate contributions this leads to different numbers of zeros of the OPE, as exhibited in Fig. 4.4.

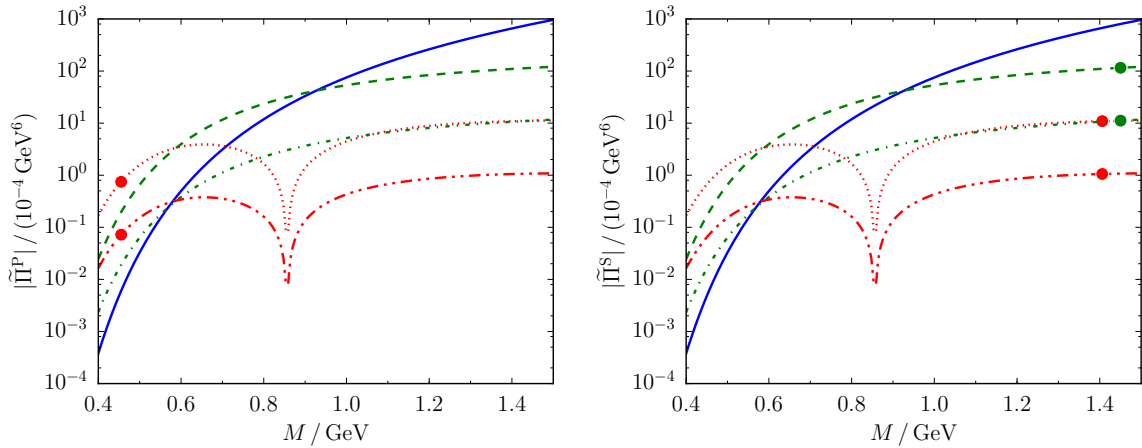


**Figure 4.5:** Modulus of the major OPE contributions of pseudo-scalar (left panel) and scalar (right panel)  $D$  mesons with fixed continuum threshold parameters  $s_0^{P,S} = 7 \text{ GeV}^2$ : the blue solid curve depicts the perturbative contribution, the green dashed and dot-dashed curves are the chiral condensates contributions in vacuum and at  $T = 0.25 \text{ GeV}$ , respectively, while the red dotted and dot-dot-dashed curves display the mixed condensate term in vacuum and at  $T = 0.25 \text{ GeV}$ , respectively. The branches with bullet markers originate from negative values.

#### 4.2.2 Borel analysis with given meson mass input

The conventional Borel analysis as performed in the previous subsection can be contrasted by an analysis which utilizes the given meson mass as input and aims for deducing the hadron's residuum and decay constant. This approach has attracted much attention in recent years [Bor04, Bor05, Luc11a, Luc11b, Luc14, Gel13, Nar13, Nar16, Wan15b], not only in the realm of QSRs [Suz16b, Fah16, Dür16], because accurate numerical values of open flavor meson decay constants could be used to constrain, inter alia, off-diagonal CKM matrix elements from weak decays of these mesons, cf. Eq. (4.4). For a pole + continuum ansatz, the continuum threshold parameter  $s_0$  is adjusted to reproduce the given meson mass parameter  $m$  from the respective mass Borel curve (2.134) employing the flatness criterion (2.137). Subsequently, the Borel averaged residuum  $R$  is calculated from Eq. (2.135) with the extracted continuum threshold parameter and the meson mass. The corresponding decay constant  $f$  is readily obtained from Eq. (4.8).

In order to improve the flatness of the mass Borel curve within the Borel window one may introduce a Borel mass dependent continuum threshold parameter [Luc10]

$$s_0(M) = \sum_{n=0}^{n_{\max}} \frac{s_0^{(n)}}{M^{2n}}, \quad (4.13)$$

where the coefficients  $s_0^{(n)}$  are chosen to minimize deviations of the mass Borel curve from the known actual meson mass according to the requirement (2.137). This approach has been checked for toy models with potentials, where the spectral information of the lowest resonance as well as the OPE are precisely known. As an effective continuum threshold (4.13) produces more accurate results than a fixed continuum threshold parameter in these test cases [Luc09] one may infer that the Borel mass dependent  $s_0$  reduces the contamination

of the lowest resonance by continuum states, thus, rendering the semi-local quark-hadron duality (2.128) exact if the fixed value of  $s_0$  on the r.h.s. of Eq. (2.128) is substituted by the  $M$ -dependent one [Luc11b]. Due to the  $M$ -dependent continuum threshold parameter, further terms contribute to the derivative sum rule used to determine the mass Borel curve, i.e. for an original QSR of the form

$$\int_0^{s_0(M)} ds e^{-s/M^2} \rho^{\text{res}}(s) = \frac{1}{\pi} \int_{m_Q^2}^{s_0(M)} ds e^{-s/M^2} \text{Im}\Pi^{\text{pert}}(s) + \text{power corrections} \quad (4.14)$$

the derivative sum rule reads

$$\begin{aligned} & \int_0^{s_0(M)} ds s e^{-s/M^2} \rho^{\text{res}}(s) - \rho^{\text{res}}(s_0(M)) e^{-s_0(M)/M^2} \frac{ds_0(M)}{d(1/M^2)} \\ &= \frac{1}{\pi} \int_{m_Q^2}^{s_0(M)} ds s e^{-s/M^2} \text{Im}\Pi^{\text{pert}}(s) - \frac{1}{\pi} \text{Im}\Pi^{\text{pert}}(s_0(M)) e^{-s_0(M)/M^2} \frac{ds_0(M)}{d(1/M^2)} \\ & \quad - \frac{d}{d(1/M^2)} (\text{power corrections}). \end{aligned} \quad (4.15)$$

While  $\rho^{\text{res}}(s_0(M)) = 0$  for a pole ansatz, because we assume  $m_h^2 < s_0$ , the continuum contribution merged with the perturbative term is altered if the derivative of the continuum threshold parameter w.r.t.  $1/M^2$  does not vanish.

## Vacuum

Our studies show that the minimization method yields acceptable results only for a fixed Borel window and fails for continuum threshold parameter dependent upper Borel window boundaries  $M_{\text{max}}(s_0)$ . In Ref. [Luc11b], the fixed Borel window [1.4 GeV, 3.2 GeV] for the pseudo-scalar D meson QSR is determined requiring that the power corrections do not exceed a contribution of 30 % to the OPE (sets  $M_{\text{min}}$ ) and that the resonance contribution to the spectral integral does not fall below 10 % (sets  $M_{\text{max}}$ ). However, at the lower boundary the continuum already contributes 50 % to the spectral strength causing a closed Borel window determined from standard criteria [Lei97].

**Table 4.2:** Continuum threshold coefficients  $s_0^{S(n)}$  of the Borel mass dependent continuum threshold parameter  $s_0^S$  obtained from minimization requirement (2.137) with the actual scalar D meson mass input. The corresponding Borel curves are depicted in Fig. 4.6.

$n_{\text{max}}$	$s_0^{S(0)} / \text{GeV}^2$	$s_0^{S(1)} / \text{GeV}^4$	$s_0^{S(2)} / \text{GeV}^6$	$s_0^{S(3)} / \text{GeV}^8$
0	7.4371			
1	7.5009	0.00012		
2	7.4755	-0.00026	0.00029	
3	7.3781	-0.00661	0.01040	-0.00535



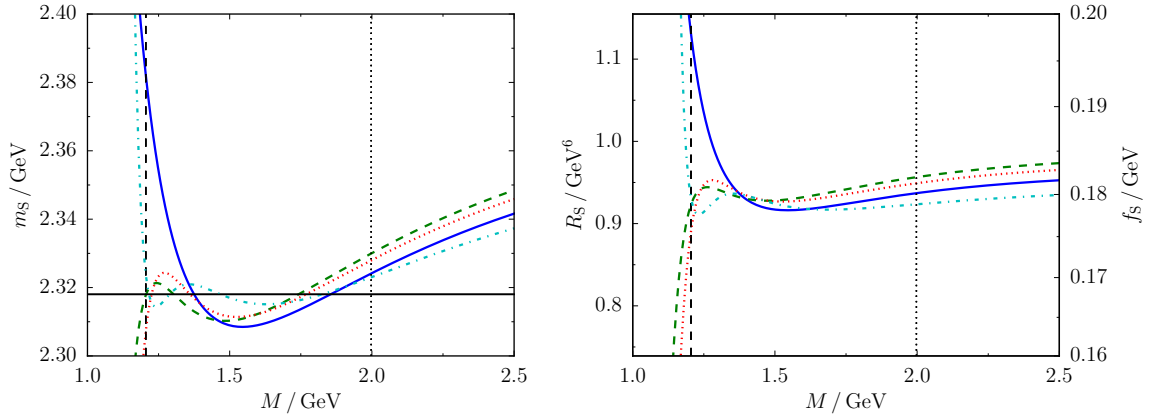


**Figure 4.6:** Vacuum scalar  $D$  meson mass Borel curves (left panel) for  $M$ -dependent continuum threshold parameters (4.13) with minimized deviations from the actual meson mass depicted by the solid horizontal line. The blue solid, green dashed, red dotted and cyan dot-dashed curves correspond to continuum thresholds with the degree of the polynomial ansatz  $n_{\max} = 0, 1, 2$  and  $3$ , respectively, where the numerical values of the coefficients are listed in Tab. 4.2. The residuum and decay constant Borel curves depicted in the right panel are associated with the mass Borel curves in the left panel, i. e. the same color code applies. The vertical dashed and dotted lines denote the lower and upper Borel window boundaries.

To reduce the impact of the continuum on the spectral properties of the scalar  $D$  meson resonance the Borel window from the conventional analysis,  $[1.2 \text{ GeV}, 2 \text{ GeV}]$ , cf. Fig. 4.2 upper left panel, has been utilized to obtain the results in Fig. 4.6. The mass Borel curves for increasing degree polynomials contributing to the  $M$ -dependent continuum threshold parameter adapt closer to the actual scalar  $D$  meson mass, indeed. However, the tendency of rising residuum and decay constant values for increasing  $n_{\max}$  as reported in [Luc11a] for pseudo-scalar  $D$  mesons do not occur in the scalar channel. While vacuum scalar  $D$  meson decay constants deduced from a QSR with perturbative term in order  $\alpha_s^2$  are reported to reside in the range of  $f_S = 0.217 - 0.221 \text{ GeV}$  in Refs. [Nar05, Nar16] the determination [Col91] building on the perturbative term in order  $\alpha_s$ , used throughout this thesis, yield  $f_S = 0.17 \text{ GeV}$  which is compatible with our findings depicted in the (lower) right panel of Fig. 4.6 (Fig. 4.7).

## Medium

Extracting the decay constant from a fixed meson mass by adjusting multiple coefficients of a Borel mass dependent continuum threshold is also viable in a strongly interacting medium if the temperature and/or net-baryon density dependence of the respective meson is at our disposal. Due to lacking experimental information available temperature dependent  $D$  meson masses may serve as input, which are calculated from an effective theory comprising chiral symmetry breaking terms [Sas14].

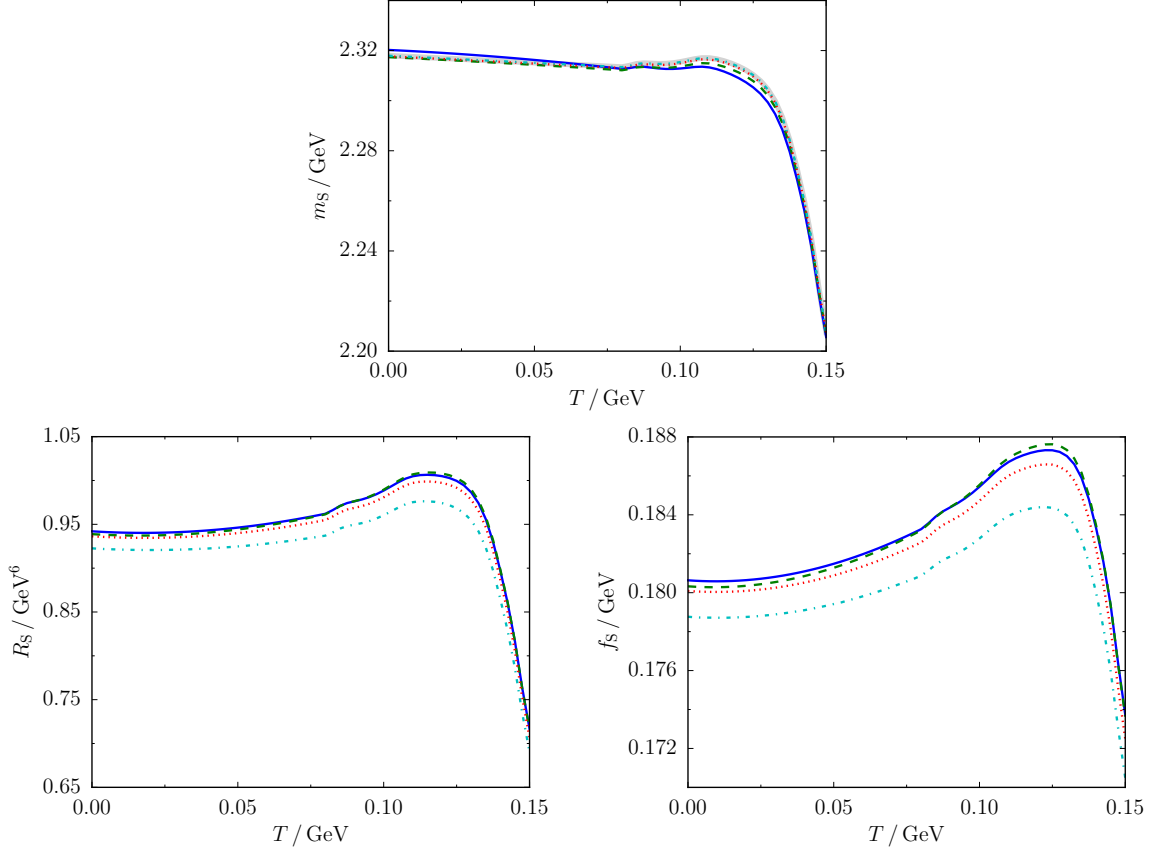


**Figure 4.7:** Temperature dependences of the scalar D meson mass (upper panel), residuum (lower left panel) and decay constant (lower right panel). The blue solid, green dashed, red dotted and cyan dot-dashed curves correspond to continuum thresholds with the degree of the polynomial ansatz  $n_{\max} = 0, 1, 2$  and  $3$ , respectively. The light gray thick curve in the upper panel depicts the input mass parameters calculated in Ref. [Sas14].

We studied various Borel window configurations building on the vacuum and  $T = 0.15$  GeV Borel windows from the 'orthodox analysis',<sup>3</sup> cf. Fig. 4.2, e.g. temperature independent intersection and union of the two Borel windows, or a simple construction where the lower boundary changes linearly from its vacuum value  $M_{\min}(T=0) \simeq 1.2$  GeV to  $M_{\min}(T=0.15 \text{ GeV}) \simeq 1.1$  GeV and  $M_{\max}$  alike. The extracted numerical values are sensitive to the definition of the temperature dependent Borel window or even produce implausible optimization results for the degree  $n_{\max} = 3$  of the polynomial ansatz (4.13). Reliable numerical results, displayed in Fig. 4.7, are obtained with the temperature independent Borel window adopted from the evaluation in vacuum.

The temperature dependent scalar D meson masses  $m_S$  are well reproduced from the QSR analysis, where the curves adapt more closely to the input meson mass for increasing  $n_{\max}$ . For rising temperatures the residuum  $R_S$  increases 5 % at  $T = 0.12$  GeV before falling

<sup>3</sup>In accordance with the vacuum evaluation,  $s_0$ -dependent upper Borel boundaries  $M_{\max}(s_0)$  obstruct the optimization procedure also at finite temperatures. Hence, a fixed Borel window has to be deployed for each temperature. The Borel windows from the conventional analysis can provide a rough estimate only, because they refer to an optimized continuum threshold parameter at a given temperature.

off rapidly. The associated temperature behavior of the decay constant  $f_S$  exhibits a similar pattern, but with more pronounced increase up to  $T = 0.12$  GeV. While the decreasing residuum  $R_S = |\langle \Omega | j_S(0) | S \rangle|^2$  – signaling the decoupling of the quark current from the meson states – is a prerequisite for deconfinement at high temperatures, the decrease of the decay constant  $f_S$  seems counter-intuitive, because it dominates the temperature behavior of the decay rate  $\Gamma_S$ , cf. Eq. (4.4), corresponding to the meson’s (partial) width which is expected to grow in a strongly interacting environment, cf. the  $\rho$  meson in [Rap97, Kli97, Fri97, Pet98, Pos04, Kwo08]. Considering the relation (4.8) one may attribute the fall of the decay constant for rising temperatures to the scalar D meson mass, decreasing not fast enough to counteract the decreasing residuum; or vice versa, a too rapid fall of the residuum which can not be compensated by the decreasing meson mass causes the dropping decay constant.

### 4.3 Weinberg sum rules

The Weinberg sum rules (WSRs), originally deduced from current algebra [Wei67b],

$$\int_0^\infty ds \, s^{-1} \rho_{V-A}(s) = f_\pi^2, \quad (4.16a)$$

$$\int_0^\infty ds \, \rho_{V-A}(s) = -2m_q \langle \bar{q}q \rangle, \quad (4.16b)$$

$$\int_0^\infty ds \, s \rho_{V-A}(s) = 2\pi\alpha_s \langle \mathcal{O}_{4q}^{\text{odd}} \rangle \quad (4.16c)$$

link moments of the difference of vector and axial-vector meson spectra,  $\rho_{V-A} = \rho_V - \rho_A$ , to order parameters of chiral symmetry, i. e. the pion decay constant  $f_\pi$ , the chiral condensate  $\langle \bar{q}q \rangle$  and chirally odd four-quark condensates  $\langle \mathcal{O}_{4q}^{\text{odd}} \rangle$ . In this spirit, chirally odd condensates being order parameters of D $\chi$ SB quantify the difference of chiral partner spectra. The moments (4.16) are sensitive to single order parameters and hence overcome the shortcomings of channel-specific QSRs where a multitude of condensates enters blurring the contribution of a particular order parameter, i. e. allowing for its extraction with limited accuracy only. Since the WSRs solely quantify D $\chi$ SB effects whereas the standard QSRs are channel-specific, they provide independent information [Hoh14].

WSRs at finite temperature  $T$  were first formulated in Ref. [Kap94] by subtracting the vector and axial-vector in-medium QSRs from one another, Taylor-expanding the Borel exponential, and equating powers of the squared Borel mass  $M^2$  on each side of the sum rule. Such difference sum rules attract much attention, because they can be utilized to investigate the medium behavior of vector and axial-vector spectral functions in the light-meson sector building on the well constrained  $\rho$  and  $a_1$  vacuum spectral densities [Bar98] and the (in principle) experimentally accessible  $\rho$  spectrum in a strongly interacting environment [Aga12, Sal13]. Thus, the WSRs of the chiral partner mesons  $\rho$  and  $a_1$  have been studied extensively, e. g. to study chiral restoration driven by the order parameters of chiral symmetry [Hoh14, Aya14], to further restrict spectral functions containing more than one low-lying

resonance [Hoh12] as well as to check their compatibility with chiral mixing [Hol13] and hadronic models [Kwo10].

### 4.3.1 Extending Weinberg-type sum rules for spin-0 heavy-light mesons

According to the arguments of Sec. 4.1, one can derive in-medium Weinberg-type sum rules along the lines of Ref. [Kap94] as differences of chiral partner QSRs of heavy-light mesons in the  $V - A$  (spin-1) as well as in the  $P - S$  (spin-0) channels [Buc16a]

$$\int_{-\infty}^{\infty} d\omega \frac{\rho_{\text{c.p.}}(\omega, \vec{p})}{\omega - p_0} \tanh\left(\frac{\omega}{2T}\right) = \Pi_{\text{c.p.}}(p_0, \vec{p}), \quad (4.17)$$

where the subscript 'c.p.' symbolizes either  $V - A$  or  $P - S$ , and  $\Pi_{V-A, P-S} = \Pi_{V, P} - \Pi_{A, S}$  with contracted Lorentz indices in the spin-1 channels is understood. The quantities  $\Pi_{V, A, P, S}$  denote current-current correlators (2.1) defined with vector, axial-vector, pseudo-scalar and scalar interpolating currents,  $j_X = \bar{q}_1 \Gamma_X q_2$  with  $\Gamma_X \in \{\gamma^\mu, \gamma^\mu \gamma_5, i\gamma_5, \mathbb{1}_4\}$ , respectively, cf. Eqs. (B.15)–(B.18) with a suitable combination of flavor matrices  $\tau^a$  and  $\mathbb{1}_{N_f}$ .

Considering the difference of chiral partner QSRs considerably reduces computational efforts, because chirally even terms cancel in the chiral difference OPE  $\Pi_{\text{c.p.}}$ , in particular perturbative contributions and gluon condensates, cf. Fig. 3.1 diagrams (a)–(f). Thus, to LO in the strong coupling the fully Wick-contracted term  $\Pi_{\text{c.p.}}^{(0)}$  does not yield chirally odd terms but they exclusively enter from the two-quark term  $\Pi_{\text{c.p.}}^{(2)}$ , where the notation  $\Pi_{\text{c.p.}} = \Pi_{\text{c.p.}}^{(0)} + \Pi_{\text{c.p.}}^{(2)}$  is adopted from the decomposition of the pseudo-scalar correlator due to the application of Wick's theorem (3.6). Furthermore, the projection of the Dirac structure of occurring anti-commutators incorporating the quark propagators  $S_{1,2}$  and the Dirac matrix  $\gamma_5$  onto basis elements  $\Gamma$  of the Clifford algebra yields vanishing projection coefficients, cf. App. C.1.1. Hence, the chiral partner two-quark terms read [Hil11]

$$\begin{aligned} \Pi_{V-A}^{(2)}(p) = & - \sum_n \frac{(-i)^n}{n!} 2 \sum_{\Gamma}^{\{\mathbb{1}_4, i\gamma_5\}} \langle\langle : \bar{q}_1 \overleftarrow{D}_{\vec{\alpha}_n} \Gamma \partial^{\vec{\alpha}_n} (\text{Tr}_D[\Gamma S_2(p)]) q_1 \\ & + \bar{q}_2 \Gamma \partial^{\vec{\alpha}_n} (\text{Tr}_D[\Gamma S_1(-p)]) D_{\vec{\alpha}_n} q_2 : \rangle\rangle, \end{aligned} \quad (4.18)$$

$$\begin{aligned} \Pi_{P-S}^{(2)}(p) = & - \sum_n \frac{(-i)^n}{n!} \frac{1}{2} \sum_{\Gamma}^{\{\mathbb{1}_4, \sigma_{\alpha < \beta}, \gamma_5\}} \langle\langle : \bar{q}_1 \overleftarrow{D}_{\vec{\alpha}_n} \Gamma \partial^{\vec{\alpha}_n} (\text{Tr}_D[\Gamma S_2(p)]) q_1 \\ & + \bar{q}_2 \Gamma \partial^{\vec{\alpha}_n} (\text{Tr}_D[\Gamma S_1(-p)]) D_{\vec{\alpha}_n} q_2 : \rangle\rangle, \end{aligned} \quad (4.19)$$

where the full quark propagators  $S_{1,2}$  are approximated by the perturbative propagators according to Eq. (2.44). As we are particularly interested in spin-0 chiral partner D mesons we exploit Eq. (4.19) with  $q_1 = q$  and  $q_2 = Q$ , as well as  $S_{1,2} = S_{q,Q}$  correspondingly, in the light chiral limit,  $m_q \rightarrow 0$ .

Evaluation of in-medium sum rules distinguishes even and odd parts of the OPE with respect to the meson energy  $p_0$ , cf. Eqs. (2.19) and (2.20), allowing for a Borel transformation

$\Pi_{\text{c.p.}}^{\text{even,odd}}(Q^2) \rightarrow \hat{\Pi}_{\text{c.p.}}^{\text{even,odd}}(M^2)$  after a Wick rotation  $p_0 = iQ$ . In the medium's rest frame,  $v_\mu = (1, \vec{0})$ , for  $qQ$  mesons at rest, we are able to extend the previous findings in the P – S channel contributing solely to the even OPE [Hil11, Hil12b]

$$\begin{aligned} \int_{-\infty}^{\infty} d\omega \, \omega e^{-\omega^2/M^2} \tanh\left(\frac{\omega}{2T}\right) \rho_{\text{P-S}}(\omega) &= \hat{\Pi}_{\text{P-S}}^{(2)\text{even}}(M^2) \\ &= e^{-m_Q^2/M^2} \left[ -2m_Q \langle\langle \bar{q}q \rangle\rangle + \left( \frac{m_Q^3}{2M^4} - \frac{m_Q}{M^2} \right) \left( \langle\langle \bar{q}g\sigma Gq \rangle\rangle - \langle\langle \Delta \rangle\rangle \right) \right] \end{aligned} \quad (4.20)$$

to mass dimension 6 by adding the chirally odd four-quark condensate contribution occurring in the odd OPE

$$\begin{aligned} \int_{-\infty}^{\infty} d\omega \, e^{-\omega^2/M^2} \tanh\left(\frac{\omega}{2T}\right) \rho_{\text{P-S}}(\omega) &= \hat{\Pi}_{\text{P-S}}^{(2)\text{odd}}(M^2) \\ &= \frac{2e^{-m_Q^2/M^2} m_Q}{M^4} g^2 \langle\langle \bar{q}t^A q \sum_f f^\dagger t^A f \rangle\rangle. \end{aligned} \quad (4.21)$$

The expectation value  $\langle\langle \bar{q}g\sigma Gq \rangle\rangle$  is the mixed quark-gluon condensate of mass dimension 5 and  $\langle\langle \Delta \rangle\rangle = \langle\langle \bar{q}g\sigma Gq \rangle\rangle - 8\langle\langle \bar{q}D_0^2 q \rangle\rangle$  [Hil11] stands for a medium-specific condensate [Buc15a] of mass dimension 5. In contrast to the original WSRs (4.16) for light spin-1 chiral partner mesons, moments of the spectral density  $\rho_{\text{c.p.}}$  of  $qQ$  mesons do in general not depend on a single order parameter, but higher spectral moments contain the full set of chirally odd condensates of the previous moments, due to the common exponential factor  $e^{-m_Q^2/M^2}$  entering the OPE of  $qQ$  mesons. Thus, if heavy-light mesons are considered, an analysis of the Borel mass dependent chiral partner sum rules in a reasonable Borel range is to be preferable to an evaluation of the corresponding Weinberg-type sum rules, which are derivatives of the chiral partner sum rules w. r. t.  $1/M^2$  evaluated at  $1/M^2 = 0$  and lack the beneficial sensitivity to single order parameters.

### 4.3.2 Comments on chirally odd condensates

Pseudo-scalar D and B meson sum rule analyses in the nuclear medium [Hil09] show that the odd OPE drives the mass splitting of D(B) and  $\bar{D}(\bar{B})$  mesons. However, at zero nucleon density, particles and anti-particles are degenerate even at finite temperature involving a vanishing odd OPE (4.21). Although, this requires a zero chirally odd four-quark condensate, chiral symmetry is not restored since the chirally odd condensates entering the even OPE (4.20) do not vanish per se. Therefore, chiral symmetry restoration does not emerge by vanishing of a single chirally odd condensate, but requires vanishing of all chirally odd condensates. A recent study [Kan15], which is based on a particular D $\chi$ SB pattern described below, substantiates this insight.

Inspired by spontaneous magnetization effects in (anti-)ferromagnets breaking the rotation symmetry of the spin systems [Kne94], an alternative pattern of D $\chi$ SB in QCD has been outlined in Ref. [Ste98] leading to a vanishing chiral condensate while further order parameters, e.g. the pion decay constant and the mixed quark-gluon condensate, remain

non-zero. The regime considered in [Ste98] is natural if the pattern of D $\chi$ SB is not the conventional  $SU(N_f)_V \times SU(N_f)_A \rightarrow SU(N_f)_V$  but rather the unorthodox [Kog99]

$$SU(N_f)_V \times SU(N_f)_A \rightarrow SU(N_f)_V \times Z(N_f)_A, \quad (4.22)$$

where  $Z(N_f)_A$  denotes the axial center symmetry group associated with the transformations  $\psi \rightarrow \psi' = e^{2\pi i \gamma_5 k / N_f} \psi$  and  $k = 1, \dots, N_f$ . As the chiral condensate is not invariant under these transformations, the vanishing of  $\langle \bar{q}q \rangle$  in the chiral limit is ensured by the unbroken  $Z(N_f)_A$  symmetry [Kog99]. At this point it is evident that, to obtain a discriminating order parameter, probing solely a single symmetry, it must be invariant under all further symmetry transformations. In a scenario resembling the D $\chi$ SB pattern (4.22) particular four-quark condensates can serve as meaningful chiral order parameters [Kog99]. Although, this explicit breaking pattern can not be ruled out by means of rigorous QCD inequalities, based on Cauchy-Schwarz inequalities of correlators composed of axial and pseudo-scalar currents, it is unlikely to be realized in nature as the inequalities are not satisfied for all energies, also at non-zero temperatures [Kog99]. However, at finite net-baryon densities the breaking pattern (4.22) is conceivable [Kan15]. Although, these studies address particular phases with zero chiral condensate but further non-vanishing order parameters, while we are concerned with zero chirally odd condensates, vanishing due to their medium-specific character, they still emphasize the vital point that vanishing of single order parameters is insufficient to verify chiral restoration.

All chirally odd condensates of a certain mass dimension  $\dim_m$  appear either in the even or in the odd OPE of the LO correlator, i.e. they have either an even or odd Lorentz tensor rank  $n$ . The four-quark condensate given e.g. in Eq. (4.21) is a particular example of a condensate which is characterized by its non-trivial chiral transformation properties, similar to the famous chiral condensate  $\langle \bar{q}q \rangle$ , as an order parameter of D $\chi$ SB. However, as it is a Lorentz-odd condensate, it must be zero at any temperature for zero net density if particle and anti-particle are to remain degenerate (see App. C.2.2). This exemplifies why the vanishing of a chirally odd condensate, such as the chiral condensate, is not a sufficient condition for chiral symmetry restoration if only the non-trivial chiral transformation properties of such a condensate are taken into account [Hil16].

The exclusive occurrence of chirally odd condensates with fixed mass dimension either in the even or in the odd OPE can be deduced from chiral partner OPEs, where chirally even condensates cancel. In the EVs of Eqs. (4.20) and (4.21), only elements of the Clifford algebra  $\Gamma$  with an even number of Lorentz indices enter:

$$\Pi_{\text{c.p.}}^{(2)} \propto \sum_{k,l,m} \sum_{\Gamma}^{\{\mathbb{1}_4, \sigma_{\alpha\beta}, \gamma_5\}} \langle \bar{q} \overleftrightarrow{D}_{\alpha_1} \cdots \overleftrightarrow{D}_{\alpha_k} \Gamma S(D_{\mu_1}, \dots, D_{\mu_l}; G_{\nu_1 \lambda_1}, \dots, G_{\nu_m \lambda_m}) q \rangle, \quad (4.23)$$

where the mass dimension  $\dim_m$  of the EV is given by  $\dim_m = 3 + k + l + 2m$ .<sup>4</sup> In the above relation  $S$  denotes a term of the expansion of the perturbative quark propagator (2.44) in a classical, weak, gluonic background field specified by  $l$  and  $m$ . It is merely a function of the field strength tensor and derivatives thereof. Thus, the Dirac matrices  $\Gamma$  do not alter

<sup>4</sup>A more detailed mass formula which is based on the order of the quark field expansion and the expansion of the perturbative quark propagator can be found in [Hil12a]. Note that Eq. (4.23) holds true solely for quark condensates from the correlator in LO  $\alpha_s$ .

the spin parity of the EV. Since the number of Lorentz indices and the order of the mass dimension are increased by the same integer if  $G_{\mu\nu}$  and  $D_\mu$  are added, one can stick with the mass dimension of the individual operators contributing to the EV to determine the rank of this Lorentz tensor. Hence, the Lorentz tensor rank of the EV is  $n = \dim_m - 3$ , where 3 is the mass dimension of the two quark operators. From relation (4.23) we, therefore, infer that all chirally odd condensates of the fixed mass dimension  $\dim_m$  enter the odd (even) OPE with respect to the meson energy  $p_0$ , due to their odd (even) tensor rank  $n$ . At this point it becomes apparent, that chirally odd condensates in mass dimension 6 originating from the LO correlator must enter the chirally odd OPE. Hence, these contributions do not directly extend the open flavor chiral sum rule (4.20) calculated in [Hil11], which includes even OPE contributions with condensates of mass dimension 3 and 5, but they establish an associated open flavor chiral sum rule (4.21) containing condensates with even mass dimension originating from the correlator in LO  $\alpha_s$ .

## 4.4 D meson properties from chiral partner sum rules

In order to assess the compatibility of chiral partner sum rules with  $qQ$  meson phenomenology, we need the pseudo-scalar and scalar D meson spectral functions, provided by experimental data or hadronic models. As chiral partner sum rules quantify the degree of D $\chi$ SB one is tempted to check whether the temperature dependences of the involved spectral functions are consistent with the in-medium P–S sum rule (4.20) which exhibits signals of chiral restoration for increasing temperatures. Currently, there are no experimental finite-temperature spectral functions of D mesons available. However, the recent hadronic model of chiral partner heavy-light mesons from Ref. [Sas14] provides temperature dependent D meson masses, but no further information about the spectral functions. The incomplete spectral information obstructs the desired consistency check, i.e. even if we resort to the pole + continuum ansatz (4.7) for both particles employing the given meson masses  $m_X$  and degenerate continuum threshold parameters  $s_0^X$  residing at high energies, where chiral symmetry is assumed to hold, the unrestricted chiral partner residua  $R_X$  prohibit the quantification of the phenomenological side of the chiral partner sum rule.<sup>5</sup>

Although the temperature dependence of the chiral partner D meson masses [Sas14] is insufficient to check the compatibility of the underlying hadronic model with the chiral partner sum rules they can be utilized to determine the meson residua and corresponding decay constants from the P–S sum rule and its first derivative w.r.t.  $1/M^2$ . To derive comparable results for the decay constants extracted in recent vacuum QSRs we consider also here the spin-0 currents (4.1) deviating from the ones defined below Eq. (4.17) by the quark mass factors. The experimental value of the relevant leptonic branching fraction (listed in Ref. [Pat16]), which corresponds to the decay constant and the residuum of the pseudo-scalar D meson in vacuum, agrees with the results in Ref. [Nar13]. However, such valuable experimental information is not available for the broad scalar D meson. In order to treat scalar as well as pseudo-scalar particles on the same footing, in particular at finite

---

<sup>5</sup>Extraction of the needed parameters from channel-specific QSRs does not cure the problem, because these parameters always yield spectral functions which perfectly satisfy the chiral partner sum rules, displaying the consistency of the QSR framework, thus, obscuring the compatibility check provided by chiral partner sum rules.

temperatures, where no data is available, we use the pole + continuum ansatz (4.7) and the continuum threshold parameters are determined from channel-specific QSRs for pseudo-scalar and scalar D mesons separately. Hence, the finite-temperature P – S sum rule (4.20) reads

$$R_P e^{-m_P^2/M^2} - R_S e^{-m_S^2/M^2} + \int_{s_0^P}^{s_0^S} ds e^{-s/M^2} \text{Im}\Pi^{\text{pert}}(s) = \hat{\Pi}_{P-S}^{(2)\text{even}}(M^2)$$

$$= m_Q^2 e^{-m_Q^2/M^2} \left[ -2m_Q \langle \bar{q}q \rangle_T + \left( \frac{m_Q^3}{2M^4} - \frac{m_Q}{M^2} \right) (\langle \bar{q}g\sigma Gq \rangle_T - \langle \Delta \rangle_T) \right], \quad (4.24)$$

where the temperature dependent tanh-term in the spectral integral kernel has been neglected as argued in Sec. 4.2. After taking the derivative w. r. t.  $1/M^2$  of the phenomenological and OPE sides, solving for the residua yields

$$R_P(M) = m_Q^2 e^{(m_P^2 - m_Q^2)/M^2} \left[ -2m_Q \frac{m_Q^2 - m_S^2}{m_P^2 - m_S^2} \langle \bar{q}q \rangle_T \right. \\ \left. + \left( \frac{m_Q^3}{2M^4} \frac{m_Q^2 - m_S^2}{m_P^2 - m_S^2} - \frac{m_Q}{M^2} \frac{2m_Q^2 - m_S^2}{m_P^2 - m_S^2} + \frac{m_Q}{m_P^2 - m_S^2} \right) (\langle \bar{q}g\sigma Gq \rangle_T - \langle \Delta \rangle_T) \right] \\ - \frac{1}{\pi} \int_{s_0^P}^{s_0^S} ds \frac{s - m_S^2}{m_P^2 - m_S^2} e^{(m_P^2 - s)/M^2} \text{Im}\Pi^{\text{pert}}(s), \quad (4.25a)$$

$$R_S(M) = -m_Q^2 e^{(m_S^2 - m_Q^2)/M^2} \left[ -2m_Q \frac{m_Q^2 - m_P^2}{m_S^2 - m_P^2} \langle \bar{q}q \rangle_T \right. \\ \left. + \left( \frac{m_Q^3}{2M^4} \frac{m_Q^2 - m_P^2}{m_S^2 - m_P^2} - \frac{m_Q}{M^2} \frac{2m_Q^2 - m_P^2}{m_S^2 - m_P^2} + \frac{m_Q}{m_S^2 - m_P^2} \right) (\langle \bar{q}g\sigma Gq \rangle_T - \langle \Delta \rangle_T) \right] \\ + \frac{1}{\pi} \int_{s_0^P}^{s_0^S} ds \frac{s - m_P^2}{m_S^2 - m_P^2} e^{(m_S^2 - s)/M^2} \text{Im}\Pi^{\text{pert}}(s). \quad (4.25b)$$

Using the numerical condensate values in Tab. 4.1 as well as the temperature dependences of  $m_{P,S}$  from Ref. [Sas14], these chiral partner sum rule is evaluated in the overlap Borel window of the channel-specific P and S sum rules, i.e. we average the resulting residuum Borel curves (4.25) in

$$[M_{\min}^{P-S}, M_{\max}^{P-S}] = [M_{\min}^P, M_{\max}^P] \cap [M_{\min}^S, M_{\max}^S] \quad (4.26)$$

to obtain the residua for the pseudo-scalar and scalar D mesons, which can be readily converted to the respective decay constants by virtue of Eq. (4.8).

We obtain the results depicted in Fig. 4.8. The pseudo-scalar D meson residuum  $R_P$  hardly changes with rising temperature as suggested by the conventional QSR analysis demonstrating an insensitivity against temperature effects. However, the corresponding decay constant  $f_P$  being the  $m_P(T)$ -rescaled square root of the residuum seems to acquire a



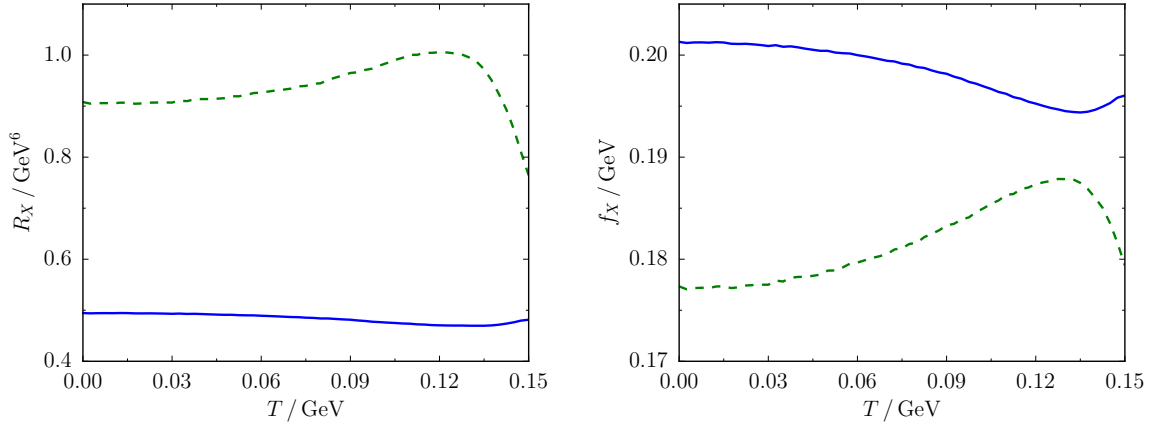


**Figure 4.8:** Temperature dependences of residues (left panel) and decay constants (right panel) of pseudo-scalar (blue solid curve) and scalar (green dashed curve) D mesons from chiral partner sum rules.

mild temperature dependence. Its vacuum value,  $f_P(T = 0) = 0.201 \text{ GeV}$ , is in agreement with previous findings [Luc11b, Nar13]. In contrast, the scalar D meson residuum  $R_S$  and decay constant  $f_S$  exhibit stronger temperature dependences. In fact, the resulting curves are similar to the ones with  $M$ -dependent continuum threshold, cf. Fig. 4.7, as these evaluations share the same input parameters, albeit a less pronounced fall of the residuum above  $T = 0.12 \text{ GeV}$  leads to a higher decay constants towards the upper end of the depicted temperature range. Although, the approaching chiral partner D meson masses have been used as an input to the chiral sum rules (4.25) the corresponding decay constant curves diverge for  $T > 0.12 \text{ GeV}$  after showing signals of partial chiral restoration. However, the residues directly entering the pole ansatz of the spectral density exhibit approaching curves for higher temperatures in accordance with the D meson masses. Thus, their behavior accumulates indications for chiral symmetry restoration in a strongly interacting medium which would be characterized by degenerate chiral partner spectra. The discrepancy might be attributed to the decay constant quantifying a specific leptonic decay mode while modifications of spectral densities due to chiral symmetry restoration affect all decay channels contributing to the total width of the respective meson. Thus, as the leptonic decay constants do not dominate the decay properties of the D mesons, the residues parameterizing the spectral densities in a comprehensive manner are better suited to judge implications of the medium modifications of D mesons.

## 4.5 Interim summary

Besides confinement, chiral symmetry is the central phenomenon of QCD because it provides a mass generating mechanism giving essentially mass to the light hadrons. As this mechanism is based on a spontaneous symmetry breaking principle the chiral symmetry breaking pattern as well as its restoration in a strongly interacting medium are subject to a large variety of investigations. While previous studies often consider chiral effects on light mesons [Dom89, Dom04, Dom15b, Kap94, Kwo08, Kwo10, Hoh12, Hoh14, Aya14], we shift the focus to the heavy-

light sector evaluating pseudo-scalar and scalar D meson QSRs, because the notions of chiral symmetry can be translated into the heavy-light sector if the symmetry transformations are restricted to the light-quark content. While pseudo-scalar D mesons have already been investigated in the framework of QSRs in the vacuum [Ali83, Luc11b, Nar13] and in the medium [Hay00, Hil09, Suz16a, Wan16a], the investigations in this chapter provides QSR results in vacuum and at finite temperatures for pseudo-scalar as well as scalar D mesons, allowing for insights into the D $\chi$ SB phenomenology.

While the conventional QSR analysis is inadequate to extract the pseudo-scalar D meson mass, its scalar counterpart can be treated successfully. However, from intermediate steps of the analysis a particular insensitivity of the pseudo-scalar QSR to temperature changes is evident, suggesting negligible modification of the pseudo-scalar D meson spectral properties. As the scalar QSR evaluation yields a decreasing mass for growing temperatures the channel-specific chiral partner sum rules signal partial chiral restoration up to  $T = 0.15$  GeV (conservatively) limiting the range of validity of the employed low-temperature approximation. This qualitative behavior is in agreement with the findings of Ref. [Sas14], but the parabolic temperature curve deviates from the scalar D meson mass curve presented there. Interestingly, the scalar D meson mass and decay constant approximately follows the temperature dependence adapted from chiral perturbation theory.

Although, medium modifications of the D meson masses do not lead to measurable changes of the D meson production in a statistical hadronization model [And08], the D meson yields in heavy-ion collisions may be sensitive to their altered decay properties in an ambient strongly interacting medium. Accordingly, we have extracted the temperature dependences of the pseudo-scalar and scalar D meson decay constants utilizing channel-specific as well as chiral partner QSRs. Due to their connection to particular leptonic branching fractions these decay constants are of large interest allowing for the determination of the off-diagonal CKM matrix element  $|V_{cd}|^2$  at  $T = 0$  as a bonus.

The growing interest in decay constants of open charm mesons has led to QSRs for these quantities using the experimentally determined vacuum masses as phenomenological input [Nar01, Luc11b]. Hence, employing the estimated temperature behavior of these masses [Sas14] allows for the prediction of their in-medium decay constants. An improvement of the QSR analysis by introduction of a Borel mass dependent continuum threshold parameter, which is supposed to suppress contaminations of the lowest resonance from continuum excitations of the spectral density, results in residuum and decay constant temperature curves deviating from the ones of the conventional analysis, i. e. albeit showing signals of chiral restoration at high temperatures the scalar residuum and decay constant do not decrease monotonically.

The difference of chiral partner spectra can be quantified by WSRs, i. e. in the light-meson sector, they are sensitive to single chiral order parameters, e. g. the chiral condensate and chirally odd four-quark condensates. As promising experiments measured the dilepton spectra of decaying light vector mesons in a strongly interacting medium [Sal13] the in-medium WSRs of  $\rho$  and  $a_1$  chiral partner mesons are eligible to test the contemporary understanding of the D $\chi$ SB pattern. As open charm chiral partner sum rules are equally well suited to study chiral effects driven by these order parameters they are extended to four-quark condensate contributions of mass dimension 6 which turn out to contribute to the odd OPE, i. e. they are of relevance at finite baryon densities only. Evaluating finite-temperature

chiral partner sum rules with spectral input from Ref. [Sas14] one can deduce the residua and subsequently the decay constants of pseudo-scalar and scalar D mesons. While the residua parameterizing the spectral density resemble the expected partial chiral restoration signature at high temperatures the decay constants of the chiral partner D mesons diverge suggesting that the associated leptonic decays do not dominate the D meson widths but other decay modes are important instead. This counter-intuitive behavior elucidates the conceptional distinction of decay-channel specific decay constants and spectral parameters, e. g. width and residuum.

While the planned facilities at NICA, FAIR and J-PARC are going to address charm DoF in a baryonic dense medium, the running collider experiments at LHC and RHIC are delivering at present a wealth of data on charm and bottom DoF in a high-temperature environment at very small net-baryon density. The firm application of QSRs on these quite different experimental conditions and the relation to observables, in particular such ones supporting the quest for chiral restoration signatures, deserve much more dedicated investigations on the theory side.



## 5 Summary and outlook

QSRs are a powerful, contemporary tool to determine spectral properties of hadrons in an active field of research [Nar13, Nar15, Dom14, Dom15a, Che15, Jia15, Wan15b, Zho15, Mao15, Luc15, Far16, Zan16] competing with the growing success of  $\ell$ QCD which is predictably facing a dominant role in the realm of hadron spectroscopy due to increasing computational capabilities. A major advantage of the QSR approach over other methods is its comprehensive and unproblematic generalization to hadrons embedded in a strongly interacting environment. Thereby, the approach demonstrates its conceptional strength allowing for testable predictions of medium modifications of hadrons at finite temperature [Wan15a, Wan16a, Kim16], nucleon density [Buc15b, Gub15b, Suz16a] and magnetic fields [Mac14, Cho15, Gub16]. The evaluation of the impact of higher order contributions on in-medium D meson QSRs is one of the main goals of this thesis. Furthermore, the QSR framework benefits from its easy application to exotic states, because it can be used to uncover the internal structure of the newly observed hadrons with exotic quantum numbers [Dia13, Nie14, Alb16, Wan16b, Wan16c, Dia16, Aga16a, Aga16c, Aga16b, Che16].

This work grounds on a careful introduction to the in-medium QSR framework which is an inevitable prerequisite for a rigorous application of OPE techniques to higher mass dimension in-medium contributions envisaged in this thesis. By virtue of a dispersion relation, integrated spectral properties of hadrons are linked to QCD condensates which are EVs of quark and gluon operators. As the strongly interacting matter breaks Poincaré invariance its characteristic velocity  $v_\mu$  must be used to build invariants resulting in a multitude of additional in-medium condensates which obey the assumed symmetries of the in-medium ground state. Apart from the occurrence of new terms in the medium, a medium dependence is inherent to all condensates, the additional in-medium contributions as well as the condensates already occurring in the vacuum. This is of particular interest, because there are order parameters of chiral symmetry among these condensates offering the opportunity to study chiral dynamics within the framework of QSRs and WSRs. A recent discussion on the origin and meaning of condensates has been launched by the consideration of cosmological arguments favoring in-hadron condensates with restricted spatial support over space-time independent quantities.

As QSRs are capable of probing integrated spectral properties only, assumptions about the spectral shape are to be specified. In order to enhance the sensitivity on the lowest resonance a Borel transformation can be employed simultaneously reducing the impact of the continuum region. To go beyond ansätze for the spectral density of the hadron under consideration, Bayesian methods may be applied or model-independent information can be derived from moments of a spectral function with a single peak structure.

One of the main results presented in this thesis is the first in-medium evaluation of the pseudo-scalar D meson OPE for light-quark operators of mass dimension 6 [Buc15b]. It requires the introduction of medium-specific condensates [Buc14b, Buc15a] defined to obtain a smooth transition from medium to vacuum. These medium-specific condensates bear

implications for the vacuum EVs of the contributing operator combinations [Buc16b]. The calculation of the respective Wilson coefficients is performed and the numerical impact of the complete light-quark mass dimension 6 condensate terms with a density dependence dominated by four-quark condensates is estimated. In contrast to the  $\rho$  meson sum rule, these contributions are numerically small which can be attributed to the heavy-quark mass entering the D meson OPE as a new scale and to the absence of light four-quark terms originating from diagrams with hard gluons, i.e. from the NLO correlator, substituted in the D meson sum rule by four-quark condensates containing heavy quarks. These contributions are assumed to be negligible due to the static heavy quark which hardly condenses. Although leading to cumbersome expressions, four-quark condensate from the NLO heavy-light correlator with heavy-quark content could be included into the heavy-light QSR [Hil12b] performing a HQE [Buc14a].

Aside from their numerical impact, four quark condensates possess relevance due to their close connection to chiral symmetry. By virtue of its non-trivial behavior under chiral transformations, we can identify the chirally odd four-quark condensate  $\langle \bar{q}t^A q \sum_f \bar{f} \not{t} t^A f \rangle$  as a potential order parameter quantifying the degree of chiral symmetry breaking, similar to the famous chiral condensate  $\langle \bar{q}q \rangle$ .

In this work, we advocate pseudo-scalar and scalar D mesons as probes of chiral dynamics, because such effects can be translated into the heavy-light sector if the related chiral transformations are restricted to the light-quark content [Buc16a]. As pseudo-scalar D mesons have been frequently studied we shift the focus on its scalar counterpart. A conventional sum rule analysis yields different temperature behaviors of pseudo-scalar and scalar D meson masses which can be explained to some extent in the scope of QSRs by a comparison of the temperature dependences of the dominant OPE contributions. While the pseudo-scalar D meson mass hardly changes, the scalar mass and decay constant decrease parabolically, in agreement with results from chiral perturbation theory. There is growing interest from the hadron physics community in decay properties of heavy-light mesons, as they may influence open flavor meson production rates in contrast to the negligible impact of their mass modifications. In particular, decay constants attracted much attention, as they provide access to off-diagonal CKM matrix elements in the vacuum. Accordingly, we determine the temperature dependence of the scalar D meson residuum and decay constant from channel-specific QSRs using temperature dependent masses as input.

Although, the D meson OPE is dominated by the chiral condensates  $\langle \bar{q}q \rangle$ , being an order parameter of  $D\chi SB$ , the sensitivity on further potential order parameters can be enhanced if the difference of chiral partner sum rules is considered, which would lead to the well known Weinberg sum rules for light spin-1 mesons. Due to cancellation of chirally even contributions chiral partner sum rules establish a relation between the difference of the integrated chiral partner spectra and potential order parameters. We extend these sum rules to mass dimension 6, which enter the odd OPE and, thus, are relevant to finite-density situations only. Evaluations of the in-medium chiral partner sum rules with temperature dependent input masses in order to deduce residua and decay constants disclose their conceptual differences. These studies of pseudo-scalar and scalar D mesons in a heat bath yield approaching meson residua which exhibit signals of chiral restoration at higher temperatures approving also heavy-light spin-0 mesons as adequate probes of partial chiral symmetry restoration.

---

Driven by the desire for understanding the thermodynamics of strongly interacting matter, a series of current and forthcoming large scale experiments is set up to explore the QCD phase diagram. As they produce a plenitude of open charm and bottom states at finite temperatures or net-baryon densities, many efforts are made to treat heavy open flavor hadrons under these circumstances theoretically. While one branch of research focuses on the medium modifications of the hadrons themselves, another branch deals with the influence of penetrating, open flavor particles on the fireball of a heavy-ion collision, e.g. transport properties are determined or their impact on the hadronization process towards the end of a collision is studied. By evaluation of the in-medium QSRs up to high orders, we deduce changing spectral properties of D mesons which may also involve and indicate chiral dynamics. Hence, this thesis contributes to the understanding of open charm mesons as probes of hot and dense strongly interacting matter allowing for a mutual judging of the different approaches.

As has been already stressed in the introduction, low-energy QCD faces multiple problems: The large coupling denies perturbative expansions. Confinement is not yet derived from QCD. Although  $\ell$ QCD looks promising for the calculation of many Green's functions it has resistant issues with reproducing the pion mass and finite chemical potentials, due to the sign problem in the Metropolis algorithm. Many approaches are model calculations covering only certain aspects of full QCD, e.g. the linear sigma model, or rely on conjectures, e.g. holographic methods. In this difficult milieu, QSRs seem an appealing analytic approach with intimate contact to QCD, i.e. hadronic properties are traced to quark and gluon DoF by means of a dispersion relation, where a rigorous separation of scales allows for perturbative methods supplemented by a few condensate values encoding the long-range, i.e. non-perturbative, effects.

A key to reliable results determined from QSRs are the evaluational strategies. Parameterizing the shape of hadronic spectral functions requires the extraction of several parameters from a single equation calling for derivative sum rules in order to arrive at a system of equations which can be solved for the wanted spectral information. However, the reliability of higher order derivative sum rules is questionable, which is the reason we do not proceed beyond the first derivative following the orthodox approach. An evaluational strategy that overcomes the shortcomings of derivative sum rules is provided by the Monte-Carlo sum rule analysis based solely on the genuine QSR. This analysis procedure, where hadronic parameters of the spectral density ansatz are extracted by means of a maximum likelihood method for Gaussianly distributed input parameters, allows for a rigorous uncertainty analysis. However, it heavily relies on sophisticated optimization routines capable of producing credible results. Once a reliable optimization is obtained the results genuinely reflect low-energy QCD as intended by Shifman, Vainshtein and Zakharov, the inventors of the framework. Thus, the Monte-Carlo sum rule analysis might be a promising tool to extract hadron properties from QCD with the benefit of a statistical analysis of input uncertainties.

In the scope of this thesis, we pushed QSRs to the frontiers of its applicability in the spirit of their inventors. In particular, in-medium OPEs in higher orders are flooded with numerous condensates with yet unknown numerical values. While we could show from algebraic relations that the ground state EVs of additional in-medium light-quark condensates of mass dimension 6 can be related to known condensates of lower mass dimension or to four-

quark condensates, the details of their medium dependences remain unsettled. Aiming for even higher mass dimension terms further increases the complexity of entering in-medium contributions with presumably small numerical impact. However, if the involved Wilson coefficients suggest a sizable impact of such contributions they would spoil the predictive power of the sum rule. This very dilemma discloses one of the shortcomings inherent to the QSR framework which lacks control over higher order power correction such that the influence of these condensate contributions on the extracted spectral properties of the hadron under consideration is a priori unclear. In contrast, the rigorous power counting rules in effective theories avoid any of these difficulties. The crux of these approaches, however, is the knowledge of the exact numerical values of the involved low-energy constants, e.g. particle couplings, which are accessible in QSRs. Although, the applicability of the QSR framework is limited to low-temperature/density approximations of lower order mass dimension condensates its value beyond that may be strengthened when QSRs are used to extract low-energy constants leaving the thermodynamics to an effective model.



## A Quantum chromodynamics. An overview

This chapter must not be understood as an introduction to QCD, but it specifies the notation employed throughout this thesis and collects the essential definitions and relations. In particular, no details of the quantization and BRS transformations are provided. A review of the Lagrangian density<sup>1</sup> of classical chromodynamics suffices to introduce the used conventions. The gauge invariant Lagrangian density, which is the basis of QCD, reads

$$\mathcal{L} = \bar{\psi} (i\gamma^\mu D_\mu - M) \psi - \frac{1}{4} G_{\mu\nu}^A G^{A\mu\nu} \quad (\text{A.1})$$

with the following notation:

$$D_\mu^{\alpha\beta}(x) = \partial_\mu(\mathbb{1}_{N_c})^{\alpha\beta} - igA_\mu^{\alpha\beta}(x) \quad \text{gauge covariant derivative,} \quad (\text{A.2a})$$

$$A_\mu^{\alpha\beta}(x) = (t^A)^{\alpha\beta} A_\mu^A(x) \quad \text{gluon field,} \quad (\text{A.2b})$$

$$G_{\mu\nu}(x) = \frac{i}{g} [D_\mu(x), D_\nu(x)] = t^A G_{\mu\nu}^A(x) \quad \text{gluon field strength tensor,} \quad (\text{A.2c})$$

$$\psi_i^\alpha(x) \quad \text{quark fields,} \quad (\text{A.2d})$$

$$(\gamma^\mu)_{ij} \quad \text{Dirac matrices,} \quad (\text{A.2e})$$

$$t^A = \frac{1}{2} \lambda^A \quad \text{generators of gauge group SU}(N_c), \quad (\text{A.2f})$$

$$\lambda^A \quad \text{Gell-Mann matrices for } N_c = 3, \quad (\text{A.2g})$$

where Lorentz indices are denoted by Greek letters  $\mu, \nu, \lambda, \dots$ , Dirac indices by Latin letters  $i, j, k, \dots$ , color indices by Greek letters  $\alpha, \beta, \gamma, \dots$  (fundamental representation) and generator indices by Latin capitals  $A, B, C, \dots$  (adjoint representation).  $N_c$  is the number of colors; in QCD one has  $N_c = 3$ . Generator indices which occur twice are to be summed over from 1 to  $N_c^2 - 1$  and Einstein's summation is applied to contracted Lorentz indices. The generators of the symmetry group  $\text{SU}(N_c)$  satisfy the following relations:

$$[t^A, t^B] = if^{ABC} t^C, \quad (\text{A.3})$$

$$\text{Tr}_c [t^A] = 0, \quad \text{Tr}_c [t^A t^B] = \frac{1}{2} \delta^{AB}, \quad \text{Tr}_c [t^A t^B t^C] = \frac{1}{4} (d^{ABC} + if^{ABC}), \quad (\text{A.4})$$

where  $f^{ABC}$  is the totally anti-symmetric structure constant of  $\text{SU}(N_c)$ , while the symmetric quantity  $d^{ABC}$  is defined by the anti-commutator

$$\{t^A, t^B\} = \frac{1}{N_c} \delta^{AB} \mathbb{1}_{N_c} + d^{ABC} t^C. \quad (\text{A.5})$$

---

<sup>1</sup>The Lagrangian density is often referred to as simply the Lagrangian in quantum field theory and in particular in this work, keeping in mind that an integration over the spatial coordinates gives the actual Lagrangian, i.e. the quantity which is related to the Hamiltonian of the system by a Legendre transformation.

Thus, the gluon field strength tensor (A.2c) can be expressed as

$$G_{\mu\nu}^A = \partial_\mu A_\nu^A - \partial_\nu A_\mu^A + gf^{ABC} A_\mu^B A_\nu^C \quad \text{and} \quad G_{\mu\nu}^A = -G_{\nu\mu}^A. \quad (\text{A.6})$$

The gluon field strength tensor fulfills the Bianchi identity

$$[D_\lambda, G_{\mu\nu}] + [D_\mu, G_{\nu\lambda}] + [D_\nu, G_{\lambda\mu}] = 0. \quad (\text{A.7})$$

Equation (A.6) exhibits the gluon self-interaction, i. e. three- and four-gluon vertices, entering in the last term of the Lagrangian (A.1).

The Dirac matrices satisfy the relations

$$\{\gamma^\mu, \gamma^\nu\} = 2g^{\mu\nu} \mathbb{1}_4, \quad (\text{A.8})$$

$$\text{Tr}_D[\gamma^\mu] = 0, \quad \text{Tr}_D[\gamma^\mu \gamma^\nu] = 4g^{\mu\nu}, \quad \text{Tr}_D[\text{odd number of } \gamma^\mu] = 0 \quad (\text{A.9})$$

with Minkowski metric  $g^{\mu\nu} = \text{diag}(1, -1, -1, -1)$ . Traces with a higher number of Dirac matrices can be calculated with Eq. (A.8) exploiting cyclicity of the trace operation. The Feynman slash notation  $\not{a} = \gamma^\mu a_\mu$  of four-vectors  $a_\mu$  is often used, e. g. the gauge invariant Lagrangian can be expressed with the covariant derivative  $\not{D}$ . The Levi-Civita symbol

$$\varepsilon^{\mu\nu\lambda\kappa} = \begin{cases} +1 & (\mu\nu\lambda\kappa) \text{ is an even permutation of } (1234) \\ -1 & (\mu\nu\lambda\kappa) \text{ is an odd permutation of } (1234) \\ 0 & \text{otherwise} \end{cases} \quad (\text{A.10})$$

may be used to define the Dirac matrix  $\gamma_5 = \frac{i}{4!} \varepsilon_{\mu\nu\lambda\kappa} \gamma^\mu \gamma^\nu \gamma^\lambda \gamma^\kappa = i\gamma^0 \gamma^1 \gamma^2 \gamma^3$  which satisfies the relations

$$\{\gamma^\mu, \gamma_5\} = 0, \quad (\text{A.11})$$

$$\text{Tr}_D[\gamma_5] = \text{Tr}_D[\gamma^\mu \gamma^\nu \gamma_5] = 0, \quad \text{Tr}_D[\gamma^\mu \gamma^\nu \gamma^\lambda \gamma^\kappa \gamma_5] = 4i\varepsilon^{\mu\nu\lambda\kappa} \quad (\text{A.12})$$

as well as the identity

$$i\varepsilon^{\rho\mu\nu\lambda} \gamma_5 \gamma_\rho = \gamma^\mu \gamma^\nu \gamma^\lambda - g^{\mu\nu} \gamma^\lambda - g^{\nu\lambda} \gamma^\mu + g^{\mu\lambda} \gamma^\nu = g^{\mu\lambda} \gamma^\nu - g^{\nu\lambda} \gamma^\mu - i\sigma^{\mu\nu} \gamma^\lambda, \quad (\text{A.13})$$

where the Dirac matrices  $\sigma^{\mu\nu}$  are defined by

$$\sigma^{\mu\nu} = \frac{i}{2} [\gamma^\mu, \gamma^\nu] = i(\gamma^\mu \gamma^\nu - g^{\mu\nu}). \quad (\text{A.14})$$

The quark field  $\psi = (u, d, c, s, t, b)^T$  is a vector in the quark flavor space with diagonal mass matrix  $M$ . Thus, the quark field also carries a flavor index suppressed in the above definition (A.2d). The flavor symmetries of the Lagrangian (A.1) are an integral part of this work and are detailed in App. B. According to the quark masses, which are reviewed in Ref. [Pat16], light and heavy quarks can be distinguished. While the up- and down-quarks are approximately massless, followed by the heavier strange-quark, the masses of the heavy quarks of charm-, bottom- and top-type are orders of magnitude larger. Throughout this thesis, quark fields of an individual flavor are denoted by  $q$ ,  $f$  or  $Q$  depending on their respective masses.

---

The coupling strength  $g$  of QCD entering the interaction part

$$\begin{aligned}\mathcal{L}_{\text{int}}(x) &= g\bar{\psi}(x)\gamma^\mu t^A \psi(x) A_\mu^A(x) \\ &\quad - \frac{1}{2}gf^{ABC} [\partial_\mu A_\nu^A(x) - \partial_\nu A_\mu^A(x)] A^{B\mu}(x) A^{C\nu}(x) \\ &\quad - \frac{1}{4}g^2 f^{ABC} f^{ADE} A_\mu^B(x) A_\nu^C(x) A^{D\mu}(x) A^{E\nu}(x)\end{aligned}\tag{A.15}$$

of the Lagrangian (A.1) is defined as

$$g = \sqrt{4\pi\alpha_s},\tag{A.16}$$

where  $\alpha_s$  is the running coupling given to one- and two-loop order by Eqs. (2.75) and (2.74), respectively. Due to the decreasing coupling for growing momentum transfer QCD is referred to as asymptotically free.

The quark and gluon EoMs may be inferred from Euler-Lagrange equations (or the Heisenberg EoMs on quantum level) using Eq. (A.1):

$$\gamma^\mu D_\mu q = -imq,\tag{A.17}$$

$$\bar{q}\gamma^\mu \overleftarrow{D}_\mu = im\bar{q},\tag{A.18}$$

$$[D^\mu, G_{\mu\nu}] = -gt^A \sum_f \bar{f}\gamma_\nu t^A f,\tag{A.19}$$

where for soft gluons the sum over quark flavors  $f$  is restricted to light quarks, i.e.  $f = u, d, s$ . Utilizing the EoM one can show

$$D^2 \equiv g^{\mu\nu} D_\mu D_\nu = \gamma^\mu D_\mu \gamma^\nu D_\nu + \frac{1}{2}g\sigma^{\mu\nu} G_{\mu\nu},\tag{A.20}$$

$$D^2 q = \left( \frac{1}{2}g\sigma^{\mu\nu} G_{\mu\nu} - m_q^2 \right) q.\tag{A.21}$$

The Green's functions of the differential operators contained in (A.1) yield (as 2-point functions in momentum space) the free quark propagator

$$S^{(0)}(p) = \frac{\not{p} + m}{p^2 - m^2 + i\eta}\tag{A.22}$$

and the free gluon propagator

$$D_{\mu\nu}^{(0)}(k) = \frac{1}{k^2 + i\eta} \left[ -g_{\mu\nu} + (1 - \xi) \frac{k_\mu k_\nu}{k^2 + i\eta} \right]\tag{A.23}$$

with gauge fixing parameter  $\xi$  and  $\eta \rightarrow 0^+$ . The gauge is fixed by including the term  $-\frac{1}{2\xi}(D^\mu A_\mu^A)^2$  into the Lagrangian (A.1) in order to satisfy canonical commutation relations of the fields with their canonically conjugated momenta. Without the gauge fixing term the zeroth component of the canonically conjugated momentum, associated with the gluon field, vanishes and an important step in the canonical quantization procedure of the Lagrangian of chromodynamics would fail. Throughout this thesis, the Feynman gauge with  $\xi = 1$  is used.

The Lagrangian (A.1) is deduced from requiring invariance of  $\mathcal{L}$  under the local gauge transformation

$$\psi^\alpha(x) \longrightarrow \psi'^\alpha(x) = U^{\alpha\beta}(x)\psi^\beta(x) \quad (\text{A.24})$$

with a unitary ( $N_c \times N_c$ ) matrix

$$U(x) = e^{-igt^A \Theta^A(x)}, \quad (\text{A.25})$$

where  $\Theta^A(x)$  are the space-time dependent rotation parameters. Therefore, one obtains the following transformations in color space:

$$\bar{\psi}(x) \longrightarrow \bar{\psi}'(x) = \bar{\psi}(x)U^\dagger(x), \quad (\text{A.26a})$$

$$D_\mu \psi(x) \longrightarrow D'_\mu \psi'(x) = U(x)D_\mu \psi(x), \quad (\text{A.26b})$$

$$D_\mu(x) \longrightarrow D'_\mu(x) = U(x)D_\mu(x)U^\dagger(x), \quad (\text{A.26c})$$

$$A_\mu(x) \longrightarrow A'_\mu(x) = U(x)A_\mu(x)U^\dagger(x) + \frac{1}{ig} [\partial_\mu U(x)] U^\dagger(x), \quad (\text{A.26d})$$

$$G_{\mu\nu}(x) \longrightarrow G'_{\mu\nu}(x) = U(x)G_{\mu\nu}(x)U^\dagger(x). \quad (\text{A.26e})$$

Particular gauge invariants occurring in QCD condensates are usually abbreviated throughout this work, i. e.

$$G^2 = G_{\mu\nu}^A G^{A\mu\nu}, \quad (\text{A.27a})$$

$$\bar{q}\sigma Gq = \bar{q}\sigma^{\mu\nu} G_{\mu\nu} q, \quad (\text{A.27b})$$

$$G^3 = f^{ABC} G_{\mu\nu}^A G^{B\nu}{}_\lambda G^{C\lambda\mu}. \quad (\text{A.27c})$$

Among the discrete symmetries of the Lagrangian (A.1) are parity and time reversal, which are assumed to be manifested in the QCD ground state as well as in the in-medium ground state throughout this thesis. A parity transformation ( $P$ ) changes sign of the spatial components, while a time reversal transformation ( $T$ ) inverts sign of the temporal component of  $x_\mu = (x_0, \vec{x})$ , i. e.<sup>2</sup>

$$P \quad \vec{x} \longrightarrow \vec{x}' = -\vec{x}, \quad (\text{A.28})$$

$$T \quad x_0 \longrightarrow x'_0 = -x_0. \quad (\text{A.29})$$

The  $P$  transformation is mediated by a unitary operator  $\mathcal{P}$  satisfying

$$\mathcal{P}\psi(x_0, \vec{x})\mathcal{P}^\dagger = \eta_P \gamma^0 \psi(x_0, -\vec{x}) \quad (\text{A.30})$$

with  $|\eta_P| = 1$ , where  $\gamma^0 \psi(x_0, -\vec{x})$  satisfies the parity transformed Dirac equation (A.17). Analogously, the action of the time reversal operator  $\mathcal{T}$  can be inferred from rewriting the time reversed Dirac equation into its usual form (A.17) yielding

$$\mathcal{T}\psi(x_0, \vec{x})\mathcal{T}^\dagger = \eta_T i\gamma^1 \gamma^3 \psi(-x_0, \vec{x}) \quad (\text{A.31})$$

---

<sup>2</sup>The symbol  $T$  denoting the time reversal transformation is employed only within this Appendix and must not be confused with the temperature  $T$  used frequently in the thesis' main body.

---

with  $|\eta_T| = 1$  in standard representation of the Dirac matrices. However, the  $T$  transformation requires an anti-unitary operator  $\mathcal{T}$  to preserve time-translation invariance, i. e. the operator obeys  $\langle \mathcal{T}\psi | \mathcal{T}\phi \rangle = \langle \phi | \psi \rangle$  and in particular  $\mathcal{T}i\mathcal{T}^\dagger = -i$ . Utilizing these transformations on quark spinors, the transformation properties of further QCD operators may be deduced from the invariance of  $\mathcal{L}$ . The behavior of fermion bilinears and further operators entering QCD condensates under parity and time reversal transformations is summarized in Tab. A.1.

**Table A.1:** Transformation properties of quark and gluon operator combinations as well as further components of in-medium condensates under parity ( $P$ ) and time reversal ( $T$ ) transformations, where the shorthand notation  $(-1)^\mu = 1$  for  $\mu = 0$  and  $(-1)^\mu = -1$  for  $\mu = 1, 2, 3$  is employed.

	$\bar{\psi}\psi$	$i\bar{\psi}\gamma_5\psi$	$\bar{\psi}\gamma^\mu\psi$	$\bar{\psi}\gamma^\mu\gamma_5\psi$	$\bar{\psi}\sigma^{\mu\nu}\psi$	$D^\mu$	$G^{\mu\nu}$	$v^\mu$
$P$	+1	-1	$(-1)^\mu$	$-(-1)^\mu$	$(-1)^\mu(-1)^\nu$	$(-1)^\mu$	$(-1)^\mu(-1)^\nu$	$(-1)^\mu$
$T$	+1	-1	$(-1)^\mu$	$(-1)^\mu$	$-(-1)^\mu(-1)^\nu$	$-(-1)^\mu$	$-(-1)^\mu(-1)^\nu$	$(-1)^\mu$



## B Chiral symmetry

The purpose of this chapter is the introduction of the terms and notions of chiral symmetry which provides the essential mass generating mechanism for light hadrons. Hence, the influence of chiral symmetry and its breaking patterns on the observable world is of utmost interest. Chiral symmetry aspects in the heavy-light sector are non-standard, thus, the related notions and formulae frequently used throughout this thesis, especially in Chap. 4, deserve a careful introduction specifying our notation simultaneously.

### B.1 Chiral symmetry group, related transformations and currents

The classical chromodynamic Lagrangian (A.1), which QCD is based on, obeys a set of global flavor symmetries in the massless quark limit  $M = 0$  manifested in the chiral symmetry group  $U(N_f)_L \times U(N_f)_R$ . Since the gauge fields are insensitive to the quark flavor, relevant considerations involve the quark part of the Lagrangian (A.1) only. Upon introduction of the left and right handed projectors

$$P_{L,R} = \frac{1}{2}(1 \mp \gamma_5), \quad (B.1)$$

satisfying  $P_{L,R}^2 = P_{L,R}$ ,  $P_L P_R = P_R P_L = 0$  and  $P_L + P_R = 1$ , the quark fields can be decomposed in two chiral sectors

$$\psi_{L,R} = P_{L,R} \psi \quad (B.2)$$

building the  $N_f$ -dimensional light-flavor vector  $\psi = \psi_L + \psi_R$ . The free fermion Lagrangian in terms of left and right handed spinors reads

$$\mathcal{L} = \bar{\psi}_L i \not{\partial} \psi_L - \bar{\psi}_L M \psi_R + \text{L} \longleftrightarrow \text{R}. \quad (B.3)$$

The independence of the symmetries  $U(N_f)_L$  and  $U(N_f)_R$  expresses the decoupling of left and right helicity states. In the assumed chiral limit,  $M = 0$ , where helicity and chirality coincide (similarly in the infinite momentum frame), this corresponds to the decoupling of left and right handed quark field dynamics, cf. Eq. (B.3).

Employing the decomposition of an unitary group  $U(N) \simeq U(1) \times SU(N)$ ,<sup>1</sup> the chiral symmetry group may be rewritten  $U(1)_L \times U(1)_R \times SU(N_f)_L \times SU(N_f)_R$  with the corresponding transformations

$$U(1)_{L,R} \quad \psi_{L,R} \longrightarrow \psi'_{L,R} = e^{-i\Theta_{L,R}} \psi_{L,R}, \quad (B.4)$$

$$SU(N_f)_{L,R} \quad \psi_{L,R} \longrightarrow \psi'_{L,R} = e^{-i\Theta_{L,R}^a \tau^a} \psi_{L,R} \quad (B.5)$$

---

<sup>1</sup>One may not consider the given decomposition as an exact equality, because the center symmetry group  $Z(N)$ , with associated transformation  $\psi \longrightarrow \psi' = e^{2\pi i k/N} \psi$  for  $k = 1, \dots, N$ , is a subgroup of  $SU(N)$  but also contained in  $U(1)$ , and thus, redundant in this expression [Fuk13].

in a matrix representation characterized by arbitrary angles  $\Theta_{L,R}$  or sets of angles  $\Theta_{L,R}^a$  with implicit summation over  $a = 1, \dots, N_f^2 - 1$ , respectively. The matrices  $\tau^a = \lambda^a/2$  acting on the flavor indices are the  $N_f^2 - 1$  traceless generators of the special unitary group being normalized by  $\text{Tr}_f[\tau^a \tau^b] = \delta^{ab}/2$  and satisfying the equivalent relations to (A.3)–(A.5) for the generators of the gauge group.

Using the infinite transformations  $\psi'_C \simeq (1 - i\Theta_C)\psi_C \equiv \psi_C + \delta\psi_C$  and  $\psi'_C \simeq (1 - i\Theta_C^a \tau^a)\psi_C \equiv \psi_C + \Theta_C^a \delta^a \psi_C$ , where  $C$  denotes a common subscript for either L or R, one can deduce the Noether currents

$$j_C^{(a)\mu} = \frac{\partial \mathcal{L}}{\partial(\partial_\mu \psi_C)} \delta^{(a)} \psi_C \quad (\text{B.6})$$

from the assumed invariance of the Lagrangian, i. e.  $\delta_C^{(a)} \mathcal{L} = \mathcal{L}(\psi_C + \delta^{(a)} \psi_C) - \mathcal{L}(\psi_C) = 0$ . They read

$$j_C^\mu = \bar{\psi}_C \gamma^\mu \psi_C \quad \text{and} \quad j_C^{a\mu} = \bar{\psi}_C \gamma^\mu \tau^a \psi_C. \quad (\text{B.7})$$

However, for finite quark masses,  $M \neq 0$ , these currents are not conserved and their divergence can be read off the change of the Lagrangian  $\delta_C^{(a)} \mathcal{L}$  under these transformation, i. e.

$$\partial_\mu j_{L,R}^\mu = \delta_{L,R} \mathcal{L} = -i (\bar{\psi}_{L,R} M \psi_{R,L} - \bar{\psi}_{R,L} M \psi_{L,R}), \quad (\text{B.8a})$$

$$\partial_\mu j_{L,R}^{a\mu} = \delta_{L,R}^a \mathcal{L} = -i (\bar{\psi}_{L,R} \tau^a M \psi_{R,L} - \bar{\psi}_{R,L} M \tau^a \psi_{L,R}). \quad (\text{B.8b})$$

These relations explicitly show how the symmetry breaking term of the Lagrangian is related to the non-conservation of the current.

As various objects built from quark operators, e. g. bilinears or QCD condensates, exhibit invariant or non-invariant behavior under the chiral transformations, we introduce the notions of chirally even and chirally odd objects, respectively. If a quark operator object is invariant under the transformations (B.5) for arbitrary angles  $\Theta_{L,R}^a$  it is dubbed chirally even, otherwise it is considered chirally odd, although this very term is apparent only for suitable chiral transformations, i. g. for a specific choices of rotation parameters  $\Theta_{L,R}^a$ , which transform the operator object into its negative.

While utilizing infinite transformations are sufficient to deduce the Noether currents (B.7) they are inadequate to unveil the chirally odd nature of various objects explicitly, i. e. in general they do not transform chirally odd objects into their negatives. For  $N_f = 2$  the finite chiral transformations (B.5) can be cast into a matrix analogon to Euler's formula which considerably simplifies the search for angles  $\Theta_{L,R}^a$  transforming chirally odd QCD condensates into their negatives or parity partner currents into each other. Expanding the exponential into a power series separating the even and odd polynomials and multiple application of the Pauli matrix algebra  $\{\sigma^a, \sigma^b\} = 2\delta^{ab}$  yields

$$e^{-i\Theta_C^a \sigma^a/2} = \cos \frac{|\Theta_C|}{2} - i \frac{\Theta_C^a \sigma^a}{|\Theta_C|} \sin \frac{|\Theta_C|}{2} \quad (\text{B.9})$$

with  $|\Theta_C| = \sqrt{\sum_{a=1}^3 (\Theta_C^a)^2}$ . Analogously, also for  $N_f > 2$  one can use finite transformations in  $\dot{a}$ -direction (no summation over dotted indices)

$$e^{-i\Theta_C^{\dot{a}} \tau^{\dot{a}}} = \cos \frac{\Theta_C^{\dot{a}}}{\sqrt{2N_f}} - i \sqrt{2N_f} \tau^{\dot{a}} \sin \frac{\Theta_C^{\dot{a}}}{\sqrt{2N_f}}, \quad (\text{B.10})$$



which might suffice to exhibit chirally odd behavior. In order to derive Eq. (B.10) the flavor equivalent to Eq. (A.5) with  $d^{ab} = 0$  has been employed.

The above provided chiral symmetry group based on the decomposition of quark states into left and right handed parts can be equivalently expressed  $U(1)_V \times U(1)_A \times SU(N_f)_V \times SU(N_f)_A$ , i. e. in terms of the well known vector and axial-vector transformations

$$U(1)_V \quad \psi \longrightarrow \psi' = e^{-i\Theta_V} \psi, \quad U(1)_A \quad \psi \longrightarrow \psi' = e^{-i\Theta_A \gamma_5} \psi, \quad (B.11)$$

$$SU(N_f)_V \quad \psi \longrightarrow \psi' = e^{-i\Theta_V^a \tau^a} \psi, \quad SU(N_f)_A \quad \psi \longrightarrow \psi' = e^{-i\Theta_A^a \tau^a \gamma_5} \psi, \quad (B.12)$$

choosing the vector and axial-vector angles to be

$$\Theta_V^{(a)} = \frac{1}{2} \left( \Theta_R^{(a)} + \Theta_L^{(a)} \right), \quad (B.13a)$$

$$\Theta_A^{(a)} = \frac{1}{2} \left( \Theta_R^{(a)} - \Theta_L^{(a)} \right), \quad (B.13b)$$

respectively. Thus, invariance under the transformations (B.4) and (B.5) for arbitrary left and right handed angles is equivalent to invariance under the transformations (B.11) and (B.12) for arbitrary vector and axial-vector angles, i. e. they are related by

$$\begin{aligned} \psi = \psi_L + \psi_R &\longrightarrow \psi' = e^{-i(\Theta_V^a - \Theta_A^a) \tau^a} P_L \psi + e^{-i(\Theta_V^a + \Theta_A^a) \tau^a} P_R \psi \\ &= e^{-i\Theta_V^a \tau^a} e^{-i\Theta_A^a \tau^a \gamma_5} \left[ e^{+i\Theta_A^a \tau^a (1+\gamma_5)} P_L + e^{-i\Theta_A^a \tau^a (1-\gamma_5)} P_R \right] \psi \\ &= e^{-i\Theta_V^a \tau^a} e^{-i\Theta_A^a \tau^a \gamma_5} \left\{ \left[ 1 + P_R \sum_{n=1}^{\infty} \frac{1}{n!} (2i\Theta_A^a \tau^a)^n \right] P_L \right. \\ &\quad \left. + \left[ 1 + P_L \sum_{n=1}^{\infty} \frac{1}{n!} (-2i\Theta_A^a \tau^a)^n \right] P_R \right\} \psi \\ &= e^{-i\Theta_V^a \tau^a} e^{-i\Theta_A^a \tau^a \gamma_5} (P_L + P_R) \psi \\ &= e^{-i\Theta_V^a \tau^a} e^{-i\Theta_A^a \tau^a \gamma_5} \psi, \end{aligned} \quad (B.14)$$

where the inverted Eqs. (B.13),  $\Theta_L^a = \Theta_V^a - \Theta_A^a$  and  $\Theta_R^a = \Theta_V^a + \Theta_A^a$ , as well as the three projector relations, given above, have been employed. An analogous relation holds for the  $U(1)$  transformations, too.

The conserved Noether currents of the transformations (B.11) and (B.12), which can be deduced analogously to (B.6) from invariance of the QCD Lagrangian, are the (iso-vector-)vector and (iso-vector-)axial-vector currents

$$U(1)_V \quad j_V^\mu = \bar{\psi} \gamma^\mu \psi, \quad U(1)_A \quad j_A^\mu = \bar{\psi} \gamma^\mu \gamma_5 \psi, \quad (B.15)$$

$$SU(N_f)_V \quad j_V^{a\mu} = \bar{\psi} \gamma^\mu \tau^a \psi, \quad SU(N_f)_A \quad j_A^{a\mu} = \bar{\psi} \gamma^\mu \gamma_5 \tau^a \psi, \quad (B.16)$$

respectively. The vector and axial-vector currents can be related to the corresponding left and right handed currents (B.7) via  $j_V^{(a)\mu} = j_L^{(a)\mu} + j_R^{(a)\mu}$  and  $j_A^{(a)\mu} = j_L^{(a)\mu} - j_R^{(a)\mu}$ . According to the behavior of  $j_V^{(a)\mu}$  and  $j_A^{(a)\mu}$  under Lorentz transformation, they are currents with internal angular momentum 1. Analogously one may define (iso-vector-)scalar and (iso-vector-)pseudo-scalar currents

$$j_S = \bar{\psi} \psi, \quad j_P = i \bar{\psi} \gamma_5 \psi, \quad (B.17)$$

$$j_S^a = \bar{\psi} \tau^a \psi, \quad j_P^a = i \bar{\psi} \gamma_5 \tau^a \psi \quad (B.18)$$

with internal angular momentum 0. They can be also expressed in terms of left and right handed currents  $j_{\text{LR}} = \bar{\psi}_{\text{L}}\psi_{\text{R}}$  and  $j_{\text{RL}} = \bar{\psi}_{\text{R}}\psi_{\text{L}}$  or  $j_{\text{LR}}^a = \bar{\psi}_{\text{L}}\tau^a\psi_{\text{R}}$  and  $j_{\text{RL}}^a = \bar{\psi}_{\text{R}}\tau^a\psi_{\text{L}}$ , yielding the relations  $j_{\text{S}}^{(a)} = j_{\text{LR}}^{(a)} + j_{\text{RL}}^{(a)}$  and  $j_{\text{P}}^{(a)} = i(j_{\text{LR}}^{(a)} - j_{\text{RL}}^{(a)})$ .

For currents that share the same internal angular momentum but have opposite parity we introduce the notion chiral partner currents, because they can be transformed into each other by suitable, finite chiral transformations. Thus, if the system is invariant under such transformations the exchange of chiral partners does not alter observables. The appropriate angles to convert chiral partner currents into each other are conveniently obtained from the representation in left and right handed currents to which the finite transformations (B.5) are applied employing Eq. (B.9), cf. the specific example in App. B.3.

Evaluating the divergence of (iso-vector-)vector and (iso-vector-)axial-vector currents by virtue of Eqs. (B.8), where  $\partial_{\mu}j_{\text{V,A}}^{(a)\mu}$  are to be expressed in terms of  $\partial_{\mu}j_{\text{L,R}}^{(a)\mu}$ , allows to infer the requirements under which the classical theory obeys the chiral symmetries  $\text{U}(1)_{\text{V,A}}$  and  $\text{SU}(N_{\text{f}})_{\text{V,A}}$ . While the  $\text{U}(1)_{\text{V}}$  symmetry causing the conservation of the vector current  $j_{\text{V}}^{\mu}$  and thus the total baryon number is always realized, even for arbitrary quark masses, the classical  $\text{U}(1)_{\text{A}}$  symmetry is preserved only in the massless quark limit,  $M = 0$ . It is special, because it is not conserved on quantum level due to the QCD axial anomaly. The discussion on the behavior of condensates under chiral transformation mainly focuses on the remaining  $\text{SU}(N_{\text{f}})_{\text{V}} \times \text{SU}(N_{\text{f}})_{\text{A}}$  symmetry.

In the presence of identical finite masses for all quark DoF, where the diagonal mass matrix reduces to  $M = m\mathbb{1}_{N_{\text{f}}}$ , the theory obeys iso-vector-vector symmetry  $\text{SU}(N_{\text{f}})_{\text{V}}$ , often abbreviated iso-spin symmetry, because the reduced mass matrix and the generator of the vector symmetry commute,  $[M, \tau^a] = 0$ . In contrast, the iso-vector-axial-vector symmetry  $\text{SU}(N_{\text{f}})_{\text{A}}$  is violated by any non-zero quark mass. Even if the generator of the symmetry,  $\tau^a\gamma_5$ , commutes with the quark mass matrix, it does not commute with the Dirac matrix  $\gamma_0$  of the conjugate quark field  $\bar{\psi} = \psi^{\dagger}\gamma_0$ , i. e. from the infinite iso-vector-axial-vector transformation  $\psi' \simeq (1 - i\Theta_{\text{A}}^a\tau^a\gamma_5)\psi$  one obtains  $\partial_{\mu}j_{\text{A}}^{a\mu} = \delta_{\text{A}}^a\mathcal{L} = -(i\psi^{\dagger}\gamma_5\gamma_0\tau^aM\psi - i\bar{\psi}M\tau^a\gamma_5\psi) \neq 0$ . Thus, the mass matrix must vanish in order to obtain an invariant Lagrangian.

Although the up- and down-quark masses deviate slightly they are both negligible in comparison to hadronic mass scales. Hence, iso-spin symmetry is approximately realized in nature, e. g. the neutron and proton masses coincide nearly (in terms of hadronic scales). However, the masses of mesons which couple to different chiral partner currents, e. g. the vector meson  $\rho$  and the axial-vector meson  $a_1$ , possess vastly different masses,  $m_{\rho} \simeq 776$  MeV and  $m_{a_1} \simeq 1240$  MeV. This mass splitting is not caused by the explicit breaking of the  $\text{SU}(N_{\text{f}})_{\text{A}}$  symmetry due to the tiny quark masses, because the meson mass difference is of the order of hadronic scales, but rather points to a spontaneous symmetry breaking mechanism. This mechanism can generate the essential part of light hadron masses. As this symmetry violation is not manifest in the Lagrangian but is due to a non-symmetric ground state of the theory one relies on order parameters to quantify the degree of violation. Chirally odd QCD condensates which appear in QSR evaluations are candidates for such order parameter. Thus, they are subject to more detailed considerations in Subsec. 2.3.2.

## B.2 Derivation of the GOR relation

The notions of order parameters, as presented in Subsec. 2.3.2, allow for the derivation of the famous Gell-Mann–Oakes–Renner (GOR) relation [GM68] relating the chiral condensate to pion properties [Hil12a]. This relation was known before the introduction of QSRs and is used to estimate the numerical value of the chiral condensate from known pion properties.

The Goldstone theorem ensures that the Goldstone bosons, interpreted as pions described by the one-pion state  $|\pi^b(\vec{p})\rangle$  with momentum  $p$ , couple to the current  $j_A^{a\mu}(x) = \bar{\psi}(x)\gamma^\mu\gamma_5\tau^a\psi(x)$  of the charge  $Q_A^a$  (2.106), i.e.

$$\langle\Omega|j_A^{a\mu}(x)|\pi^b(\vec{p})\rangle = i\delta^{ab}p^\mu f_\pi(p^2)e^{-ipx}, \quad (\text{B.19})$$

where the coordinate dependence has been extracted employing the unitary space-time translation operator, and the projection of the Lorentz structure has been performed, cf. App. C.2. The decay constant  $f_\pi(p^2)$  is defined as (no summation over dotted indices)

$$if_\pi(p^2) = \frac{1}{m_\pi^2}\langle\Omega|p_\mu j_A^{\dot{a}\mu}(0)|\pi^{\dot{a}}(\vec{p})\rangle, \quad (\text{B.20})$$

which may be verified by multiplying Eq. (B.19) by  $p_\mu$  evaluated at  $x = 0$  with  $a = b = \dot{a}$ . By applying  $\partial_\mu$  to Eq. (B.19), the pseudo-scalar current is introduced which has the quantum numbers of the pion. Thus, employing the quark EoMs (A.17) and (A.18) yields

$$\langle\Omega|\partial_\mu j_A^{a\mu}(x)|\pi^b(\vec{p})\rangle = \langle\Omega|i\bar{\psi}(x)\gamma_5\{M, \tau^a\}\psi(x)|\pi^b(\vec{p})\rangle = i\delta^{ab}m_\pi^2 f_\pi(p^2)e^{-ipx} \quad (\text{B.21})$$

for a diagonal mass matrix  $M$ . This relation is often considered to exhibit partial conservation of the axial-vector current (PCAC), because the violation scales with the pion mass squared being a very small quantity compared to other hadronic scales; and in the chiral limit, where pions are massless, the current is conserved. For the light two-flavor systems, i.e.  $2\tau^a = \sigma^a$  are Pauli matrices, the diagonal mass matrix is readily expressed by  $M = \frac{1}{2}[m_u(\mathbb{1}_2 + \sigma^3) + m_d(\mathbb{1}_2 - \sigma^3)]$  leading to  $\{M, \tau^a\} = (m_u + m_d)\sigma^a + (m_u - m_d)\delta^{a3}\mathbb{1}_2$ , and therefore the commutator (2.104) reads

$$\begin{aligned} \langle\Omega|[Q_A^a(x_0), \partial_\mu j_A^{b\mu}(x)]|\Omega\rangle &= -i\delta^{ab}\frac{m_u + m_d}{2}\langle\Omega|\bar{\psi}\psi|\Omega\rangle \\ &\quad - i\delta^{b3}\frac{m_u - m_d}{2}\langle\Omega|\bar{\psi}\sigma^a\psi|\Omega\rangle, \end{aligned} \quad (\text{B.22})$$

where the second term on the r. h. s. may be neglected due to iso-spin symmetry. Inserting a complete set of covariantly normalized one-pion states  $\mathbb{1} = \sum_c \int \frac{d^3p}{(2\pi)^3 2E_p} |\pi^c(\vec{p})\rangle \langle\pi^c(\vec{p})|$  into Eq. (B.22), using the definition of the charge (2.98) together with (B.19) for  $\mu = 0$  and the PCAC relation (B.21) as well as taking the trace w.r.t. flavor indices, one arrives at the GOR relation

$$-m_\pi^2 f_\pi^2 = \frac{m_u + m_d}{2} \langle\Omega|\bar{u}u + \bar{d}d|\Omega\rangle, \quad (\text{B.23})$$

which is also often expressed in terms of iso-spin averaged quantities  $m_q = (m_u + m_d)/2$  and  $\langle\Omega|\bar{q}q|\Omega\rangle = \langle\Omega|\bar{u}u + \bar{d}d|\Omega\rangle/2$  as  $-m_\pi^2 f_\pi^2 = 2m_q \langle\Omega|\bar{q}q|\Omega\rangle$ .

### B.3 Finite chiral transformations in the heavy-light sector

General pseudo-scalar and scalar two-quark currents read

$$j_P^\tau = i\bar{\psi}\gamma_5\tau\psi \quad \text{and} \quad j_S^\tau = \bar{\psi}\tau\psi \quad (\text{B.24})$$

with flavor matrix  $\tau$ . They are decomposable into the (iso-vector) currents (B.17) and (B.18). One can rewrite these general currents as follows:

$$\begin{aligned} j_P^\tau &= i\bar{\psi}_L\gamma_5\tau\psi_R + i\bar{\psi}_R\gamma_5\tau\psi_L \\ &= i\bar{\psi}_L\gamma_5\tau\frac{1}{2}(1+\gamma_5)\psi_R + i\bar{\psi}_R\gamma_5\tau\frac{1}{2}(1-\gamma_5)\psi_L \\ &= \frac{i}{2}\left(\frac{1}{i}j_P^\tau + \bar{\psi}_L\tau\psi_R - \bar{\psi}_R\tau\psi_L\right) \\ &= i(\bar{\psi}_L\tau\psi_R - \bar{\psi}_R\tau\psi_L) \\ &\equiv i(j_{LR}^\tau - j_{RL}^\tau) \end{aligned} \quad (\text{B.25a})$$

and

$$j_S^\tau = \bar{\psi}_L\tau\psi_R + \bar{\psi}_R\tau\psi_L \quad (\text{B.26a})$$

$$\equiv j_{LR}^\tau + j_{RL}^\tau \quad (\text{B.26b})$$

in terms of the left-right and right-left handed currents  $j_{LR}^\tau$  and  $j_{RL}^\tau$ , respectively.

Heavy-light meson currents are recovered, e. g., for  $\psi = (u, d, c)^T$  and the choice  $\tau = \tilde{\tau} = (\lambda^4 + i\lambda^5)/2$ . Accordingly, we obtain

$$\begin{aligned} j_P^{\tilde{\tau}} &= i\bar{\psi}\gamma_5\tilde{\tau}\psi = i(\bar{u}, \bar{d}, \bar{c})\gamma_5 \begin{pmatrix} 0 & 0 & 1 \\ 0 & 0 & 0 \\ 0 & 0 & 0 \end{pmatrix} \begin{pmatrix} u \\ d \\ c \end{pmatrix} = i\bar{u}\gamma_5 c \\ &= i(\bar{u}_L c_R - \bar{u}_R c_L) \end{aligned} \quad (\text{B.27})$$

and

$$\begin{aligned} j_S^{\tilde{\tau}} &= \psi\tilde{\tau}\psi = \bar{u}c \\ &= \bar{u}_L c_R + \bar{u}_R c_L. \end{aligned} \quad (\text{B.28})$$

General chiral transformations restricted to the light parts of the left and right handed flavor vectors  $\psi_{L,R}$  read

$$\psi_{L,R} = \begin{pmatrix} u \\ d \\ c \end{pmatrix}_{L,R} \longrightarrow \psi'_{L,R} = e^{-i\Theta_{L,R}^a \lambda^a/2} \psi_{L,R} \quad (\text{B.29})$$

with the rotation parameters  $\Theta_{L,R}^a = (\Theta_{L,R}^1, \Theta_{L,R}^2, \Theta_{L,R}^3, 0, \dots, 0)$  and the Gell-Mann matrices  $\lambda^a$ . Applying the  $SU(N_f = 2)$  finite chiral transformation formula (B.5) expressed by

Eq. (B.9) to the light-flavor components  $\varphi = (u, d)^T$  we can explicate the desired finite transformations

$$\begin{aligned}\psi_C &= \begin{pmatrix} \varphi_C \\ c_C \end{pmatrix} \longrightarrow \psi'_C = \begin{pmatrix} \varphi'_C \\ c_C \end{pmatrix} = \begin{pmatrix} \left[ \cos \frac{|\Theta_C|}{2} - i \frac{\Theta_C^a \sigma^a}{|\Theta_C|} \sin \frac{|\Theta_C|}{2} \right] \varphi_C \\ c_C \end{pmatrix}, \\ \bar{\psi}_C &= (\bar{\varphi}_C, \bar{c}_C) \longrightarrow \bar{\psi}'_C = (\bar{\varphi}'_C, \bar{c}_C) = \left( \bar{\varphi}_C \left[ \cos \frac{|\Theta_C|}{2} + i \frac{\Theta_C^a \sigma^a}{|\Theta_C|} \sin \frac{|\Theta_C|}{2} \right], \bar{c}_C \right),\end{aligned}\tag{B.30}$$

where again  $C$  is a common label for either L or R,  $\varphi_C = (u_C, d_C)^T$ ,  $\sigma^a$  are the Pauli matrices and  $\Theta_C^a$  the three non-vanishing rotation parameters. Employing the finite transformations restricted to the light part of the flavor vector  $\psi$  we aim for a set of rotation parameters  $\Theta_{L,R}^a$  which transforms the pseudo-scalar into the scalar heavy-light current, i.e.  $j_P^{\tilde{\tau}} \longrightarrow (j_P^{\tilde{\tau}})' = j_S^{\tilde{\tau}} = \bar{u}_L c_R + \bar{u}_R c_L$ :

$$\begin{aligned}(j_P^{\tilde{\tau}})' &= i (\bar{\psi}'_L \tilde{\tau} \psi'_R - \bar{\psi}'_R \tilde{\tau} \psi'_L) \\ &= i (\bar{u}_L, \bar{d}_L, \bar{c}_L) \begin{pmatrix} \left[ \cos \frac{|\Theta_L|}{2} + i \frac{\Theta_L^a \sigma^a}{|\Theta_L|} \sin \frac{|\Theta_L|}{2} \right] & 0 \\ 0 & 0 \\ 0 & 0 & 1 \end{pmatrix} \begin{pmatrix} 0 & 0 & 1 \\ 0 & 0 & 0 \\ 0 & 0 & 0 \end{pmatrix} \\ &\quad \times \begin{pmatrix} \left[ \cos \frac{|\Theta_R|}{2} - i \frac{\Theta_R^a \sigma^a}{|\Theta_R|} \sin \frac{|\Theta_R|}{2} \right] & 0 \\ 0 & 0 \\ 0 & 0 & 1 \end{pmatrix} \begin{pmatrix} u_R \\ d_R \\ c_R \end{pmatrix} - (L \longleftrightarrow R) \\ &= i \left( \bar{u}_L \left[ \cos \frac{|\Theta_L|}{2} + i \frac{\Theta_L^3}{|\Theta_L|} \sin \frac{|\Theta_L|}{2} \right] c_R + \bar{d}_L \left[ i \frac{\Theta_L^1 + i \Theta_L^2}{|\Theta_L|} \sin \frac{|\Theta_L|}{2} \right] c_R \right) \\ &\quad - (L \longleftrightarrow R).\end{aligned}\tag{B.31}$$

Choosing

$$\begin{aligned}\Theta_L^1 &= \Theta_L^2 = 0, & \Theta_L^3 &= (4k-1)\pi, & |\Theta_L| &= |\Theta_L^3|, \\ \Theta_R^1 &= \Theta_R^2 = 0, & \Theta_R^3 &= (4k+1)\pi, & |\Theta_R| &= |\Theta_R^3|\end{aligned}\tag{B.32}$$

with integer  $k$  we obtain

$$\begin{aligned}(j_P^{\tilde{\tau}})' &= i \left[ \bar{u}_L \left( \cos \frac{\pi}{2} + i \frac{-\pi}{\pi} \sin \frac{\pi}{2} \right) c_R + \bar{d}_L \left( i \frac{0}{\pi} \sin \frac{\pi}{2} \right) c_R \right] \\ &\quad - i \left[ \bar{u}_R \left( \cos \frac{\pi}{2} + i \frac{\pi}{\pi} \sin \frac{\pi}{2} \right) c_L + \bar{d}_R \left( i \frac{0}{\pi} \sin \frac{\pi}{2} \right) c_L \right] \\ &= \bar{u}_L c_R + \bar{u}_R c_L \\ &= j_S^{\tilde{\tau}},\end{aligned}\tag{B.33}$$

where  $k = 0$  has been used, exemplarily.

The chiral transformation (B.29) specified by the rotation parameters (B.32) also exhibits the chirally odd nature of the chiral condensate

$$\begin{aligned}
 \langle \bar{\varphi} \varphi \rangle' &= \langle \bar{\varphi}'_L \varphi'_R + \bar{\varphi}'_R \varphi'_L \rangle \\
 &= \langle \bar{\varphi}_L e^{i\pi\sigma^3} \varphi_R \rangle + \langle \bar{\varphi}_R e^{-i\pi\sigma^3} \varphi_L \rangle \\
 &= -\langle \bar{\varphi}_L \varphi_R + \bar{\varphi}_R \varphi_L \rangle \\
 &= -\langle \bar{\varphi} \varphi \rangle,
 \end{aligned} \tag{B.34}$$

i.e., as expected, it turns the chiral condensate into its negative.

## C Operator product expansion. Addendum

In this chapter, further important details of an OPE evaluation are provided bridging the gap from the basic ideas of the expansion to the resulting expressions presented in Chaps. 3 and 4. While the cornerstones of the computation, building on Wick's theorem and the background field expansion, are provided in Sec. 2.2, the physical implications of the condensates involved are outlined in Sec. 2.3. To arrive at operator combinations which form meaningful condensates a sequence of manipulations is in order. The intricate calculation of contributions to the in-medium OPE with higher order mass dimension condensates, as employed in this thesis, require a thorough application of these computation steps given below.

### C.1 Technicalities on condensates

QCD condensates introduced in Sec. 2.2 and described in Sec. 2.3 are to be color singlets as well as Dirac and Lorentz scalars to share the assumed symmetries of the QCD ground state. They emerge as decomposition coefficients of non-scalar operator products. However, in intermediate steps of the OPE one naturally encounters the EVs of quark and gluon operators which are color, Dirac and Lorentz matrices, i.e. non-scalars. Therefore, the projection of color, Dirac and Lorentz indices is needed to obtain non-zero ground state EVs of these operators which can be interpreted as QCD condensates. Thereby, the decomposition into Lorentz scalars is special, as only there the difference between vacuum and medium in the scope of an OPE comes into play.

#### C.1.1 Projection of Dirac indices

The projection of Dirac indices builds on the basis elements of the Clifford algebra. Thanks to the 16 basis elements with lower Lorentz indices  $\Gamma_a \in \{\mathbb{1}_4, \gamma_\mu, \sigma_{\mu<\nu}, i\gamma_5\gamma_\mu, \gamma_5\}$  and upper Lorentz indices  $\Gamma^b \in \{\mathbb{1}_4, \gamma^\mu, \sigma^{\mu<\nu}, i\gamma_5\gamma^\mu, \gamma_5\}$  each  $(4 \times 4)$  matrix in Dirac space  $O_{ij}$  can be decomposed into

$$O_{ij} = \sum_a d_a (\Gamma^a)_{ij} . \quad (\text{C.1})$$

Multiplication with  $(\Gamma_b)_{ji}$  and summation over  $i$  and  $j$  yields

$$d_a = \frac{1}{4} \text{Tr}_D [\Gamma_a O] , \quad (\text{C.2})$$

where the normalization of the basis elements of the Clifford algebra with the Dirac trace  $\text{Tr}_D [\Gamma_a \Gamma^b] = 4\delta_a^b$  is employed. Interpreting this trace as a scalar product reveals that the basis elements  $\Gamma_a$  and  $\Gamma^b$  form an orthogonal basis of the Clifford algebra. The normalization

relation can be expressed in that simple manner only if the basis elements are chosen as above. (In the literature, one often encounters an inconvenient notation of the basis elements of the Clifford algebra  $\Gamma_a$  and  $\Gamma^b$  without ' $<$ ' in the element  $\sigma_{\mu<\nu}$  and without the imaginary unit in the element  $i\gamma_5\gamma_\mu$ . In this case a further factor  $\epsilon_a$  is necessary in Eq. (C.1), which acquires the value  $\epsilon_a = 1/2$  for projections with  $\sigma_{\mu\nu}$  and  $\epsilon_a = -1$  for projections with  $\gamma_5\gamma_\mu$ .)

For typical structures entering the OPE,  $\langle \bar{q}_i \cdots q_j \rangle$ , which are to be projected, one obtains (with suppressed color indices)

$$\langle \bar{q}_i \cdots q_j \rangle = \sum_a d_a^{\text{OPE}} (\Gamma^a)_{ji} , \quad (\text{C.3})$$

with

$$d_a^{\text{OPE}} = \frac{1}{4} \langle \bar{q} \Gamma_a \cdots q \rangle . \quad (\text{C.4})$$

In comparison with Eq. (C.1) the Dirac indices of the basis element  $\Gamma^a$  are interchanged, because a Dirac scalar has to appear in the coefficient  $d_a^{\text{OPE}}$ , which is commonly not expressed as a trace. Thus, the basis element of the Clifford algebra needs to be placed in-between the spinors  $\bar{q}$  and  $q$ .

### C.1.2 Projection of color indices

The projection of color indices also relies on an orthogonal basis. For  $(N_c \times N_c)$  matrices, this basis is provided by the generators of the symmetry group  $\text{SU}(N_c)$  supplemented by the  $N_c$ -dimensional identity matrix. To reduce notation the identity matrix is included into the generator notation:

$$T^A = \begin{cases} \mathbb{1}_{N_c}/\sqrt{2N_c} & \text{for } A = 0, \\ t^A & \text{otherwise,} \end{cases} \quad (\text{C.5})$$

where the generators  $t^A = \lambda^A/2$  incorporate the  $N_c$ -dimensional generalization of the Gell-Mann matrices  $\lambda^A$  and satisfy the normalization relation  $\text{Tr}_c [T^A T^B] = \delta^{AB}/2$ . Therefore, each color matrix  $O_{\alpha\beta}$  can be decomposed as

$$O_{\alpha\beta} = \sum_A c_A (T^A)_{\alpha\beta} . \quad (\text{C.6})$$

Multiplication with  $(T^B)_{\beta\alpha}$  and summation over  $\alpha$  and  $\beta$  yields the coefficients

$$c_A = 2\text{Tr}_c [T^A O] . \quad (\text{C.7})$$

For structures entering the OPE up to mass dimension 5, which are to be projected, one obtains with  $N_c = 3$  the single color singlet structure (with suppressed Dirac indices)

$$\langle \bar{q}_\alpha \cdots q_\beta \rangle = \frac{1}{3} \langle \bar{q} \cdots q \rangle (\mathbb{1}_3)_{\beta\alpha} . \quad (\text{C.8})$$

If four-quark condensates and condensates of mass dimension 6 or higher are considered, further color singlet structures arise. Two color singlet structures formed by contraction



with the identity matrix of color space or the generators  $t^A$  exist for four-quark condensates leading to the projection formula (with suppressed Dirac indices and implicit summation over generator indices)

$$\langle \bar{q}_1^\alpha q_2^\beta \bar{q}_3^\gamma q_4^\delta \rangle = \frac{1}{9} \langle \bar{q}_1 q_2 \bar{q}_3 q_4 \rangle (\mathbb{1}_3)_{\beta\alpha} (\mathbb{1}_3)_{\delta\gamma} + \frac{1}{2} \langle \bar{q}_1 t^A q_2 \bar{q}_3 t^A q_4 \rangle (t^B)_{\beta\alpha} (t^B)_{\delta\gamma}, \quad (\text{C.9})$$

where the subscript labels potentially different quark flavors. This is the corrected projection formula of Eq. (39) in [Tho07] which contained a typographical error and was included for pedagogical purposes only [Tho12].

### C.1.3 Fierz transformations

In this subsection, general Fierz transformations [Pes95, Nie04] are presented as well as Fierz transformations with symmetry restrictions [Zha10]. Despite the different notation for the sums over basis elements of the Clifford algebra or generators of the symmetry group  $\text{SU}(N_c)$  the close connection between Fierz transformations and the projections of Dirac and color indices of four quark condensates is obvious. The considered quark fields carry Dirac and color indices, i. e. the Fierz rearrangement in Dirac and color space must be applied to transform the four-quark condensates with the structures  $\langle : \bar{q}_1 \Gamma_a q_2 \bar{q}_3 \Gamma_b q_4 : \rangle$  and  $\langle : \bar{q}_1 t^A \Gamma_a q_2 \bar{q}_3 t^A \Gamma_b q_4 : \rangle$  to condensates with interchanged quark fields  $q_2$  and  $q_4$ , i. e.  $\langle : \bar{q}_1 \Gamma_c q_4 \bar{q}_3 \Gamma_d q_2 : \rangle$  and  $\langle : \bar{q}_1 t^A \Gamma_c q_4 \bar{q}_3 t^A \Gamma_d q_2 : \rangle$ .

In Dirac space, the relation between  $(\Gamma_a)_{ij}(\Gamma_b)_{kl}$  and  $(\Gamma_c)_{il}(\Gamma_d)_{kj}$  is wanted. In general it is given by the linear combination

$$(\Gamma_a)_{ij}(\Gamma_b)_{kl} = \sum_{c,d} C_{ab}^{cd} (\Gamma_c)_{il}(\Gamma_d)_{kj}, \quad (\text{C.10})$$

where  $\Gamma_a \in \{\mathbb{1}_4, \gamma_\mu, \sigma_{\mu<\nu}, i\gamma_5 \gamma_\mu, \gamma_5\}$  is the basis of the Clifford algebra with the scalar product  $\text{Tr}_D [\Gamma_a \Gamma_b] = 4\delta_{ab} \equiv \eta_{ab}$  which induces a metric  $\eta_{ab}$  with  $\Gamma_a = \sum_b \eta_{ab} \Gamma^b$ , thus, one has  $4\Gamma^a \in \{\mathbb{1}_4, \gamma^\mu, \sigma^{\mu<\nu}, i\gamma_5 \gamma^\mu, \gamma_5\}$ . Multiplication of Eq. (C.10) with  $(\Gamma_e)_{li}(\Gamma_f)_{jk}$  yields

$$C_{ab}^{cd} = \frac{1}{16} \text{Tr}_D [\Gamma_a \Gamma_d \Gamma_b \Gamma_c]. \quad (\text{C.11})$$

The general Fierz transformation (C.10) with the coefficients  $C_{abcd} = \text{Tr} [\Gamma_a \Gamma_d \Gamma_b \Gamma_c]$  is not restricted to the Clifford algebra of the Dirac space, but is valid for all groups with basis elements which can be represented by matrices  $\Gamma_a$  and with a scalar product that induces an invertible metric  $\eta_{ab} = \text{Tr} [\Gamma_a \Gamma_b]$ .

The Fierz transformation in color space is a special case of the transformation (C.10) due to the required invariance of four-quark condensates under symmetry transformations of  $\text{SU}(N_c = 3)$ . Not all combinations of matrices which form color space meet this requirement. Invariants of a particular irreducible representation  $\mathcal{A}$  of an arbitrary symmetry group are of the form  $\sum_a (\Gamma_a^{\mathcal{A}})_{mn} (\Gamma_a^{\mathcal{A}})_{rs}$  ( $a = 1, \dots, \dim \mathcal{A}$ ). Therefore, a Fierz transformation which obeys a particular symmetry is a rearrangement of invariants of the symmetry group (instead of components of basis matrices):

$$\sum_a (\Gamma_a^{\mathcal{A}})_{ij} (\Gamma_a^{\mathcal{A}})_{kl} = \sum_{\mathcal{B}} C^{\mathcal{AB}} \sum_b (\Gamma_b^{\mathcal{B}})_{il} (\Gamma_b^{\mathcal{B}})_{kj}, \quad (\text{C.12})$$

where the Fierz coefficients  $C^{\mathcal{AB}}$  depend only on the associated representations. Summation of Eq. (C.10) with  $a = b$  over  $a$  and considering that coefficients (C.11) do not vanish for  $c = d$  only, yields

$$C^{\mathcal{AB}} = \sum_a C_a^{ab} = \sum_a \text{Tr} \left[ \Gamma_a^{\mathcal{A}} \Gamma_b^{\mathcal{B}} \Gamma^{Aa} \Gamma^{Bb} \right]. \quad (\text{C.13})$$

In color space of  $\text{SU}(N_c)$ , the one-dimensional representation  $\mathcal{I}$  and the fundamental representation  $\mathcal{T}$  ( $\dim \mathcal{T} = N_c^2 - 1$ ) with generators  $t^a$  exist, which are normalized by the scalar product  $\text{Tr}_c [t^a t^b] = \delta^{ab}/2$ .<sup>1</sup> To harmonize notation and in accordance with the generalized Fierz transformation the generator index  $a$  instead of  $A$  is used here and the sums over generator indices are written explicitly. The final transformation formulae are provided in standard notation with indices  $A$  and implicit summation. Due to the definition of the metrics for the choice  $\Gamma_a^{\mathcal{I}} = \mathbb{1}_{N_c}$  and  $\Gamma_a^{\mathcal{T}} = t^a$  one has

$$\eta_{ab}^{\mathcal{I}} \equiv \text{Tr} [\Gamma_a^{\mathcal{I}} \Gamma_b^{\mathcal{I}}] = \text{Tr}_c [\mathbb{1}_{N_c}] = N_c, \quad (\text{C.14a})$$

$$\eta_{ab}^{\mathcal{T}} \equiv \text{Tr} [\Gamma_a^{\mathcal{T}} \Gamma_b^{\mathcal{T}}] = \text{Tr}_c [t^a t^b] = \frac{1}{2} \delta^{ab} \quad (\text{C.14b})$$

and consequently  $\Gamma^{\mathcal{I}a} = \mathbb{1}_{N_c}/N_c$  and  $\Gamma^{\mathcal{T}a} = 2t^a$ . Thus, the Fierz coefficients read

$$C^{\mathcal{II}} = \frac{1}{N_c}, \quad C^{\mathcal{IT}} = \frac{1}{N_c}, \quad C^{\mathcal{TI}} = \frac{N_c^2 - 1}{N_c}, \quad C^{\mathcal{TT}} = -\frac{1}{N_c}. \quad (\text{C.15})$$

Utilizing Eq. (C.12) with the coefficients (C.15) one obtains for the symmetry group  $\text{SU}(N_c)$  the following Fierz transformations:

$$(\mathbb{1}_{N_c})_{ij} (\mathbb{1}_{N_c})_{kl} = \frac{1}{N_c} (\mathbb{1}_{N_c})_{il} (\mathbb{1}_{N_c})_{kj} + 2 \sum_a (t^a)_{il} (t^a)_{kj}, \quad (\text{C.16a})$$

$$\sum_a (t^a)_{ij} (t^a)_{kl} = \frac{N_c^2 - 1}{2N_c^2} (\mathbb{1}_{N_c})_{il} (\mathbb{1}_{N_c})_{kj} - \frac{1}{N_c} \sum_a (t^a)_{il} (t^a)_{kj}. \quad (\text{C.16b})$$

Setting  $N_c = 3$  and rewriting the Fierz transformations in standard notation with the generator indices  $A$  and implicit summation as well as color indices with Greek letters  $\alpha, \beta, \gamma$  and  $\delta$  yields

$$(\mathbb{1}_3)_{\alpha\beta} (\mathbb{1}_3)_{\gamma\delta} = \frac{1}{3} (\mathbb{1}_3)_{\alpha\delta} (\mathbb{1}_3)_{\gamma\beta} + 2 (t^A)_{\alpha\delta} (t^A)_{\gamma\beta}, \quad (\text{C.17a})$$

$$(t^A)_{\alpha\beta} (t^A)_{\gamma\delta} = \frac{4}{9} (\mathbb{1}_3)_{\alpha\delta} (\mathbb{1}_3)_{\gamma\beta} - \frac{1}{3} (t^A)_{\alpha\delta} (t^A)_{\gamma\beta}. \quad (\text{C.17b})$$

---

<sup>1</sup>The symbol  $\mathcal{T}$  denoting the fundamental representation of the color group must not be confused with the anti-unitary operator  $\mathcal{T}$  mediating the time reversal transformation.

## C.2 In-medium projection of Lorentz tensors and algebraic vacuum limits of QCD condensates

Based on the notions of vacuum- and medium-specific condensates, introduced in Sec. 3.7 and illustrated in Fig. 3.7, we are going to present a comprehensively formalized framework suitable to deal with the decomposition of Lorentz tensors entering higher mass dimension condensates [Buc14b, Buc15a, Buc16b]. The framework builds on ideas first considered in finite-density nucleon QSRs [Coh91, Coh92, Fur92, Jin93], where the authors realized that a tensor decomposition of local operators, as needed in OPE evaluations, depends on the available tensors, e. g. the metric tensor  $g_{\mu\nu}$  and the Levi-Civita symbol  $\varepsilon_{\mu\nu\kappa\lambda}$ . In a strongly interacting medium the ground state is not Poincaré invariant, but there is an additional four-vector, the medium velocity  $v_\mu$ , which must be transformed when comparing observations in different reference frames and which must be included to build tensors or invariants [Jin93]. Thus, additional condensates give non-zero in-medium contributions which vanish in vacuum. The goal is a decomposition scheme for tensor structures which accomplishes the smooth transition of the OPE of current-current correlators in a medium to the vacuum.

### C.2.1 General framework

QCD condensates constitute the decomposition coefficients of ground state EVs  $\langle\Omega|O_\mu|\Omega\rangle$  and/or Gibbs' averages  $\langle\langle O_\mu\rangle\rangle$  of local spin- $n$  operators  $O_\mu$ . We use the short notation  $\langle O_\mu\rangle$  for both in this paragraph. The label  $\mu$  is understood here as a shorthand notation for  $n$  Lorentz indices  $O_{\mu_1\ldots\mu_n}$  (irrespective of the number of space-time dimensions). The corresponding Lorentz indices are projected onto a set of independent Lorentz tensors collected in the projection vector  $\vec{l}_\mu$  which represents the dependences of the EV under consideration.<sup>2</sup> We now assume that the following decomposition holds:

$$\langle O_\mu\rangle = \vec{l}_\mu \cdot \vec{a}, \quad (\text{C.18})$$

where ' $\cdot$ ' denotes the scalar product. It follows that the desired decomposition is given by

$$\vec{a} = \left(\vec{l} \circ \vec{l}\right)^{-1} \vec{l}_\nu \langle O^\nu\rangle, \quad (\text{C.19a})$$

$$\langle O_\mu\rangle = \text{Tr} \left[ \left(\vec{l} \circ \vec{l}\right)^{-1} \left(\vec{l}_\mu \circ \vec{l}_\nu\right) \right] \langle O^\nu\rangle, \quad (\text{C.19b})$$

where ' $\circ$ ' is the dyadic product, to which the trace refers to and contracted indices are understood if omitted. The projection matrix  $L = \left(\vec{l}_\alpha \circ \vec{l}^\alpha\right) = \left(\vec{l} \circ \vec{l}\right)$  is symmetric and

$$P_{\mu\nu} = \text{Tr} \left[ \left(\vec{l} \circ \vec{l}\right)^{-1} \left(\vec{l}_\mu \circ \vec{l}_\nu\right) \right] \quad (\text{C.20})$$

is the wanted projection tensor, satisfying  $P_{\mu\nu}P^\nu{}_\kappa = P_{\mu\kappa}$ . Obviously, a valid set of Lorentz tensors and a valid projection vector is only given if the projection matrix  $L$  is invertible.

<sup>2</sup>Note that we do not explicate the index notation as in the App. C.1. However, we do not refer to  $\vec{l}_\mu$  as an element of a vector space, but only make use of the vector notation for the sake of conciseness.

Therefore, the components of  $\vec{l}_\mu$  must be linearly independent. As  $L$  is symmetric,  $L^{-1}$  is likewise.

In general, one writes down all possible Lorentz tensors which can be constructed from the set on which the EV depends and performs the projection for each EV independently. However, as can be seen from (C.19b), the procedure of decomposing an operator into a set of Lorentz scalars only depends on the tensor rank and is, thus, actually independent of the operator. Once  $P_{\mu\nu}$  is known, it is the same for all operators  $O_\mu$ . On the other hand, a specific operator  $O_\mu$  may occur in different OPEs. This in turn may impose different symmetry conditions on the operator by contraction of its Lorentz indices with symmetric or anti-symmetric tensors. It is therefore advisable to (anti-)symmetrize the Lorentz indices of  $\vec{l}_\mu$ .

### Vacuum

In vacuum, we assume that an operator  $O_\mu$  decomposes as

$$\langle \Omega | O_\mu | \Omega \rangle = \langle \Omega | O_\mu | \Omega \rangle_0 = \vec{l}_\mu^{(0)} \cdot \vec{a}_0, \quad (\text{C.21})$$

where the metric tensor  $g_{\mu_1\mu_2}$  and the Levi-Civita pseudo tensor  $\varepsilon_{\mu_1\mu_2\mu_3\mu_4}$  are the only independent Lorentz tensors to construct the projection vector  $\vec{l}_\mu^{(0)}$ . From these,  $\vec{l}_\mu^{(0)}$  can be constructed only for even rank tensors. Hence, the Lorentz-odd OPE vanishes.

**Examples** For a second-rank tensor (two Lorentz indices)  $\langle \Omega | O_{\mu_1\mu_2} | \Omega \rangle$ , only the metric tensor  $g_{\mu_1\mu_2} = \vec{l}_{\mu_1\mu_2}^{(0)}$  contributes and the decomposition tensor is trivially given by

$$P_{\mu_1\mu_2\nu_1\nu_2}^0 = \frac{1}{4} g_{\mu_1\mu_2} g_{\nu_1\nu_2}. \quad (\text{C.22})$$

Clearly, only symmetric tensors can give non-vanishing condensates. For a fourth-rank tensor (four Lorentz indices)  $\langle \Omega | O_{\mu_1\mu_2\mu_3\mu_4} | \Omega \rangle$ , three combinations of metric tensors and the Levi-Civita symbol,  $\vec{l}_{\mu_1\mu_2\mu_3\mu_4}^{(0)} = (\varepsilon_{\mu_1\mu_2\mu_3\mu_4}, g_{\mu_1\mu_2}g_{\mu_3\mu_4}, g_{\mu_1\mu_3}g_{\mu_2\mu_4}, g_{\mu_1\mu_4}g_{\mu_2\mu_3})^T$  (with  $\vec{l}_{\nu_1\nu_2\nu_3\nu_4}^{(0)}$  analogously), serve as decomposition basis yielding

$$P_{\mu_1\mu_2\mu_3\mu_4\nu_1\nu_2\nu_3\nu_4}^0 = \frac{1}{72} \text{Tr} \left[ \begin{pmatrix} -3 & & & \\ & 5 & -1 & -1 \\ & -1 & 5 & -1 \\ & -1 & -1 & 5 \end{pmatrix} \left( \vec{l}_{\mu_1\mu_2\mu_3\mu_4}^{(0)} \circ \vec{l}_{\nu_1\nu_2\nu_3\nu_4}^{(0)} \right) \right]. \quad (\text{C.23})$$

Due to different (anti-)symmetries of the decomposition elements, the projection matrix  $L_0$  is in block-diagonal form.<sup>3</sup> Equivalently, a set of (anti-)symmetrized tensors,  $\vec{l}_{\{\mu_1\mu_2\}\{\mu_3\mu_4\}}^{(0)}$ ,

---

<sup>3</sup>The projection matrix  $L$  can be cast in diagonal form employing an orthogonal set of tensors for decomposition, i. e.  $(\vec{l}_\mu \circ \vec{l}^\mu) = \text{diag}(b_1, b_2, \dots)$ , which can be generated, e. g., by the Gram-Schmidt orthogonalization. However, this merely shifts the problem from inversion of  $L$  to finding an orthogonal set of tensors, which themselves have no relation to the properties of the operator under consideration unlike tensors which reflect the (anti-)symmetries of particular index pairs of the operator.

may be employed, which simplifies the projection tensor to

$$P_{\mu_1\mu_2\mu_3\mu_4\nu_1\nu_2\nu_3\nu_4}^0 = \frac{1}{72} \text{Tr} \left[ \begin{pmatrix} -3 & & & \\ & 3 & & \\ & & 2 & -1 \\ & & -1 & 5 \end{pmatrix} \left( \vec{l}_{\{\mu_1\mu_2\}\{\mu_3\mu_4\}}^{(0)} \circ \vec{l}_{\{\nu_1\nu_2\}\{\nu_3\nu_4\}}^{(0)} \right) \right] \quad (\text{C.24})$$

with

$$\vec{l}_{\{\mu_1\mu_2\}\{\mu_3\mu_4\}}^{(0)} = \begin{pmatrix} \varepsilon_{\mu_1\mu_2\mu_3\mu_4} \\ g_{\mu_1\mu_3}g_{\mu_2\mu_4} - g_{\mu_1\mu_4}g_{\mu_2\mu_3} \\ g_{\mu_1\mu_3}g_{\mu_2\mu_4} + g_{\mu_1\mu_4}g_{\mu_2\mu_3} \\ g_{\mu_1\mu_2}g_{\mu_3\mu_4} \end{pmatrix} \quad (\text{C.25})$$

and  $\vec{l}_{\{\nu_1\nu_2\}\{\nu_3\nu_4\}}^{(0)}$  analogously.

## Medium

At non-zero density and/or temperature, the medium four-velocity  $v_\mu$  provides a new element allowing for a number of additional Lorentz tensors to be projected onto (cf. [Buc14b] for a list of tensors up to 5 Lorentz indices). We assume that in medium the following decomposition holds for any operator  $O_\mu$ :

$$\langle\langle O_\mu \rangle\rangle = \langle\langle O_\mu \rangle\rangle_\rho = \vec{l}_\mu^{(\rho)} \cdot \vec{a}_\rho, \quad (\text{C.26})$$

where  $\rho$  is a generalized medium parameter, i.e.  $\rho = 0$  in vacuum, and  $\rho > 0$  in the medium.<sup>4</sup> The projection vector  $\vec{l}_\mu^{(\rho)} = (\vec{l}_\mu^{(\rho_0)}, \vec{l}_\mu^{(\rho_1)})^T$  contains all tensors which already occur in vacuum, i.e.  $\vec{l}_\mu^{(\rho_0)} = \vec{l}_\mu^{(0)}$ . All remaining tensors which incorporate the medium four-velocity  $v_\mu$  are collected in  $\vec{l}_\mu^{(\rho_1)}$ . Analogously,  $\vec{a}_\rho = (\vec{a}_{\rho_0}, \vec{a}_{\rho_1})^T$ , but  $\vec{a}_{\rho_0} \neq \vec{a}_0$  due to  $\vec{l}^{(0)} \circ \vec{l}^{(\rho_1)} \neq 0$ .

The coefficient vectors are given as

$$\vec{a}_{\rho_0} = L_0^{-1} \left( \vec{l}_\nu^{(0)} \langle\langle O^\nu \rangle\rangle - L_{0,\rho_1} \vec{a}_{\rho_1} \right), \quad (\text{C.27a})$$

$$\vec{a}_{\rho_1} = L_{\rho_1}^{-1} \left( \vec{l}_\nu^{(\rho_1)} \langle\langle O^\nu \rangle\rangle - L_{\rho_1,0} \vec{a}_{\rho_0} \right), \quad (\text{C.27b})$$

and in disentangled form they read

$$\vec{a}_{\rho_0} = (L_0 - L_{0,\rho_1} L_{\rho_1}^{-1} L_{\rho_1,0})^{-1} \left( \vec{l}_\nu^{(0)} - L_{0,\rho_1} L_{\rho_1}^{-1} \vec{l}_\nu^{(\rho_1)} \right) \langle\langle O^\nu \rangle\rangle, \quad (\text{C.28a})$$

$$\vec{a}_{\rho_1} = (L_{\rho_1} - L_{\rho_1,0} L_0^{-1} L_{0,\rho_1})^{-1} \left( \vec{l}_\nu^{(\rho_1)} - L_{\rho_1,0} L_0^{-1} \vec{l}_\nu^{(0)} \right) \langle\langle O^\nu \rangle\rangle, \quad (\text{C.28b})$$

<sup>4</sup>The general medium parameter  $\rho$ , here mainly used as an distinguishing index, must not be confused with the spectral density of a hadron introduced in Sec. 2.1.

where the sub-matrices  $L_0$ ,  $L_{0,\rho_1}$ ,  $L_{\rho_1,0}$  and  $L_{\rho_1}$  of the projection matrix  $L_\rho = (\vec{l}^{(\rho)} \circ \vec{l}^{(\rho)})$  are given explicitly in Eq. (C.90) below. As can be seen, having pre-evaluated the vacuum decomposition is of little use. Both decomposition vectors have to be evaluated and will, in general, contain all occurring condensates, irrespective of their vacuum limit.

Naturally, one wishes to reduce evaluational efforts in case the vacuum decomposition is already at our disposal and only the additional medium-specific contribution has to be determined. At this stage, however, the full decomposition has to be performed and the vacuum contribution subtracted to identify the medium-specific term. In particular, the construction of a medium-specific projection vector  $\vec{l}_\mu^{(1)}$ , which directly gives the additional terms, is wanted.

We now define the 'algebraic' vacuum decomposition in full analogy to (C.19a) and (C.21) as

$$\langle\langle O_\mu \rangle\rangle_0 = \vec{l}_\mu^{(0)} \cdot \vec{a}_0 \equiv \text{Tr} \left[ L_0^{-1} \left( \vec{l}_\mu^{(0)} \circ \vec{l}_\nu^{(0)} \right) \right] \langle\langle O^\nu \rangle\rangle, \quad (\text{C.29})$$

which is algebraically given by the same operators as the decomposition (C.21). However, in general, the ground state EVs are now medium dependent. Here and in the following, 'algebraic' means that the projection vector  $\vec{l}_\mu$  is specified and the projection tensor  $P_{\mu\nu}$  is applied to the EV irrespective if it is the ground state EV or Gibbs average. We explicitly separate the algebraic vacuum-specific terms

$$\langle\langle O_\mu \rangle\rangle \equiv \langle\langle O_\mu \rangle\rangle_0 + \langle\langle O_\mu \rangle\rangle_1 \equiv \vec{l}_\mu^{(0)} \cdot \vec{a}_0 + \vec{l}_\mu^{(1)} \cdot \vec{a}_1, \quad (\text{C.30})$$

which, together with Eq. (C.21), defines the 'algebraic' medium-specific contribution  $\langle\langle O_\mu \rangle\rangle_1$ .

Note that (C.30) is an algebraic separation. This means, that the vacuum-specific condensates generated by the vacuum-specific decomposition (C.21) exhibit a density dependence when entering the in-medium decomposition in (C.30). Furthermore, it is important to emphasize that the medium-specific projection vector  $\vec{l}_\mu^{(1)}$  is not only constituted by the medium four-velocity or tensors that contain the latter. The elements in  $\vec{l}_\mu^{(0)}$  are completely contained in  $\vec{l}_\mu^{(1)}$ . Medium-specific condensates have zero vacuum limit and are contained in  $\vec{a}_1$ .

Using (C.27) together with (C.29), equality of the definitions (C.30) and (C.26) leads to the following orthogonality requirement for  $\vec{l}_\mu^{(0)}$  and the medium-specific projection vector

$$0 = \vec{l}^{(1)} \circ \vec{l}^{(0)}. \quad (\text{C.31})$$

It can be shown that (C.30) and (C.31) are equivalent definitions (cf. App. C.2.4).

The according prescription is detailed in the following. From orthogonality (C.31), the relation  $\vec{a}_0 = L_0^{-1} (\vec{l}^{(0)} \circ \vec{l}^{(\rho)}) \vec{a}_\rho$  follows, which imposes  $\text{dim}(\vec{l}_\mu^{(0)})$  constraints on the coefficients  $\vec{a}^{(\rho)}$  and  $\vec{a}^{(0)}$  leaving  $\text{dim}(\vec{l}_\mu^{(\rho)})$  independent elements. Substituting the obtained constraints

$$\vec{a}_{\rho_0} = \vec{a}_0 - L_0^{-1} L_{0,\rho_1} \vec{a}_{\rho_1} \quad (\text{C.32})$$

in definition (C.30) allows (together with Eq. (C.21)) to construct a medium-specific projection vector

$$\vec{l}_\mu^{(1)} = L_{\rho_1,0} L_0^{-1} \vec{l}_\mu^{(0)} - \vec{l}_\mu^{(\rho_1)}. \quad (\text{C.33})$$

Note that  $\vec{l}_\mu^{(1)}$  is not unique. A constant factor and symmetry properties may be chosen differently. Due to orthogonality (C.31), vacuum- and medium-specific parts of the tensor decomposition can be evaluated independently of each other and the general decomposition procedure (C.19b) can be applied utilizing the medium-specific projection vector (C.33).

The medium-specific contribution  $\langle\langle O_\mu \rangle\rangle_1$  of a decomposed Gibbs averaged operator is also referred to as a higher-twist contribution  $\langle\langle \mathcal{ST} O_\mu \rangle\rangle$ , where  $\mathcal{ST}$  renders the operator symmetric and traceless w.r.t. Lorentz indices [Hat93, Leu98]. The numerical values of these quantities can be obtained from DIS amplitudes [Gub15a]. In the very same fashion numerical values can be found for medium-specific condensates or at least for linear combinations of the latter. For medium-specific condensates up to mass dimension 5, the corresponding numerical values and their medium behaviors from DIS amplitudes to leading order in the nucleon density are explicated in [Jin93].

**Examples** For a second-rank tensor (two Lorentz indices)  $\langle\langle O_{\mu_1\mu_2} \rangle\rangle_1$ , only the metric tensor  $g_{\mu_1\mu_2} = \vec{l}_{\mu_1\mu_2}^{(0)}$  and  $v_{\mu_1}v_{\mu_2}/v^2 = \vec{l}_{\mu_1\mu_2}^{(\rho_1)}$  contribute, and the decomposition tensor reads

$$P_{\mu_1\mu_2\nu_1\nu_2}^1 = \frac{1}{12} \left( g_{\mu_1\mu_2} - 4 \frac{v_{\mu_1}v_{\mu_2}}{v^2} \right) \left( g_{\nu_1\nu_2} - 4 \frac{v_{\nu_1}v_{\nu_2}}{v^2} \right), \quad (\text{C.34})$$

where non-vanishing results are obtained for symmetric Lorentz indices only. For a fourth-rank tensor (four Lorentz indices)  $\langle\langle O_{\mu_1\mu_2\mu_3\mu_4} \rangle\rangle_1$  fourteen tensors contribute. Four of them, which incorporate the Levi-Civita symbol, can be evaluated separately (cf. Eq. (C.23)). Thus, we restrict the consideration to the remaining ten tensors, giving

$$P_{\mu_1\mu_2\mu_3\mu_4\nu_1\nu_2\nu_3\nu_4}^1 = \frac{1}{240} \times \text{Tr} \left[ \begin{pmatrix} 7 & -\frac{1}{2} & -\frac{1}{2} & 2 & -\frac{1}{2} & -\frac{1}{2} & -1 \\ -\frac{1}{2} & 7 & -\frac{1}{2} & -\frac{1}{2} & 2 & -\frac{1}{2} & -1 \\ -\frac{1}{2} & -\frac{1}{2} & 7 & -\frac{1}{2} & -\frac{1}{2} & 2 & -1 \\ 2 & -\frac{1}{2} & -\frac{1}{2} & 7 & -\frac{1}{2} & -\frac{1}{2} & -1 \\ -\frac{1}{2} & 2 & -\frac{1}{2} & -\frac{1}{2} & 7 & -\frac{1}{2} & -1 \\ -\frac{1}{2} & -\frac{1}{2} & 2 & -\frac{1}{2} & -\frac{1}{2} & 7 & -1 \\ -1 & -1 & -1 & -1 & -1 & -1 & \frac{4}{3} \end{pmatrix} \left( \vec{l}_{\mu_1\mu_2\mu_3\mu_4}^{(1)} \circ \vec{l}_{\nu_1\nu_2\nu_3\nu_4}^{(1)} \right) \right] \quad (\text{C.35})$$

with

$$\vec{l}_{\mu_1\mu_2\mu_3\mu_4}^{(1)} = \left( g_{\mu_1\mu_2}g_{\mu_3\mu_4} - 4g_{\mu_1\mu_2}\frac{v_{\mu_3}v_{\mu_4}}{v^2}, g_{\mu_1\mu_3}g_{\mu_2\mu_4} - 4g_{\mu_1\mu_3}\frac{v_{\mu_2}v_{\mu_4}}{v^2}, \right. \\ g_{\mu_1\mu_4}g_{\mu_2\mu_3} - 4g_{\mu_1\mu_4}\frac{v_{\mu_2}v_{\mu_3}}{v^2}, g_{\mu_3\mu_4}g_{\mu_1\mu_2} - 4g_{\mu_3\mu_4}\frac{v_{\mu_1}v_{\mu_2}}{v^2}, \\ g_{\mu_2\mu_4}g_{\mu_1\mu_3} - 4g_{\mu_2\mu_4}\frac{v_{\mu_1}v_{\mu_3}}{v^2}, g_{\mu_2\mu_3}g_{\mu_1\mu_4} - 4g_{\mu_2\mu_3}\frac{v_{\mu_1}v_{\mu_4}}{v^2}, \\ \left. g_{\mu_1\mu_2}g_{\mu_3\mu_4} + g_{\mu_1\mu_3}g_{\mu_2\mu_4} + g_{\mu_1\mu_4}g_{\mu_2\mu_3} - 24\frac{v_{\mu_1}v_{\mu_2}v_{\mu_3}v_{\mu_4}}{v^4} \right)^T \quad (\text{C.36})$$

and  $\vec{l}_{\nu_1\nu_2\nu_3\nu_4}^{(1)}$  analogously. Decomposing the components of the projection vector into tensors symmetric and anti-symmetric in the index pairs  $\mu_1\mu_2$  and  $\mu_3\mu_4$  yields

$$P_{\mu_1\mu_2\mu_3\mu_4\nu_1\nu_2\nu_3\nu_4}^1 = \frac{1}{240} \times \text{Tr} \left[ \begin{pmatrix} 10 & & & & \\ & 20 & & & \\ & & 20 & & \\ & & & 8 & -1 & -1 & -2 \\ & & & -1 & 7 & 2 & -1 \\ & & & -1 & 2 & 7 & -1 \\ & & & -2 & -1 & -1 & \frac{4}{3} \end{pmatrix} \left( \vec{l}_{\{\mu_1\mu_2\}\{\mu_3\mu_4\}}^{(1)} \circ \vec{l}_{\{\nu_1\nu_2\}\{\nu_3\nu_4\}}^{(1)} \right) \right] \quad (\text{C.37})$$

with

$$\vec{l}_{\{\mu_1\mu_2\}\{\mu_3\mu_4\}}^{(1)} = \left( l_{[\mu_1\mu_2][\mu_3\mu_4]}^{(1)}, l_{(\mu_1\mu_2)[\mu_3\mu_4]}^{(1)}, l_{[\mu_1\mu_2](\mu_3\mu_4)}^{(1)}, \vec{l}_{(\mu_1\mu_2)(\mu_3\mu_4)}^{(1)} \right)^T, \quad (\text{C.38})$$

$$l_{[\mu_1\mu_2][\mu_3\mu_4]}^{(1)} = g_{\mu_1\mu_3}g_{\mu_2\mu_4} - g_{\mu_1\mu_4}g_{\mu_2\mu_3} - \frac{2}{v^2}(g_{\mu_1\mu_3}v_{\mu_2}v_{\mu_4} - g_{\mu_1\mu_4}v_{\mu_2}v_{\mu_3} + g_{\mu_2\mu_4}v_{\mu_1}v_{\mu_3} - g_{\mu_2\mu_3}v_{\mu_1}v_{\mu_4}), \quad (\text{C.39a})$$

$$l_{(\mu_1\mu_2)[\mu_3\mu_4]}^{(1)} = \frac{1}{v^2}(g_{\mu_1\mu_3}v_{\mu_2}v_{\mu_4} - g_{\mu_1\mu_4}v_{\mu_2}v_{\mu_3} - g_{\mu_2\mu_4}v_{\mu_1}v_{\mu_3} + g_{\mu_2\mu_3}v_{\mu_1}v_{\mu_4}), \quad (\text{C.39b})$$

$$l_{[\mu_1\mu_2](\mu_3\mu_4)}^{(1)} = \frac{1}{v^2}(g_{\mu_1\mu_3}v_{\mu_2}v_{\mu_4} + g_{\mu_1\mu_4}v_{\mu_2}v_{\mu_3} - g_{\mu_2\mu_4}v_{\mu_1}v_{\mu_3} - g_{\mu_2\mu_3}v_{\mu_1}v_{\mu_4}), \quad (\text{C.39c})$$

$$\begin{aligned} \vec{l}_{(\mu_1\mu_2)(\mu_3\mu_4)}^{(1)} = & \left( g_{\mu_1\mu_3}g_{\mu_2\mu_4} + g_{\mu_1\mu_4}g_{\mu_2\mu_3} - \frac{2}{v^2}(g_{\mu_1\mu_3}v_{\mu_2}v_{\mu_4} \right. \\ & \left. + g_{\mu_1\mu_4}v_{\mu_2}v_{\mu_3} + g_{\mu_2\mu_4}v_{\mu_1}v_{\mu_3} + g_{\mu_2\mu_3}v_{\mu_1}v_{\mu_4}), \right. \\ & g_{\mu_1\mu_2}g_{\mu_3\mu_4} - 4g_{\mu_1\mu_2}\frac{v_{\mu_3}v_{\mu_4}}{v^2}, \quad g_{\mu_1\mu_2}g_{\mu_3\mu_4} - 4g_{\mu_3\mu_4}\frac{v_{\mu_1}v_{\mu_2}}{v^2}, \\ & \left. g_{\mu_1\mu_2}g_{\mu_3\mu_4} + g_{\mu_1\mu_3}g_{\mu_2\mu_4} + g_{\mu_1\mu_4}g_{\mu_2\mu_3} - 24\frac{v_{\mu_1}v_{\mu_2}v_{\mu_3}v_{\mu_4}}{v^4} \right)^T \end{aligned} \quad (\text{C.39d})$$

and  $\vec{l}_{\{\nu_1\nu_2\}\{\nu_3\nu_4\}}^{(1)}$  analogously, where the Bach bracket notation is employed to the bracketed index pair  $\{\dots\}$ .

Due to the anti-symmetry of the indices of the gluon field strength tensor, the medium-specific gluon condensate can be identified by the decomposition [Zsc11]

$$\begin{aligned} \langle\langle G_{\mu_1\mu_2}^A G_{\mu_3\mu_4}^A \rangle\rangle_1 = & \frac{1}{24} \langle\langle \left( \frac{G^2}{4} - \frac{(vG)^2}{v^2} \right) \rangle\rangle \left[ g_{\mu_1\mu_3}g_{\mu_2\mu_4} - g_{\mu_1\mu_4}g_{\mu_2\mu_3} \right. \\ & \left. - \frac{2}{v^2}(g_{\mu_1\mu_3}v_{\mu_2}v_{\mu_4} - g_{\mu_1\mu_4}v_{\mu_2}v_{\mu_3} + g_{\mu_2\mu_4}v_{\mu_1}v_{\mu_3} - g_{\mu_2\mu_3}v_{\mu_1}v_{\mu_4}) \right] \end{aligned} \quad (\text{C.40})$$

which features only the decomposition in Eq. (C.39a).



### Vacuum constraints

Although the (anti-)symmetrized projection vector exhibits a more complicated structure, it considerably simplifies the decomposition of tensors with known symmetries among the Lorentz indices and allows for an unambiguous identification of medium-specific condensates.

In vacuum, Gibbs averaging reduces to the ground state EV of the operators under consideration,  $\langle\langle O_\mu \rangle\rangle \rightarrow \langle\Omega|O_\mu|\Omega\rangle$ . Hence, in the vacuum limit the non-orthogonal decomposition must satisfy

$$\vec{l}_\mu^{(0)} \cdot \vec{a}_{\rho_0} + \vec{l}_\mu^{(\rho_1)} \cdot \vec{a}_{\rho_1} \rightarrow \vec{l}_\mu^{(0)} \cdot \vec{a}_0, \quad (\text{C.41})$$

which can be expressed by the following vacuum constraint

$$\begin{pmatrix} \vec{l}_\mu^{(0)} \\ \vec{l}_\mu^{(\rho_1)} \end{pmatrix}^T \left[ L_\rho^{-1} - \begin{pmatrix} L_0^{-1} & 0 \\ 0 & 0 \end{pmatrix} \right] \begin{pmatrix} \vec{l}_\nu^{(0)} \\ \vec{l}_\nu^{(\rho_1)} \end{pmatrix} \langle\Omega|O^\nu|\Omega\rangle = 0. \quad (\text{C.42})$$

As the components of  $\vec{l}_\mu^{(\rho)}$  must be linearly independent, (C.42) can only be fulfilled if

$$\left[ L_\rho^{-1} - \begin{pmatrix} L_0^{-1} & 0 \\ 0 & 0 \end{pmatrix} \right] \begin{pmatrix} \vec{l}_\nu^{(0)} \\ \vec{l}_\nu^{(\rho_1)} \end{pmatrix} \langle\Omega|O^\nu|\Omega\rangle = 0. \quad (\text{C.43})$$

On the other hand  $\vec{l}_\mu^{(\rho)} \langle\Omega|O^\mu|\Omega\rangle \neq 0$  must hold, if  $\vec{l}_\mu^{(0)} \langle\Omega|O^\mu|\Omega\rangle \neq 0$ .<sup>5</sup> Consequently, the vector of condensates  $\vec{l}_\mu^{(\rho)} \langle\Omega|O^\mu|\Omega\rangle$  must satisfy

$$\vec{l}_\mu^{(\rho)} \langle\Omega|O^\mu|\Omega\rangle \in \ker \left[ L_\rho^{-1} - \begin{pmatrix} L_0^{-1} & 0 \\ 0 & 0 \end{pmatrix} \right] \quad (\text{C.44})$$

for all operators  $O_\mu$ . Note that, in general, the kernel of the matrix is degenerate. Thus, the imposed vacuum constraints are not unique in the sense that (C.43) is the strongest constraint which can be deduced. In particular, because of the non-orthogonality of  $\vec{l}_\mu^{(0)}$  and  $\vec{l}_\mu^{(\rho_1)}$ , the matrix in (C.43) has no block-diagonal form and possible interrelations among the additional medium terms remain hidden.

Because the matrix in (C.43) must have a non-trivial kernel, thus being not invertible, there is no matrix  $\bar{L}$  with

$$\bar{L}^{-1} = \left[ L_\rho^{-1} - \begin{pmatrix} L_0^{-1} & 0 \\ 0 & 0 \end{pmatrix} \right]. \quad (\text{C.45})$$

This is merely another formulation of the problem that the full decomposition has to be reevaluated in case additional tensors enter the projection vector although the vacuum decomposition is known.

<sup>5</sup> In case  $\vec{l}_\mu^{(0)} \langle\Omega|O^\mu|\Omega\rangle = 0$ ,  $\vec{l}_\mu^{(\rho)} \langle\Omega|O^\mu|\Omega\rangle = 0$  must be fulfilled element-wise. For an odd number of indices  $\vec{l}_\mu^{(0)}$  does not exist, thus  $\vec{l}_\mu^{(\rho_1)} = \vec{l}_\mu^{(1)}$  and the arguments for the orthogonal decomposition apply.

For the orthogonal decomposition, the vacuum limit reads

$$0 = \langle \Omega | O_\mu | \Omega \rangle_1 = \vec{l}_\mu^{(1)} \cdot \vec{a}_1. \quad (\text{C.46})$$

As the components of  $\vec{l}_\mu^{(1)}$  must be linearly independent and the kernel of the invertible medium-specific projection matrix is trivial, i. e.  $\ker \left( \vec{l}^{(1)} \circ \vec{l}^{(1)} \right)^{-1} = \{0\}$ , this is equivalent to  $\vec{a}_1 \rightarrow 0$  with element-wise vanishing of the medium-specific condensates

$$0 = \vec{l}_\mu^{(1)} \langle \Omega | O^\mu | \Omega \rangle, \quad (\text{C.47})$$

cf. Eq. (C.19a). From (C.33) it can be seen that medium-specific condensates  $\vec{l}_\mu^{(1)} \langle \langle O^\mu \rangle \rangle$  contain algebraic vacuum condensates  $\vec{l}_\mu^{(0)} \langle \langle O^\mu \rangle \rangle$ . Accordingly, the requirement of vanishing medium-specific condensates gives rise to vacuum constraints as interrelations among the  $\vec{l}_\mu^{(\rho)} \langle \Omega | O^\mu | \Omega \rangle$  entering the medium-specific part of the decomposition, in particular also between terms which already occur in vacuum, i. e.  $\vec{l}_\mu^{(0)} \langle \Omega | O^\mu | \Omega \rangle$ . Thus, the vacuum limit of non-vacuum condensates  $\vec{l}_\mu^{(\rho_1)} \langle \Omega | O^\mu | \Omega \rangle$  is restricted by vacuum condensates:

$$\vec{l}_\mu^{(\rho_1)} \langle \Omega | O^\mu | \Omega \rangle = L_{\rho_1,0} L_0^{-1} \vec{l}_\mu^{(0)} \langle \Omega | O^\mu | \Omega \rangle. \quad (\text{C.48})$$

In particular, non-vacuum condensates have a non-zero vacuum limit.

Summarizing, the Lorentz tensors which enter the decomposition upon the onset of a continuous parameter  $\rho$ , as e. g. the density, lead to additional condensates. The limit of these condensates for  $\rho \rightarrow 0$  is however constrained by (C.48) if the transition is assumed to be continuous. It is remarkable that these vacuum constraints are independent of the operator  $O_\mu$ , but only depend on the rank of this Lorentz tensor. Finally, the arguments given above are not restricted to the occurrence of a medium velocity  $v_\mu$  and can in principle be applied to any decomposition where additional tensors enter.

### Transformation to canonical condensates

Utilizing quark and gluon EoMs, i. e. Eqs. (A.17), (A.18) and (A.19), as well as Dirac matrix identities, e. g. Eq. (A.13), and the symmetries of the QCD ground state, the elements of the vector of condensates can be mapped to a smaller set of (canonical) condensates,

$$\vec{l}_\mu^{(\rho)} \langle O^\mu \rangle = K \langle \vec{q} \rangle, \quad (\text{C.49})$$

where  $K$  is a linear transformation matrix. It maps the canonical condensates  $\langle \vec{q} \rangle = (\langle \vec{q} \rangle^{(0)}, \langle \vec{q} \rangle^{(\rho_1)})^T$  onto the contracted EVs  $\vec{l}_\mu^{(\rho)} \langle O^\mu \rangle$ . Canonical condensates contain the minimal number of covariant derivatives. Whereas the Lorentz decomposition of a QCD operator depends only on its tensor rank, the operator itself might be identified by its transformation to canonical condensates. Having fixed a set of canonical condensates in the medium, any operator  $O$  may be specified by its matrix  $K$ .

Since vacuum and non-vacuum parts of the  $(m \times n)$  matrix  $K$  separate according to

$$K = \begin{pmatrix} K_0 & 0 \\ 0 & K_{\rho_1} \end{pmatrix} \quad (\text{C.50})$$

the vacuum constraints (C.48) read

$$K_{\rho_1} \langle \vec{q} \rangle^{(\rho_1)} = L_{\rho_1,0} L_0^{-1} K_0 \langle \vec{q} \rangle^{(0)}, \quad (\text{C.51})$$

requiring the left inverse of  $K_{\rho_1}$  to cast the vacuum constraints in the desired form. Since columns and rows in  $K$  might show linear dependences the inverse  $K_{\rho_1}^{-1}$  does not exist in general. However, a left inverse  $K_{\rho_1}^+$  can always be constructed from a matrix with linearly independent columns which can be obtained by appropriate redefinition of  $\langle \vec{q} \rangle$ . Then the vacuum constraints of canonical condensates read

$$\langle \vec{q} \rangle^{(\rho_1)} = K_{\rho_1}^+ L_{\rho_1,0} L_0^{-1} K_0 \langle \vec{q} \rangle^{(0)}. \quad (\text{C.52})$$

### C.2.2 Application to four-quark condensates

The above derived formulae are essential for setting up in-medium QSRs for mesons and baryons. Depending on the order of the OPE of the correlator, operators with an increasing number of Lorentz indices occur. To illustrate the definitions of vacuum- and medium-specific contributions and to shed light on the effect of vacuum constraints we choose four-quark condensates as an example with up to five Lorentz indices. The evaluation of leading order  $\alpha_s$  four-quark condensate terms using the Fock-Schwinger gauge method [Nov84, Pas84] requires the computation of three distinct contributions to the meson current-current correlator (cf. App. C.3):  $\langle \langle \bar{q} \overleftrightarrow{D}_\mu \overleftrightarrow{D}_\nu \overleftrightarrow{D}_\lambda \Gamma q \rangle \rangle$ ,  $\langle \langle \bar{q} \Gamma [D_\nu, G_{\kappa\lambda}] q \rangle \rangle$ ,  $\langle \langle \bar{q} \overleftrightarrow{D}_\mu \Gamma G_{\nu\lambda} q \rangle \rangle$ . Specifying the Dirac structure  $\Gamma$  for a light vector current, such as for the  $\rho$  or  $\omega$  meson, we end up with the following Gibbs averaged operators:

even OPE

$$\begin{aligned} (\text{e1}) \quad & \langle \langle \bar{q} \overleftrightarrow{D}_\mu \overleftrightarrow{D}_\nu \overleftrightarrow{D}_\lambda \gamma_\alpha q \rangle \rangle \\ (\text{e2}) \quad & \langle \langle \bar{q} \gamma_\mu [D_\nu, G_{\kappa\lambda}] q \rangle \rangle \\ (\text{e3}) \quad & \langle \langle \bar{q} \gamma_5 \gamma_\mu [D_\nu, G_{\kappa\lambda}] q \rangle \rangle \\ (\text{e4}) \quad & \langle \langle \bar{q} \overleftrightarrow{D}_\mu \gamma_\alpha G_{\nu\lambda} q \rangle \rangle \\ (\text{e5}) \quad & \langle \langle \bar{q} \overleftrightarrow{D}_\mu \gamma_5 \gamma_\alpha G_{\nu\lambda} q \rangle \rangle \end{aligned}$$

odd OPE

$$\begin{aligned} (\text{o1}) \quad & \langle \langle \bar{q} \overleftrightarrow{D}_\mu \overleftrightarrow{D}_\nu \overleftrightarrow{D}_\lambda q \rangle \rangle \\ (\text{o2}) \quad & \langle \langle \bar{q} [D_\nu, G_{\kappa\lambda}] q \rangle \rangle \\ (\text{o3}) \quad & \langle \langle \bar{q} \sigma_{\alpha\beta} [D_\sigma G_{\nu\lambda}] q \rangle \rangle \\ (\text{o4}) \quad & \langle \langle \bar{q} \overleftrightarrow{D}_\mu G_{\nu\lambda} q \rangle \rangle \\ (\text{o5}) \quad & \langle \langle \bar{q} \overleftrightarrow{D}_\mu \sigma_{\alpha\beta} G_{\nu\lambda} q \rangle \rangle \end{aligned}$$

and equivalent objects with covariant derivatives acting on the right quark operator, i.e.  $\bar{q} \overleftrightarrow{D}_\mu \cdots q \longrightarrow \bar{q} \cdots D_\mu q$ . Four-quark condensates in LO of  $\alpha_s$  also occur in the NLO correlator with inserted interaction term:

even OPE

$$\begin{aligned} (\text{e6}) \quad & \langle \langle \bar{q} \gamma_\mu T^A q \bar{q}' \gamma_\nu T^A q' \rangle \rangle \\ (\text{e7}) \quad & \langle \langle \bar{q} \gamma_5 \gamma_\mu T^A q \bar{q}' \gamma_5 \gamma_\nu T^A q' \rangle \rangle \end{aligned}$$

odd OPE

$$\begin{aligned} (\text{o6}) \quad & \langle \langle \bar{q} T^A q \bar{q}' \gamma_\mu T^A q' \rangle \rangle \\ (\text{o7}) \quad & \langle \langle \bar{q} \gamma_5 \gamma_\mu T^A q \bar{q}' \sigma_{\nu\lambda} T^A q' \rangle \rangle, \end{aligned}$$

where  $q$  and  $q'$  denote light-quark flavors, which may coincide, and  $T^A$  with  $A = 0, \dots, 8$  symbolize the generators of the color group  $\text{SU}(N_c = 3)$ ,  $t^A$ , added by the unit element for  $A = 0$ .

In the following we provide vacuum- and medium-specific decompositions of those OPE operators (e1)–(e7) and (o1)–(o7) which do not vanish in the light (axial-)vector meson OPE (due to (anti-)symmetries among the Lorentz indices or vanishing Dirac trace results). The Lorentz-contracted operators occurring in the decomposition coefficients are transformed to canonical condensates. The corresponding transformation matrices are presented along with the vacuum constraints in terms of these canonical condensates.

In pseudo-scalar, scalar, vector and axial-vector meson currents the Dirac trace results of the OPE differ only by a constant (non-zero) factor/sign, except for traces with Dirac projection matrix  $\sigma_{\alpha\beta}$ , where vector and axial-vector currents give zero results. Hence, up to prefactors all four-quark condensate contributions in LO of  $\alpha_s$  to spin-1 OPEs already enter spin-0 OPEs. The presented constraints are therefore valid in both channels. In particular, they do not mutually contradict.

### Even OPE

To extend conveniently the following results to mesons consisting of a light and a heavy quark, such as D and B mesons, we first present the vacuum constraints set up by the contributions of (e1)–(e5) and include additional vacuum constraints from (e6) and (e7) originating from the NLO correlator later on.

(i) The first EV (e1) decomposes into vacuum- and medium-specific terms as (cf. (C.30))

$$\begin{aligned} & \langle\langle \bar{q} \overleftrightarrow{D}_\mu \overleftrightarrow{D}_\nu \overleftrightarrow{D}_\lambda \gamma_\alpha q \rangle\rangle_0 \\ &= \frac{1}{72} \begin{pmatrix} g_{\mu\lambda} g_{\nu\alpha} + g_{\mu\alpha} g_{\nu\lambda} \\ g_{\mu\nu} g_{\lambda\alpha} \end{pmatrix}^T \begin{pmatrix} 2 & -1 \\ -1 & 5 \end{pmatrix} \begin{pmatrix} \langle\langle \bar{q} \overleftrightarrow{D}^\mu \overleftrightarrow{D}^\nu \overleftrightarrow{D}_\mu q + \bar{q} \overleftrightarrow{D}^\mu \overleftrightarrow{D}^2 q \rangle\rangle \\ \langle\langle \bar{q} \overleftrightarrow{D}^2 \overleftrightarrow{D} q \rangle\rangle \end{pmatrix}, \quad (\text{C.53}) \end{aligned}$$

$$\begin{aligned} & \langle\langle \bar{q} \overleftrightarrow{D}_\mu \overleftrightarrow{D}_\nu \overleftrightarrow{D}_\lambda \gamma_\alpha q \rangle\rangle_1 \\ &= \frac{1}{240} \begin{pmatrix} g_{\mu\lambda} g_{\nu\alpha} + g_{\mu\alpha} g_{\nu\lambda} - \frac{2}{v^2} (g_{\mu\lambda} v_\nu v_\alpha \\ + g_{\mu\alpha} v_\nu v_\lambda + g_{\nu\alpha} v_\mu v_\lambda + g_{\nu\lambda} v_\mu v_\alpha) \\ g_{\mu\nu} g_{\lambda\alpha} - \frac{4}{v^2} g_{\mu\nu} v_\lambda v_\alpha \\ g_{\mu\nu} g_{\lambda\alpha} - \frac{4}{v^2} g_{\lambda\alpha} v_\mu v_\nu \\ g_{\mu\lambda} g_{\nu\alpha} + g_{\mu\alpha} g_{\nu\lambda} + g_{\mu\nu} g_{\lambda\alpha} - \frac{48}{v^4} v_\mu v_\nu v_\lambda v_\alpha \end{pmatrix}^T \begin{pmatrix} 8 & -1 & -1 & -2 \\ -1 & 7 & 1 & -1 \\ -1 & 1 & 7 & -1 \\ -2 & -1 & -1 & \frac{4}{3} \end{pmatrix} \\ & \times \begin{pmatrix} \langle\langle \bar{q} \overleftrightarrow{D}^{\mu'} \overleftrightarrow{D}^\nu \overleftrightarrow{D}_{\mu'} q + \bar{q} \overleftrightarrow{D}^\nu \overleftrightarrow{D}^2 q - \frac{2}{v^2} (\bar{q} \overleftrightarrow{D}^{\mu'} (v \overleftrightarrow{D}) \overleftrightarrow{D}_{\mu'} \not{q} \\ + \bar{q} \overleftrightarrow{D} (v \overleftrightarrow{D})^2 q + \bar{q} (v \overleftrightarrow{D}) \overleftrightarrow{D} (v \overleftrightarrow{D}) q + \bar{q} (v \overleftrightarrow{D}) \overleftrightarrow{D}^2 \not{q} \rangle\rangle \\ \langle\langle \bar{q} \overleftrightarrow{D}^2 \overleftrightarrow{D} q - \frac{4}{v^2} \bar{q} \overleftrightarrow{D}^2 (v \overleftrightarrow{D}) \not{q} \rangle\rangle \\ \langle\langle \bar{q} \overleftrightarrow{D}^2 \overleftrightarrow{D} q - \frac{4}{v^2} \bar{q} (v \overleftrightarrow{D})^2 \overleftrightarrow{D} q \rangle\rangle \\ \langle\langle \bar{q} \overleftrightarrow{D}^{\mu'} \overleftrightarrow{D}^\nu \overleftrightarrow{D}_{\mu'} q + \bar{q} \overleftrightarrow{D}^\nu \overleftrightarrow{D}^2 q + \bar{q} \overleftrightarrow{D}^2 \overleftrightarrow{D} q - \frac{48}{v^4} \bar{q} (v \overleftrightarrow{D})^3 \not{q} \rangle\rangle \end{pmatrix}, \quad (\text{C.54}) \end{aligned}$$

where only the part symmetric in the index pairs  $\mu\nu$  and  $\lambda\alpha$  contributes to the (axial-)vector

OPE. Transformation to canonical condensates yields

$$\begin{pmatrix} \langle \bar{q} \overleftrightarrow{D}^2 \overleftrightarrow{\not{D}} q \rangle \\ \langle \bar{q} \overleftrightarrow{D}^\mu \overleftrightarrow{\not{D}} \overleftrightarrow{D}_\mu q \rangle \\ \langle \bar{q} \overleftrightarrow{\not{D}} \overleftrightarrow{D}^2 q \rangle \\ \langle \bar{q} \overleftrightarrow{D}^2 (v \overleftrightarrow{D}) \not{q} \rangle \\ \langle \bar{q} \overleftrightarrow{D}^\mu (v \overleftrightarrow{D}) \overleftrightarrow{D}_\mu \not{q} \rangle \\ \langle \bar{q} \overleftrightarrow{\not{D}} (v \overleftrightarrow{D})^2 q \rangle \\ \langle \bar{q} (v \overleftrightarrow{D})^2 \overleftrightarrow{\not{D}} q \rangle \\ \langle \bar{q} (v \overleftrightarrow{D}) \overleftrightarrow{\not{D}} (v \overleftrightarrow{D}) q \rangle \\ \langle \bar{q} (v \overleftrightarrow{D}) \overleftrightarrow{D}^2 \not{q} \rangle \\ \langle \bar{q} (v \overleftrightarrow{D})^3 \not{q} \rangle \end{pmatrix} = \begin{pmatrix} 0 & i & & & & & & & & \\ \frac{i}{2} & i & & & & & & & & \\ 0 & i & & & & & & & & \\ & & 0 & 1 & 0 & 0 & 0 & & & \\ & & \frac{i}{2} & 1 & 0 & 0 & 0 & & & \\ & & 0 & 0 & i & 0 & 0 & & & \\ & & 0 & 0 & i & 0 & 0 & & & \\ & & 0 & 0 & i & -i & 0 & & & \\ & & 0 & 1 & 0 & -2i & 0 & & & \\ & & 0 & 0 & 0 & 0 & 1 & & & \end{pmatrix} \begin{pmatrix} g^2 \langle \bar{q} \gamma^\mu t^A q \sum_f \bar{f} \gamma_\mu t^A f \rangle \\ \frac{m_q}{2} \langle \bar{q} g \sigma G q \rangle - m_q^3 \langle \bar{q} q \rangle \\ g^2 \langle \bar{q} \not{v} t^A q \sum_f \bar{f} \not{v} t^A f \rangle \\ \frac{1}{2} \langle \bar{q} (v \overleftrightarrow{D}) g \sigma G \not{q} \rangle \\ - m_q^2 \langle \bar{q} (v \overleftrightarrow{D}) \not{q} \rangle \\ m_q \langle \bar{q} (v \overleftrightarrow{D})^2 q \rangle \\ g \langle \bar{q} (v \overleftrightarrow{D}) \gamma^\mu G_{\mu\nu} v^\nu q \rangle \\ \langle \bar{q} (v \overleftrightarrow{D})^3 \not{q} \rangle \end{pmatrix}, \quad (C.55)$$

where  $\sum_f$  denotes the sum over light-quark flavors.

(ii) The second EV (e2) decomposes into vacuum- and medium-specific terms as

$$\langle \langle \bar{q} \gamma_\mu [D_\nu, G_{\kappa\lambda}] q \rangle \rangle_0 = \frac{1}{12} (g_{\mu\kappa} g_{\nu\lambda} - g_{\mu\lambda} g_{\nu\kappa}) \langle \langle \bar{q} \gamma^\alpha [D^\beta, G_{\alpha\beta}] q \rangle \rangle, \quad (C.56)$$

$$\begin{aligned} \langle \langle \bar{q} \gamma_\mu [D_\nu, G_{\kappa\lambda}] q \rangle \rangle_1 &= \frac{1}{12} l_{[\mu\nu][\kappa\lambda]}^{(1)} \langle \langle \bar{q} \gamma^\alpha [D^\beta, G_{\alpha\beta}] q \rangle \rangle \\ &\quad - \frac{2}{v^2} \left( \bar{q} \gamma^\alpha [(vD), G_{\alpha\beta}] v^\beta q + \bar{q} \not{v} [D^\alpha, G_{\beta\alpha}] v^\beta q \right), \end{aligned} \quad (C.57)$$

where only the part anti-symmetric in both index pairs  $\mu\nu$  and  $\kappa\lambda$  contributes to the (axial-)vector OPE. Transformation to canonical condensates yields

$$\begin{pmatrix} \langle \bar{q} \gamma^\alpha [D^\beta, G_{\alpha\beta}] q \rangle \\ \langle \bar{q} \gamma^\alpha [(vD), G_{\alpha\beta}] v^\beta q \rangle \\ \langle \bar{q} \not{v} [D^\alpha, G_{\beta\alpha}] v^\beta q \rangle \end{pmatrix} = \begin{pmatrix} 1 & & \\ & 1 & 0 \\ & 0 & 1 \end{pmatrix} \begin{pmatrix} g \langle \bar{q} \gamma^\mu t^A q \sum_f \bar{f} \gamma_\mu t^A f \rangle \\ \langle \bar{q} \gamma^\alpha [(vD), G_{\alpha\beta}] v^\beta q \rangle \\ g \langle \bar{q} \not{v} t^A q \sum_f \bar{f} \not{v} t^A f \rangle \end{pmatrix}. \quad (C.58)$$

(iii) The third EV (e3) decomposes into vacuum- and medium-specific terms as

$$\langle \langle \bar{q} \gamma_5 \gamma_\alpha [D_\sigma, G_{\nu\lambda}] q \rangle \rangle_0 = -\frac{1}{24} \varepsilon_{\alpha\sigma\nu\lambda} \langle \langle \varepsilon_{\alpha'\sigma'\nu'\lambda'} \bar{q} \gamma_5 \gamma^{\alpha'} [D^{\sigma'}, G^{\nu'\lambda'}] q \rangle \rangle, \quad (C.59)$$

$$\begin{aligned} &\langle \langle \bar{q} \gamma_5 \gamma_\alpha [D_\sigma, G_{\nu\lambda}] q \rangle \rangle_1 \\ &= -\frac{1}{192} \begin{pmatrix} \varepsilon_{\alpha\sigma\nu\lambda} - \frac{4}{v^2} \varepsilon_{\alpha\nu\lambda\tau} v^\tau v_\sigma \\ -\varepsilon_{\alpha\sigma\nu\lambda} - \frac{4}{v^2} \varepsilon_{\alpha\sigma\lambda\tau} v^\tau v_\nu - (\varepsilon_{\alpha\sigma\nu\lambda} - \frac{4}{v^2} \varepsilon_{\alpha\sigma\nu\tau} v^\tau v_\lambda) \end{pmatrix}^T \begin{pmatrix} 4 & -2 \\ -2 & 3 \end{pmatrix} \\ &\quad \times \begin{pmatrix} \langle \langle \varepsilon_{\alpha'\sigma'\nu'\lambda'} \bar{q} \gamma_5 \gamma^{\alpha'} [D^{\sigma'}, G^{\nu'\lambda'}] q - \frac{4}{v^2} \varepsilon_{\alpha'\nu'\lambda'\tau'} v_{\tau'} \bar{q} \gamma_5 \gamma^{\alpha'} [(vD), G^{\nu'\lambda'}] q \rangle \rangle \\ 2 \langle \langle -\varepsilon_{\alpha'\sigma'\nu'\lambda'} \bar{q} \gamma_5 \gamma^{\alpha'} [D^{\sigma'}, G^{\nu'\lambda'}] q - \frac{4}{v^2} \varepsilon_{\alpha'\sigma'\lambda'\tau'} v_{\tau'} v^{\nu'} \bar{q} \gamma_5 \gamma^{\alpha'} [D^{\sigma'}, G^{\nu'\lambda'}] q \rangle \rangle \end{pmatrix}, \end{aligned} \quad (C.60)$$

where only the part anti-symmetric in the index pair  $\nu\lambda$  contributes to the (axial-)vector OPE. Transformation to canonical condensates yields

$$\begin{pmatrix} \langle \varepsilon_{\alpha\sigma\nu\lambda} \bar{q} \gamma_5 \gamma^\alpha [D^\sigma, G^{\nu\lambda}] q \rangle \\ \langle \varepsilon_{\alpha\nu\lambda\tau} v^\tau \bar{q} \gamma_5 \gamma^\alpha [(vD), G^{\nu\lambda}] q \rangle \\ \langle \varepsilon_{\alpha\sigma\lambda\tau} v^\tau v_\nu \bar{q} \gamma_5 \gamma^\alpha [D^\sigma, G^{\nu\lambda}] q \rangle \end{pmatrix} = \begin{pmatrix} 1 & & & \\ & -1 & 2i & 0 \\ & 0 & -i & i \end{pmatrix} \begin{pmatrix} 0 \\ \langle \bar{q} \not{v} \sigma^{\nu\lambda} [(vD), G_{\nu\lambda}] q \rangle \\ \langle \bar{q} \gamma^\lambda [(vD), G_{\nu\lambda}] v^\nu q \rangle \\ g \langle \bar{q} \not{v} t^A q \sum_f \bar{f} \not{v} t^A f \rangle \end{pmatrix}. \quad (\text{C.61})$$

(iv) The decomposition of (e4) does vanish, when contracted with the Dirac trace result of the OPE.

(v) The fifth EV (e5) decomposes into vacuum- and medium-specific terms as

$$\begin{aligned} \langle \langle \bar{q} \overleftrightarrow{D}_\mu \gamma_5 \gamma_\alpha G_{\nu\lambda} q \rangle \rangle_0 &= -\frac{1}{24} \varepsilon_{\mu\alpha\nu\lambda} \langle \langle \varepsilon_{\mu'\alpha'\nu'\lambda'} \bar{q} \overleftrightarrow{D}^{\mu'} \gamma_5 \gamma^{\alpha'} G^{\nu'\lambda'} q \rangle \rangle, \\ \langle \langle \bar{q} \overleftrightarrow{D}_\mu \gamma_5 \gamma_\alpha G_{\nu\lambda} q \rangle \rangle_1 &= -\frac{1}{192} \begin{pmatrix} \varepsilon_{\mu\alpha\nu\lambda} - \frac{4}{v^2} \varepsilon_{\mu\nu\lambda\tau} v^\tau v_\alpha \\ -\varepsilon_{\mu\alpha\nu\lambda} - \frac{4}{v^2} \varepsilon_{\mu\alpha\lambda\tau} v^\tau v_\nu - (\varepsilon_{\mu\alpha\nu\lambda} - \frac{4}{v^2} \varepsilon_{\mu\alpha\nu\tau} v^\tau v_\lambda) \end{pmatrix}^T \begin{pmatrix} 4 & -2 \\ -2 & 3 \end{pmatrix} \\ &\times \begin{pmatrix} \langle \langle \varepsilon_{\mu'\alpha'\nu'\lambda'} \bar{q} \overleftrightarrow{D}^{\mu'} \gamma_5 \gamma^{\alpha'} G^{\nu'\lambda'} q \rangle - \frac{4}{v^2} \varepsilon_{\mu'\nu'\lambda'\tau'} v^{\tau'} \bar{q} \overleftrightarrow{D}^{\mu'} \gamma_5 \not{v} G^{\nu'\lambda'} q \rangle \rangle \\ 2 \langle \langle -\varepsilon_{\mu'\alpha'\nu'\lambda'} \bar{q} \overleftrightarrow{D}^{\mu'} \gamma_5 \gamma^{\alpha'} G^{\nu'\lambda'} q - \frac{4}{v^2} \varepsilon_{\mu'\alpha'\lambda'\tau'} v^{\tau'} v_{\nu'} \bar{q} \overleftrightarrow{D}^{\mu'} \gamma_5 \gamma^{\alpha'} G^{\nu'\lambda'} q \rangle \rangle \end{pmatrix}, \end{aligned} \quad (\text{C.63})$$

where only the part anti-symmetric in the index pair  $\nu\lambda$  contributes to the (axial-)vector OPE. Transformation to canonical condensates yields

$$\begin{pmatrix} \langle \varepsilon_{\mu\alpha\nu\lambda} \bar{q} \overleftrightarrow{D}^\mu \gamma_5 \gamma^\alpha G^{\nu\lambda} q \rangle \\ \langle \varepsilon_{\mu\nu\lambda\tau} v^\tau \bar{q} \overleftrightarrow{D}^\mu \gamma_5 \not{v} G^{\nu\lambda} q \rangle \\ \langle \varepsilon_{\mu\alpha\lambda\tau} v^\tau v_\nu \bar{q} \overleftrightarrow{D}^\mu \gamma_5 \gamma^\alpha G^{\nu\lambda} q \rangle \end{pmatrix} = \begin{pmatrix} i & & \\ & 1 & 0 \\ & 0 & i \end{pmatrix} \begin{pmatrix} m_q \langle \bar{q} \sigma G q \rangle + g \langle \bar{q} \gamma^\mu t^A q \sum_f \bar{f} \gamma_\mu t^A f \rangle \\ \langle \varepsilon_{\mu\nu\lambda\tau} v^\tau \bar{q} \overleftrightarrow{D}^\mu \gamma_5 \not{v} G^{\nu\lambda} q \rangle \\ m_q \langle \bar{q} v_\mu \sigma^{\mu\nu} G_{\nu\lambda} v^\lambda q \rangle - \frac{1}{2} g \langle \bar{q} \not{v} t^A q \sum_f \bar{f} \not{v} t^A f \rangle - \langle \bar{q} (v \overleftrightarrow{D}) \gamma^\nu G_{\nu\lambda} v^\lambda q \rangle \end{pmatrix}. \quad (\text{C.64})$$

Gathering the vacuum constraints as vanishing medium-specific condensates of the decompositions (C.54), (C.57), (C.60) and (C.63) in terms of canonical condensates yields

$$\begin{aligned} 0 &= \langle \Omega | g^2 \bar{q} \gamma^\mu t^A q \sum_f \bar{f} \gamma_\mu t^A f + 2m_q \bar{q} g \sigma G q - 4m_q^3 \bar{q} q - \frac{2}{v^2} \left( g^2 \bar{q} \not{v} t^A q \sum_f \bar{f} \not{v} t^A f \right. \\ &\quad \left. - 2\bar{q} (v \overleftrightarrow{D}) g \sigma G \not{v} q + 4m_q^2 \bar{q} (v \overleftrightarrow{D}) \not{v} q - 4m_q \bar{q} (v \overleftrightarrow{D})^2 q + 6g \bar{q} (v \overleftrightarrow{D}) \gamma^\mu G_{\nu\mu} v^\nu q \right) | \Omega \rangle, \end{aligned} \quad (\text{C.65a})$$

$$0 = \langle \Omega | m_q \bar{q} g \sigma G q - 2m_q^3 \bar{q} q - \frac{4}{v^2} \left( -\bar{q} (v i \overleftrightarrow{D}) g \sigma G \not{q} + 2m_q^2 \bar{q} (v i \overleftrightarrow{D}) \not{q} \right) | \Omega \rangle, \quad (\text{C.65b})$$

$$0 = \langle \Omega | m_q \bar{q} g \sigma G q - 2m_q^3 \bar{q} q + \frac{8}{v^2} m_q \bar{q} (v i \overleftrightarrow{D})^2 q | \Omega \rangle, \quad (\text{C.65c})$$

$$0 = \langle \Omega | g^2 \bar{q} \gamma^\mu t^A q \sum_f \bar{f} \gamma_\mu t^A f + 3m_q \bar{q} g \sigma G q - 6m_q^3 \bar{q} q - \frac{48}{v^4} \bar{q} (v i \overleftrightarrow{D})^3 \not{q} | \Omega \rangle, \quad (\text{C.65d})$$

$$0 = \langle \Omega | g \bar{q} \gamma^\mu t^A q \sum_f \bar{f} \gamma_\mu t^A f - \frac{2}{v^2} \left( \bar{q} \gamma^\mu [(v D), G_{\mu\nu}] v^\nu q + g \bar{q} \not{t}^A q \sum_f \bar{f} \not{t}^A f \right) | \Omega \rangle, \quad (\text{C.65e})$$

$$0 = \langle \Omega | g \bar{q} \not{t}^A q \sum_f \bar{f} \not{t}^A f + \bar{q} \gamma^\mu [(v D), G_{\mu\nu}] v^\nu q + \bar{q} \not{t}^A \sigma^{\nu\lambda} [(v D), G_{\nu\lambda}] q | \Omega \rangle, \quad (\text{C.65f})$$

$$0 = \langle \Omega | 3g^2 \bar{q} \gamma^\mu t^A q \sum_f \bar{f} \gamma_\mu t^A f + 3m_q \bar{q} g \sigma G q - \frac{4}{v^2} \left( -g \varepsilon_{\mu\nu\lambda\tau} v^\tau \bar{q} i \overleftrightarrow{D}^\mu \gamma_5 \not{t}^A q \right. \\ \left. - 2g m_q \bar{q} v_\mu \sigma^{\mu\nu} G_{\nu\lambda} v^\lambda q + g^2 \bar{q} \not{t}^A q \sum_f \bar{f} \not{t}^A f + 2g \bar{q} (v \overleftrightarrow{D}) \gamma^\lambda G_{\nu\lambda} v^\nu q \right) | \Omega \rangle. \quad (\text{C.65g})$$

Equations (C.65) relate the known ground state EVs of vacuum operators, e. g.  $\langle \Omega | \bar{q} q | \Omega \rangle$ ,  $\langle \Omega | \bar{q} g \sigma G q | \Omega \rangle$  and  $g^2 \langle \Omega | \bar{q} \gamma^\mu t^A q \sum_f \bar{f} \gamma_\mu t^A f | \Omega \rangle$ , or the known components of medium-specific condensates up to mass dimension 5, i. e.  $\langle \Omega | \bar{q} (v i \overleftrightarrow{D}) \not{q} | \Omega \rangle$  and  $\langle \Omega | \bar{q} (v i \overleftrightarrow{D})^2 q | \Omega \rangle$ , to heretofore unknown ground state EVs of components of medium-specific condensates in mass dimension 6, e. g. the medium four-quark condensate  $g^2 \langle \Omega | \bar{q} \not{t}^A q \sum_f \bar{f} \not{t}^A f | \Omega \rangle / v^2$ . We therefore solve the above system of linear equations for the unknown condensates.

The system of equations is underdetermined, thus, the solution is not unique. In fact, the relation between vacuum and medium four-quark condensate can be tuned this way. The ground state EVs of non-vacuum operators of mass dimension 6 deduced from the algebraic vacuum constraints, where we choose

$$g^2 \langle \Omega | \bar{q} \not{t}^A q \sum_f \bar{f} \not{t}^A f | \Omega \rangle / v^2 = x_q, \quad (\text{C.66a})$$

$$g \langle \Omega | m_q \bar{q} v_\mu \sigma^{\mu\nu} G_{\nu\lambda} v^\lambda q | \Omega \rangle / v^2 = y_q \quad (\text{C.66b})$$

to be the free parameters of the solution of the system of equations (C.65), read

$$g \langle \Omega | \bar{q} (v i \overleftrightarrow{D}) \sigma G \not{q} | \Omega \rangle / v^2 = \frac{1}{4} \left( 4m_q^3 \langle \Omega | \bar{q} q | \Omega \rangle - m_q \langle \Omega | \bar{q} g \sigma G q | \Omega \rangle \right), \quad (\text{C.67a})$$

$$g \langle \Omega | \bar{q} (v i \overleftrightarrow{D}) \gamma^\mu G_{\nu\mu} v^\nu q | \Omega \rangle / v^2 = \frac{1}{12} \left( g^2 \langle \Omega | \bar{q} \gamma^\mu t^A q \sum_f \bar{f} \gamma_\mu t^A f | \Omega \rangle - 2x_q \right), \quad (\text{C.67b})$$

$$g \langle \Omega | \bar{q} \gamma^\mu [(v D), G_{\mu\nu}] v^\nu q | \Omega \rangle / v^2 = \frac{1}{2} \left( g^2 \langle \Omega | \bar{q} \gamma^\mu t^A q \sum_f \bar{f} \gamma_\mu t^A f | \Omega \rangle - 2x_q \right), \quad (\text{C.67c})$$

$$g \langle \Omega | \bar{q} \not{t}^A \sigma^{\nu\lambda} [(v i D), G_{\nu\lambda}] q | \Omega \rangle / v^2 = \frac{1}{2} \left( g^2 \langle \Omega | \bar{q} \gamma^\mu t^A q \sum_f \bar{f} \gamma_\mu t^A f | \Omega \rangle - 4x_q \right), \quad (\text{C.67d})$$

$$g\langle\Omega|\varepsilon_{\mu\nu\lambda\tau}v^\tau\bar{q}i\overleftarrow{D}^\mu\gamma_5\not{p}G^{\nu\lambda}q|\Omega\rangle/v^2 = \frac{1}{12}\left(6m_q^3\langle\Omega|\bar{q}q|\Omega\rangle - 8m_q\langle\Omega|\bar{q}g\sigma Gq|\Omega\rangle - 7g^2\langle\Omega|\bar{q}\gamma^\mu t^A q\sum_f\bar{f}\gamma_\mu t^A f|\Omega\rangle + 8x_q - 24y_q\right), \quad (\text{C.67e})$$

$$\langle\Omega|\bar{q}(vi\overleftarrow{D})^3\not{p}q|\Omega\rangle/v^4 = \frac{1}{48}\left(-6m_q^3\langle\Omega|\bar{q}q|\Omega\rangle + 3m_q\langle\Omega|\bar{q}g\sigma Gq|\Omega\rangle + g^2\langle\Omega|\bar{q}\gamma^\mu t^A q\sum_f\bar{f}\gamma_\mu t^A f|\Omega\rangle\right), \quad (\text{C.67f})$$

where the vacuum constraints

$$\langle\Omega|\bar{q}(vi\overleftarrow{D})\not{p}q|\Omega\rangle/v^2 = -\frac{1}{4}m_q\langle\Omega|\bar{q}q|\Omega\rangle, \quad (\text{C.68})$$

$$\langle\Omega|\bar{q}(vi\overleftarrow{D})^2q|\Omega\rangle/v^2 = -\frac{1}{8}\langle\Omega|\bar{q}g\sigma Gq|\Omega\rangle + \frac{1}{4}m_q^2\langle\Omega|\bar{q}q|\Omega\rangle \quad (\text{C.69})$$

from mass dimension-4 and -5 condensates have been used, respectively. The same solution holds in the light chiral limit  $m_q \rightarrow 0$ .

(vi) Gibbs averaged light four-quark operators (e6) and (e7) from the NLO correlator decompose into vacuum- and medium-specific terms as

$$\langle\langle\bar{q}\Gamma'\gamma_\mu T^A q\bar{q}'\Gamma'\gamma_\nu T^A q'\rangle\rangle_0 = \frac{1}{4}g_{\mu\nu}\langle\langle\bar{q}\Gamma'\gamma^{\mu'} T^A q\bar{q}'\Gamma'\gamma_{\mu'} T^A q'\rangle\rangle, \quad (\text{C.70})$$

$$\begin{aligned} \langle\langle\bar{q}\Gamma'\gamma_\mu T^A q\bar{q}'\Gamma'\gamma_\nu T^A q'\rangle\rangle_1 &= \frac{1}{12}\left(g_{\mu\nu} - \frac{4}{v^2}v_\mu v_\nu\right) \\ &\times \langle\langle\bar{q}\Gamma'\gamma^{\mu'} T^A q\bar{q}'\Gamma'\gamma_{\mu'} T^A q' - \frac{4}{v^2}\bar{q}\Gamma'\not{v}T^A q\bar{q}'\Gamma'\not{v}T^A q'\rangle\rangle, \end{aligned} \quad (\text{C.71})$$

where  $\Gamma'$  denotes either  $\mathbb{1}_4$  or  $\gamma_5$ . These condensates originating from two cut quark lines in the corresponding diagram of the NLO correlator are already in canonical form, cf. Fig. 3.3.

The vacuum constraints from vanishing medium-specific condensates (C.71) read

$$\langle\Omega|\bar{q}\Gamma'\not{p}T^A q\bar{q}'\Gamma'\not{p}T^A q'|\Omega\rangle/v^2 = \frac{1}{4}\langle\Omega|\bar{q}\Gamma'\gamma^\mu T^A q\bar{q}'\Gamma'\gamma_\mu T^A q'|\Omega\rangle \quad (\text{C.72})$$

which completes the list of Eqs.(C.67) for light-quark condensates. They confine the arbitrary parameter  $x_q$  in (C.67), i.e. Eq. (C.72) with  $\Gamma' = \mathbb{1}_4$  and  $T^A = t^A$  determines the relation between light four-quark condensates in vacuum and medium, such that  $x_q = \frac{1}{4}\langle\Omega|\bar{q}\gamma^\mu t^A q\sum_f\bar{f}\gamma_\mu t^A f|\Omega\rangle$  must be used in the above vacuum constraints (C.67) leading to a zero ground state EV in (C.67d).

This is a general result providing vacuum values for non-vacuum condensates. It is deduced only from the requirement of a continuous transition to vacuum terms when 'turning off the medium',  $\rho \rightarrow 0$ .

Vacuum constraints of the even OPE of  $qQ$  meson currents can be deduced from the results presented here. Besides Gibbs averaged light-quark operators also heavy-quark operators and such quantities containing both kinds of quark operators enter the OPE of  $qQ$  mesons. The Gibbs averages (e1)–(e5) are supplemented by similar contributions, where



$\bar{q}\bar{D}_\mu \cdots q \longrightarrow \bar{Q} \cdots D_\mu Q$ . The four-quark terms (e6) and (e7) are substituted by similar contributions where one  $\bar{q} \cdots q$  pair is changed for one  $\bar{Q} \cdots Q$  pair.

The decompositions of the heavy-quark terms and their vacuum constraints originating from the LO correlator can be obtained by  $q \longrightarrow Q$  in (C.54)–(C.69), where this substitution also refers to subscripts, e. g. further parameters enter the heavy-quark vacuum constraints,  $x_Q$  and  $y_Q$ , which are absent in a light-quark current OPE. The decomposition of the heavy-light four-quark terms originating from the NLO correlator can be obtained by the exchange of one quark pair  $\bar{q} \cdots q \longrightarrow \bar{Q} \cdots Q$  in (C.70)–(C.72). This substitution in Eq. (C.72) fixes the parameter  $x_Q = \frac{1}{4} \langle \Omega | \bar{Q} \gamma^\mu t^A Q \sum_f \bar{f} \gamma_\mu t^A f | \Omega \rangle$ .

A subtlety may be mentioned regarding the parameter  $x_q$  in  $qQ$  meson OPEs. Since no light four-quark terms (e6) and (e7) but exclusively corresponding four-quark terms containing heavy-quark and light-quark pairs enter such OPEs,  $x_q$  can not be determined by the  $qQ$  meson OPE alone. However, the assumed universality of condensates requires identical behavior of identical condensates in different OPEs. Thus, the light current OPE fixes the parameter  $x_q$  also in a heavy-light current OPE.

### Odd OPE

In vacuum, the Lorentz-odd OPE is always zero. Hence,  $\langle\langle O \rangle\rangle_0 = 0$  for all Lorentz-odd operators.

(i) The first EV (o1) decomposes as

$$\langle\langle \bar{q} \bar{D}_\mu \bar{D}_\nu \bar{D}_\lambda q \rangle\rangle = \frac{1}{3v^2} \begin{pmatrix} v_\mu g_{\nu\lambda} \\ v_\nu g_{\mu\lambda} \\ v_\lambda g_{\mu\nu} \\ \frac{1}{v^2} v_\mu v_\nu v_\lambda \end{pmatrix}^T \begin{pmatrix} 1 & 0 & 0 & -1 \\ 0 & 1 & 0 & -1 \\ 0 & 0 & 1 & -1 \\ -1 & -1 & -1 & 6 \end{pmatrix} \begin{pmatrix} \langle\langle \bar{q}(v\bar{D})\bar{D}^2 q \rangle\rangle \\ \langle\langle \bar{q}\bar{D}^{\mu'}(v\bar{D})\bar{D}_{\mu'} q \rangle\rangle \\ \langle\langle \bar{q}\bar{D}^2(v\bar{D})q \rangle\rangle \\ \frac{1}{v^2} \langle\langle \bar{q}(v\bar{D})^3 q \rangle\rangle \end{pmatrix}, \quad (\text{C.73})$$

where only the combination  $\langle\langle \bar{q}(v\bar{D})\bar{D}^2 q + 2\bar{q}\bar{D}^\mu(v\bar{D})\bar{D}_\mu q + \bar{q}\bar{D}^2(v\bar{D})q \rangle\rangle$  and the single term  $\langle\langle \bar{q}(v\bar{D})^3 q \rangle\rangle/v^2$  enter the (axial-)vector OPE. Transformation to canonical condensates yields

$$\begin{pmatrix} \langle\langle \bar{q}(v\bar{D})\bar{D}^2 q \rangle\rangle \\ \langle\langle \bar{q}\bar{D}^\mu(v\bar{D})\bar{D}_\mu q \rangle\rangle \\ \langle\langle \bar{q}\bar{D}^2(v\bar{D})q \rangle\rangle \\ \frac{1}{v^2} \langle\langle \bar{q}(v\bar{D})^3 q \rangle\rangle \end{pmatrix} = \begin{pmatrix} 0 & 1 & 0 & 0 \\ \frac{i}{2} & 1 & 0 & 0 \\ 0 & 0 & 1 & 0 \\ 0 & 0 & 0 & 1 \end{pmatrix} \begin{pmatrix} g^2 \langle\bar{q} t^A q \sum_f \bar{f} \phi t^A f \rangle \\ \frac{g}{2} \langle\bar{q}(v\bar{D})\sigma G q \rangle - m_q^2 \langle\bar{q}(v\bar{D})q \rangle \\ \frac{g}{2} \langle\bar{q}\sigma G(v\bar{D})q \rangle - m_q^2 \langle\bar{q}(v\bar{D})q \rangle \\ \frac{1}{v^2} \langle\bar{q}(v\bar{D})^3 q \rangle \end{pmatrix}. \quad (\text{C.74})$$

(ii) The second EV (o2) decomposes as

$$\langle\langle \bar{q}[D_\sigma, G_{\nu\lambda}]q \rangle\rangle = \frac{1}{3v^2} (v_\nu g_{\sigma\lambda} - v_\lambda g_{\sigma\nu}) \langle\langle \bar{q}[D^{\mu'}, G_{\nu'\mu'}]v^{\nu'} q \rangle\rangle, \quad (\text{C.75})$$

where only the part anti-symmetric in  $\nu\lambda$  enters the (axial-)vector OPE. Transformation to

a canonical condensate yields

$$\langle \bar{q}[D^\mu, G_{\nu\mu}]v^\nu q \rangle = g \langle \bar{q}t^A q \sum_f \bar{f}\psi t^A f \rangle. \quad (\text{C.76})$$

(iii) The third EV (o3) decomposes as

$$\begin{aligned} & \langle \langle \bar{q}\sigma_{\alpha\beta}[D_\sigma, G_{\nu\lambda}]q \rangle \rangle \\ &= \frac{1}{6v^2} \begin{pmatrix} v_\alpha g_{\beta\nu} g_{\sigma\lambda} - v_\alpha g_{\beta\lambda} g_{\sigma\nu} - v_\beta g_{\alpha\nu} g_{\sigma\lambda} + v_\beta g_{\alpha\lambda} g_{\sigma\nu} \\ v_\sigma (g_{\alpha\nu} g_{\beta\lambda} - g_{\alpha\lambda} g_{\beta\nu}) \\ v_\nu g_{\alpha\sigma} g_{\beta\lambda} - v_\lambda g_{\alpha\sigma} g_{\beta\nu} + v_\lambda g_{\alpha\nu} g_{\beta\sigma} - v_\nu g_{\alpha\lambda} g_{\beta\sigma} \\ \frac{1}{v^2} (v_\alpha v_\sigma v_\nu g_{\beta\lambda} - v_\alpha v_\sigma v_\lambda g_{\beta\nu} - v_\beta v_\sigma v_\nu g_{\alpha\lambda} + v_\beta v_\sigma v_\lambda g_{\alpha\nu}) \end{pmatrix}^T \\ & \times \begin{pmatrix} 1 & 0 & 0 & -1 \\ 0 & 2 & 0 & -2 \\ 0 & 0 & 1 & -1 \\ -1 & -2 & -1 & 6 \end{pmatrix} \begin{pmatrix} \langle \bar{q}v_{\alpha'}\sigma^{\alpha'\nu'}[D^{\lambda'}, G_{\nu'\lambda'}]q \rangle \\ \frac{1}{2} \langle \bar{q}\sigma^{\nu'\lambda'}[(vD), G_{\nu'\lambda'}]q \rangle \\ \langle \bar{q}\sigma^{\sigma'\lambda'}[D_{\sigma'}, G_{\nu'\lambda'}]v^{\nu'}q \rangle \\ \frac{1}{v^2} \langle \bar{q}v_{\alpha'}\sigma^{\alpha'\lambda'}[(vD), G_{\nu'\lambda'}]v^{\nu'}q \rangle \end{pmatrix}, \quad (\text{C.77}) \end{aligned}$$

where only the combination  $\langle \bar{q}\sigma^{\nu\lambda}[(vD), G_{\nu\lambda}]q + \bar{q}\sigma^{\sigma\lambda}[D_\sigma, G_{\nu\lambda}]v^\nu q \rangle$  enters the (pseudo-) scalar OPE. Application of the gluon EoM (A.19) to the first condensate in (C.77) yields the four-quark condensate  $\langle \bar{q}v_\alpha\sigma^{\alpha\nu}t^A q \sum_f \bar{f}\gamma_\nu t^A f \rangle$  which is not invariant under parity and time reversal transformations. The other condensates in (C.77) cannot be reduced by EoMs.

(iv) The forth EV (o4) decomposes as

$$\langle \bar{q}\overleftarrow{D}_\mu G_{\nu\lambda} q \rangle = \frac{1}{3v^2} (v_\nu g_{\mu\lambda} - v_\lambda g_{\mu\nu}) \langle \bar{q}\overleftarrow{D}^{\mu'} G_{\nu'\mu'} v^{\nu'} q \rangle, \quad (\text{C.78})$$

where only the part anti-symmetric in  $\nu\lambda$  enters the (axial-)vector OPE. Transformation to a canonical condensate yields

$$\langle \bar{q}\overleftarrow{D}^\mu G_{\nu\mu} v^\nu q \rangle = \frac{g}{2} \langle \bar{q}t^A q \sum_f \bar{f}\psi t^A f \rangle. \quad (\text{C.79})$$

(v) The fifth EV (o5) decomposes as

$$\begin{aligned} & \langle \langle \bar{q}\overleftarrow{D}_\mu \sigma_{\alpha\beta} G_{\nu\lambda} q \rangle \rangle \\ &= \frac{1}{6v^2} \begin{pmatrix} v_\alpha g_{\beta\nu} g_{\mu\lambda} - v_\alpha g_{\beta\lambda} g_{\mu\nu} - v_\beta g_{\alpha\nu} g_{\mu\lambda} + v_\beta g_{\alpha\lambda} g_{\mu\nu} \\ v_\mu (g_{\alpha\nu} g_{\beta\lambda} - g_{\alpha\lambda} g_{\beta\nu}) \\ v_\nu g_{\alpha\mu} g_{\beta\lambda} - v_\lambda g_{\alpha\mu} g_{\beta\nu} + v_\lambda g_{\alpha\nu} g_{\beta\mu} - v_\nu g_{\alpha\lambda} g_{\beta\mu} \\ \frac{1}{v^2} (v_\alpha v_\mu v_\nu g_{\beta\lambda} - v_\alpha v_\mu v_\lambda g_{\beta\nu} - v_\beta v_\mu v_\nu g_{\alpha\lambda} + v_\beta v_\mu v_\lambda g_{\alpha\nu}) \end{pmatrix}^T \end{aligned}$$

$$\times \begin{pmatrix} 1 & 0 & 0 & -1 \\ 0 & 2 & 0 & -2 \\ 0 & 0 & 1 & -1 \\ -1 & -2 & -1 & 6 \end{pmatrix} \begin{pmatrix} \langle \bar{q} \overleftrightarrow{D}^{\lambda'} v_{\alpha'} \sigma^{\alpha' \nu'} G_{\nu' \lambda'} q \rangle \\ \frac{1}{2} \langle \bar{q} (v \overleftrightarrow{D}) \sigma G q \rangle \\ \langle \bar{q} \overleftrightarrow{D}_{\alpha'} \sigma^{\sigma' \lambda'} G_{\nu' \lambda'} v^{\nu'} q \rangle \\ \frac{1}{v^2} \langle \bar{q} (v \overleftrightarrow{D}) v_{\alpha'} \sigma^{\alpha' \lambda'} G_{\nu' \lambda'} v^{\nu'} q \rangle \end{pmatrix}, \quad (\text{C.80})$$

where only the term containing  $\langle \bar{q} (v \overleftrightarrow{D}) \sigma G q \rangle$  enters the (pseudo-)scalar OPE. Application of gluon EoM (A.19) to the first condensate in (C.80) yields  $\langle \bar{q} v_{\alpha} \sigma^{\alpha \nu} t^A q \sum_f \bar{f} \gamma_{\nu} t^A f \rangle$  which is not invariant under parity and time reversal transformations. The other condensates in (C.80) cannot be reduced by EoM.

The OPE relevant combinations of condensates of the odd OPE must vanish in vacuum, thus forming the algebraic vacuum constraints:

$$0 = \frac{i}{2} g^2 \langle \Omega | \bar{q} t^A q \sum_f \bar{f} \not{t}^A f | \Omega \rangle + g \langle \Omega | \bar{q} (v \overleftrightarrow{D}) \sigma G q | \Omega \rangle + \frac{1}{2} g \langle \Omega | \bar{q} \sigma G (v \overleftrightarrow{D}) q | \Omega \rangle - 3m_q^2 \langle \Omega | \bar{q} (v \overleftrightarrow{D}) q | \Omega \rangle, \quad (\text{C.81a})$$

$$0 = \langle \Omega | \bar{q} (v \overleftrightarrow{D})^3 q | \Omega \rangle, \quad (\text{C.81b})$$

$$0 = g \langle \Omega | \bar{q} t^A q \sum_f \bar{f} \not{t}^A f | \Omega \rangle, \quad (\text{C.81c})$$

$$0 = \langle \Omega | \bar{q} \sigma^{\mu \nu} [(v D), G_{\mu \nu}] q | \Omega \rangle + \langle \Omega | \bar{q} \sigma^{\mu \lambda} [D_{\mu}, G_{\nu \lambda}] v^{\nu} q | \Omega \rangle, \quad (\text{C.81d})$$

$$0 = \langle \Omega | \bar{q} (v \overleftrightarrow{D}) \sigma G q | \Omega \rangle. \quad (\text{C.81e})$$

Therefore, the condensates in (C.81) must vanish individually in vacuum except the condensates in (C.81d) which need to cancel each other. Vanishing of the condensates in (C.81a) is ensured due to (C.81c), (C.81e) and  $\langle \Omega | \bar{q} (v \overleftrightarrow{D}) q | \Omega \rangle = -im_q \langle \Omega | \bar{q} \not{v} q | \Omega \rangle$ , where the latter condensate is a medium-specific condensate in mass dimension 4 with a zero vacuum value.

(vi) From the NLO correlator further Gibbs averaged light-quark operators (o6) and (o7) contribute in order  $\alpha_s$

$$\langle \bar{q} t^A q \bar{q} \gamma_{\mu} t^A q \rangle = \frac{v_{\mu}}{v^2} \langle \bar{q} t^A q \bar{q} \not{v} t^A q \rangle, \quad (\text{C.82})$$

$$\langle \bar{q} \gamma_5 \gamma^{\mu} t^A q \bar{q} \sigma_{\nu \lambda} t^A q \rangle = -\frac{1}{6} \varepsilon_{\mu \nu \lambda \alpha} \frac{v^{\alpha}}{v^2} \langle \varepsilon^{\mu' \nu' \lambda' \alpha'} v_{\alpha'} \bar{q} \gamma_5 \gamma_{\mu'} t^A q \bar{q} \sigma_{\nu' \lambda'} t^A q \rangle, \quad (\text{C.83})$$

originating from two cut quark lines in the corresponding diagrams, cf. Fig. 3.3. They are already in canonical form and must vanish in vacuum.

Vacuum constraints of the odd OPE of  $qQ$  meson currents can be deduced from the results presented here. Besides Gibbs averaged light-quark operators also heavy-quark operators and such quantities containing both kinds of quark operators enter the OPE of  $qQ$  mesons. The Gibbs averages (o1)–(o5) are supplemented by similar contributions where  $\bar{q} \overleftrightarrow{D}_{\mu} \cdots q \longrightarrow \bar{Q} \cdots D_{\mu} Q$ . The four-quark terms (o6) and (o7) are substituted by similar contributions where one  $\bar{q} \cdots q$  pair is changed for one  $\bar{Q} \cdots Q$  pair. Be aware that, for two-flavor four-quark terms with two different Dirac structures as in (o6) and (o7), the necessary substitution yields two structures for each term.

The decompositions of the heavy-quark terms and their vacuum constraints originating from the LO correlator can be obtained by  $q \rightarrow Q$  in (C.73)–(C.81), where this substitution also refers to subscripts. The decomposition of the heavy-light four-quark terms originating from the NLO correlator can be obtained for the exchange of one quark pair  $\bar{q} \cdots q \rightarrow \bar{Q} \cdots Q$  in (C.82) and (C.83). Analogous to the odd OPE of light-quark currents all heavy-quark condensates must vanish individually for  $\rho \rightarrow 0$ . An exception bears the analog of (C.81d), where both condensates cancel each other.

Note that the odd OPE and, thus, odd condensates drive the mass splitting of particle and anti-particle in the medium. Such splitting may intuitively be understood in an asymmetric ambient strongly interacting medium. First, heavy quarks are hardly generated dynamically (at least compared to light quarks) and hardly condense (directly). Considering a strongly interacting ambient medium consisting mainly of nuclear matter, i. e. light quarks (not anti-quarks), a meson consisting of a heavy quark and a light anti-quark is affected differently than its anti-meson, which consists of a heavy anti-quark and a light quark. Similarly, it seems reasonable to assume that at zero density, meson and anti-meson, e. g.  $D$  and  $\bar{D}$ , are degenerate. As this splitting is driven by the Lorentz-odd OPE, it vanishes at zero baryon density for arbitrary temperatures [Boc86, Hat93, Buc16a].

### C.2.3 Discussion of factorization and ground state saturation hypothesis

The common problem of presently poorly known numerical values of higher mass dimension condensates is often circumvented by a factorization into condensates of lower mass dimension, cf. Subsec. 3.3.3. The non-zero factorization results of light four-quark condensates employed in the decompositions of (e1)–(e5) and (o1)–(o5) read

$$\langle\langle \bar{q} \gamma^\mu t^A q \sum_f \bar{f} \gamma_\mu t^A f \rangle\rangle = -\frac{2}{9} \kappa_0^q(\rho) [2\langle\langle \bar{q} q \rangle\rangle^2 - \langle\langle \bar{q} \not{p} q \rangle\rangle^2 / v^2] , \quad (\text{C.84a})$$

$$\langle\langle \bar{q} \not{p} t^A q \sum_f \bar{f} \not{p} t^A f \rangle\rangle / v^2 = -\frac{1}{9} \kappa_1^q(\rho) [\langle\langle \bar{q} q \rangle\rangle^2 + \langle\langle \bar{q} \not{p} q \rangle\rangle^2 / v^2] , \quad (\text{C.84b})$$

$$\langle\langle \bar{q} t^A q \sum_f \bar{f} \not{p} t^A f \rangle\rangle = -\frac{2}{9} \kappa_2^q(\rho) \langle\langle \bar{q} q \rangle\rangle \langle\langle \bar{q} \not{p} q \rangle\rangle , \quad (\text{C.84c})$$

in full analogy to the expressions given in Tab. 3.3 but with 'fudge factors'  $\kappa_i^q$  in order to streamline the notation in this subsection. Further light four-quark condensates with the Dirac structures in (e6), (e7), (o6) and (o7) factorize as [Jin93]

$$\langle\langle \bar{q} \gamma^\mu t^A q \bar{q} \gamma_\mu t^A q \rangle\rangle = -\frac{2}{9} \kappa_0^q(\rho) [2\langle\langle \bar{q} q \rangle\rangle^2 - \langle\langle \bar{q} \not{p} q \rangle\rangle^2 / v^2] , \quad (\text{C.85a})$$

$$\langle\langle \bar{q} \not{p} t^A q \bar{q} \not{p} t^A q \rangle\rangle / v^2 = -\frac{1}{9} \kappa_1^q(\rho) [\langle\langle \bar{q} q \rangle\rangle^2 + \langle\langle \bar{q} \not{p} q \rangle\rangle^2 / v^2] , \quad (\text{C.85b})$$

$$\langle\langle \bar{q} t^A q \bar{q} \not{p} t^A q \rangle\rangle = -\frac{2}{9} \kappa_2^q(\rho) \langle\langle \bar{q} q \rangle\rangle \langle\langle \bar{q} \not{p} q \rangle\rangle , \quad (\text{C.85c})$$

$$\langle\langle \bar{q} \gamma_5 \gamma^\mu t^A q \bar{q} \gamma_5 \gamma_\mu t^A q \rangle\rangle = \frac{2}{9} \kappa_3^q(\rho) [2\langle\langle \bar{q} q \rangle\rangle^2 + \langle\langle \bar{q} \not{p} q \rangle\rangle^2 / v^2] , \quad (\text{C.85d})$$

$$\langle\langle \bar{q} \gamma_5 \not{p} t^A q \bar{q} \gamma_5 \not{p} t^A q \rangle\rangle / v^2 = \frac{1}{9} \kappa_4^q(\rho) [\langle\langle \bar{q} q \rangle\rangle^2 - \langle\langle \bar{q} \not{p} q \rangle\rangle^2 / v^2] , \quad (\text{C.85e})$$

$$\langle\langle \varepsilon^{\mu\nu\lambda\alpha} v_\alpha \bar{q} \gamma_5 \gamma_\mu t^A q \bar{q} \sigma_{\nu\lambda} t^A q \rangle\rangle = -\frac{16}{3} \kappa_5^q(\rho) \langle\langle \bar{q} q \rangle\rangle \langle\langle \bar{q} \not{p} q \rangle\rangle, \quad (\text{C.85f})$$

$$\langle\langle \bar{q} \gamma^\mu q \bar{q} \gamma_\mu q \rangle\rangle = -\frac{1}{6} \kappa_6^q(\rho) [2\langle\langle \bar{q} q \rangle\rangle^2 - 7\langle\langle \bar{q} \not{p} q \rangle\rangle^2 / v^2], \quad (\text{C.85g})$$

$$\langle\langle \bar{q} \not{p} q \bar{q} \not{p} q \rangle\rangle / v^2 = -\frac{1}{12} \kappa_7^q(\rho) [\langle\langle \bar{q} q \rangle\rangle^2 - 11\langle\langle \bar{q} \not{p} q \rangle\rangle^2 / v^2], \quad (\text{C.85h})$$

$$\langle\langle \bar{q} q \bar{q} \not{p} q \rangle\rangle = \frac{11}{12} \kappa_8^q(\rho) \langle\langle \bar{q} q \rangle\rangle \langle\langle \bar{q} \not{p} q \rangle\rangle, \quad (\text{C.85i})$$

$$\langle\langle \bar{q} \gamma_5 \gamma^\mu q \bar{q} \gamma_5 \gamma_\mu q \rangle\rangle = \frac{1}{6} \kappa_9^q(\rho) [2\langle\langle \bar{q} q \rangle\rangle^2 + \langle\langle \bar{q} \not{p} q \rangle\rangle^2 / v^2], \quad (\text{C.85j})$$

$$\langle\langle \bar{q} \gamma_5 \not{p} q \bar{q} \gamma_5 \not{p} q \rangle\rangle / v^2 = \frac{1}{12} \kappa_{10}^q(\rho) [\langle\langle \bar{q} q \rangle\rangle^2 - \langle\langle \bar{q} \not{p} q \rangle\rangle^2 / v^2], \quad (\text{C.85k})$$

$$\langle\langle \varepsilon^{\mu\nu\lambda\alpha} v_\alpha \bar{q} \gamma_5 \gamma_\mu q \bar{q} \sigma_{\nu\lambda} q \rangle\rangle = -4 \kappa_{11}^q(\rho) \langle\langle \bar{q} q \rangle\rangle \langle\langle \bar{q} \not{p} q \rangle\rangle. \quad (\text{C.85l})$$

For condensates composed of heavy- and light-quark operators with the Dirac structures in (e6), (e7), (o6) and (o7) containing the unit elements  $T^0 = \mathbb{1}_3$  as color structures one obtains [Jin93]

$$\langle\langle \bar{q} \gamma_\mu q \bar{Q} \gamma^\mu Q \rangle\rangle = \kappa_0^Q(\rho) [\langle\langle \bar{q} q \rangle\rangle \langle\langle \bar{Q} Q \rangle\rangle + \langle\langle \bar{q} \not{p} q \rangle\rangle \langle\langle \bar{Q} \not{p} Q \rangle\rangle / v^2], \quad (\text{C.86a})$$

$$\langle\langle \bar{q} \not{p} q \bar{Q} \not{p} Q \rangle\rangle / v^2 = \frac{1}{4} \kappa_1^Q(\rho) [\langle\langle \bar{q} q \rangle\rangle \langle\langle \bar{Q} Q \rangle\rangle + 4\langle\langle \bar{q} \not{p} q \rangle\rangle \langle\langle \bar{Q} \not{p} Q \rangle\rangle / v^2], \quad (\text{C.86b})$$

$$\langle\langle \bar{q} q \bar{Q} \not{p} Q \rangle\rangle = \kappa_2^Q(\rho) \langle\langle \bar{q} q \rangle\rangle \langle\langle \bar{Q} \not{p} Q \rangle\rangle, \quad (\text{C.86c})$$

$$\langle\langle \bar{q} \not{p} q \bar{Q} Q \rangle\rangle = \kappa_3^Q(\rho) \langle\langle \bar{q} \not{p} q \rangle\rangle \langle\langle \bar{Q} Q \rangle\rangle, \quad (\text{C.86d})$$

$$\langle\langle \bar{q} \gamma_5 \gamma_\mu q \bar{Q} \gamma_5 \gamma^\mu Q \rangle\rangle = -\kappa_4^Q(\rho) \langle\langle \bar{q} q \rangle\rangle \langle\langle \bar{Q} Q \rangle\rangle, \quad (\text{C.86e})$$

$$\langle\langle \bar{q} \gamma_5 \not{p} q \bar{Q} \gamma_5 \not{p} Q \rangle\rangle / v^2 = -\frac{1}{4} \kappa_5^Q(\rho) \langle\langle \bar{q} q \rangle\rangle \langle\langle \bar{Q} Q \rangle\rangle, \quad (\text{C.86f})$$

$$\langle\langle \varepsilon^{\mu\nu\lambda\alpha} v_\alpha \bar{q} \gamma_5 \gamma_\mu q \bar{Q} \sigma_{\nu\lambda} Q \rangle\rangle = 0, \quad (\text{C.86g})$$

$$\langle\langle \varepsilon^{\mu\nu\lambda\alpha} v_\alpha \bar{q} \sigma_{\mu\nu} q \bar{Q} \gamma_5 \gamma_\lambda Q \rangle\rangle = 0. \quad (\text{C.86h})$$

The same relations hold true for  $Q \rightarrow q'$  providing the factorization formulae for light two-flavor condensates.

In vacuum, where  $\langle\langle \dots \rangle\rangle$  reduces to  $\langle \Omega | \dots | \Omega \rangle$ , the medium-specific two-quark condensate  $\langle\langle \bar{q} \not{p} q \rangle\rangle$  cancels, thus further simplifying above relations and yielding zero factorization results. The vacuum constraint (C.67) from the even OPE, where light four-quark condensates are factorized, provide the following relations:

$$g \langle \Omega | \bar{q} (v i \not{D}) \sigma G \not{p} q | \Omega \rangle / v^2 = \frac{1}{4} \left( 4m_q^3 \langle \Omega | \bar{q} q | \Omega \rangle - m_q \langle \Omega | \bar{q} g \sigma G q | \Omega \rangle \right), \quad (\text{C.87a})$$

$$g \langle \Omega | \bar{q} (v i \not{D}) \gamma^\mu G_{\nu\mu} v^\nu q | \Omega \rangle / v^2 = -\frac{1}{54} \left( 2\kappa_0^q(0) - \kappa_1^q(0) \right) g^2 \langle \Omega | \bar{q} q | \Omega \rangle^2, \quad (\text{C.87b})$$

$$g \langle \Omega | \bar{q} \gamma^\mu [(v D), G_{\mu\nu}] v^\nu q | \Omega \rangle / v^2 = -\frac{1}{9} \left( 2\kappa_0^q(0) - \kappa_1^q(0) \right) g^2 \langle \Omega | \bar{q} q | \Omega \rangle^2, \quad (\text{C.87c})$$

$$g \langle \Omega | \bar{q} \not{p} \sigma^{\nu\lambda} [(v i D), G_{\nu\lambda}] q | \Omega \rangle / v^2 = -\frac{2}{9} \left( \kappa_0^q(0) - \kappa_1^q(0) \right) g^2 \langle \Omega | \bar{q} q | \Omega \rangle^2, \quad (\text{C.87d})$$

$$g\langle\Omega|\varepsilon_{\mu\nu\lambda\tau}v^\tau\bar{q}i\overleftarrow{D}^\mu\gamma_5\not{p}G^{\nu\lambda}q|\Omega\rangle/v^2 = \frac{1}{12}\left(6m_q^3\langle\Omega|\bar{q}q|\Omega\rangle - 8m_q\langle\Omega|\bar{q}g\sigma Gq|\Omega\rangle\right. \\ \left.+ \frac{4}{9}\left(7\kappa_0^q(0) - 2\kappa_1^q(0)\right)g^2\langle\Omega|\bar{q}q|\Omega\rangle^2 - 24y_q\right), \quad (\text{C.87e})$$

$$\langle\Omega|\bar{q}(vi\overleftarrow{D})^3\not{p}q|\Omega\rangle/v^4 = \frac{1}{48}\left(-6m_q^3\langle\Omega|\bar{q}q|\Omega\rangle + 3m_q\langle\Omega|\bar{q}g\sigma Gq|\Omega\rangle\right. \\ \left.- \frac{4}{9}\kappa_0^q(0)g^2\langle\Omega|\bar{q}q|\Omega\rangle^2\right) \quad (\text{C.87f})$$

supplemented by six relations contained in (C.72) (originating from NLO correlator)

$$\kappa_1^q(0) = \kappa_0^q(0), \quad (\text{C.88a})$$

$$\kappa_4^q(0) = \kappa_3^q(0), \quad (\text{C.88b})$$

$$\kappa_7^q(0) = \kappa_6^q(0), \quad (\text{C.88c})$$

$$\kappa_{10}^q(0) = \kappa_9^q(0), \quad (\text{C.88d})$$

$$\kappa_1^{q'}(0) = \kappa_0^{q'}(0), \quad (\text{C.88e})$$

$$\kappa_5^{q'}(0) = \kappa_4^{q'}(0), \quad (\text{C.88f})$$

relating the  $\kappa$  parameters for  $\rho = 0$  and simplifying the factorized algebraic vacuum constraints (C.87), where (C.87d) gives a vanishing ground state EV as can be recognized already in Eqs. (C.67d) and (C.72). The odd OPE vacuum constraints are trivial as the contained four-quark condensates vanish individually in the vacuum.

In  $qQ$  meson OPEs, the vacuum constraints in factorized form are composed of the relations (C.87) as well as these relations with  $\kappa_{0,1}^q = 0$  and  $q \longrightarrow Q$ . The vacuum constraints (C.88) are substituted by

$$\kappa_1^Q(0) = \kappa_0^Q(0), \quad (\text{C.89a})$$

$$\kappa_5^Q(0) = \kappa_4^Q(0). \quad (\text{C.89b})$$

As exhibited in Eqs. (C.87)–(C.89) factorization of four-quark condensates does not violate the algebraic vacuum constraints. Instead, it relates the  $\kappa$  factorization parameters at  $\rho = 0$  and assigns numerical vacuum values to the medium dimension-6 condensates which were previously unknown. Relating them to the known vacuum values of the chiral and the mixed quark-gluon condensate allows for their tentative numerical estimate in vacuum.

#### C.2.4 Equivalence of two approaches to the medium-specific decomposition

One may find the medium-specific decomposition either by subtraction of the algebraic vacuum decomposition (C.29) from the complete in-medium decomposition (C.26) using Eq. (C.30) or by performing the projection procedure for the medium-specific decomposition structures in (C.33) which are orthogonal to the vacuum decomposition structures. Following the former approach we show that utilizing the blockwise inversion of the total projection matrix

$$L_\rho \equiv \left(\vec{l}^{(\rho)} \circ \vec{l}^{(\rho)}\right) = \begin{pmatrix} \left(\vec{l}^{(0)} \circ \vec{l}^{(0)}\right) & \left(\vec{l}^{(0)} \circ \vec{l}^{(\rho_1)}\right) \\ \left(\vec{l}^{(\rho_1)} \circ \vec{l}^{(0)}\right) & \left(\vec{l}^{(\rho_1)} \circ \vec{l}^{(\rho_1)}\right) \end{pmatrix} \equiv \begin{pmatrix} L_0 & L_{0,\rho_1} \\ L_{\rho_1,0} & L_{\rho_1} \end{pmatrix} \quad (\text{C.90})$$

yields the same medium-specific decomposition structures  $\vec{l}_\mu^{(1)}$  as the latter approach based on orthogonality, i. e. the equivalence of both approaches to the medium-specific decomposition. We rearrange Eq. (C.30):

$$\vec{l}_\mu^{(1)} \cdot \vec{a}_1 = \vec{l}_\mu^{(\rho)} \cdot \vec{a}_\rho - \vec{l}_\mu^{(0)} \cdot \vec{a}_0 = \vec{l}_\mu^{(0)} \cdot (\vec{a}_{\rho_0} - \vec{a}_0) + \vec{l}_\mu^{(\rho_1)} \cdot \vec{a}_{\rho_1}. \quad (\text{C.91})$$

Using the projections

$$\vec{a}_0 = L_0^{-1} \vec{l}_\nu^{(0)} \langle O^\nu \rangle, \quad (\text{C.92})$$

$$\vec{a}_\rho = L_\rho^{-1} \vec{l}_\nu^{(\rho)} \langle O^\nu \rangle \quad (\text{C.93})$$

with the sub-matrix definitions<sup>6</sup> of the inverse total projection matrix

$$L_\rho^{-1} = \begin{pmatrix} (L^{-1})_0 & (L^{-1})_{0,\rho_1} \\ (L^{-1})_{\rho_1,0} & (L^{-1})_{\rho_1} \end{pmatrix} \quad (\text{C.94})$$

further decomposed to

$$\vec{a}_{\rho_0} = \left( (L^{-1})_0, (L^{-1})_{0,\rho_1} \right) \vec{l}_\nu^{(\rho)} \langle O^\nu \rangle \quad \text{and} \quad \vec{a}_{\rho_1} = \left( (L^{-1})_{\rho_1,0}, (L^{-1})_{\rho_1} \right) \vec{l}_\nu^{(\rho)} \langle O^\nu \rangle \quad (\text{C.95})$$

yields

$$\begin{aligned} \vec{l}_\mu^{(1)} \cdot \vec{a}_1 &= \vec{l}_\mu^{(0)} \cdot \left[ \left( (L^{-1})_0, (L^{-1})_{0,\rho_1} \right) \vec{l}_\nu^{(\rho)} \langle O^\nu \rangle - L_0^{-1} \vec{l}_\nu^{(0)} \langle O^\nu \rangle \right] + \vec{l}_\mu^{(\rho_1)} \cdot \vec{a}_{\rho_1} \\ &= \vec{l}_\mu^{(0)} \cdot \left[ (L^{-1})_0 - L_0^{-1} \right] \vec{l}_\nu^{(0)} \langle O^\nu \rangle + \vec{l}_\mu^{(0)} \cdot (L^{-1})_{0,\rho_1} \vec{l}_\nu^{(\rho_1)} \langle O^\nu \rangle + \vec{l}_\mu^{(\rho_1)} \cdot \vec{a}_{\rho_1}. \end{aligned} \quad (\text{C.96})$$

The formula for blockwise inversion of matrices with two square sub-matrices  $A$  and  $D$

$$\begin{bmatrix} A & B \\ C & D \end{bmatrix}^{-1} = \begin{bmatrix} A^{-1} + A^{-1} B V C A^{-1} & -A^{-1} B V \\ -V C A^{-1} & V \end{bmatrix} \quad (\text{C.97})$$

with

$$V = (D - C A^{-1} B)^{-1} \quad (\text{C.98})$$

relates the sub-matrices of the inverted matrix. We deploy this formula to the total projection matrix (C.90) and its inverse (C.94) obtaining the relations

$$(L^{-1})_0 = L_0^{-1} + L_0^{-1} L_{0,\rho_1} W L_{\rho_1,0} L_0^{-1}, \quad (\text{C.99})$$

$$(L^{-1})_{0,\rho_1} = -L_0^{-1} L_{0,\rho_1} W, \quad (\text{C.100})$$

$$(L^{-1})_{\rho_1,0} = -W L_{\rho_1,0} L_0^{-1}, \quad (\text{C.101})$$

$$(L^{-1})_{\rho_1} \equiv W = (L_{\rho_1} - L_{\rho_1,0} L_0^{-1} L_{0,\rho_1})^{-1}. \quad (\text{C.102})$$

Identifying the relevant interrelations among the sub-matrices of the inverted projection matrix yields the desired terms

$$(L^{-1})_0 = L_0^{-1} - L_0^{-1} L_{0,\rho_1} (L^{-1})_{\rho_1,0}, \quad (\text{C.103})$$

$$(L^{-1})_{0,\rho_1} = -L_0^{-1} L_{0,\rho_1} (L^{-1})_{\rho_1}. \quad (\text{C.104})$$

<sup>6</sup>Note that  $(L^{-1})_i \neq L_i^{-1}$  for  $i \in \{0; 0, \rho_1; \rho_1, 0; \rho_1\}$ .

Substituting Eqs. (C.103) and (C.104) in Eq. (C.96) yields

$$\vec{l}_\mu^{(1)} \cdot \vec{a}_1 = \vec{l}_\mu^{(0)} \cdot L_0^{-1} L_{0,\rho_1} \left( (L^{-1})_{\rho_1,0}, (L^{-1})_{\rho_1} \right) \vec{l}_\nu^{(\rho)} \langle O^\nu \rangle + \vec{l}_\mu^{(\rho_1)} \cdot \vec{a}_{\rho_1}. \quad (\text{C.105})$$

Using Eq. (C.95) we arrive at

$$\vec{l}_\mu^{(1)} \cdot \vec{a}_1 = -\vec{l}_\mu^{(0)} \cdot L_0^{-1} L_{0,\rho_1} \vec{a}_{\rho_1} + \vec{l}_\mu^{(\rho_1)} \cdot \vec{a}_{\rho_1}. \quad (\text{C.106})$$

Providing the first term in matrix notation

$$\vec{l}_\mu^{(1)} \cdot \vec{a}_1 = -\left( \vec{l}_\mu^{(0)} \right)^T L_0^{-1} L_{0,\rho_1} \vec{a}_{\rho_1} + \vec{l}_\mu^{(\rho_1)} \cdot \vec{a}_{\rho_1} = -\left( L_{\rho_1,0} L_0^{-1} \vec{l}_\mu^{(0)} \right)^T \vec{a}_{\rho_1} + \vec{l}_\mu^{(\rho_1)} \cdot \vec{a}_{\rho_1} \quad (\text{C.107})$$

finally yields

$$\vec{l}_\mu^{(1)} \cdot \vec{a}_1 = \left[ L_{\rho_1,0} L_0^{-1} \vec{l}_\mu^{(0)} - \vec{l}_\mu^{(\rho_1)} \right] \cdot (-\vec{a}_{\rho_1}) \quad (\text{C.108})$$

which is exactly the medium-specific part of the decomposition as obtained from orthogonality of vacuum- and medium-specific parts of the decomposition (cf. Eq. (C.33)). The orthogonality (C.31) can be easily shown:

$$\vec{l}^{(1)} \circ \vec{l}^{(0)} = \left( L_{\rho_1,0} L_0^{-1} \vec{l}^{(0)} - \vec{l}^{(\rho_1)} \right) \circ \vec{l}^{(0)} = L_{\rho_1,0} L_0^{-1} L_0 - L_{\rho_1,0} = 0, \quad (\text{C.109})$$

where the orthogonality  $\vec{l}^{(0)} \circ \vec{l}^{(1)} = 0$  can be deduced for the transposed of (C.109), due to the handy notation of the dyadic product.

### C.3 Calculation of Wilson coefficients of light-quark condensates of mass dimension 6

For the calculation of Wilson coefficients of light four-quark condensates corresponding to tree-level diagrams containing a soft-gluon line we utilize Eq. (3.7b). Using the heretofore presented OPE techniques – projection of Dirac indices onto elements of the Clifford algebra, Eqs. (C.3) and (C.4), as well as the covariant expansion of quark field operators exploiting the Fock-Schwinger gauge, Eq. (2.35) – the light two-quark term  $\Pi^{(2)}$  after Fourier transformation reads [Hil11]

$$\Pi^{(2)}(p) = \sum_a \frac{1}{4} \sum_{n=0}^{\infty} \frac{(-i)^n}{n!} \partial_p^{\vec{\alpha}_n} \langle : \bar{q} \overleftrightarrow{D}_{\vec{\alpha}_n} \Gamma_a \text{Tr}_D [\Gamma^a \gamma_5 S_Q(p) \gamma_5] q : \rangle, \quad (\text{C.110})$$

where heavy-quark condensates are neglected. Treated in a classical, weak, gluonic background field the interaction of the quark is modeled by soft-gluon exchange with the QCD ground state and the full propagator  $S_Q(p) = \int d^4x e^{ipx} S_Q(x, 0)$  can be approximated by the perturbative propagator (2.44), where the subscript 'Q' refers to the heavy quark.

Light-quark condensate terms in mass dimension 6 enter  $\Pi^{(2)}$  with  $n = 3$  and  $S_Q = S_Q^{(0)}$ ,  $n = 0$  and  $S_Q = S_{Q(\hat{A}^{(1)})}^{(1)}$  as well as  $n = 1$  and  $S_Q = S_{Q(\hat{A}^{(0)})}^{(1)}$  [Nov84], where the order of the



background field expansion is specified according to Eq. (2.49). The light-quark condensate contribution reads

$$\Pi_{\text{dim6}}(p) = \Pi_{\text{dim6}}^{[1]}(p) + \Pi_{\text{dim6}}^{[2]}(p) + \Pi_{\text{dim6}}^{[3]}(p) \quad (\text{C.111})$$

with the three terms

$$\Pi_{\text{dim6}}^{[1]}(p) = \sum_a \frac{1}{4} \frac{(-i)^3}{3!} \langle : \bar{q} \overleftarrow{D}_\nu \overleftarrow{D}_\lambda \overleftarrow{D}_\rho \Gamma_a q : \rangle \text{Tr}_D \left[ \Gamma^a \gamma_5 \partial_p^\nu \partial_p^\lambda \partial_p^\rho S_Q^{(0)}(p) \gamma_5 \right], \quad (\text{C.112})$$

$$\Pi_{\text{dim6}}^{[2]}(p) = \sum_a \frac{1}{4} \langle : \bar{q} \Gamma_a \text{Tr}_D \left[ \Gamma^a \gamma_5 S_{Q(\tilde{A}^{(1)})}^{(1)}(p) \gamma_5 \right] q : \rangle, \quad (\text{C.113})$$

$$\Pi_{\text{dim6}}^{[3]}(p) = \sum_a \frac{1}{4} \frac{(-i)^1}{1!} \partial_p^\nu \langle : \bar{q} \overleftarrow{D}_\nu \Gamma_a \text{Tr}_D \left[ \Gamma^a \gamma_5 S_{Q(\tilde{A}^{(0)})}^{(1)}(p) \gamma_5 \right] q : \rangle, \quad (\text{C.114})$$

where  $\Pi_{\text{dim6}}^{[1]}$  contains contributions associated with diagram (d) and  $\Pi_{\text{dim6}}^{[2,3]}$  incorporate terms associated with diagram (e) in Fig. 3.2. Using the perturbative quark propagators  $S_{Q(\tilde{A}^{(1)})}^{(1)}(p) = -S_Q^{(0)}(p) \gamma^\rho \tilde{A}_\rho^{(1)} S_Q^{(0)}(p)$  and  $S_{Q(\tilde{A}^{(0)})}^{(1)}(p) = -S_Q^{(0)}(p) \gamma^\rho \tilde{A}_\rho^{(0)} S_Q^{(0)}(p)$  with  $\tilde{A}_\rho^{(1)} = \frac{g}{3} [D_\nu, G_{\rho\lambda}] \partial_p^\lambda \partial_p^\nu$  and  $\tilde{A}_\rho^{(0)} = i \frac{g}{2} G_{\rho\lambda} \partial_p^\lambda$ , respectively, one obtains

$$\Pi_{\text{dim6}}^{[2]}(p) = -\frac{g}{12} \sum_a \langle : \bar{q} \Gamma_a [D_\nu, G_{\rho\lambda}] q : \rangle \text{Tr}_D \left[ \Gamma^a \gamma_5 S_Q^{(0)}(p) \gamma^\rho \left( \partial_p^\lambda \partial_p^\nu S_Q^{(0)}(p) \right) \gamma_5 \right], \quad (\text{C.115})$$

$$\Pi_{\text{dim6}}^{[3]}(p) = -\frac{g}{8} \sum_a \langle : \bar{q} \overleftarrow{D}_\nu \Gamma_a G_{\rho\lambda} q : \rangle \partial_p^\nu \text{Tr}_D \left[ \Gamma^a \gamma_5 S_Q^{(0)}(p) \gamma^\rho \left( \partial_p^\lambda S_Q^{(0)}(p) \right) \gamma_5 \right]. \quad (\text{C.116})$$

Subsequently,  $\Pi_{\text{dim6}}^{[1,2,3]}$  are treated analogously. Utilizing the identity

$$\partial_p^\mu S_Q^{(0)}(p) = -S_Q^{(0)}(p) \gamma^\mu S_Q^{(0)}(p) \quad (\text{C.117})$$

and insertion of the free quark propagator (A.22) yields traces of products of Dirac matrices, which stem from elements of the Clifford algebra  $\Gamma_a$  as well as free quark propagators and vertex functions. The results of the Dirac trace evaluations are to be contracted with the tensor decompositions of the Gibbs averaged operators  $\langle : \bar{q} \overleftarrow{D}_\nu \overleftarrow{D}_\lambda \overleftarrow{D}_\rho \Gamma_a q : \rangle$ ,  $\langle : \bar{q} \Gamma_a [D_\nu, G_{\rho\lambda}] q : \rangle$  and  $\langle : \bar{q} \overleftarrow{D}_\nu \Gamma_a G_{\rho\lambda} q : \rangle$ , cf. App. C.2.2.

In order to obtain a continuous transition of the OPE for  $T, n \rightarrow 0$ , the in-medium decomposition into Lorentz structures composed of  $g_{\mu\nu}$  (metric tensor),  $\varepsilon_{\mu\nu\lambda\sigma}$  (Levi-Civita symbol) and  $v_\mu$  (medium four-velocity) [Buc14b] requires the separation of vacuum- and medium-specific condensate contributions, where the former are present in vacuum, while the latter vanish at zero temperature and nucleon density, cf. App. C.2.1 for details. If the (anti-)symmetries among the Lorentz indices of the operators are imposed on the decomposition structures one is able to identify unambiguously medium-specific operators.

The resulting Gibbs averaged operators can be reduced to canonical condensates of lower mass dimension using the quark EoMs (A.17) and (A.18), cf. App. C.2.1, or they contain covariant derivatives which can not be eliminated by application of the EoMs, i.e. exhibiting light-quark condensation in mass dimension 6. Especially, the combinations  $D^\lambda D_\nu D_\lambda$ ,  $[D^\lambda, G_{\nu\lambda}]$  and  $G_{\nu\lambda} D^\lambda$  incorporate the desired four-quark condensate terms. The first and

third terms contain the second combination  $[D^\lambda, G_{\nu\lambda}]$ , which allows for the application of the gluon EoM (A.19). One obtains

$$\langle : \bar{q} \Gamma [D^\lambda, G_{\nu\lambda}] q : \rangle = g \langle : \bar{q}_i \Gamma t^A q_i \sum_f \bar{f} \gamma_\nu t^A f : \rangle, \quad (\text{C.118})$$

where  $\Gamma \in \{v^\nu, \gamma^\nu, \not{v}^\nu\}$ , because other elements of the Clifford algebra lead to expectation values which are not invariant under time reversal and parity transformations, cf. Tab. A.1. The result of these calculations is Eq. (3.8) with operators listed in Tab. 3.1 providing the complete light-quark condensate contribution to the OPE of pseudo-scalar  $qQ$  mesons in mass dimension 6.

## D Borel transformation

The QSRs emerging from the dispersion relations (2.17), (2.22) and (2.23) are not well suited to estimate the lowest hadronic resonance of the spectral density. Generically, they contain unknown subtraction terms and, apart from the lowest resonance, only limited information about the shape of the spectral density is available. Furthermore, the OPE is an asymptotic series, where only a first few terms are calculated which may not exhibit a convergent behavior. However, the evaluation can be substantially improved utilizing a Borel transformation which has been successfully employed since the early days of the QSR method [Shi79]. The Borel transformation can be defined by [Shi79]

$$\tilde{\mathcal{B}}[f(Q^2)] \equiv \lim_{\substack{n \rightarrow \infty \\ Q^2 = nM^2}} \frac{(Q^2)^n}{\Gamma(n)} \left( -\frac{d}{dQ^2} \right)^n f(Q^2) = \tilde{F}(M^2), \quad (\text{D.1})$$

and slightly deviating but equivalent definitions are introduced in the literature, e. g. [Fur92]

$$\mathcal{B}[f(Q^2)] \equiv \lim_{\substack{n \rightarrow \infty \\ Q^2 = nM^2}} \frac{(Q^2)^{n+1}}{\Gamma(n+1)} \left( -\frac{d}{dQ^2} \right)^n f(Q^2) = F(M^2), \quad (\text{D.2})$$

where in vacuum one has  $Q^2 = -q^2$  and in the medium  $Q^2 = -q_0^2$ , accordingly. The new parameter  $M$  is referred to as Borel mass and remains finite in the limit  $Q^2, n \rightarrow \infty$ . The two definitions differ in overall factors only, which cancel if the Borel transformation is applied to both sides of the QSR. We proceed with the latter definition (D.2), commonly used in finite-density QSRs. For practical purposes, a catalog of Borel transforms  $F(M^2)$  of typical functions  $f(Q^2)$  entering the OPE or the spectral integral is provided in the following.

Direct calculation from the definition (D.2) yields:

$$f(Q^2) = (Q^2)^k \quad \longrightarrow \quad F(M^2) = 0 \quad (k = 0, 1, 2, \dots), \quad (\text{D.3})$$

$$f(Q^2) = \frac{1}{(Q^2)^k} \quad \longrightarrow \quad F(M^2) = \frac{1}{(k-1)!} \frac{1}{(M^2)^{k-1}} \quad (k = 1, 2, 3, \dots), \quad (\text{D.4})$$

$$f(Q^2) = (Q^2)^k \ln Q^2 \quad \longrightarrow \quad F(M^2) = (-1)^{k+1} k! (M^2)^{k+1} \quad (k = 0, 1, 2, \dots). \quad (\text{D.5})$$

Although, the Borel transforms of simple functions, as they appear in the subtraction terms or power corrections of the QSRs, are obtained easily with the definition (D.2), the Borel transforms of complicated functions require much more effort. For complicated functions the connection between Borel transformation and Laplace transformation is helpful.

The Laplace transform is defined by [Bro08]

$$\mathcal{L}[g(t)] \equiv \int_0^\infty dt e^{-pt} g(t) = f(p), \quad (\text{D.6})$$

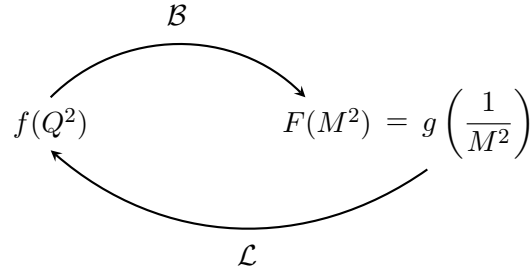


**Figure D.1:** Graphical representation of Eq. (D.10) exhibiting the link between Borel and (inverse) Laplace transformation.

where the given function  $f(p)$  (with  $p$  complex) is the Laplace transform of the function  $g(t)$  (with  $t$  real). Further requirements are:  $g(t)$  is piecewise smooth on its domain  $t \geq 0$  and it increases less than  $e^{\alpha t}$  with  $\alpha > 0$  for  $t \rightarrow \infty$ . The inverse Laplace transform satisfies

$$\mathcal{L}^{-1}[f(p)] = \int_{c-i\infty}^{c+i\infty} dp e^{pt} f(p) = g(t) \quad (\text{D.7})$$

with  $t > 0$ . The integration path of the complex integral is parallel, i.e.  $\text{Re } p = c$ , to the imaginary axis with  $c > \alpha$ . An alternative inverse Laplace transformation revealing the connection to the definition of the Borel transformation (D.2) is provided by Post-Widder's inversion formula [Hil12a]:

$$\mathcal{L}^{-1}[f(p)] = \lim_{n \rightarrow \infty} \frac{1}{n!} \left(\frac{n}{t}\right)^{n+1} \left(-\frac{d}{dp}\right)^n f(p) \Big|_{p=n/t} = g(t). \quad (\text{D.8})$$

For  $t = 1/M^2$  and  $n/t = nM^2 = Q^2$  one obtains

$$g\left(\frac{1}{M^2}\right) = \lim_{\substack{n \rightarrow \infty \\ Q^2 = nM^2}} \frac{(Q^2)^{n+1}}{n!} \left(-\frac{d}{dQ^2}\right)^n f(Q^2). \quad (\text{D.9})$$

Comparing with Eq. (D.2) one can identify

$$\mathcal{B}[f(Q^2)] = F(M^2) = g\left(\frac{1}{M^2}\right) = \mathcal{L}^{-1}[f(Q^2)]. \quad (\text{D.10})$$

The Borel transform of function  $f$  equals the inverse Laplace transform of function  $f$ . If a function  $g$  can be found which is the inverse Laplace transform of the given function  $f$ , then  $g$  is the desired Borel transform  $F$  of  $f$  (see Fig. D.1). That is, Borel transforms of numerous function can be found which are known to be the Laplace transforms of the wanted functions. Furthermore, the well established properties of the Laplace transform may be employed. The property [Bro08]

$$\mathcal{L}[e^{-at}g(t)] = f(p+a) \quad (\text{D.11})$$

simplifies the calculation of the Borel transform of numerous function. Due to the definition  $g(t) = \mathcal{L}^{-1}[f(p)]$  with  $t = 1/M^2$  and  $p = Q^2 - a$  one has

$$\mathcal{B}[f(Q^2 - a)] = e^{a/M^2} \mathcal{B}[f(Q^2)]. \quad (\text{D.12})$$

---

For functions entering the hadronic integral of the dispersion relation one obtains the Borel transformation

$$f(Q^2) = \frac{1}{(Q^2 + a)^k} \quad \longrightarrow \quad F(M^2) = \frac{1}{(k-1)!} \frac{e^{-a/M^2}}{(M^2)^{k-1}} \quad (k = 1, 2, 3, \dots). \quad (\text{D.13})$$

Employing the identity

$$\frac{(Q^2)^m}{Q^2 + a} = (Q^2)^{m-1} - \frac{a(Q^2)^{m-1}}{Q^2 + a} \quad (\text{D.14})$$

iteratively and Eq. (D.13), the Borel transformation of Wilson coefficients emerging from propagators of particles with finite masses can be obtained:

$$\begin{aligned} f(Q^2) = \frac{(Q^2)^m}{(Q^2 + a)^k} \quad &\longrightarrow \\ F(M^2) = \sum_{i=0}^m \binom{m}{i} \frac{(-a)^i}{(k-m+i-1)!} \frac{e^{-a/M^2}}{(M^2)^{k-m+i-1}} \quad &(\text{D.15}) \\ (k > m, \ k = 1, 2, 3, \dots, \ m = 0, 1, 2, \dots). \end{aligned}$$

In general, one has

$$\begin{aligned} f(Q^2) = \frac{(Q^2)^m}{(Q^2 + a)^k} \quad &\longrightarrow \\ F(M^2) = \frac{(-1)^m}{(k-1)!} \left( \frac{d}{dt} \right)^m \left( \left( \frac{1}{M^2} - t \right)^{k-1} e^{-a(1/M^2 - t)} \right) \Bigg|_{t=0} \quad &(\text{D.16}) \\ (k = 1, 2, 3, \dots, \ m = 0, 1, 2, \dots). \end{aligned}$$

The Borel transformation is tailored to improve the extraction of the properties of the lowest hadronic resonance from QSRs emerging from the subtracted dispersion relations (2.17), (2.22) and (2.23) in a threefold manner: It *(i)* eliminates the subtraction terms, due to Eq. (D.3), and *(ii)* improves the convergence of the asymptotic OPE series by suppressing higher order contributions factorially, due to Eq. (D.4) and its generalizations (D.13), (D.15) and (D.16). By virtue of exponential factors in the integrand of the spectral integral the Borel transformation *(iii)* enhances the sensitivity of the QSR at low values of  $M$  close to the lowest resonance, while suppressing higher hadronic excitations of the spectrum.



## E Monte-Carlo sum rule analysis

The Monte-Carlo QSR analysis introduced in Ref. [Lei97] does genuinely rely on the original QSR (2.130) avoiding the shortcomings of derivative sum rules (2.140) given in Sec. 2.4.2. In this approach, the parameters of the pole ansatz (2.133) of the spectral density (2.126), i. e.  $s_0$ ,  $m_h$  and  $R_h$ , are not evaluated consecutively, but they are fitted from the very same chi-squared function  $\chi^2(m_h, R_h, s_0)$  measuring the deviations of the phenomenological side of the QSR (2.130) from the OPE side. For each considered Borel mass parameter  $M_j$  in the Borel window this deviation is weighted by an OPE uncertainty  $\sigma_{\text{OPE}}^2(M_j)$  emerging from Gaussianly distributed condensate values. The presentation of this QSR analysis method closely follows Ref. [Lei97].

An OPE in Borel space,  $\Pi_i^{\text{OPE}}(M)$ , is constructed from a set (labeled by subscript 'i') of Gaussianly-distributed randomly-selected QCD condensate values. By repeating this procedure  $n_C$  times, an uncertainty for the OPE at a fixed Borel mass  $M_j$  can be given by

$$\sigma_{\text{OPE}}^2(M_j) = \frac{1}{n_C - 1} \sum_{i=1}^{n_C} \left[ \Pi_i^{\text{OPE}}(M_j) - \overline{\Pi^{\text{OPE}}}(M_j) \right]^2 \quad (\text{E.1})$$

with the OPE mean

$$\overline{\Pi^{\text{OPE}}}(M_j) = \frac{1}{n_C} \sum_{i=1}^{n_C} \Pi_i^{\text{OPE}}(M_j). \quad (\text{E.2})$$

The uncertainties  $\sigma_{\text{OPE}}^2$  are not uniform throughout the relevant Borel range. They are larger at the lower, non-perturbative end of the Borel range, where uncertainties in the higher dimensional vacuum condensates dominate. Hence, it is crucial to have knowledge about the higher mass dimension condensates and to use the appropriate weight in the calculation of  $\chi^2$ . Having determined the OPE uncertainty (E.1) for  $n_B$  equidistantly distributed Borel masses  $M_j$  throughout the relevant Borel region<sup>1</sup> a  $\chi^2$  measure is easily constructed. For the OPE,  $\Pi_k^{\text{OPE}}(M)$ , obtained from the  $k$ -th set of QCD parameters, the  $\chi_k^2$  per degree of freedom reads

$$\frac{\chi_k^2}{N_{\text{DoF}}} = \frac{1}{n_B^{(k)} - n_{\text{phen}}} \sum_{j=1}^{n_B^{(k)}} \frac{\left[ \Pi_k^{\text{OPE}}(M_j) - \Pi^{\text{phen}}(M_j; m_h^{(k)}, R_h^{(k)}, s_0^{(k)}) \right]^2}{\sigma_{\text{OPE}}^2(M_j)}, \quad (\text{E.3})$$

where the sum runs over the  $n_B^{(k)}$  Borel masses within the  $k$ -th Borel window, typically  $n_B^{(k)} \sim 50$ . The quantity  $n_{\text{phen}}$  is the number of phenomenological fit parameters ( $n_{\text{phen}} = 3$  for the pole + continuum ansatz), and  $\Pi^{\text{phen}}(M_j; m_h^{(k)}, R_h^{(k)}, s_0^{(k)})$  denotes the phenomenological spectral representation of the QSR, i. e. the r. h. s. of Eq. (2.130) with the ansatz (2.133).

---

<sup>1</sup>The number of evaluated Borel masses  $n_B$  must not be confused with the Bose-Einstein distribution  $n_B$  used in Subsec. 2.3.3.

The measure  $\chi_k^2$  is minimized by adjusting the phenomenological parameters including the hadron mass  $m_h^{(k)}$ , the pole residue  $R_h^{(k)}$  and the continuum threshold parameter  $s_0^{(k)}$ .

Distributions for the phenomenological parameters are obtained by minimizing  $\chi_k^2$  for  $N$  QCD parameter sets, where  $N$  may or may not coincide with  $n_C$ . Provided the resulting distributions are Gaussian, an estimate of the uncertainty in the phenomenological results such as the hadron mass  $m_h$  is obtained from

$$\sigma_{m_h}^2 = \frac{1}{N-1} \sum_{k=1}^N (m_h^{(k)} - m_h)^2 \quad (\text{E.4})$$

with

$$m_h = \frac{1}{N} \sum_{k=1}^N m_h^{(k)} \quad (\text{E.5})$$

being the mean hadron mass, which may be considered the result of the QSR evaluation following the Monte-Carlo approach. Analogously, mean and uncertainty can be obtained for further phenomenological parameters, i.e. pole residue  $R_h$  and continuum threshold parameter  $s_0$ . If the resulting distributions are not Gaussian, one may provide median and asymmetric standard deviations. In contrast to the error of the distribution  $\sigma^2/N$ , the standard deviation (E.4) is roughly independent of the number  $N$  of QCD parameter sets used in the analysis, and directly reflects the input parameter uncertainties. While  $N \sim 100$  QCD parameter configurations are sufficient for obtaining reliable uncertainty estimates,  $N \sim 1000$  should be used to explore more subtle correlations among the QCD parameters and the phenomenological fit parameters.

Some care must be taken in the interpretation of the  $\chi_k^2/N_{\text{DoF}}$ . While we are free to choose any number of points  $n_B$  along the Borel axis for fitting the two sides of the QSR, it is important to recognize that the actual number of DoF is determined by the number of QCD parameters in the OPE. For the  $\chi_k^2/N_{\text{DoF}}$  to have true statistical meaning, a correlated  $\chi_k^2$  calculation is required:

$$\begin{aligned} \chi_k^2 = \sum_{j,j'=1}^{n_B^{(k)}} & \left[ \Pi_k^{\text{OPE}}(M_j) - \Pi^{\text{phen}}(M_j; m_h^{(k)}, R_h^{(k)}, s_0^{(k)}) \right] \\ & \times C_{jj'}^{-1} \left[ \Pi_k^{\text{OPE}}(M_{j'}) - \Pi^{\text{phen}}(M_{j'}; m_h^{(k)}, R_h^{(k)}, s_0^{(k)}) \right], \quad (\text{E.6}) \end{aligned}$$

where  $C_{jj'}^{-1}$  is the inverse of the covariance matrix, which may be estimated by

$$C_{jj'} = \frac{1}{n_C - 1} \sum_{i=1}^{n_C} \left[ \Pi_i^{\text{OPE}}(M_j) - \overline{\Pi^{\text{OPE}}}(M_j) \right] \left[ \Pi_i^{\text{OPE}}(M_{j'}) - \overline{\Pi^{\text{OPE}}}(M_{j'}) \right]. \quad (\text{E.7})$$

Unfortunately, on many occasions the covariance matrix is ill-conditioned. Thus, inversion of the covariance matrix leads to pathological problems [Mic95].

Even if some correlation among the data is suspected, due to  $n_B^{(k)} > \text{number of QCD parameters in the OPE}$ , it is still acceptable to use the uncorrelated  $\chi_k^2$  fit (E.3) provided



---

the errors on the fit parameters are estimated using a Monte-Carlo based procedure, like that one presented here, rather than from the dependence of  $\chi_k^2$  on the fit parameters. The only drawback of such a practice is that it may be difficult to estimate the goodness of the fit since the correlation among the data may not have been adequately treated [Mic94].

Sophisticated algorithms are needed to find the minimum of the  $\chi^2$  function (E.3) in order to genuinely extract the hadronic spectral properties from the QSRs rather than to (re)construct results by fine-tuning the initial values of the optimization [Lei97]. As the parameters of the spectral density enter the QSR in the integrand of the spectral integral, the integral value itself might not be sufficiently sensitive on the individual parameters impeding the fitting procedure, in particular, if a large number of parameters is used to shape the spectral density.

The Monte-Carlo QSR analysis has been successfully tested by the  $\rho$  meson and the nucleon sum rules [Lei97]. Based on this approach also finite-density QSRs for the  $\rho$  meson [Jin95] and the nucleon [Fur96] have been evaluated, where the statistical analysis supports a  $\rho$  mass drop for finite net-baryon densities and demonstrates qualitative consistency of the obtained nucleon self-energies close to nuclear saturation density with expectations from mean-field phenomenology.



## Acronyms

AdS/CFT	Anti-de Sitter/Conformal Field Theory
CBM	Compressed Baryonic Matter
CERN	Conseil Européen pour la Recherche Nucléaire
CKM	Cabibbo-Kobayashi-Maskawa
D $\chi$ SB	dynamical chiral symmetry breaking
DIS	deep inelastic scattering
DoF	degrees of freedom
EoM	equation of motion
EV	expectation value
FAIR	Facility for Anti-proton and Ion Research
GOR	Gell-Mann–Oakes–Renner
GSI	Gesellschaft für SchwerIonenforschung
HQE	heavy-quark expansion
J-PARC	Japan Proton Accelerator Research Complex
JLab	Jefferson Laboratory
KEK	Kō Enerugi Kasokuki Kenkyū Kikō
LHC	Large Hadron Collider

LO	leading order
$\ell$ QCD	lattice QCD
NICA	Nuclotron-based Ion Collider fAcility
NLO	next-to-leading order
OPE	operator product expansion
PANDA	anti-Proton ANnihilation at DArmstadt
PCAC	partial conservation of the axial-vector current
QCD	quantum chromodynamics
QED	quantum electrodynamics
QSR	QCD sum rule
RGE	renormalization group equation
RGI	renormalization group invariant
RHIC	Relativistic Heavy Ion Collider
SPS	Super Proton Synchrotron
SVZ	Shifman, Vainshtein and Zakharov
WSR	Weinberg sum rule

## List of Figures

2.1	Integration contours for derivation of dispersion relations in complex plain . .	16
2.2	Diagrammatic representation of the perturbative quark propagator . . . . .	22
2.3	Diagrammatic representation of the perturbative gluon propagator . . . . .	25
2.4	Diagrammatic representation of the loop expansion of the correlator . . . . .	33
2.5	Diagrammatic representation of the QCD quark propagator . . . . .	34
2.6	Sketches of generic spectral densities . . . . .	44
3.1	Diagrammatic representation of the fully Wick-contracted contribution to the LO correlator . . . . .	56
3.2	Diagrammatic representation of the two-quark contribution to the LO correlator	57
3.3	Diagrammatic representation of the tree-level four-quark condensate contri- bution to the NLO correlator . . . . .	58
3.4	Various (combined) contributions to the even OPE of the $qQ$ sum rule . . . .	64
3.5	Individual contributions to the OPE of the $qQ$ sum rule . . . . .	65
3.6	Comparison of $\rho$ meson and D meson OPE contributions . . . . .	67
3.7	Density dependence of the vacuum- and medium-specific condensates . . . . .	71
3.8	Heavy-quark mass dependence of the HQE compatibility . . . . .	74
4.1	Comparison of pseudo-scalar and scalar D meson mass contours . . . . .	82
4.2	Scalar D meson mass contours with optimized mass Borel curves . . . . .	83
4.3	Temperature dependences of the spectral properties of the scalar D meson . .	84
4.4	Comparison of temperature behavior of pseudo-scalar and scalar D meson OPE Borel curves . . . . .	86
4.5	Temperature behavior of the predominant D meson OPE contributions . . . .	87
4.6	Scalar D meson Borel curves optimized with $M$ -dependent continuum threshold	89
4.7	Temperature dependences of the scalar D meson spectral properties . . . . .	90
4.8	Temperature dependences of residua and decay constants of D mesons from chiral partner sum rules . . . . .	97
D.1	Link between Borel and (inverse) Laplace transformations . . . . .	148



## List of Tables

3.1	List of light-quark operators $O_k$ of mass dimension 6 forming condensates which enter the LO correlator . . . . .	59
3.2	List of medium-specific light-quark operator combinations in mass dimension 6 incorporating operators related to $O_1$ . . . . .	59
3.3	List of light four-quark condensates $\langle\langle :O_k: \rangle\rangle$ , with $k = 1, 2$ and 9 in genuine and factorized form . . . . .	61
4.1	List of relevant condensates entering the finite-temperature OPEs . . . . .	81
4.2	Coefficients $s_0^{S(n)}$ of the $M$ -dependent continuum threshold . . . . .	88
A.1	Transformation of components of condensates under $P$ and $T$ transformations	109





## Bibliography

- [Aad12] G. Aad et al. (ATLAS Collaboration): *Observation of a new particle in the search for the Standard Model Higgs boson with the ATLAS detector at the LHC*, Phys. Lett. B **716**, 1 (2012).
- [Aam08] K. Aamodt et al. (ALICE Collaboration): *The ALICE experiment at the CERN LHC*, JINST **3**, S08002 (2008).
- [Ada05] J. Adams et al. (STAR Collaboration): *Experimental and theoretical challenges in the search for the quark-gluon plasma: The STAR Collaboration's critical assessment of the evidence from RHIC collisions*, Nucl. Phys. A **757**, 102 (2005).
- [Adc05] K. Adcox et al. (PHENIX Collaboration): *Formation of dense partonic matter in relativistic nucleus-nucleus collisions at RHIC: Experimental evaluation by the PHENIX collaboration*, Nucl. Phys. A **757**, 184 (2005).
- [Aga95] G. Agakichiev et al. (CERES Collaboration): *Enhanced Production of Low-Mass Electron Pairs in 200 GeV/Nucleon S-Au Collisions at the CERN Super Proton Synchrotron*, Phys. Rev. Lett. **75**, 1272 (1995).
- [Aga07] G. Agakichiev et al. (HADES Collaboration): *Dielectron Production in  $^{12}\text{C}+^{12}\text{C}$  Collisions at 2A GeV with the HADES Spectrometer*, Phys. Rev. Lett. **98**, 052302 (2007).
- [Aga12] G. Agakishiev et al. (HADES Collaboration): *First measurement of proton-induced low-momentum dielectron radiation off cold nuclear matter*, Phys. Lett. B **715**, 304 (2012).
- [Aga16a] S. S. Agaev, K. Azizi and H. Sundu: *Charmed partner of the exotic  $X(5568)$  state and its properties*, Phys. Rev. D **93**, 094006 (2016).
- [Aga16b] S. S. Agaev, K. Azizi and H. Sundu: *Mass and decay constant of the newly observed exotic  $X(5568)$  state*, Phys. Rev. D **93**, 074024 (2016).
- [Aga16c] S. S. Agaev, K. Azizi and H. Sundu: *Width of the exotic  $X_b(5568)$  state through its strong decay to  $B_s^0\pi^+$* , Phys. Rev. D **93**, 114007 (2016).
- [Alb16] R. Albuquerque, S. Narison, A. Rabemananjara and D. Rabetiariivony: *Nature of the  $X(5568)$  – A critical Laplace sum rule analysis at  $N^2\text{LO}$* , Int. J. Mod. Phys. A **31**, 1650093 (2016).
- [Ali83] T. M. Aliiev and V. L. Eletsky: *On the leptonic decay constants of pseudoscalar  $D$  and  $B$  mesons*, Sov. J. Nucl. Phys. **38**, 936 (1983), [Yad. Fiz. **38**, 1537 (1983)].
- [And08] A. Andronic, P. Braun-Munzinger, K. Redlich and J. Stachel: *Charmonium and open charm production in nuclear collisions at SPS/FAIR energies and the possible influence of a hot hadronic medium*, Phys. Lett. B **659**, 149 (2008).
- [Arn06] R. Arnaldi et al. (NA60 Collaboration): *First Measurement of the  $\rho$  Spectral*

- Function in High-Energy Nuclear Collisions*, Phys. Rev. Lett. **96**, 162302 (2006).
- [Aya14] A. AYALA, C. A. DOMINGUEZ, M. LOEWE and Y. ZHANG: *Weinberg sum rules at finite temperature*, Phys. Rev. D **90**, 034012 (2014).
- [Bag85] E. BAGAN, J. I. LATORRE, P. PASCUAL and R. TARRACH: *Heavy-quark expansion, factorization and 8-dimensional gluon condensates*, Nucl. Phys. B **254**, 555 (1985).
- [Bag86] E. BAGAN, J. I. LATORRE and P. PASCUAL: *Heavy and heavy to light quark expansions*, Z. Phys. C **32**, 43 (1986).
- [Bag94] E. BAGAN, M. R. AHMADY, V. ELIAS and T. G. STEELE: *Plane-wave, coordinate-space, and moment techniques in the operator-product expansion: equivalence, improved methods, and the heavy quark expansion*, Z. Phys. C **61**, 157 (1994).
- [Bal89] I. I. BALITSKY, V. M. BRAUN and A. V. KOLESNICHENKO: *Radiative decay  $\sigma^+ \rightarrow p\gamma$  in quantum chromodynamics*, Nucl. Phys. B **312**, 509 (1989).
- [Bar98] R. BARATE et al.: *Measurement of the axial-vector  $\tau$  spectral functions and determination of  $\alpha_s(M_\tau^2)$  from hadronic  $\tau$  decays*, Eur. Phys. J. C **4**, 409 (1998).
- [Ben95] M. BENMERROUCHE, G. ORLANDINI and T. G. STEELE: *Constraints on QCD sum rules from the Hölder inequalities*, Phys. Lett. B **356**, 573 (1995).
- [Bla12] D. BLASCHKE, P. COSTA and YU. L. KALINOVSKY: *D mesons at finite temperature and density in the Polyakov–Nambu–Jona-Lasinio model*, Phys. Rev. D **85**, 034005 (2012).
- [Boc86] A. I. BOCHKAREV and M. E. SHAPOSHNIKOV: *The spectrum of hot hadronic matter and finite-temperature QCD sum rules*, Nucl. Phys. B **268**, 220 (1986).
- [Bor04] J. BORDES, J. PENARROCHA and K. SCHILCHER: *B and  $B_s$  decay constants from QCD duality at three loops*, JHEP **12**, 064 (2004).
- [Bor05] J. BORDES, J. PENARROCHA and K. SCHILCHER: *D and  $D_s$  decay constants from QCD duality at three loops*, JHEP **11**, 014 (2005).
- [Bor10] S. BORSANYI, Z. FODOR, C. HOELBLING, S. D. KATZ, S. KRIEG, C. RATTI and K. K. SZABO: *Is there still any  $T_c$  mystery in lattice QCD? Results with physical masses in the continuum limit III*, JHEP **09**, 073 (2010).
- [Bra89] V. M. BRAUN and I. E. FILYANOV: *QCD sum rules in exclusive kinematics and pion wave function*, Z. Phys. C **44**, 157 (1989), [Yad. Fiz. 50, 818 (1989)].
- [Bra15] F. L. BRAGHIN and F. S. NAVARRA: *Factorization breaking of four-quark condensates in the Nambu–Jona-Lasinio model*, Phys. Rev. D **91**, 074008 (2015).
- [Bri07] K. T. BRINKMANN (PANDA Collaboration): *Physics with the  $\bar{P}$ ANDA detector at FAIR*, Nucl. Phys. A **790**, 75 (2007).
- [Bro91] G. E. BROWN and M. RHO: *Scaling Effective Lagrangians in a Dense Medium*, Phys. Rev. Lett. **66**, 2720 (1991).
- [Bro08] I. N. BRONSTEIN, K. A. SEMENDJAJEW, G. MUSIOL and H. MÜHLIG: *Taschenbuch der Mathematik*, Harri Deutsch, 2008.

- 
- [Bro10] S. J. BRODSKY, C. D. ROBERTS, R. SHROCK and P. C. TANDY: *New perspectives on the quark condensate*, Phys. Rev. C **82**, 022201 (2010).
  - [Bro11] S. J. BRODSKY and R. SHROCK: *Condensates in quantum chromodynamics and the cosmological constant*, Proc. Nat. Acad. Sci. **108**, 45 (2011).
  - [Bro12] S. J. BRODSKY, C. D. ROBERTS, R. SHROCK and P. C. TANDY: *Confinement contains condensates*, Phys. Rev. C **85**, 065202 (2012).
  - [Buc12] T. BUCHHEIM: *QCD Summenregeln: Berechnung der Wilson-Koeffizienten von Vier-Quark-Kondensaten in  $Q\bar{q}$ -Mesonen*, Diploma thesis, Technische Universität Dresden (2012).
  - [Buc14a] T. BUCHHEIM, T. HILGER and B. KÄMPFER: *Heavy-quark expansion for  $D$  and  $B$  mesons in nuclear matter*, EPJ Web Conf. **81**, 05007 (2014).
  - [Buc14b] T. BUCHHEIM, T. HILGER and B. KÄMPFER: *In-medium QCD sum rules for  $D$  mesons: A projection method for higher order contributions*, J. Phys. Conf. Ser. **503**, 012006 (2014).
  - [Buc15a] T. BUCHHEIM, T. HILGER and B. KÄMPFER: *Defining medium-specific condensates in QCD sum rules for  $D$  and  $B$  mesons*, Nucl. Part. Phys. Proc. **258-259**, 213 (2015).
  - [Buc15b] T. BUCHHEIM, T. HILGER and B. KÄMPFER: *Wilson coefficients and four-quark condensates in QCD sum rules for medium modifications of  $D$  mesons*, Phys. Rev. C **91**, 015205 (2015).
  - [Buc16a] T. BUCHHEIM, T. HILGER and B. KÄMPFER: *Chiral symmetry aspects in the open charm sector*, J. Phys. Conf. Ser. **668**, 012047 (2016).
  - [Buc16b] T. BUCHHEIM, B. KÄMPFER and T. HILGER: *Algebraic vacuum limits of QCD condensates from in-medium projections of Lorentz tensors*, J. Phys. G **43**, 055105 (2016).
  - [Bur00] C. P. BURGESS: *Goldstone and pseudo-Goldstone bosons in nuclear, particle and condensed-matter physics*, Phys. Rept. **330**, 193 (2000).
  - [Bur13] Y. BURNIER and A. ROTHKOPF: *Bayesian Approach to Spectral Function Reconstruction for Euclidean Quantum Field Theories*, Phys. Rev. Lett. **111**, 182003 (2013).
  - [Cas74] A. CASHER and L. SUSSKIND: *Chiral magnetism (or magnetohydrochironics)*, Phys. Rev. D **9**, 436 (1974).
  - [Cha12] S. CHATRCHYAN et al. (CMS Collaboration): *Observation of a new boson at a mass of 125 GeV with the CMS experiment at the LHC*, Phys. Lett. B **716**, 30 (2012).
  - [Cha13] L. CHANG, C. D. ROBERTS and S. M. SCHMIDT: *Light front distribution of the chiral condensate*, Phys. Lett. B **727**, 255 (2013).
  - [Che90] V. L. CHERNYAK and I. R. ZHITNITSKY:  *$B$ -meson exclusive decays into baryons*, Nucl. Phys. B **345**, 137 (1990).
  - [Che15] H.-X. CHEN, W. CHEN, Q. MAO, A. HOSAKA, X. LIU and S.-L. ZHU:  *$P$ -wave charmed baryons from QCD sum rules*, Phys. Rev. D **91**, 054034 (2015).

- [Che16] W. CHEN, H.-X. CHEN, X. LIU, T. G. STEELE and S.-L. ZHU: *Decoding the  $X(5568)$  as a Fully Open-Flavor  $sub\bar{d}$  Tetraquark State*, Phys. Rev. Lett. **117**, 022002 (2016).
- [Cho15] S. CHO, K. HATTORI, S. H. LEE, K. MORITA and S. OZAKI: *Charmonium spectroscopy in strong magnetic fields by QCD sum rules: S-wave ground states*, Phys. Rev. D **91**, 045025 (2015).
- [Clo14] I. C. CLOËT and C. D. ROBERTS: *Explanation and prediction of observables using continuum strong QCD*, Prog. Part. Nucl. Phys. **77**, 1 (2014).
- [Coh91] T. D. COHEN, R. J. FURNSTAHL and D. K. GRIEGEL: *From QCD Sum Rules to Relativistic Nuclear Physics*, Phys. Rev. Lett. **67**, 961 (1991).
- [Coh92] T. D. COHEN, R. J. FURNSTAHL and D. K. GRIEGEL: *Quark and gluon condensates in nuclear matter*, Phys. Rev. C **45**, 1881 (1992).
- [Coh95] T. D. COHEN, R. J. FURNSTAHL, D. K. GRIEGEL and X.-M. JIN: *QCD sum rules and applications to nuclear physics*, Prog. Part. Nucl. Phys. **35**, 221 (1995).
- [Col91] P. COLANGELO, G. NARDULLI, A. A. OVCHINNIKOV and N. PAVER: *Semileptonic B-decays into positive-parity charmed mesons*, Phys. Lett. B **269**, 201 (1991).
- [Col01] P. COLANGELO and A. KHODJAMIRIAN: *QCD sum rules, a modern perspective*, in M. A. SHIFMAN (Editor), *At the Frontier of Particle Physics / Handbook of QCD*, volume 3, page 1495, World Scientific, Singapore, 2001.
- [Dia13] J. M. DIAS, F. S. NAVARRA, M. NIELSEN and C. M. ZANETTI:  *$Z_c^+(3900)$  decay width in QCD sum rules*, Phys. Rev. D **88**, 016004 (2013).
- [Dia16] J. M. DIAS, K. P. KHEMCHANDANI, A. MARTÍNEZ TORRES, M. NIELSEN and C. M. ZANETTI: *A QCD sum rule calculation of the  $X^\pm(5568) \rightarrow B_s^0 \pi^\pm$  decay width*, Phys. Lett. B **758**, 235 (2016).
- [Dom89] C. A. DOMINGUEZ and M. LOEWE: *Deconfinement and chiral-symmetry restoration at finite temperature*, Phys. Lett. B **233**, 201 (1989).
- [Dom04] C. A. DOMINGUEZ and K. SCHILCHER: *Finite energy chiral sum rules in QCD*, Phys. Lett. B **581**, 193 (2004).
- [Dom14] C. A. DOMINGUEZ: *Analytical determination of the QCD quark masses*, Int. J. Mod. Phys. A **29**, 1430069 (2014).
- [Dom15a] C. A. DOMINGUEZ, L. A. HERNANDEZ and K. SCHILCHER: *Determination of the gluon condensate from data in the charm-quark region*, JHEP **07**, 110 (2015).
- [Dom15b] C. A. DOMINGUEZ, L. A. HERNANDEZ, K. SCHILCHER and H. SPIESBERGER: *Chiral sum rules and vacuum condensates from tau-lepton decay data*, JHEP **03**, 053 (2015).
- [Dru91] E. G. DRUKAREV and E. M. LEVIN: *Structure of nuclear matter and QCD sum rules*, Prog. Part. Nucl. Phys. **27**, 77 (1991).
- [Dru02] E. G. DRUKAREV, M. G. RYSKIN, V. A. SADOVNIKOVA and A. FAESSLER: *Expectation values of four-quark operators in pions*, Phys. Rev. D **65**, 074015 (2002), [Erratum: Phys. Rev. D **66**, 039903 (2002)].
- [Dru03] E. G. DRUKAREV, M. G. RYSKIN, V. A. SADOVNIKOVA, V. E. LYUBOVITSKIJ,

- 
- T. GUTSCHE and A. FAESSLER: *Expectation values of four-quark operators in the nucleon*, Phys. Rev. D **68**, 054021 (2003).
- [Dru12] E. G. DRUKAREV, M. G. RYSKIN and V. A. SADOVNIKOVA: *Role of the in-medium four-quark condensates reexamined*, Phys. Rev. C **86**, 035201 (2012).
- [Dür16] S. DÜRR et al.: *Leptonic decay-constant ratio  $f_K/f_\pi$  from lattice QCD using 2+1 clover-improved fermion flavors with 2-HEX smearing* (2016), [arXiv: 1601.05998].
- [Dys49] F. J. DYSON: *The S Matrix in Quantum Electrodynamics*, Phys. Rev. **75**, 1736 (1949).
- [Eng64] F. ENGLERT and R. BROUT: *Broken Symmetry and the Mass of Gauge Vector Mesons*, Phys. Rev. Lett. **13**, 321 (1964).
- [Fah16] B. FAHY, G. COSSU, S. HASHIMOTO, T. KANEKO, J. NOAKI and M. TOMII: *Decay constants and spectroscopy of mesons in lattice QCD using domain-wall fermions*, PoS LATTICE2015, 074 (2016).
- [Far16] A. H. FARIBORZ, A. POKRAKA and T. G. STEELE: *Connections between chiral Lagrangians and QCD sum-rules*, Mod. Phys. Lett. A **31**, 1650023 (2016).
- [Fio12] S. FIORILLA, N. KAISER and W. WEISE: *Nuclear thermodynamics and the in-medium chiral condensate*, Phys. Lett. B **714**, 251 (2012).
- [Foc37] V. FOCK: *Proper time in classical and quantum mechanics*, Phys. Z. Sowjetunion **12**, 404 (1937).
- [Fri73] H. FRITZSCH, M. GELL-MANN and H. LEUTWYLER: *Advantages of the color octet gluon picture*, Phys. Lett. B **47**, 365 (1973).
- [Fri97] B. FRIMAN and H. J. PIRNER: *P-wave polarization of the  $\rho$ -meson and the dilepton spectrum in dense matter*, Nucl. Phys. A **617**, 496 (1997).
- [Fri06] V. FRIESE (CBM Collaboration): *The CBM experiment at GSI/FAIR*, Nucl. Phys. A **774**, 377 (2006).
- [Fri11] B. FRIMAN, C. HÖHNE, J. KNOLL, S. LEUPOLD, J. RANDRUP, R. RAPP and P. SENGGER (Editors): *The CBM Physics Book: Compressed Baryonic Matter in Laboratory Experiments*, Lect. Notes Phys. **814**, 1 (2011).
- [Fuk13] K. FUKUSHIMA and C. SASAKI: *The phase diagram of nuclear and quark matter at high baryon density*, Prog. Part. Nucl. Phys. **72**, 99 (2013).
- [Fur92] R. J. FURNSTAHL, D. K. GRIEGEL and T. D. COHEN: *QCD sum rules for nucleons in nuclear matter*, Phys. Rev. C **46**, 1507 (1992).
- [Fur96] R. J. FURNSTAHL, X.-M. JIN and D. B. LEINWEBER: *New QCD sum rules for nucleons in nuclear matter*, Phys. Lett. B **387**, 253 (1996).
- [Gas87] J. GASSER and H. LEUTWYLER: *Light quarks at low temperatures*, Phys. Lett. B **184**, 83 (1987).
- [Gel13] P. GELHAUSEN, A. KHODJAMIRIAN, A. A. PIVOVAROV and D. ROSENTHAL: *Decay constants of heavy-light vector mesons from QCD sum rules*, Phys. Rev. D **88**, 014015 (2013), [Errata: Phys. Rev. D **89**, 099901 (2014), Phys. Rev. D **91**, 099901 (2015)].

- [Gen84] S. C. GENERALIS and D. J. BROADHURST: *The heavy-quark expansion and QCD sum rules for light quarks*, Phys. Lett. B **139**, 85 (1984).
- [Ger89] P. GERBER and H. LEUTWYLER: *Hadrons below the chiral phase transition*, Nucl. Phys. B **321**, 387 (1989).
- [Gle92] J. GLEICK: *Genius: The Life and Science of Richard Feynman*, Pantheon Books, 1992.
- [GM51] M. GELL-MANN and F. LOW: *Bound States in Quantum Field Theory*, Phys. Rev. **84**, 350 (1951).
- [GM62] M. GELL-MANN: *Symmetries of Baryons and Mesons*, Phys. Rev. **125**, 1067 (1962).
- [GM64] M. GELL-MANN: *A schematic model of baryons and mesons*, Phys. Lett. **8**, 214 (1964).
- [GM68] M. GELL-MANN, R. J. OAKES and B. RENNER: *Behavior of Current Divergences under  $SU_3 \times SU_3$* , Phys. Rev. **175**, 2195 (1968).
- [God13] S. GODA and D. JIDO: *Chiral condensate at finite density using the chiral Ward identity*, Phys. Rev. C **88**, 065204 (2013).
- [Gre02] W. GREINER, S. SCHRAMM and E. STEIN: *Quantum Chromodynamics*, Springer-Verlag, 2002.
- [Gri89] B. GRINSTEIN and L. RANDALL: *The renormalization of  $G^2$* , Phys. Lett. B **217**, 335 (1989).
- [Gro73] D. J. GROSS and F. WILCZEK: *Ultraviolet Behavior of Nonabelian Gauge Theories*, Phys. Rev. Lett. **30**, 1343 (1973).
- [Gro95] A. G. GROZIN: *Methods of calculation of higher power corrections in QCD*, Int. J. Mod. Phys. A **10**, 3497 (1995).
- [Gub10] P. GUBLER and M. OKA: *A bayesian approach to QCD sum rules*, Prog. Theor. Phys. **124**, 995 (2010).
- [Gub15a] P. GUBLER, K. S. JEONG and S. H. LEE: *New determination of  $ST\langle N|\bar{q}D_\mu D_\nu q|N\rangle$  based on recent experimental constraints*, Phys. Rev. D **92**, 014010 (2015).
- [Gub15b] P. GUBLER and W. WEISE: *Moments of  $\phi$  meson spectral functions in vacuum and nuclear matter*, Phys. Lett. B **751**, 396 (2015).
- [Gub16] P. GUBLER, K. HATTORI, S. H. LEE, M. OKA, S. OZAKI and K. SUZUKI: *D mesons in a magnetic field*, Phys. Rev. D **93**, 054026 (2016).
- [Har06] M. HARADA and C. SASAKI: *Dropping  $\rho$  and  $A_1$  meson masses at chiral phase transition in the generalized hidden local symmetry*, Phys. Rev. D **73**, 036001 (2006).
- [Hat92a] T. HATSUDA and T. KUNIHIRO: *Strange quark, heavy quark, and gluon contents of light hadrons*, Nucl. Phys. B **387**, 715 (1992).
- [Hat92b] T. HATSUDA and S. H. LEE: *QCD sum rules for vector mesons in the nuclear medium*, Phys. Rev. C **46**, 34 (1992).

- 
- [Hat93] T. HATSUDA, Y. KOIKE and S. H. LEE: *Finite-temperature QCD sum rules reexamined:  $\rho$ ,  $\omega$  and  $A_1$  mesons*, Nucl. Phys. B **394**, 221 (1993).
  - [Hat95] T. HATSUDA, S. H. LEE and H. SHIOMI: *QCD sum rules, scattering length, and the vector mesons in the nuclear medium*, Phys. Rev. C **52**, 3364 (1995).
  - [Hay00] A. HAYASHIGAKI: *Mass modification of D-meson at finite density in QCD sum rule*, Phys. Lett. B **487**, 96 (2000).
  - [Hay04] A. HAYASHIGAKI and K. TERASAKI: *Charmed-meson spectroscopy in QCD sum rule* (2004), [arXiv: hep-ph/0411285].
  - [He13] M. HE, R. J. FRIES and R. RAPP:  *$D_s$  Meson as Quantitative Probe of Diffusion and Hadronization in Nuclear Collisions*, Phys. Rev. Lett. **110**, 112301 (2013).
  - [Hig64a] P. W. HIGGS: *Broken Symmetries and the Masses of Gauge Bosons*, Phys. Rev. Lett. **13**, 508 (1964).
  - [Hig64b] P. W. HIGGS: *Broken symmetries, massless particles and gauge fields*, Phys. Lett. **12**, 132 (1964).
  - [Hil09] T. HILGER, R. THOMAS and B. KÄMPFER: *QCD sum rules for D and B mesons in nuclear matter*, Phys. Rev. C **79**, 025202 (2009).
  - [Hil10] T. HILGER and B. KÄMPFER: *In-medium modifications of scalar charm mesons in nuclear matter*, Nucl. Phys. Proc. Suppl. **207-208**, 277 (2010).
  - [Hil11] T. HILGER, B. KÄMPFER and S. LEUPOLD: *Chiral QCD sum rules for open-charm mesons*, Phys. Rev. C **84**, 045202 (2011).
  - [Hil12a] T. HILGER: *Medium Modifications of Mesons*, Ph.D. thesis, Technische Universität Dresden (2012).
  - [Hil12b] T. HILGER, T. BUCHHEIM, B. KÄMPFER and S. LEUPOLD: *Four-quark condensates in open-charm chiral QCD sum rules*, Prog. Part. Nucl. Phys. **67**, 188 (2012).
  - [Hil12c] T. HILGER, R. THOMAS, B. KÄMPFER and S. LEUPOLD: *The impact of chirally odd condensates on the rho meson*, Phys. Lett. B **709**, 200 (2012).
  - [Hil16] T. HILGER: *Poincaré covariant pseudoscalar and scalar meson spectroscopy in Wigner-Weyl phase*, Phys. Rev. D **93**, 054020 (2016).
  - [Hoh12] P. M. HOHLER and R. RAPP: *Sum rule analysis of vector and axial-vector spectral functions with excited states in vacuum*, Nucl. Phys. A **892**, 58 (2012).
  - [Hoh14] P. M. HOHLER and R. RAPP: *Is  $\rho$ -meson melting compatible with chiral restoration?*, Phys. Lett. B **731**, 103 (2014).
  - [Hol13] N. P. M. HOLT, P. M. HOHLER and R. RAPP: *Quantitative sum rule analysis of low-temperature spectral functions*, Phys. Rev. D **87**, 076010 (2013).
  - [Iof81] B. L. IOFFE: *Calculation of baryon masses in quantum chromodynamics*, Nucl. Phys. B **188**, 317 (1981).
  - [Itz80] C. ITZYKSON and J.-B. ZUBER: *Quantum Field Theory*, McGraw-Hill, 1980.
  - [Jam86] M. JAMIN and M. KREMER: *Anomalous dimensions of spin-zero four-quark operators without derivatives*, Nucl. Phys. B **277**, 349 (1986).

- [Jam93] M. JAMIN and M. MÜNZ: *Current correlators to all orders in the quark masses*, Z. Phys. C **60**, 569 (1993).
- [Jia15] J.-F. JIANG and S.-L. ZHU: *Radial excitations of mesons and nucleons from QCD sum rules*, Phys. Rev. D **92**, 074002 (2015).
- [Jin93] X.-M. JIN, T. D. COHEN, R. J. FURNSTAHL and D. K. GRIEGEL: *QCD sum rules for nucleons in nuclear matter II*, Phys. Rev. C **47**, 2882 (1993).
- [Jin95] X.-M. JIN and D. B. LEINWEBER: *Valid QCD sum rules for vector mesons in nuclear matter*, Phys. Rev. C **52**, 3344 (1995).
- [Käl52] G. KÄLLÉN: *On the Definition of the Renormalization Constants in Quantum Electrodynamics*, Helv. Phys. Acta **25**, 417 (1952).
- [Kan15] T. KANAZAWA: *Chiral symmetry breaking with no bilinear condensate revisited*, JHEP **10**, 010 (2015).
- [Kap94] J. I. KAPUSTA and E. V. SHURYAK: *Weinberg-type sum rules at zero and finite temperature*, Phys. Rev. D **49**, 4694 (1994).
- [Kek16] V. KEKELIDZE, A. KOVALENKO, R. LEDNICKY, V. MATVEEV, I. MESHKOV, A. SORIN and G. TRUBNIKOV (NICA Collaboration): *Prospects for the dense baryonic matter research at NICA*, Nucl. Phys. A **956**, 846 (2016).
- [Kim16] H. KIM, K. MORITA and S. H. LEE: *Temperature dependence of dimension-6 gluon operators and their effects on charmonium*, Phys. Rev. D **93**, 016001 (2016).
- [Kli97] F. KLINGL, N. KAISER and W. WEISE: *Current correlation functions, QCD sum rules and vector mesons in baryonic matter*, Nucl. Phys. A **624**, 527 (1997).
- [Kne94] M. KNECHT and J. STERN: *Generalized chiral perturbation theory*, in *2nd DAPHNE Physics Handbook*, pages 169–190, 1994.
- [Kog99] I. I. KOGAN, A. KOVNER and M. A. SHIFMAN: *Chiral symmetry breaking without bilinear condensates, unbroken axial  $Z_N$  symmetry, and exact QCD inequalities*, Phys. Rev. D **59**, 016001 (1999).
- [Koi93] Y. KOIKE: *Octet baryons at finite temperature: QCD sum rules versus chiral symmetry*, Phys. Rev. D **48**, 2313 (1993).
- [Koi95] Y. KOIKE:  *$\rho$ ,  $\omega$ ,  $\phi$  meson-nucleon scattering lengths from QCD sum rules*, Phys. Rev. C **51**, 1488 (1995).
- [Koi97] Y. KOIKE and A. HAYASHIGAKI: *QCD sum rules for  $\rho$ ,  $\omega$ ,  $\phi$  meson-nucleon scattering lengths and the mass shifts in nuclear medium*, Prog. Theor. Phys. **98**, 631 (1997).
- [Kug97] T. KUGO: *Eichtheorie*, Springer-Verlag, 1997.
- [Kum10] A. KUMAR and A. MISHRA: *D mesons and charmonium states in asymmetric nuclear matter at finite temperatures*, Phys. Rev. C **81**, 065204 (2010).
- [Kum11] A. KUMAR and A. MISHRA: *D-mesons and charmonium states in hot isospin asymmetric strange hadronic matter*, Eur. Phys. J. A **47**, 164 (2011).
- [Kwo08] Y. KWON, M. PROCURA and W. WEISE: *QCD sum rules for  $\rho$  mesons in vacuum and in-medium, re-examined*, Phys. Rev. C **78**, 055203 (2008).



- 
- [Kwo10] Y. KWON, C. SASAKI and W. WEISE: *Vector mesons at finite temperature and QCD sum rules*, Phys. Rev. C **81**, 065203 (2010).
  - [Lat85] J. I. LATORRE and P. PASCUAL: *QCD sum rules and the  $\bar{q}q\bar{q}q$  system*, J. Phys. G **11**, L231 (1985).
  - [Lau84] G. LAUNER, S. NARISON and R. TARRACH: *Non-perturbative QCD vacuum from  $e^+e^- \rightarrow I = 1$  hadron data*, Z. Phys. C **26**, 433 (1984).
  - [Leh54] H. LEHMANN: *On the properties of propagation functions and renormalization constants of quantized fields*, Nuovo Cim. **11**, 342 (1954).
  - [Lei97] D. B. LEINWEBER: *QCD Sum Rules for Skeptics*, Annals Phys. **254**, 328 (1997).
  - [Lei99] D. B. LEINWEBER: *Visualizations of the QCD vacuum*, in *Light-Cone QCD and Nonperturbative Hadron Physics. Proceedings, Workshop, Adelaide, Australia, December 13-22, 1999*, page 138, 1999.
  - [Leu98] S. LEUPOLD and U. MOSEL: *On QCD sum rules for vector mesons in nuclear medium*, Phys. Rev. C **58**, 2939 (1998).
  - [Leu05] S. LEUPOLD: *Factorization and non-factorization of in-medium four-quark condensates*, Phys. Lett. B **616**, 203 (2005).
  - [Leu06] S. LEUPOLD: *Four-quark condensates and chiral symmetry restoration in a resonance gas model*, J. Phys. G **32**, 2199 (2006).
  - [Luc09] W. LUCHA, D. MELIKHOV and S. SIMULA: *Effective continuum threshold in dispersive sum rules*, Phys. Rev. D **79**, 096011 (2009).
  - [Luc10] W. LUCHA, D. MELIKHOV and S. SIMULA: *Extraction of ground-state decay constant from dispersive sum rules: QCD versus potential models*, Phys. Lett. B **687**, 48 (2010).
  - [Luc11a] W. LUCHA, D. MELIKHOV and S. SIMULA: *Decay constants of heavy pseudoscalar mesons from QCD sum rules*, J. Phys. G **38**, 105002 (2011).
  - [Luc11b] W. LUCHA, D. MELIKHOV and S. SIMULA: *OPE, charm-quark mass, and decay constants of  $D$  and  $D_s$  mesons from QCD sum rules*, Phys. Lett. B **701**, 82 (2011).
  - [Luc14] W. LUCHA, D. MELIKHOV and S. SIMULA: *Decay constants of the charmed vector mesons  $D^*$  and  $D_s^*$  from QCD sum rules*, Phys. Lett. B **735**, 12 (2014).
  - [Luc15] W. LUCHA, D. MELIKHOV and S. SIMULA: *Accurate decay-constant ratios  $f_{B^*}/f_B$  and  $f_{B_s^*}/f_{B_s}$  from Borel QCD sum rules*, Phys. Rev. D **91**, 116009 (2015).
  - [Mac14] C. S. MACHADO, S. I. FINAZZO, R. D. MATHEUS and J. NORONHA: *Modification of the  $B$  meson mass in a magnetic field from QCD sum rules*, Phys. Rev. D **89**, 074027 (2014).
  - [Mao15] Q. MAO, H.-X. CHEN, W. CHEN, A. HOSAKA, X. LIU and S.-L. ZHU: *QCD sum rule calculation for  $P$ -wave bottom baryons*, Phys. Rev. D **92**, 114007 (2015).
  - [Mic94] C. MICHAEL: *Fitting correlated data*, Phys. Rev. D **49**, 2616 (1994).
  - [Mic95] C. MICHAEL and A. MCKERRELL: *Fitting correlated hadron mass spectrum data*, Phys. Rev. D **51**, 3745 (1995).
  - [Mun92] H. J. MUNCZEK and P. JAIN: *Relativistic pseudoscalar  $q\bar{q}$  bound states: Results on*

- Bethe-Salpeter wave functions and decay constants*, Phys. Rev. D **46**, 438 (1992).
- [Nak99] Y. NAKAHARA, M. ASAKAWA and T. HATSUDA: *Hadronic spectral functions in lattice QCD*, Phys. Rev. D **60**, 091503 (1999).
- [Nar83] S. NARISON and R. TARRACH: *Higher dimensional renormalization group invariant vacuum condensates in quantum chromodynamics*, Phys. Lett. B **125**, 217 (1983).
- [Nar88] S. NARISON: *Beautiful mesons from QCD spectral sum rules*, Phys. Lett. B **210**, 238 (1988).
- [Nar89] S. NARISON: *QCD spectral sum rules*, World Sci. Lect. Notes Phys. **26**, 1 (1989).
- [Nar94] S. NARISON: *A fresh look into the heavy quark-mass values*, Phys. Lett. B **341**, 73 (1994).
- [Nar99] S. NARISON: *Extracting  $\bar{m}_c(M_c)$  and  $f_{D_{(s)},B}$  from the pseudoscalar sum rules*, Nucl. Phys. B (Proc. Suppl.) **74**, 304 (1999).
- [Nar01] S. NARISON:  *$c, b$  quark masses and  $f_{D_{(s)}}, f_{B_{(s)}}$  decay constants from pseudoscalar sum rules in full QCD to order  $\alpha_s^2$* , Phys. Lett. B **520**, 115 (2001).
- [Nar05] S. NARISON: *Open charm and beauty chiral multiplets in QCD*, Phys. Lett. B **605**, 319 (2005).
- [Nar06] M. NARUKI et al. (E325 Collaboration): *Experimental Signature of Medium Modification for  $\rho$  and  $\omega$  Mesons in the 12 GeV  $p + A$  Reactions*, Phys. Rev. Lett. **96**, 092301 (2006).
- [Nar07] S. NARISON: *QCD as a Theory of Hadrons – From Partons to Confinement*, Cambridge University Press, 2007.
- [Nar13] S. NARISON: *A fresh look into  $\bar{m}_{c,b}(\bar{m}_{c,b})$  and precise  $f_{D_{(s)},B_{(s)}}$  from heavy-light QCD spectral sum rules*, Phys. Lett. B **718**, 1321 (2013).
- [Nar15] S. NARISON: *Improved  $f_{D_{(s)}}^*, f_{B_{(s)}}^*$  and  $f_{B_c}$  from QCD Laplace sum rules*, Int. J. Mod. Phys. A **30**, 1550116 (2015).
- [Nar16] S. NARISON: *Decay constants of heavy-light mesons from QCD*, Nucl. Part. Phys. Proc. **270-272**, 143 (2016).
- [Nas07] R. NASSERIPOUR et al. (CLAS Collaboration): *Search for Medium Modification of the  $\rho$  Meson*, Phys. Rev. Lett. **99**, 262302 (2007).
- [Neg88] J. W. NEGELE and H. ORLAND: *Quantum many-particle systems*, Addison-Wesley, 1988.
- [Nes82] V. A. NESTERENKO and A. V. RADYUSHKIN: *Sum rules and pion form factor in QCD*, Phys. Lett. B **115**, 410 (1982).
- [Nie04] J. F. NIEVES and P. B. PAL: *Generalized Fierz identities*, Am. J. Phys. **72**, 1100 (2004).
- [Nie14] M. NIELSEN and F. S. NAVARRA: *Charged exotic charmonium states*, Mod. Phys. Lett. A **29**, 1430005 (2014).
- [Nov84] V. A. NOVIKOV, M. A. SHIFMAN, A. I. VAINSHTEIN and V. I. ZAKHAROV: *Calculations in External Fields in Quantum Chromodynamics. Technical Review*,

- Fortsch. Phys. **32**, 585 (1984).
- [Pas84] P. PASCUAL and R. TARRACH: *QCD: Renormalization for the Practitioner*, Lect. Notes Phys. **194**, 1 (1984).
- [Pat16] C. PATRIGNANI et al. (Particle Data Group): *Review of Particle Physics*, Chin. Phys. C **40**, 100001 (2016).
- [Pes95] M. E. PESKIN and D. V. SCHROEDER: *An Introduction to Quantum Field Theory*, Perseus Books, 1995.
- [Pet98] W. PETERS, M. POST, H. LENSKE, S. LEUPOLD and U. MOSEL: *The Spectral function of the rho meson in nuclear matter*, Nucl. Phys. A **632**, 109 (1998).
- [Pol73] H. D. POLITZER: *Reliable Perturbative Results for Strong Interactions?*, Phys. Rev. Lett. **30**, 1346 (1973).
- [Pos04] M. POST, S. LEUPOLD and U. MOSEL: *Hadronic spectral functions in nuclear matter*, Nucl. Phys. A **741**, 81 (2004).
- [Pre16] E. PRENCIPE (PANDA Collaboration): *Status and perspectives for  $\bar{P}$ ANDA at FAIR*, Nucl. Part. Phys. Proc. **273-275**, 231 (2016).
- [Rap97] R. RAPP, G. CHANFRAY and J. WAMBACH: *Rho meson propagation and dilepton enhancement in hot hadronic matter*, Nucl. Phys. A **617**, 472 (1997).
- [Rap99] R. RAPP and J. WAMBACH: *Low-mass dileptons at the CERN-SpS: evidence for chiral restoration?*, Eur. Phys. J. A **6**, 415 (1999).
- [Rap00] R. RAPP and J. WAMBACH: *Chiral symmetry restoration and dileptons in relativistic heavy-ion collisions*, Adv. Nucl. Phys. **25**, 1 (2000).
- [Rap10] R. RAPP, J. WAMBACH and H. VAN HEES: *The Chiral Restoration Transition of QCD and Low Mass Dileptons*, in R. STOCK (Editor), *Relativistic Heavy Ion Physics*, volume I/23 of *Landolt-Börnstein*, Springer-Verlag, 2010.
- [Rap11] R. RAPP et al.: *In-Medium Excitations*, Lect. Notes Phys. **814**, 335 (2011).
- [Rei83] L. J. REINDERS, H. RUBINSTEIN and S. YAZAKI: *Hadron couplings to Goldstone bosons in QCD*, Nucl. Phys. B **213**, 109 (1983).
- [Rei85] L. J. REINDERS, H. RUBINSTEIN and S. YAZAKI: *Hadron properties from QCD sum rules*, Phys. Rept. **127**, 1 (1985).
- [Rom69] P. ROMAN: *Introduction to Quantum Field Theory*, John Wiley and Sons, 1969.
- [Sak14] H. SAKO et al. (J-PARC-HI Collaboration): *Towards the heavy-ion program at J-PARC*, Nucl. Phys. A **931**, 1158 (2014).
- [Sal51] E. E. SALPETER and H. A. BETHE: *A Relativistic Equation for Bound-State Problems*, Phys. Rev. **84**, 1232 (1951).
- [Sal13] P. SALABURA et al. (HADES Collaboration): *Hades experiments: investigation of hadron in-medium properties*, J. Phys. Conf. Ser. **420**, 012013 (2013).
- [Sas14] C. SASAKI: *Fate of charmed mesons near chiral symmetry restoration in hot matter*, Phys. Rev. D **90**, 114007 (2014).
- [Sch51a] J. S. SCHWINGER: *On Gauge Invariance and Vacuum Polarization*, Phys. Rev. **82**, 664 (1951).

- [Sch51b] J. S. SCHWINGER: *On the Green's functions of quantized fields. I*, Proc. Nat. Acad. Sci. **37**, 452 (1951).
- [Sch14] H. R. SCHMIDT (CBM Collaboration): *Status and challenges of the compressed baryonic matter (CBM) experiment at FAIR*, J. Phys. Conf. Ser. **509**, 012084 (2014).
- [Shi79] M. A. SHIFMAN, A. I. VAINSHTEIN and V. I. ZAKHAROV: *QCD and resonance physics. Theoretical foundations*, Nucl. Phys. B **147**, 385 (1979).
- [Shi98] M. A. SHIFMAN: *Snapshots of hadrons – or the story of how the vacuum medium determines the properties of the classical mesons which are produced, live and die in the QCD vacuum*, Prog. Theor. Phys. Suppl. **131**, 1 (1998).
- [Shu82a] E. V. SHURYAK: *Hadrons containing a heavy quark and QCD sum rules*, Nucl. Phys. B **198**, 83 (1982).
- [Shu82b] E. V. SHURYAK and A. I. VAINSHTEIN: *Theory of power corrections to deep inelastic scattering in quantum chromodynamics (I).  $Q^{-2}$  effects*, Nucl. Phys. B **199**, 451 (1982).
- [Shu04] E. V. SHURYAK: *The QCD vacuum, hadrons and the superdense matter*, World Sci. Lect. Notes Phys. **71**, 1 (2004).
- [Sis09] A. N. SISSAKIAN and A. S. SORIN (NICA Collaboration): *The nuclotron-based ion collider facility (NICA) at JINR: new prospects for heavy ion collisions and spin physics*, J. Phys. G **36**, 064069 (2009).
- [Ste93] G. STERMAN: *An Introduction to Quantum Field Theory*, Cambridge University Press, 1993.
- [Ste98] J. STERN: *Light Quark Masses and Condensates in QCD*, Lect. Notes Phys. **513**, 26 (1998).
- [Sug61] M. SUGAWARA and A. KANAZAWA: *Subtractions in Dispersion Relations*, Phys. Rev. **123**, 1895 (1961).
- [Sun10] J. Y. SUNGU, H. SUNDU, K. AZIZI, N. YINELEK and S. SAHIN: *Heavy-light scalar and axial-vector mesons decay constants and masses in QCD sum rule approach*, PoS **FACESQCD**, 045 (2010).
- [Suz16a] K. SUZUKI, P. GUBLER and M. OKA: *D meson mass increase by restoration of chiral symmetry in nuclear matter*, Phys. Rev. C **93**, 045209 (2016).
- [Suz16b] T. SUZUKI, Y.-G. CHO, H. FUKAYA, S. HASHIMOTO, T. KANEKO and J. NOAKI: *D meson semileptonic decays from lattice QCD with chiral fermions*, PoS **LATTICE2015**, 337 (2016).
- [Tar82] R. TARRACH: *The renormalization of FF*, Nucl. Phys. B **196**, 45 (1982).
- [Tho06] R. THOMAS, S. ZSCHOCKE, T. HILGER and B. KÄMPFER: *Hunting medium modifications of the chiral condensate*, in *Proceedings, 44th International Winter Meeting on Nuclear Physics (Bormio 2006)*, 2006.
- [Tho07] R. THOMAS, T. HILGER and B. KÄMPFER: *Four-quark condensates in nucleon QCD sum rules*, Nucl. Phys. A **795**, 19 (2007).
- [Tho08a] R. THOMAS: *In-Medium QCD Sum Rules for  $\omega$  Meson, Nucleon and D Meson*,

- Ph.D. thesis, Technische Universität Dresden (2008).
- [Tho08b] R. THOMAS, T. HILGER and B. KÄMPFER: *Role of four-quark condensates in QCD sum rules*, Prog. Part. Nucl. Phys. **61**, 297 (2008).
- [Tho12] R. THOMAS: private communication (2012).
- [Tol09] L. TOLOS, C. GARCIA-RECIO and J. NIEVES: *The properties of  $D$  and  $D^*$  mesons in the nuclear medium*, Phys. Rev. C **80**, 065202 (2009).
- [Tol13] L. TOLOS and J. M. TORRES-RINCON: *D-meson propagation in hot dense matter*, Phys. Rev. D **88**, 074019 (2013).
- [Wan11] Z.-G. WANG and T. HUANG: *In-medium mass modifications of the  $D_0$  and  $B_0$  mesons from QCD sum rules*, Phys. Rev. C **84**, 048201 (2011).
- [Wan13] Z.-G. WANG: *Analysis of mass modifications of the vector and axial vector heavy mesons in the nuclear matter with the QCD sum rules*, Int. J. Mod. Phys. A **28**, 1350049 (2013).
- [Wan15a] Z.-B. WANG and Z.-G. WANG: *Analysis of the  $a_0(1450)$  and  $K_0^*(1430)$  with the thermal QCD sum rules*, Acta Phys. Polon. B **46**, 2467 (2015).
- [Wan15b] Z.-G. WANG: *Analysis of the masses and decay constants of the heavy-light mesons with QCD sum rules*, Eur. Phys. J. C **75**, 427 (2015).
- [Wan16a] Z.-B. WANG and Z.-G. WANG: *Analysis of the heavy pseudoscalar mesons with thermal QCD sum rules*, Int. J. Theor. Phys. **55**, 3137 (2016).
- [Wan16b] Z.-G. WANG: *Analysis of the strong decay  $X(5568) \rightarrow B_s^0 \pi^+$  with QCD sum rules*, Eur. Phys. J. C **76**, 279 (2016).
- [Wan16c] Z.-G. WANG: *Tetraquark state candidates:  $Y(4260)$ ,  $Y(4360)$ ,  $Y(4660)$ , and  $Z_c(4020/4025)$* , Eur. Phys. J. C **76**, 387 (2016).
- [Wei67a] S. WEINBERG: *Dynamical Approach to Current Algebra*, Phys. Rev. Lett. **18**, 188 (1967).
- [Wei67b] S. WEINBERG: *Precise Relations between the Spectra of Vector and Axial-Vector Mesons*, Phys. Rev. Lett. **18**, 507 (1967).
- [Wei68] S. WEINBERG: *Nonlinear Realizations of Chiral Symmetry*, Phys. Rev. **166**, 1568 (1968).
- [Wei94] W. WEISE: *Hadrons in dense matter*, Nucl. Phys. A **574**, 347C (1994).
- [Wei00] W. WEISE: *QCD aspects of hadron physics*, Nucl. Phys. A **670**, 3 (2000).
- [Wil69] K. G. WILSON: *Non-Lagrangian Models of Current Algebra*, Phys. Rev. **179**, 1499 (1969).
- [Wil74] K. G. WILSON: *Confinement of quarks*, Phys. Rev. D **10**, 2445 (1974).
- [Yas13a] S. YASUI and K. SUDOH: *Heavy-quark dynamics for charm and bottom flavor on the Fermi surface at zero temperature*, Phys. Rev. C **88**, 015201 (2013).
- [Yas13b] S. YASUI and K. SUDOH:  *$\bar{D}$  and  $B$  mesons in nuclear medium*, Phys. Rev. C **87**, 015202 (2013).
- [Yas14] S. YASUI and K. SUDOH: *Probing gluon dynamics by charm and bottom mesons*

- in nuclear matter in heavy-meson effective theory with  $1/M$  corrections*, Phys. Rev. C **89**, 015201 (2014).
- [Ynd06] F. J. YNDURÁIN: *The Theory of Quark and Gluon Interactions*, Springer-Verlag, 2006.
- [Zan16] C. M. ZANETTI, M. NIELSEN and K. P. KHEMCHANDANI: *QCD sum rule study of a charged bottom-strange scalar meson*, Phys. Rev. D **93**, 096011 (2016).
- [Zha10] T. ZHANG, T. BRAUNER and D. H. RISCHKE: *QCD-like theories at nonzero temperature and density*, JHEP **06**, 064 (2010).
- [Zho15] D. ZHOU, H.-X. CHEN, L.-S. GENG, X. LIU and S.-L. ZHU: *F-wave heavy-light meson spectroscopy in QCD sum rules and heavy quark effective theory*, Phys. Rev. D **92**, 114015 (2015).
- [Zhu03] S.-L. ZHU: *Understanding Pentaquark States in QCD*, Phys. Rev. Lett. **91**, 232002 (2003).
- [Zim73] W. ZIMMERMANN: *Composite Operators in the Perturbation Theory of Renormalizable Interactions*, Annals Phys. **77**, 536 (1973), [Lect. Notes Phys. 558, 244 (2000)].
- [Zsc02] S. ZSCHOCKE, O. P. PAVLENKO and B. KÄMPFER: *Evaluation of QCD sum rules for light vector mesons at finite density and temperature*, Eur. Phys. J. A **15**, 529 (2002).
- [Zsc11] S. ZSCHOCKE, T. HILGER and B. KÄMPFER: *In-medium operator product expansion for heavy-light-quark pseudoscalar mesons*, Eur. Phys. J. A **47**, 151 (2011).
- [Zwe64] G. ZWEIG: *An  $SU_3$  model for strong interaction symmetry and its breaking. Version 2*, in D. LICHTENBERG and S. P. ROSEN (Editors), *Developments in the quark theory of hadrons*, volume 1, pages 22–101, 1964.

# Acknowledgements

I would like to thank Prof. Dr. Burkhard Kämpfer for the opportunity to explore this very interesting topic and for the many stimulating discussions which guaranteed the continuous progress of the project at Helmholtz-Zentrum Dresden-Rossendorf. His vast hadron physics expertise helped to develop an interpretation of the results leading to insights on the in-medium effects of D mesons. I am grateful to have had the opportunity to present this work to the hadron physics community at international conferences.

I would particularly like to thank Dr. Thomas Hilger for his assistance on the topic of QCD sum rules while I was working on my diploma thesis. I would also like to thank him for our numerous discussions on technical and conceptional aspects of the framework which helped me to develop a deep understanding of this particular field of hadron physics. His continuous support and encouragement, especially when things became tedious, contributed to the successful completion of this thesis. Despite his distant affiliation to Karl-Franzens-Universität Graz we established regular contact which resulted in a fruitful collaboration.

I also gratefully acknowledge the kind hospitality and excellent working conditions at the Institut für Theoretische Physik at Technische Universität Dresden. In particular, thank you to all the members of our research group for their support and the friendly atmosphere in the office.

I would also like to thank my fellow students, in particular, Klaus, Roland, Mo and Flo, who became good friends of mine during the years I spent in Dresden. Bruno's philosophical insights shared during lunch are highly appreciated.

I would sincerely like to thank Margarete as well as my parents and my brother Michael for the confidence they placed in me and for their relentless moral support.





# Erklärung

Hiermit versichere ich, dass ich die vorliegende Arbeit ohne unzulässige Hilfe Dritter und ohne Benutzung anderer als der angegebenen Hilfsmittel angefertigt habe; die aus fremden Quellen direkt oder indirekt übernommenen Gedanken sind als solche kenntlich gemacht. Die Arbeit wurde bisher weder im Inland noch im Ausland in gleicher oder ähnlicher Form einer anderen Prüfungsbehörde vorgelegt.

Diese Dissertation wurde am Helmholtz-Zentrum Dresden-Rossendorf e. V. unter der wissenschaftlichen Betreuung von Herrn Prof. Dr. Burkhard Kämpfer angefertigt. Ich habe bisher an keiner Institution, weder im Inland noch im Ausland, einen Antrag auf Eröffnung eines Promotionsverfahrens gestellt. Ferner erkläre ich, dass ich die Promotionsordnung der Fakultät Mathematik und Naturwissenschaften der Technischen Universität Dresden vom 23. Februar 2011 anerkenne.

Thomas Buchheim

Dresden, den 02. Dezember 2016